

21-0002-82

~~TOP SECRET~~ G

~~0010-82~~

BIF-008-W-C-019838-RI-80

This document contains 172 classified sheets including the front and back cover.

PHOTOGRAPHIC SYSTEM REFERENCE HANDBOOK
FOR
GAMBIT RECONNAISSANCE SYSTEM
WITH
EXTENDED ALTITUDE CAPABILITY
(EAC)

VOLUME 1

Prepared by
BIF-008

Under Contract

[Redacted box]

25X1

USER:
SAFE NO:

Approved by:

[Handwritten signature]

1 July 1980

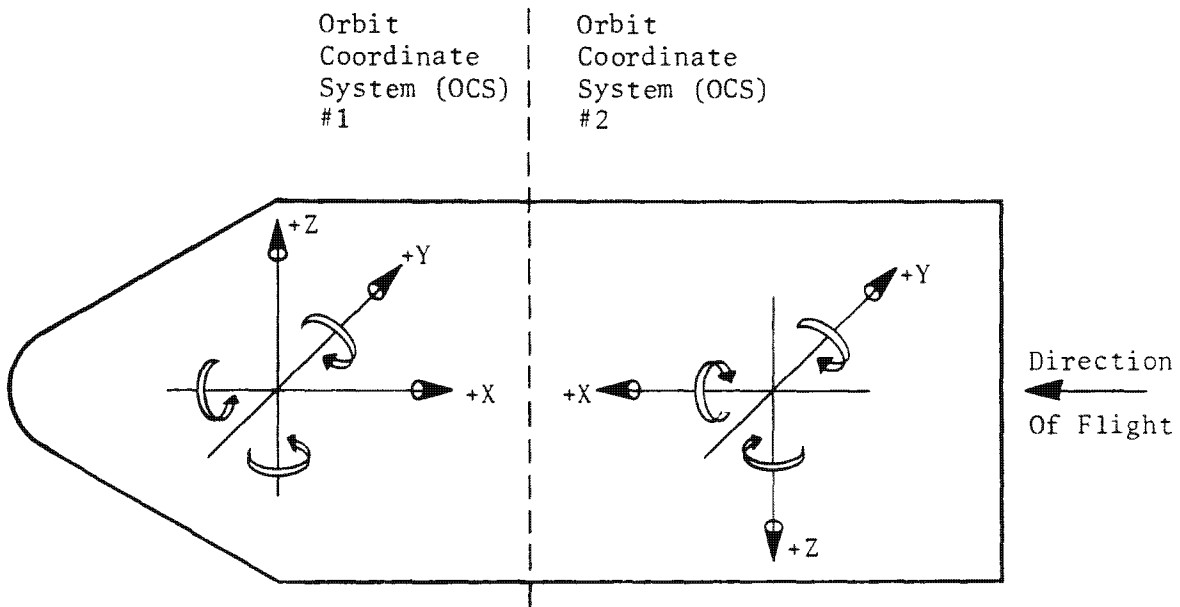
"WARNING - THIS DOCUMENT SHALL NOT BE USED AS A SOURCE FOR DERIVATIVE CLASSIFICATION"

~~TOP SECRET~~ G

Handle via **BYEMAN**
Control System Only

~~TOP SECRET~~ G

BIF-008- W-C-019838-RI-80



BIF-008 Uses OCS #1

OCS #1 Is Used In This Document

Orbit Coordinate Systems Sign Convention

FRONTISPIECE

"WARNING - THIS DOCUMENT SHALL NOT BE USED AS A SOURCE FOR DERIVATIVE CLASSIFICATION"

I
~~TOP SECRET~~ G

Handle via **BYEMAN**
Control System Only

~~TOP SECRET~~ GBIF-008- W-C-019838-RI-80

TABLE OF CONTENTS

VOLUME 1	<u>Page</u>
PART 1 SYSTEM OVERVIEW	
1.0 THE GAMBIT RECONNAISSANCE SYSTEM	1.1-1
1.1 System Definition	1.1-1
1.2 Mission Definition	1.1-1
1.2.1 Mission Requirements	1.1-2
1.2.2 Mission Orbits	1.1-3
1.2.3 Mission Duration	1.1-3
1.3 System Description	1.1-3
1.3.1 Hardware	1.1-4
1.3.2 Software	1.1-4
1.3.3 Support Activities	1.1-6
1.4 Mission Description	1.1-6
2.0 THE BIF-008 SUBSYSTEM	1.2-1
2.1 Mission	1.2-1
2.1.1 General Mission Description	1.2-1
2.1.2 Photographic Modes Of Operation	1.2-2
2.1.3 Image Motion Compensation	1.2-6
2.1.4 Exposure Control	1.2-10
2.1.5 Mission Orbits	1.2-13
2.1.6 Mission Duration	1.2-13
2.1.7 Films	1.2-13

II

~~TOP SECRET~~ GHandle via BYEMAN
Control System Only

~~TOP SECRET G~~BIF-008- W-C-019838-RI-80

TABLE OF CONTENTS (Continued)

VOLUME 1	<u>Page</u>
2.2 Aerospace Flight Equipment-Modular Subsystems	1.2-14
2.2.1 Supply and Electronics Module (SEM)	1.2-14
2.2.2 Camera Optics Module (COM)	1.2-14
2.2.3 Dual Recovery Module (DRM)	1.2-14
2.3 Aerospace Flight Equipment - Functional Subsystems	1.2-16
2.3.1 External	1.2-16
2.3.2 Film Handling Subsystem and Camera	1.2-16
2.3.3 Optics Subsystem	1.2-16
2.3.4 Servos	1.2-16
2.3.5 Viewport Door Subsystem	1.2-17
2.3.6 Focus Detection Subsystem	1.2-17
2.3.7 Power Subsystem	1.2-17
2.3.8 Thermal Control Subsystem	1.2-17
2.3.9 Command Subsystem	1.2-17
2.3.10 Telemetry and Instrumentation Subsystem	1.2-18
2.3.11 Cutter Sealer and Splicer Subsystem	1.2-18
2.3.12 Recovery Subsystem	1.2-18
2.4 Experimental Subsystems	1.2-18
2.4.1 S-1/Platen Reference Gauge	1.2-18
2.4.2 	1.2-19
 PART 2 ANALYSIS	
1.0 REFERENCE FRAMES	2.1-1
1.1 Coordinate System Conventions	2.1-1
1.2 Vehicle and Orbit Coordinate Systems	2.1-1
1.3 Image Plane and Ground Coordinate Systems	2.1-3
1.4 PPS/DP EAC Cylindrical Coordinate System	2.1-3

25X1

III

~~TOP SECRET G~~Handle via BYEMAN
Control System Only

~~TOP SECRET~~ GBIF-008- W-C-019838-RI-80

TABLE OF CONTENTS (Continued)

VOLUME 1		<u>Page</u>
2.0	POINTING AND TARGET ACQUISITION	2.2-1
2.1	Swath Width	2.2-1
2.2	5-Inch Pointing Biases	2.2-2
2.3	Target Acquisition	2.2-6
2.3.1	Slant Range	2.2-7
2.3.2	In-Track Acquisition	2.2-8
2.3.3	Cross-Track Target Acquisition	2.2-17
2.4	Pointing Error Analysis	2.2-20
2.4.1	Pointing Error Contributors	2.2-20
2.4.2	Pointing Error Limits	2.2-35
3.0	IMAGE MOTION COMPENSATION (IMC)	2.3-1
3.1	Crab	2.3-2
3.1.1	Nine-Inch System	2.3-2
3.1.2	Five-Inch System	2.3-4
3.2	Film-Drive Speed	2.3-4
3.2.1	Nine-Inch System	2.3-4
3.2.2	Five-Inch System	2.3-7
4.0	IMAGE SMEAR	2.4-1
4.1	Effects of Smear	2.4-1
4.1.1	Smear Descriptors	2.4-2
4.1.2	Modulation Transfer Function (MTF)	2.4-5
4.1.3	SMTF Application	2.4-9
4.2	Conventions and Coordinate Systems	2.4-13
4.2.1	Image Plane Coordinate System	2.4.13
4.2.2	Transformation of Smear Rates	2.4-15

IV

~~TOP SECRET~~ GHandle via BYEMAN
Control System Only

~~TOP SECRET~~ G

BIF-008- W-C-019838-RI-80

TABLE OF CONTENTS (Continued)

VOLUME 1		<u>Page</u>
4.3	Smear Contributors	2.4-17
4.3.1	PPS/DP EAC Contributors	2.4-17
4.3.2	SCS Contributors	2.4-31
4.3.3	Telemetry, Tracking and Command (T T and C) Contributors	2.4-32
4.3.4	9-Inch Smear Equations	2.4-33
4.3.5	5-Inch System Smear	2.4-33
4.4	Smear Budgeting	2.4-36
4.4.1	Between-Mission and Within-Mission Linear Smear Contributors	2-4-36
4.4.2	Nonlinear Smear Contributors	2.4-38
4.4.3	Smear Contributors for the PSV	2.4-38
4.4.4	Smear Rate Statistical Combination	2.4-38
4.5	Smear Detection and Measurement	2.4-42
4.5.1	Smear Slit Theory	2.4-42
4.5.2	Smear Slit Design	2.4-42
4.5.3	Smear Slit Operation	2.4-42
5.0	FOCUS	2.5-1
5.1	Focus Requirement	2.5-1
5.2	Focus Maintenance	2.5-2
5.2.1	Focus Detection Subsystem	2.5-2
5.2.2	Platen Adjustment Subsystems	2.5-19
5.3	Error Contributors	2.5-20
5.3.1	Error Sources	2.5-22
5.3.2	Error Budget	2.5-23
5.4	Calibration	2.5-25

V
~~TOP SECRET~~ GHandle via BYEMAN
Control System Only

~~TOP SECRET~~ G

BIF-008-W-C-009887-RH-76

TABLE OF CONTENTS (Continued)

VOLUME 1		<u>Page</u>
6.0	EXPOSURE	2.6-1
6.1	Spectral Dependency	2.6-1
6.2	Exposure Determination	2.6-2
6.2.1	Geometric Considerations	2.6-2
6.2.2	Slit-Width	2.6-2
6.3	Slit Selection, Graphical Approximation	2.6-2
6.4	Slit Selection, Operational Software	2.6-3
6.4.1	Slit Selection Algorithm Inputs	2.6-7
6.4.2	Slit Selection Algorithm	2.6-10
7.0	FILM CHARACTERISTICS	2.7-1
7.1	Physical Characteristics	2.7-1
7.1.1	Base	2.7-1
7.1.2	Emulsion	2.7-4
7.1.3	Backing	2.7-5
7.1.4	Anti-Halation Undercoat (AHU)	2.7-5
7.1.5	Dye Layers	2.7-6
7.1.6	Emulsion Matte	2.7-6
7.1.7	Total Film Properties	2.7-6
7.2	Sensitometric Characteristics	2.7-21
7.2.1	Characteristic Curve	2.7.21
7.2.2	Sensitometric Parameters	2.7-24
7.2.3	Spectral Sensitivity	2.7-27
7.2.4	Fog	2.7-27
7.2.5	Special Films	2.7-27

VI

~~TOP SECRET~~ GHandle via BYEMAN
Control System Only

~~TOP SECRET~~ GBIF-008- W-C-019838-RI-80

TABLE OF CONTENTS (Continued)

VOLUME 1	<u>Page</u>
7.3 Noise Characteristics (Signal/Noise)	2.7-29
7.3.1 Film Granularity	2.7-30
7.3.2 Threshold Modulation	2.7-30
7.3.3 Duplication	2.7-31
7.4 Film Characteristics Summary	2.7-31
8.0 MISSION SIMULATIONS	2.8-1
8.1 Orbit Generation	2.8-1
8.2 Target Acquisition	2.8-3
8.3 Target Selection	2.8-3
8.4 Photographic Performance Model	2.8-12
8.5 Equipment Usage Model	2.8-12
8.6 Photographic Performance Estimates	2.8-16
8.7 Equipment Usage Estimates	2.8-23
8.8 High-Mode Orbit Generation	2.8-26
8.9 Target Acquisition/Selection	2.8-26
9.0 IMAGE QUALITY EVALUATION	2.9-1
9.1 Limiting Resolution	2.9-2
9.1.1 Prediction	2.9-2
9.1.2 Measurement	2.9-4
9.2 Objective Quality Measures	2.9-4
9.2.1 Power Spectral Analysis	2.9-4
9.2.2 Image Noise	2.9-12
9.2.3 Specific Quality Measures	2.9-14
9.2.4 Reliability of Quality Measures	2.9-18

VII

~~TOP SECRET~~ GHandle via **BYEMAN**
Control System Only

~~TOP SECRET~~ G

BIF-008-W-C-019838-RI-80

TABLE OF CONTENTS (Continued)

VOLUME 1		<u>Page</u>
9.3	National Imagery Interpretability Rating Scale (NIIRS)	2.9-19
9.3.1	Construction of the Rating Scale	2.9-19
9.3.2	Design Objectives	2.9-19
9.4	Data Tracks as User Aids	2.9-20
9.4.1	Data Track Decoding	2.9-20
9.4.2	Decoding Procedure	2.9-20
10.0	OPERATIONAL ENVELOPE	2.10-1
10.1	Launch, Orbit and Recovery Limits	2.10-1
10.2	Photographic Limits	2.10-1
10.2.1	Timing Constraints	2.10-1
10.2.2	Focus Limits	2.10-9

VIII

~~TOP SECRET~~ GHandle via **BYEMAN**
Control System Only

~~TOP SECRET~~ GBIF-008- W-C-019838-RI-80

TABLE OF CONTENTS (Continued)

	<u>Page</u>
VOLUME 2	
PART 2 ANALYSIS	
11.0 SCENE LUMINANCE	2.11-1
11.1 Solar Irradiance at the Target	2.11-3
11.1.1 Sun Angle	2.11-3
11.1.2 Insolation and Atmospheric Transmission	2.11-3
11.2 Target Reflectance	2.11-7
11.3 Atmospheric Transmission	2.11-11
11.4 Haze	2.11-13
11.5 Radiation Effect	2.11-13
11.6 Summary	2.11-13
12.0 OPTICAL ANALYSIS	2.12-1
12.1 Analytic Tools	2.12-1
12.1.1 Spread Functions	2.12-1
12.1.2 Test Objects	2.12-3
12.1.3 Modulation	2.12-6
12.2 Modulation Transfer Function (MTF)	2.12-8
12.2.1 Linear System	2.12-9
12.2.2 Nonlinear System	2.12-11
12.2.3 System MTF	2.12-15
12.3 Threshold Modulation	2.12-16
12.3.1 Measurement	2.12-17
12.3.2 Assumptions	2.12-18

IX

~~TOP SECRET~~ GHandle via **BYEMAN**
Control System Only

~~TOP SECRET~~ GBIF-008- W-C-019838-RI-80

TABLE OF CONTENTS (Continued)

	<u>Page</u>
VOLUME 2	
12.4 Optical Quality Factor (OQF)	2.12-19
12.4.1 Calculation	2.12-19
12.4.2 Contributors to OQF Reduction	2.12-21
12.5 Lens Performance	2.12-26
12.5.1 Lens MTF and OQF	2.12-26
12.5.2 Resolution Predictions	2.12-28
12.6 Through-Focus Characteristics	2.12-31
12.6.1 Heterochromatic, Off-Axis, Through-Focus Characteristics	2.12-31
12.6.2 Monochromatic, Through-Focus Characteristics	2.12-34
12.7 Thermally Induced Focus Changes	2.12-34
12.7.1 Isothermal Analysis	2.12-34
12.7.2 Transient Thermal Analysis	2.12-36
13.0 VENTING ANALYSIS	2.13-1
13.1 Shipment	2.13-1
13.2 Venting Model	2.13-1
13.3 Ascent Venting	2.13-2
13.4 Conditioned Air Flow	2.13-5
14.0 THERMAL ANALYSIS	2.14-1
14.1 Prelaunch	2.14-1
14.1.1 Cold Environment	2.14-2
14.1.2 Hot Environment	2.14-4
14.2 Ascent	2.14-5
14.2.1 Design Requirements	2.14-5
14.2.2 Design Predictions	2.14-6

X
~~TOP SECRET~~ GHandle via BYEMAN
Control System Only

~~TOP SECRET~~ GBIF-008- W-C-019838-RI-80

TABLE OF CONTENTS (Continued)

	<u>Page</u>
VOLUME 2	
14.3 Orbital	2.14-10
14.3.1 Design Parameters	2.14-10
14.3.2 Design Requirements	2.14-10
14.3.3 Orbital Design	2.14-14
14.4 PPS/DP EAC Overage Analysis	2.14-42
14.5 Thermal Analysis	2.14-44
14.6 Recovery	2.14-46
14.6.1 Nose-Aft Flight	2.14-49
14.6.2 Pitchdown	2.14-49
14.6.3 PPS/DP EAC Recovery	2.14-50
14.7 Additional Considerations	2.14-53
14.7-1 Tumbling	2.14-53
14.7-2 Hotdogging	2.14-56
15.0 EJECTION ANALYSIS	2.15-1
15.1 Main Hatch	2.15-1
15.2 Dual Recovery Module (DRM) Ejectable Components	2.15-1
15.2.1 SRV 1 and SRV 2	2.15-3
15.2.2 Ejectable Adapter (EA)	2.15-3
15.3 Ejection Model	2.15-3
15.3.1 General Free-Body Equations	2.15-4
15.3.2 Spring Ejectors	2.15-5
15.3.3 Mass Properties	2.15-8
15.3.4 Monte Carlo Approach	2.15-9
15.4 Application of the Model	2.15-10
15.4.1 Ejectable Adapter Geometry	2.15-10
15.4.2 SRV 2 Geometry	2.15-14
15.5 Results	2.15-14

25X1

XI

~~TOP SECRET~~ GHandle via **BYEMAN**
Control System Only

~~TOP SECRET~~ GBIF-008- W-C-019838-RI-80

TABLE OF CONTENTS (Continued)

	<u>Page</u>
VOLUME 2	
15.6 Conclusions	2.15-18
15.6.1 SRV 1	2.15-18
15.6.2 Ejectable Adapter	2.15-18
15.6-3 SRV 2	2.15-18
16.0 CONSUMABLES MANAGEMENT	2.16-1
16.1 Photographic Film	2.16-1
16.1.1 Film Usage Control	2.16-1
16.1.2 Film Usage Influences	2.16-2
16.2 Electrical Power	2.16-2
16.2.1 Power Usage Control	2.16-2
16.2.2 Power Usage Influences	2.16-2
16.3 Attitude Control Gas	2.16-3
16.3.1 Control Gas Usage Control	2.16-3
16.3.2 Control Gas Usage Influences	2.16-3
16.4 Orbit Maintenance Fuel	2.16-4
16.4.1 Orbit Maintenance Fuel Usage Control	2.16-4
16.4.2 Orbit Maintenance Fuel Usage Influences	2.16-4
 PART 3 HARDWARE DESCRIPTION	
1.0 PHOTOGRAPHIC PAYLOAD SECTION/DUAL PLATEN EXTENDED ALTITUDE CAPABILITY	3.1-1
1.1 PPS/DP EAC General Description	3.1-1
1.1.1 PPS/DP EAC Assembly Modules	3.1-1
1.1.2 PPS/DP EAC External Finish	3.1-6
1.2 Dual Recovery Module	3.1-6
1.2.1 DRM Access Panels	3.1-11
1.2.2 DRM Structure and Internal Components	3.1.11

XII

~~TOP SECRET~~ GHandle via **BYEMAN**
Control System Only

~~TOP SECRET~~ GBIF-008- W-C-019838-RI-80

TABLE OF CONTENTS (Continued)

VOLUME 2		<u>Page</u>
1.3	Supply and Electronics	3.1-26
1.3.1	Supply Electronics Structure	3.1-26
1.3.2	SEM Components	3.1-39
1.3.3	SEM/COM Mating	3.1-44
1.4	Camera Optics Module	3.1-44
1.4.1	Camera Optics Module - External Sources	3.1-46
1.4.2	Camera Optics Assembly (Internal Structure)	3.1-59
1.4.3	PPS/DP EAC - SCS Interface	3.1-73

~~TOP SECRET~~ G

~~TOP SECRET G~~

BIF-008-W-C-019838-RI-80

TABLE OF CONTENTS (Continued)

	<u>Page</u>
VOLUME 3	
PART 3 HARDWARE DESCRIPTION	
2.0 9x5 DUAL PLATEN CAMERA AND FILM HANDLING SUBSYSTEM	3.2-1
2.1 Film Handling Subsystem Description	3.2-1
2.1.1 9 and 5 Supply Assemblies	3.2-5
2.1.2 9x5 Take-up Assemblies	3.2-29
2.2 9x5 Dual Platen Camera Description	3.2-42
2.2.1 Camera Housing	3.2-45
2.2.2 9 and 5 Pivot Frame Assemblies	3.2-47
2.3 Film Path Distances	3.2-71
2.4 Operational Description	3.2-71
2.4.1 Simplified Photographic Cycle	3.2-77
2.4.2 Simplified Take-up Cycle	3.2-79
2.5 9x5 Dual Platen Camera and Film Handling Subsystem Electronic Control Units	3.2-84
2.5.1 Film Control Electronics	3.2-84
2.5.2 Film Handling Electronics	3.2-93
2.5.3 9 and 5 Frequency Phase Lock Loop Electronics	3.2-103
2.5.4 9 and 5 Camera Electronics Assemblies	3.2-113
2.6 9x5 Dual Platen Camera and Film Handling Subsystem Instrumentation	3.2-133
2.7 Command Summary	3.2-157
2.7.1 CP Select Commands	3.2-157
2.7.2 Operational Power Commands	3.2-158
2.7.3 5 Parking Brake	3.2-160
2.7.4 Film Drive Commands	3.2-162
2.7.5 Take-up Control Commands	3.2-169

XIV

~~TOP SECRET G~~Handle via **BYEMAN**
Control System Only

~~TOP SECRET~~ G

BIF-008-W-C-019838-RI-80

TABLE OF CONTENTS (Continued)

	<u>Page</u>
VOLUME 3	
2.7.6 Variable Exposure Mechanism (Slit Mechanism) Commands	3.2-172
2.7.7 Slant Range Compensation Commands	3.2-174
2.7.8 Focus Adjustment (NPA) Commands	3.2-177
3.0 OPTICAL SUBSYSTEM	3.3-1
3.1 Optical Subsystem Configuration	3.3-1
3.2 Elements of the Optical Subsystem	3.3-5
3.2.1 Stereo Mirror	3.3-5
3.2.2 Primary Mirror (Asphere)	3.3-10
3.2.3 Ross Corrector and Field Lens Assembly	3.3-11
3.3 Optical Performance Parameters	3.3-11
3.3.1 Aperture Obstructions and Vignetting	3.3-12
3.3.2 Lens Spectral Transmittance	3.3-15
3.4 Instrumentation	3.3-15
4.0 MIRROR POSITIONING SUBSYSTEM	3.4-1
4.1 Stereo Servo Subsystem	3.4-4
4.1.1 Stereo Drive Components	3.4-4
4.1.2 Stereo Servo Electronic Control	3.4-6
4.1.3 Stereo Angle Instrumentation	3.4-13
4.2 Crab Servo Subsystem	3.4-15
4.2.1 Crab Drive Components	3.4-18
4.2.2 Crab Servo Electronic Control	3.4-18
4.2.3 Crab Angle Instrumentation	3.4-25
4.3 Instrumentation Summary	3.4-26

~~TOP SECRET~~ G

~~TOP SECRET~~ GBIF-008- W-C-019838-RI-80

TABLE OF CONTENTS (Continued)

	<u>Page</u>
VOLUME 3	
4.4 Mirror Positioning Command Summary	3.4-26
4.4.1 CP Select Commands	3.4-26
4.4.2 14V WORD Command	3.4-30
4.4.3 13V WORD Command (13V2bWXYZ)	3.4-31
4.4.4 Operational Power ON Commands	3.4-32
4.4.5 Operational Power OFF Commands	3.4-33
4.4.6 9/5 RUNOUT ON Command (MCS)	3.4-34
4.4.7 Power OFF Commands (MCS)	3.4-34

XVI

~~TOP SECRET~~ GHandle via **BYEMAN**
Control System Only

~~TOP SECRET~~ GBIF-008- W-C-019838-RI-80

TABLE OF CONTENTS (Continued)

VOLUME 4

PART 3 - HARDWARE DESCRIPTION

	<u>Page</u>
5.0 VIEWPORT DOOR SUBSYSTEM	3.5-1
5.1 Ejectable Hatch	3.5-1
5.2 Viewport Doors and Door Drive Linkage	3.5-3
5.2.1 Viewport Door Structure	3.5-3
5.2.2 Viewport Door Drive Mechanism	3.5-7
5.3 Viewport Door Electronics Module	3.5-9
5.3.1 Viewport Door Control	3.5-11
5.4 Viewport Door Subsystem Instrumentation	3.5-19
5.5 Viewport Door Subsystem Command Summary	3.5-32
5.5.1 HATCH EJECT Command	3.5-32
5.5.2 DOOR BACKUP Command	3.5-32
5.5.3 DOOR BLOW Command	3.5-32
5.5.4 4V WORD Command (Bit 36: Door Open/Close)	3.5-33
5.5.5 DOOR CLOSE Command (MCS)	3.5-34
6.0 FOCUS DETECTION SUBSYSTEM	3.6-1
6.1 System Description	3.6-1
6.1.1 Focus Sensor Head Assembly (Unit 15A2)	3.6-1
6.1.2 Signal Normalizing Module (Unit 15A3)	3.6-9
6.1.3 Instrumentation and Control Module (Unit 15A1)	3.6-9
6.1.4 Dual Photodiode Detector	3.6-12
6.1.5 Light-Emitting Diode (LED) Array	3.6-12
6.2 System Operation	3.6-15
6.2.1 Focus System Head Assembly	3.6-15
6.2.2 Signal Normalizing Module	3.6-24
6.2.3 Instrumentation and Control Module	3.6-26
6.3 Focus Detection Subsystem Commanding	3.6-30
6.3.1 Focus Electronics Power	3.6-30
6.4 Instrumentation	3.6-30

~~TOP SECRET~~ G

~~TOP SECRET~~ GB1F-008- W-C-019838-RI-80

TABLE OF CONTENTS (Continued)

VOLUME 4		<u>Page</u>
7.0	POWER DISTRIBUTION SUBSYSTEM	3.7-1
7.1	Power Source	3.7-1
	7.1.1 Power Distribution	3.7-3
	7.1.2 Solar Array	3.7-3
	7.1.3 Batteries	3.7-5
7.2	Power Monitor and Control Unit	3.7-8
	7.2.1 PM and C Assembly	3.7-8
	7.2.2 PM and C Logic	3.7-14
	7.2.3 PM and C Unipoint Power Return	3.7-29
	7.2.4 Power Conversion (+5/±15 Volts)	3.7-32
	7.2.5 Ampere-Hour Meter	3.7-32
	7.2.6 PM and C Instrumentation	3.7-33
7.3	Initiator Electronics Unit	3.7-34
	7.3.1 IEU Assembly	3.7-35
	7.3.2 IEU Operation	3.7-35
	7.3.3 IEU Logic	3.7-52
7.4	PPS/DP EAC Electromagnetic Interference (EMI) Control	3.7-70
	7.4.1 Filters	3.7-70
	7.4.2 Grounding	3.7-71
	7.4.3 Power Distribution	3.7-72
	7.4.4 Shielding	3.7-72
7.5	Instrumentation Summary	3.7-72
7.6	Command Summary	3.7-72

XVIII

~~TOP SECRET~~ GHandle via **BYEMAN**
Control System Only

~~TOP SECRET~~ GBIF-008- W-C-019838-RI-80

TABLE OF CONTENTS (Continued)

VOLUME 4		<u>Page</u>
8.0	ENVIRONMENTAL CONTROL	3.8-1
8.1	Ground Conditioning	3.8-1
	8.1.1 Manufacturing Environment	3.8-2
	8.1.2 Storage and Shipment	3.8-6
	8.1.3 Launch Site Ground Conditioning	3.8-6
8.2	Ascent	3.8-15
	8.2.1 Ascent Thermal Environment	3.8-15
	8.2.2 Ascent Venting	3.8-16
8.3	Orbital Environment	3.8-17
	8.3.1 Optics	3.8-18
	8.3.2 Film	3.8-19
	8.3.3 Electronic Boxes	3.8-21
	8.3.4 External Thermal Control Finishes	3.8-21
	8.3.5 Internal Design	3.8-28
8.4	Instrumentation	3.8-54
8.5	Environmental Control Command Summary	3.8-72
	8.5.1 Heater Power On	3.8-72
	8.5.2 Heater Power Off Commands	3.8-72
	8.5.3 EPSM ON Commands	3.8-72
	8.5.4 EPSM OFF Commands	3.8-73
	8.5.5 Heater Power ON/OFF (M6V Word)	3.8-73

~~TOP SECRET~~ G

~~TOP SECRET~~ GBIF-008- W-C-019838-RI-80

TABLE OF CONTENTS (Continued)

	<u>Page</u>
VOLUME 5	
PART 3 HARDWARE DESCRIPTION	
9.0 COMMAND SUBSYSTEM	3.9-1
9.1 Vehicle-Ground Communications Link	3.9-2
9.2 Command Types	3.9-2
9.3 Command Bit Structure	3.9-6
9.3.1 Decoder Selection	3.9-9
9.3.2 RTC Bit Structure	3.9-10
9.4 ECS Simultaneous Commanding	3.9-11
9.5 Timing Signals and Command Pulse Characteristics	3.9-12
9.5.1 Command Pulse Characteristics	3.9-14
9.6 Extended Command Subsystem/Minimal Command Subsystem Overview	3.9-18
9.6.1 Extended Command Subsystem	3.9-19
9.6.2 Minimal Command Subsystem	3.9-23
9.7 ECS Real-Time Bias	3.9-25
9.8 Command Processor	3.9-25
9.8.1 Command Processor Physical Properties	3.9-26
9.8.2 CP Operation	3.9-28
9.9 Command Processor Instrumentation	3.9-85
10.0 INSTRUMENTATION AND TELEMETRY	3.10-1
10.1 Instrumentation	3.10-4
10.1.1 Instrumentation Signal Characteristics	3.10.4
10.1.2 Test Points (TSP's) and Umbilical Monitoring Points (BIL's)	3.10-5
10.2 Instrumentation Processor	3.10-6
10.2.1 IP Mechanical	3.10-6
10.2.2 IP Electrical	3.10-9

XX

~~TOP SECRET~~ GHandle via **BYEMAN**
Control System Only

TABLE OF CONTENTS (Continued)

	<u>Page</u>
VOLUME 5	
10.3 PPS/DP EAC Slave Digital Telemetry Unit	3.10-12
10.3.1 DTU Assembly	3.10-30
10.3.2 Slave DTU Power Control	3.10-35
10.3.3 DTU Redundancy and Block Functions	3.10-36
10.3.4 Slave DTU Address/Reply Timing	3.10-64
10.4 Master DTU	3.10-71
10.4.1 MDTU Capabilities	3.10-71
10.4.2 Slave DTU/MDTU Communication	3.10-74
10.4.3 MDTU Telemetry Output	3.10-80
10.4.4 Telemetry Transmission and Processing	3.10-83
10.5 Telemetry Formats	3.10-85
10.5.1 Format Selection	3.10-88
10.5.2 Photographic Satellite Vehicle Telemetry Formats	3.10-88
10.5.3 Data Position Coding	3.10-90
10.5.4 Photographic Satellite Vehicle (PSV) Telemetry Modes	3.10-95
10.6 MDTU Programming	3.10-101
10.6.1 MDTU Memory Organization	3.10-101
10.6.2 Subroutine Construction	3.10-104
10.7 End-to-End Telemetry Accuracy	3.10-107
10.7.1 Analog Instrumentation Error	3.10-107
10.7.2 End-to-End Analog Accuracy Summary	3.10-112
10.7.3 Discrete Instrumentation Error	3.10-113
10.8 Instrumentation Summary	3.10-113
10.9 Command Summary	3.10-113
10.9.1 10V WORD Command (Bits 29 and 30)	3.10-113
10.9.2 M6V WORD (Bits 33 and 34)	3.10-116
10.9.3 DTU ON Commands (MR)	3.10-117
10.9.4 DTU OFF Command (Umbilical)	3.10-117

~~TOP SECRET~~ G

BIF-008-W-C-019838-RI-80

TABLE OF CONTENTS (Continued)

VOLUME 5		<u>Page</u>
11.0	CUTTER/SEALER AND SPLICER MECHANISMS	3.11-1
11.1	Function	3.11-1
11.2	The Cutter/Sealer Mechanism	3.11-2
	11.2.1 Latching Mechanism	3.11-2
	11.2.2 Pivot Door Assembly	3.11-9
	11.2.3 Electrical Interconnection and Instrumentation	3.11-9
	11.2.4 Cutter/Sealer Operation	3.11-10
11.3	Splicer Mechanism	3.11-10
	11.3.1 Dimple Motors and Drive Linkage	3.11-10
	11.3.2 Shuttle Assembly	3.11-14
	11.3.3 Platen Assembly	3.11-14
	11.3.4 Electrical Connectors and Instrumentation	3.11-16
	11.3.5 Splicer Mechanism Operation	3.11-17
11.4	Instrumentation Summary	3.11-18
11.5	Command Summary	3.11-25
	11.5.1 Splice and Cut Commands	3.11-25
	11.5.2 Cut and Seal 1 Command	3.11-25
	11.5.3 Cut and Seal 2 Command	3.11-26

~~TOP SECRET~~ GHandle via **BYEMAN**
Control System Only

~~TOP SECRET~~ G81F-008- W-C-019838-RI-80

TABLE OF CONTENTS (Continued)

VOLUME 5

PART 3 - HARDWARE DESCRIPTION

	<u>Page</u>
12.0 TERMINATION AND RECOVERY	3.12-1
12.1 Dual Recovery Module (DRM)	3.12.1
12.2 Photographic Satellite Vehicle (PSV) Recovery Maneuvers	3.12-1
12.2.1 Powered Maneuver	3.12-5
12.2.2 Inertial Maneuver	3.12-5
12.2.3 Thermal Constraints	3.12-5
12.2.4 Timing	3.12.5
12.3 Ejection	3.12-9
12.3.1 SRV 1 Ejection Sequence	3.12-9
12.3.2 Ejectable Adapter and SRV 2 Ejection	3.12-11
12.4 Satellite Reentry Vehicle	3.12-19
12.5 SRV Deorbit and Recovery Events	3.12-19
12.6 SRV Structure	3.12-22
12.7 Deorbit Subsystem	3.12-23
12.7.1 Dual Ejection Programmer and Thermal Relay Modules	3.12-25
12.7.2 Thermal Batteries	3.12-25
12.7.3 Retro-Rocket Motor	3.12-25
12.7.4 Spin and Despin Subsystem	3.12-26
12.7.5 Thrust Cone Ejection	3.12-26
12.8 Recovery Subsystem	3.12-26
12.8.1 Recovery Batteries and Battery Heaters	3.12-27
12.8.2 Orbital Heaters	3.12-27
12.8.3 Recovery Programmer	3.12-30
12.8.4 Parachute Assembly and Deployment	3.12-30
12.8.5 Recovery Beacons	3.12-31
12.8.6 Capsule Valving Hardware	3.12-31

XXIII

~~TOP SECRET~~ GHandle via **BYEMAN**
Control System Only

~~TOP SECRET~~ GBIF-008- W-C-019838-RI-80

TABLE OF CONTENTS (Continued)

VOLUME 5		<u>Page</u>
12.9	Instrumentation	3.12-32
12.9.1	Satellite Reentry Vehicle Instrumentation	3.12-32
12.9.2	Termination and Recovery Related PPS/DP EAC Instrumentation	3.12-32
12.10	Command Summary	3.12-46
12.10.1	Splice and Cut Commands	3.12-46
12.10.2	Roll-In Terminate Commands	3.12-46
12.10.3	Cut and Seal 1 Command	3.12-47
12.10.4	SRV 1 Arm Command	3.12-47
12.10.5	SRV 1 Transfer Command	3.12-48
12.10.6	SRV 1 Separate Command	3.12-48
12.10.7	Spinoff Disconnect 2 (EA Disconnect) Command	3.12-48
12.10.8	EA Separation Command	3.12-49
12.10.9	Cut and Seal 2 Command	3.12-49
12.10.10	SRV 2 Arm Command	3.12-49
12.10.11	SRV 2 Transfer Command	3.12-50
12.10.12	SRV 2 Separate Command	3.12-50
12.10.13	MCS Termination Enable 1 Command	3.12-50
12.10.14	MCS Termination Enable 2 Command	3.12-51
12.10.15	Heater Power ON Command	3.12-51
12.10.16	Heater Branch OFF Commands (Branches 1 and 6 Only)	3.12-51
12.10.17	EPSM ON Commands	3.12-51
12.10.18	EPSM OFF Commands	3.12-52
12.10.19	19 M6V WORD Command	3.12-52

XXIV

~~TOP SECRET~~ GHandle via **BYEMAN**
Control System Only

~~TOP SECRET~~ GBIF-008- W-C-019838-RI-80

TABLE OF CONTENTS (Continued)

VOLUME 5		<u>Page</u>
13.0	S1-PRG SENSOR EXPERIMENT	3.13.1
13.1	Measured Parameter	3.13-2
13.2	Sensor System Function	3.13-2
	13.2.1 Method of Sensing	3.13-3
	3.2.2 Targets	3.13-3
13.3	S1 Sensor Mechanical Configuration	3.13-4
	13.3.1 Rod and Truss Assembly	3.13-4
	13.3.2 S1 Gage Assembly	3.13-4
	13.3.3 Rod, Truss, and Gage Interface	3.13-4
	13.3.4 S1 Sensor Nominal Separations	3.13-7
13.4	PRG Sensor Mechanical Configurations	3.13-7
	13.4.1 Sensor Geometry	3.13-7
	13.4.2 PRG Sensor Mounting	3.13-8
13.5	Sensor Targets	3.13-8
13.6	Health Check (Calibration) Slide	3.13-12
13.7	S1-PRG Sensor System Electronics	3.13-14
	13.7.1 Sensor Encoder and Processing Electronics (SEPE) Unit	3.13-14
13.8	System Operation	3.13-18
	13.8.1 Factory Use	3.13-18
	13.8.2 Pre-Launch Use	3.13-19
	13.8.2 On-Orbit Use	3.13-20
13.9	S1-PRG Instrumentation Summary	3.13-21
13.10	S1-PRG Sensor System Command Summary	3.13-25
	13.10.1 S1-PRG Command	3.13-25
	13.10.2 S1-PRG CAL Command	3.13-26
	13.10.3 S1-PRG DISABLE Command	3.13-26

XXV

~~TOP SECRET~~ GHandle via **BYEMAN**
Control System Only

~~TOP SECRET~~ GBIF-008- W-C-019838-RI-80

TABLE OF CONTENTS (Continued)

VOLUME 5		<u>Page</u>
PART 4 DESIGN, MANUFACTURE, TEST AND FIELD SUPPORT		
1.0	DESIGN	4.1-1
1.1	Design Baseline (Non-EAC)	4.1-1
1.1.1	Frequency Phase Lock Loop (FPLL) Drive	4.1-2
1.1.2	Variable Width Slit	4.1-2
1.1.3	Improved Focus Detection System	4.1-2
1.1.4	Replacement of Separation Controller and Switchover Electronics with Initiator Electronics Unit (IEU)	4.1-2
1.1.5	Redesigned Command Processor	4.1-3
1.2	Extended Altitude Capability (EAC) Baseline	4.1-3
1.2.1	Frequency Phase Lock Loop (FPLL) Drive	4.1-3
1.2.2	Focus Detection System	4.1-3
1.2.3	Dual Platen Camera	4.1-3
1.2.4	Command Processor	4.1-4
1.3	Non-Baseline Items	4.1-4
2.0	RELIABILITY	4.2-1
2.1	Reliability by Attention to Design Details	4.2-1
2.2	Reliability Through Redundancy	4.2-2
2.2.1	Initiator Subsystem	4.2-3
2.2.2	Mirror Positioning Subsystem	4.2-5
2.2.3	Instrumentation Subsystem	4.2-8
2.2.4	9 and 5 Camera Platen Drive Subsystems	4.2-13
2.2.5	Nominal Platen Adjust (NPA) Subsystem	4.2-13
2.2.6	Slant Range Compensation (SRC) Subsystem	4.2-15
2.2.7	Variable Exposure Mechanism (VEM) Subsystem	4.2-18
2.2.8	9 Film Handling System	4.2-18
2.2.9	5 Film Handling System	4.2-21
2.2.10	Thermal Environment Control Subsystem	4.2-23

XXVI

~~TOP SECRET~~ GHandle via **BYEMAN**
Control System Only

~~TOP SECRET~~ GBIF-008- W-C-019838-RI-80

TABLE OF CONTENTS (Continued)

VOLUME 5		<u>Page</u>
2.3	Qualification Program	4.2-27
2.3.1	Philosophy	4.2-27
2.3.2	Purpose	4.2-28
2.3.3	Qualification Testing	4.2-28
2.3.4	Demonstrated Qualification Summary	4.2-29
3.0	MANUFACTURING	4.3-1
3.1	Aerospace Vehicle Buildup	4.3-1
3.1.1	Factory-to-Pad Concept	4.3-1
3.1.2	Manufacture/Test Interdependency	4.3-1
3.2	PPS/DP EAC Modules	4.3-3
3.2.1	Camera Optics Assembly (COA)	4.3-3
3.2.2	External Structure	4.3-12
3.2.3	COM Assembly	4.3-13
3.2.4	SEM Assembly	4.3-19
3.2.5	DRM Assembly	4.3-23
3.2.6	PPS/DP EAC Assembly	4.3-26
4.0	TESTING	4.4-1
4.1	Optical Components and Camera Optics Assembly Testing	4.4-1
4.1.1	Lens and Mirror Components Testing	4.4-1
4.1.2	Lens Assembly and COA Testing	4.4-3
4.2	Electrical/Mechanical Components Testing	4.4-13
4.2.1	Acceptance Testing	4.4-13
4.3	Major Assembly Electro/Mechanical Testing	4.4-16
4.3.1	Camera Optics Module (COM) Acceptance Testing	4.4-18
4.3.2	Supply and Electronics Module (SEM) Acceptance Testing	4.4-18
4.3.3	Dual Recovery Module (DRM) Acceptance Testing	4.4-21

XXVII

~~TOP SECRET~~ GHandle via **BYEMAN**
Control System Only

~~TOP SECRET~~ G

BIF-008- W-C-019838-RI-80

TABLE OF CONTENTS (Continued)

VOLUME 5

	<u>Page</u>
4.3.4 Photographic Payload Section/Dual Platen Extended Altitude Capability (PPS/DP EAC)	4.4-26
4.3.5 Pyrotechnic Subsystem Testing	4.4-52
4.3.6 PPS/DP EAC Revalidation Testing	4.4-53
4.3.7 Computerized System Level Testing	4.4-55

XXVIII

~~TOP SECRET~~ G

Handle via **BYEMAN**
Control System Only

~~TOP SECRET~~ G

BIF-008-W-C-019838-RI-80

TABLE OF CONTENTS (Continued)

VOLUME 6

PART 4 DESIGN, MANUFACTURE, TEST AND FIELD SUPPORT

5.0	STORAGE AND SHIPMENT	4.5-1
5.1	Storage	4.5-1
5.1.1	Factory Storage	4.5-1
5.1.2	Storage at Vandenberg AFB	4.5-2
5.2	Shipment	4.5-2
5.2.1	Shipping Preparation	4.5-2
5.2.2	Shipping Container	4.5-4
5.2.3	Ground Transportation	4.5-4
5.2.4		4.5-6
6.0	LAUNCH SUPPORT	4.6-1
6.1	Support Activiity Overview	4.6-1
6.1.1	FAS Functional Overview	4.6-1
6.1.2	FAS Organization	4.6-3
6.2	FAS Facility Overview	4.6-9
6.2.1	Vehicle Service Building (VSB)	4.6-9
6.2.2	A and B/C Rooms	4.6.9
6.2.3	Blockhouse L Room	4.6-11
6.2.4	Missile Assembly Building (MAB)	4.6-11
6.2.5	FAS Administration Office	4.6-13
6.3	Launch Support Activities	4.6-13
6.3.1	Off-Loading (L-12 Days)	4.6-13
6.3.2	Transportation and/or Storage	4.6-17
6.3.3	Mating	4.6-17

25X1

XXIX

~~TOP SECRET~~ GHandle via BYEMAN
Control System Only

~~TOP SECRET~~ GBIF-008- W-C-019838-RI-80

TABLE OF CONTENTS (Continued)

VOLUME 6		<u>Page</u>
6.3.4	Simulated Flight Testing Activities	4.6-19
6.3.5	Data Review and Buy-Off	4.6-21
6.3.6	Countdown Activities	4.6-21
6.4	Between Cycles Activities	4.6-22
6.4.1	Hardware	4.6-22
6.4.2	Software	4.6-23
6.4.3	Factory/Field Liaison	4.6-23
6.4.4	Training for FAS Cycle	4.6-23
7.0	FIELD ACTIVITY, NORTH (FAN)	4.7-1
7.1		4.7-1
7.1.1	Remote Tracking Stations (RTS's)	4.7-1
7.1.2	Communications	4.7-2
7.2	Program 110 Operations Director	4.7-2
7.2.1	Test Control	4.7-3
7.2.2	Orbit Plans	4.7-4
7.2.3	Weather	4.7-4
7.2.4	Technical Advisors	4.7-5
7.3	WCEO Activities	4.7-5
7.3.1	Pre-Flight	4.7-5
7.3.2	On-Orbit	4.7-7
7.3.3	Post-Flight	4.7-11
7.4	Vehicle Commanding	4.7-11
7.4.1	System IIB Software	4.7-13
7.4.2	Gambit-Specific Software	4.7-14
7.5	Message Generation	4.7-17
7.5.1	Mission Requirements Subsystem (Pre-Mission)	4.7-17
7.5.2	Event Generator Subsystem (Daily Cycle)	4.7-18

25X1

XXX

~~TOP SECRET~~ GHandle via **BYEMAN**
Control System Only

~~TOP SECRET~~ GBIF-008- W-C-019838-RI-80

TABLE OF CONTENTS (Continued)

VOLUME 6

	<u>Page</u>
7.5.3 Event Generator Subsystem (Message Cycle)	4.7-22
7.5.4 Command Assembly Subsystem (Message Cycle)	4.7-32
7.5.5 Telemetry Predict Subsystem (Message Cycle)	4.7-34
7.5.6 Mission Analysis Subsystem (Daily Cycle)	4.7-35
7.5.7 Mission Requirements Subsystem (Intra- and Post-Mission)	4.7-36
7.6 Payload Message Checking	4.7-37
7.6.1 Normal Mode	4.7-37
7.6.2 Priority Mode	4.7-39
7.7 Telemetry Data Processing System	4.7-40
7.7.1 Telemetry Mode Definition	4.7-40
7.7.2 Telemetry Limits Compare (TLC)	4.7-43
7.7.3 'LPROFIT	4.7-48
7.7.4 RTS <input type="checkbox"/> Processing	4.7-48
7.7.5 Modes Matrix	4.7-50
8.0 FIELD ENGINEERING OPERATIONS SUPPORT ACTIVITIES	4.8-1
8.1 Preflight	4.8-1
8.2 Launch Support	4.8-1
8.3 On-Orbit Liaison	4.8-3
8.4 Post-Flight Support	4.8-3
8.5 Between Flight Activity	4.8-4
8.6 Factory/STC Data Link Computer System	4.8-6
8.6.1 Factory System	4.8-6
8.6.2 FAN System	4.8-7
8.6.3 Stand Alone Operation	4.8-7
8.6.4 Joint Operation	4.8-7

25X1

XXXI

~~TOP SECRET~~ GHandle via **BYEMAN**
Control System Only

~~TOP SECRET~~ GBIF-008- W-C-019838-RI-80

TABLE OF CONTENTS (Continued)

VOLUME 6		<u>Page</u>
APPENDIX A	Reference Documents	A-1
APPENDIX B	Electrical Diagram	B-1
APPENDIX C	Software	C-1
APPENDIX D	Functional Description of Aerospace Support Equipment	D-1
APPENDIX E	E (95,95)Statistical Combination of Error Contributors	E-1
APPENDIX F	Numerical Summary and Mass Properties	F-1
APPENDIX G	PPS/DP EAC Instrumentation Summary	G-1
APPENDIX H	PPS/DP EAC Command List	H-1
APPENDIX J	GLOSSARY	J-1
APPENDIX K	Pyrotechnics	K-1
INDEX		I

XXXII

~~TOP SECRET~~ GHandle via **BYEMAN**
Control System Only

~~TOP SECRET~~ GBIF-008- W-C-019838-RI-80

LIST OF ILLUSTRATIONS

VOLUME 1
FigureTitlePage

1.1-1	Gambit Aerospace Vehicle	1.1-5
1.1-2	Gambit Reconnaissance System Operational Block Diagram	1.1-7
1.2-1	The Photographic Satellite Vehicle	1.2-3
1.2-2	Stereo Pair Geometry	1.2-4
1.2-3	Half-Stereo Pair Geometry	1.2-5
1.2-4	Stereo Triplet Geometry	1.2-7
1.2-5	Lateral Pair Geometry	1.2-8
1.2-6	Object Velocity Components	1.2-9
1.2-7	Mirror Movements for Stereo and IMC	1.2-11
1.2-8	Illustration of the Effect of Crab	1.2-12
1.2-9	Photographic Payload Section/Dual Platen Extended Altitude Capability	1.2-15
2.1-1	BIF-008 and LMSC Coordinate Systems	2.1-2
2.1-2	Simplified Schematic of Coordinate System Requirements	2.1-5
2.1-3	PPS/DP EAC Cylindrical Coordinates	2.1-7
2.2-1	9 System Swath Width vs Obliquity	2.2-3
2.2-2	5 System Swath Width vs Obliquity	2.2-4
2.2-3	Effect of Offset of 5-Inch System on Pointing	2.2-5
2.2-4	Slant Range Approximation	2.2-9
2.2-5	In-Track Monoscopic Acquisition	2.2-11
2.2-6	Probability of High Resolution Before Target Acquisition	2.2-12
2.2-7	Stereoscopic Acquisition	2.2-13
2.2-8	In-Track Stereo Coverage	2.2-16
2.2-9	Target-Swath Relationship	2.2-18
2.2-10	Probability of Target Within Swath	2.2-21

XXXIII

~~TOP SECRET~~ GHandle via **BYEMAN**
Control System Only

~~TOP SECRET~~ GBIF-008- W-C-019838-RI-80

LIST OF ILLUSTRATIONS (Continued)

VOLUME 1

<u>Figure</u>	<u>Title</u>	<u>Page</u>
2.2-11	Pointing Error vs Error Contributor	2.2-27
2.2-12	Pointing Error vs Contributor	2.2-28
2.2-13	Pointing Error vs Contributor	2.2-29
2.2-14	Error Parameter vs Pointing Error	2.2-30
2.2-15	Error Parameter vs Pointing Error	2.2-31
2.2-16	Pointing Error vs Contributor	2.2-32
2.2-17	Pointing Error Multiplier vs Slant Range	2.2-34
2.3-1	Roll, Crab and Obliquity	2.3-2
2.3-2	Ground Velocity for Circular Orbit (V_{cx})	2.3-6
2.3-3	Required Film Velocity vs Altitude	2.3-8
2.3-4	Film-Drive Speed Bias Approximation	2.3-9
2.4-1	Limiting Effect of Smear	2.4-3
2.4-2	Ideal Shutter Function	2.4-7
2.4-3	Linear Smear MTF	2.4-8
2.4-4	Strip Camera Shutter Function	2.4-10
2.4-5	Application of MTF Techniques	2.4-11
2.4-6	Geometric Mean Resolution Given Smear and Film Type	2.4-12
2.4-7	9-Inch Image Plane Coordinate System	2.4-14
2.4-8	Equivalent Smear Rate Due to Film-Drive Speed Error	2.4-24
2.4-9	Crab Angle Error Contributor	2.4-25
2.4-10	Geometric Smear Source	2.4-27
2.4-11	OFF-Axis Smear Rates	2.4-28
2.4-12	Five-Inch System Offset	2.4-33
2.4-13	Five-Inch Field Position	2.4-35
2.4-14	Smear Slit Configuration	2.4-43
2.5-1	Focus Detection Subsystem Functional Block Diagram	2.5-3

XXXIV

~~TOP SECRET~~ GHandle via **BYEMAN**
Control System Only

~~TOP SECRET~~ G

BIF-008-W-C-019838-RI-80

LIST OF ILLUSTRATIONS (Continued)

<u>VOLUME 1</u> <u>Figure</u>	<u>Title</u>	<u>Page</u>
2.5-2	Heterochromatic, 14 lpmm Through-Focus MTF	2.5-5
2.5-3	Earth's Wiener Spectrum (with 175 inch FL, 85% OQF Optics)	2.5-6
2.5-4	Typical Chevron Reticle	2.5-7
2.5-5	Reticle Transfer Function	2.5-9
2.5-6	Channel A and B Signals	2.5-11
2.5-7	Signal vs Defocus	2.5-12
2.5-8	Focus System, Physical Layout	2.5-13
2.5-9	Polarization Effect	2.5-15
2.5-10	Focus Position vs Slant Range	2.5-21
2.6-1	Exposure Model, Graph 1	2.6-4
2.6-2	Exposure Model, Graph 2	2.6-5
2.6-3	Slit Selection Algorithm	2.6-11
2.7-1	Typical Film Cross-Section	2.7-2
2.7-2	Halation	2.7-5
2.7-3	Window Splice	2.7-8
2.7-4	Standard Ultrasonic Weld Splice	2.7-9
2.7-5	Typical Curl	2.7-10
2.7-6	Electrification of a Film Strand	2.7-12
2.7-7	Typical Resistivity of Emulsion and Gel Backings	2.7-13
2.7-8	Temperature Conditioning Curves for 9.5-and 5-Inch Wide Films	2.7-16
2.7-9	Film Keeping Limits	2.7-17
2.7-10	Spectral Transmission of Film	2.7-20
2.7-11	Typical Characteristic Curve	2.7-22
2.7-12	Sensitometric Properties	2.7-25
2.7-13	Process Comparison	2.7-26

XXXV

~~TOP SECRET~~ GHandle via **BYEMAN**
Control System Only

~~TOP SECRET~~ GBIF-008- W-C-019838-RI-80

LIST OF ILLUSTRATIONS (Continued)

<u>VOLUME 1</u> <u>Figure</u>	<u>Title</u>	<u>Page</u>
2.7-14	Typical Spectral Sensitivity, Black-and White Film	2.7-28
2.8-1	Target Distribution	2.8-5
2.8-2	Cumulative Simulated Resolution (Tribar)	2.8-17
2.8-3	Cumulative Simulated Resolution (2:1 Contrast)	2.8-18
2.8-4	Cumulative Simulated Resolution (Operational)	2.8-19
2.8-5	Contrast Distribution	2.8-22
2.8-6	Gambit Dual Mode Search Satisfaction	2.8-28
2.8-7	Gambit Dual Mode Search Accomplishment	2.8-29
2.8-8	Gambit Dual Mode Search Satisfaction	2.8-30
2.8-9	Gambit Dual Mode Search Accomplishment	2.8-31
2.8-10	NIIRS Distribution	2.8-33
2.9-1	Limiting Resolution Illustration	2.9-3
2.9-2	Controlled Range Network (CORN) Target	2.9-5
2.9-3	Electromagnetic Field Vectors	2.9-6
2.9-4	Simplified Scene Transparency	2.9-7
2.9-5	Optically Generated Fourier Transform	2.9-9
2.9-6	Solid-State Detector for PSD Analysis	2.9-11
2.9-7	Estimation of Phase Noise	2.9-13
2.9-8	LOCMO	2.9-15
2.9-9	Information Content and BPI	2.9-17
2.9-10	Time Word Decoding	2.9-21
2.10-1	Stereo/Timing	2.10-3
2.10-2	Typical Film Velocity Profile	2.10-6
2.10-3	High-Resoluton Distance	2.10-7
2.10-4	Focus Limits	2.10-10

XXXVI

~~TOP SECRET~~ GHandle via **BYEMAN**
Control System Only

~~TOP SECRET~~ GBIF-008-W-C-019838-RI-80

LIST OF ILLUSTRATIONS (Continued)

<u>VOLUME 2</u> <u>Figure</u>	<u>Title</u>	<u>Page</u>
2.11-1	Radiance Parameters	2.11-2
2.11-2	Sun Angle Geometry	2.11-4
2.11-3	Sun Angle vs Latitude	2.11-5
2.11-4	Sun Angle vs Latitude	2.11-6
2.11-5	Solar Spectral Irradiance	2.11-8
2.11-6	Relative Irradiance vs Sun Angle	2.11-9
2.11-7	Spectral Reflectance of Ground Scenes	2.11-10
2.11-8	Zenith Angle and Obliquity	2.11-11
2.11-9	Atmospheric Transmission	2.11-12
2.11-10	Haze Radiance	2.11-14
2.11-11	Radiation-Induced Fog	2.11-15
2.12-1	Point-Spread Function	2.12-2
2.12-2	Light Scattering by the Emulsion	2.12-2
2.12-3	Actual and Geometric Image Distributions	2.12-4
2.12-4	Image Distributions of Sinusoidal Object	2.12-5
2.12-5	Low-Frequency Modulation	2.12-7
2.12-6	High-Frequency Modulation	2.12-8
2.12-7	MTF Concept	2.12-8
2.12-8	Transfer Characteristics of a Linear System	2.12-9
2.12-9	Nonlinear Transfer Concept	2.12-11
2.12-10	Transfer Characteristics of a Nonlinear System	2.12-12
2.12-11	Typical Lens MTF	2.12-15
2.12-12	Typical TM Curve	2.12-16
2.12-13	OQF vs RMS Wavefront Error	2.12-20
2.12-14	R-5 Lens MTF	2.12-29
2.12-15	AIM Illustration	2.12-30
2.12-16	Limiting Resolution	2.12-32

XXXVII
~~TOP SECRET~~ GHandle via **BYEMAN**
Control System Only

~~TOP SECRET~~ GBIF-008- W-C-019838-RI-80

LIST OF ILLUSTRATIONS (Continued)

VOLUME 2 <u>Figure</u>	<u>Title</u>	<u>Page</u>
2.12-17	Heterochromatic Off-Axis Through-Focus Curve	2.12-33
2.12-18	Monochromatic Through-Focus Curves	2.12-35
2.12-19	Thermal Focus Shift	2.12-37
2.13-1	Venting Model Illustration	2.13-3
2.13-2	Recommended Operating Limits for Clean Room	2.13-7
2.14-1	Time vs Temperature, +Z FSE Panel	2.14-3
2.14-2	Ascent Maximum Longitudinal Skin Temperature Distribution	2.14-7
2.14-3	Ascent Maximum Longitudinal Skin Temperature Distribution EAC Finish Patterns	2.14-8
2.14-4	Ascent Pinpuller Temperatures	2.14-9
2.14-5	Film Temperature vs Time Limits	2.14-12
2.14-6	Fixed Adapter Skin Temperature Minimum Altitude 67 nmi, Beta Angle: 0 Degrees	2.14-16
2.14-7	Fixed Adapter Skin Temperature Minimum Altitude 85 nmi, Beta Angle: 0 Degrees	2.14-17
2.14-8	Fixed Adapter Skin Temperature Minimum Altitude 85 nmi, Beta Angle: 60 Degrees	2.14-18
2.14-9	IBS Blanket Temperature Minimum Altitude 65 nmi	2.14-20
2.14-10	Orbit Average Heat Fluxes, Cylindrical Section	2.14-22
2.14-11	SEM Orbital Average Skin Temperature Distributions	2.14-23
2.14-12	COM Skin Temperature vs Orbit Position Angle ($\beta=0^\circ$, Roll= 0°) for Pattern $-60^\circ \leq \beta \leq 60^\circ$	2.14-26
2.14-13	COM Paint Pattern Temperature Range	2.14-27
2.14-14	COM Environmental Energy Requirements, 60-Degree Pattern	2.14-28
2.14-15	COM Environmental Energy Requirement, 48-Degree Pattern	2.14-29
2.14-16	COM Environmental Energy Requirement, 30-Degree Pattern	2.14-30

XXXVIII
~~TOP SECRET~~ GHandle via **BYEMAN**
Control System Only

~~TOP SECRET~~ GBIF-008- W-C-019838-RI-80

LIST OF ILLUSTRATIONS (Continued)

<u>VOLUME 2</u> <u>Figure</u>	<u>Title</u>	<u>Page</u>
2.14-17	COM Environmental Energy Requirement, Sun-Synchronous Pattern	2.14-31
2.14-18	COM Environmental Energy Requirements (Watt-Hours/Day) EAC Symmetric Pattern	2.14-32
2.14-19	COM Environmental Energy Requirements (Watt-Hours/Day) EAC Asymmetric Pattern (0 to +40, or 0 to -40 Degrees)	2.14-33
2.14-20	Predicted COM Curvature	2.14-36
2.14-21	Predicted COM Curvature	2.14-37
2.14-22	Predicted COM Curvature	2.14-38
2.14-23	Rotation of COA Optical Axis	2.14-39
2.14-24	Operating Constraint EAC Symmetric Finish Pattern	2.14-43
2.14-25	Operating Constraint EAC Asymmetric Finish Pattern	2.14-45
2.14-26	Lens Tube Constraints on Viewport Door Open Time	2.14-47
2.14-27	Ross Corrector Constraints on Viewport Door Open Time	2.14-48
2.14-28	COM Predictions for 68 nmi Recovery	2.14-51
2.14-29	COM Predictions for 65 nmi Recovery	2.14-52
2.14-30	COM Skin Temperatures, Tumbling Rev 3	2.14-54
2.14-31	COM Curvature, Tumbling Rev 3	2.14-55
2.14-32	Pinpuller Temperature, Tumbling Rev	2.14-57
2.14-33	COM Curvature Derivation	2.14-58
2.14-34	COA Suspension System Geometry	2.14-61
2.14-35	COA Suspension System Model	2.14-62
2.14-36	External Structure Centerline Deflection Model	2.14-63
2.14-37	Angular Rotation of COA Axis with Respect to SCS Axis	2.14-70
2.14-38	Operating and Nonoperating Curvature Constraints	2.14-73

XXXIX
~~TOP SECRET~~ GHandle via **BYEMAN**
Control System Only

~~TOP SECRET~~ GBIF-008- W-C-019838-RI-80

LIST OF ILLUSTRATIONS (Continued)

<u>VOLUME 2</u> <u>Figure</u>	<u>Title</u>	<u>Page</u>
2.15-1	PPS/DP EAC Ejectable Components	2.15-2
2.15-2	Free-Body Reference Plane	2.15-4
2.15-3	Theoretical Force-Displacement Curve	2.15-5
2.15-4	Spring Ejector Assembly	2.15-7
2.15-5	Ejection Force Geometry, Ejectable Adapter	2.15-11
2.15-6	Free-Body Diagram, Ejectable Adapter	2.15-12
2.15-7	Ejectable Adapter Configuration	2.15-13
2.15-8	Ejection Force Geometry, SRV	2.15-15
2.15-9	Free-Body Diagram, SRV	2.15-16
3.1-1	PPS/DP EAC Assembly	3.1-2
3.1-2	PPS/DP EAC Major Components	3.1-3
3.1-3	DRM Internal Components	3.1-7
3.1-4	DRM Film Path Details (Internal SRV)	3.1-9
3.1-5	Dual Recovery Module Access Panels	3.1-13
3.1-6	Ejectable Adapter (-X View)	3.1-16
3.1-7	Ejectable Adapter (-Z View)	3.1-17
3.1-8	Fixed Adapter (-Z View)	3.1-21
3.1-9	Fixed Adapter (+X View, EA Attached)	3.1-23
3.1-10	Supply Electronics Module (+Y Side)	3.1-27
3.1-11	SEM Access Panels	3.1-29
3.1-12	FSE Internal Components	3.1-31
3.1-13	SEM Internal Temperature Monitors (-Y Side)	3.1-35
3.1-14	SEM Internal Temperature Monitors (+Y Side)	3.1-36
3.1-15	SEM Aft Bulkhead	3.1-37
3.1-16	SEM Electronic Unit Locations (-Y Side)	3.1-40
3.1-17	SEM Electronic Unit Locations (+Y Side)	3.1-41

XL

~~TOP SECRET~~ GHandle via **BYEMAN**
Control System Only

~~TOP SECRET~~ GBIF-008- W-C-019838-RI-80

LIST OF ILLUSTRATIONS (Continued)

<u>VOLUME 2</u> <u>Figure</u>	<u>Title</u>	<u>Page</u>
3.1-18	SEM/COM Interface	3.1-45
3.1-19	COM Access Panels	3.1-48
3.1-20	COM Forward Barrel	3.1-49
3.1-21	COM Forward Barrel Structure	3.1-51
3.1-22	COM Aft Barrel Structure	3.1-57
3.1-23	Camera Optics Assembly	3.1-61
3.1-24	COA Structural Cylinder (-Y Side)	3.1-63
3.1-25	COA (-Y Side) Showing Adjustable A-Frame	3.1-65
3.1-26	Primary Mirror Mount(-X View)	3.1-67
3.1-27	COA Internal Structure	3.1-69
3.1-28	Stereo Mirror Yoke Assembly	3.1-71
3.1-29	COA Double Bulkhead (-X View)	3.1-74
3.1-30	PPS/SCS Alignment Scheme	3.1-76

XLI

~~TOP SECRET~~ GHandle via **BYEMAN**
Control System Only

~~TOP SECRET~~ GBIF-008- W-C-019838-RI-80

LIST OF ILLUSTRATIONS (Continued)

VOLUME 3 <u>Figure</u>	<u>Title</u>	<u>Page</u>
3.2-1	9x5 Dual Platen Camera and Film Handling Subsystem Block Diagram	3.2-2
3.2-2	9x5 Camera and Film Handling Subsystem Major Components	3.2-3
3.2-3	9 Supply and Looper Assembly Without Supply Spool	3.2-6
3.2-4	5 Supply Assembly (Breadboard)	3.2-7
3.2-5	9 Supply Spool Assembly	3.2-8
3.2-6	5 Supply Spool Assembly	3.2-10
3.2-7	9 and 5 Supply Assemblies	3.2-13
3.2-8	9 and 5 Looper Carriage Assemblies and Instrumentation	3.2-15
3.2-9	5 Supply Assembly (-Y View)	3.2-17
3.2-10	9 and 5 Tension Arm Assemblies	3.2-19
3.2-11	General Tension Arm Instrumentation Circuit	3.2-23
3.2-12	General Tension Arm Instrumentation Output	3.2-24
3.2-13	Film Velocity Sensor Conceptual Representation	3.2-26
3.2-14	9 and 5 Film Quantity Sensor Assemblies	3.2-27
3.2-15	9x5 Take-up Assembly (-Y View)	3.2-30
3.2-16	9x5 Take-up Assembly (-Z View)	3.2-31
3.2-17	9 Take-up Spool Assembly	3.2-34
3.2-18	9 T/U Motor Performance Curves	3.2-35
3.2-19	9 T/U Motor Speed-Torque Envelope	3.2-36
3.2-20	5 Take-up Spool Assembly	3.2-37
3.2-21	5 T/U Motor Performance Curves	3.2-39
3.2-22	9x5 Dual Platen Camera Internal Configuration	3.2-43
3.2-23	Camera Housing (Cover Removed)	3.2-46
3.2-24	9 Pivot Frame Assembly	3.2-48

XLII

~~TOP SECRET~~ GHandle via **BYEMAN**
Control System Only

~~TOP SECRET~~ GBIF-008-W-C-019838-RI-80

LIST OF ILLUSTRATIONS (Continued)

<u>VOLUME 3</u> <u>Figure</u>	<u>Title</u>	<u>Page</u>
3.2-25	5 Pivot Frame Assembly	3.2-49
3.2-26	9 Variable Exposure Mechanism	3.2-52
3.2-27	9 Variable Exposure Mechanism	3.2-54
3.2-28	5 Variable Exposure Mechanism	3.2-55
3.2-29	Variable Exposure Mechanism Drive System Schematic	3.2-58
3.2-30	9 Film Format	3.2-59
3.2-31	5 Film Format	3.2-60
3.2-32	9 and 5 Slit Blade Details	3.2-63
3.2-33	9 and 5 Pivot Frame Assemblies	3.2-66
3.2-34	Focus Adjust Mechanism Gearbox	3.2-68
3.2-35	Focus Adjust Mechanism Gear Train	3.2-69
3.2-36	PPS/DP EAC Film Path Distances	3.2-73
3.2-37	Film Handling Operational Schematic	3.2-76
3.2-38	Film Control Electronics Logic Diagram	3.2-87
3.2-39	Clamp Circuit and Comparator Operation	3.2-92
3.2-40	Film Tension vs Elapsed Time	3.2-94
3.2-41	5 Film Handling Subsystem Logic Diagram	3.2-97
3.2-42	FPLLE Subsystem Block Diagram	3.2-104
3.2-43	FPLLE Block Diagram (Single Channel)	3.2-108
3.2-44	CEA Subsystem Block Diagram	3.2-115
3.2-45	SRC Block Diagram	3.2-117
3.2-46	Primary NPA Block Diagram	3.2-123
3.2-47	Backup NPA Block Diagram	3.2-124
3.2-48	VEM Block Diagram (Channel A)	3.2-128
3.2-49	Data Track and Interframe Marker Block Diagram	3.2-130

XLIII

~~TOP SECRET~~ GHandle via **BYEMAN**
Control System Only

~~TOP SECRET~~ GBIF-008-W-C-019838-RI-80

LIST OF ILLUSTRATIONS (Continued)

VOLUME 3

<u>Figure</u>	<u>Title</u>	<u>Page</u>
3.3-1	Optical Configuration of the R-5 Lens and Stereo Mirror	3.3-3
3.3-2	Stereo Mirror Vignetting	3.3-13
3.3-3	Central and S-1 Sensor Vignetting	3.3-14
3.3-4	Typical Spectral Transmittance, R-5 Optics (Unobstructed)	3.3-16
3.4-1	Stereo Mirror Movements (Conceptual Presentation)	3.4-2
3.4-2	Crab and Stereo Servos	3.4-3
3.4-3	Stereo Servo and Drive	3.4-5
3.4-4	Hypocycloid Drive Assembly	3.4-7
3.4-5	Hypocycloid Drive (Conceptual Representation)	3.4-8
3.4-6	Typical Position - Time Curve for Stereo Mirror with Hypocycloid Drive	3.4-9
3.4-7	Stereo Servo Subsystem Electrical Block Diagram	3.4-10
3.4-8	Stereo and Crab Servo Instrumentation	3.4-14
3.4-9	Stereo Mirror Servos and Instrumentation	3.4-16
3.4-10	Crab Hysteresis Effect	3.4-17
3.4-11	Crab Servo	3.4-19
3.4-12	Crab Servo Subsystem Electrical Block Diagram	3.4-21

XLIV

~~TOP SECRET~~ GHandle via **BYEMAN**
Control System Only

~~TOP SECRET~~ GBIF-008- W-C-019838-RI-80

LIST OF ILLUSTRATIONS (Continued)

<u>VOLUME 4</u>			
<u>Figure</u>	<u>Title</u>		<u>Page</u>
3.5-1	Forward Barrel and Viewport Doors		3.5-2
3.5-2	Hatch Ejection Mechanism		3.5-4
3.5-3	Viewport Door Drive Mechanism and Instrumentation		3.5-5
3.5-4	Spider Linkage (-X View)		3.5-10
3.5-5	Viewport Door Subsystem Electronics		3.5-13
3.5-6	Motor Drive Control		3.5-17
3.5-7	Ratio of Lens Area As A Function of Viewport Door Position		3.5-20
3.5-8	Door Open Primary Mode		3.5-21
3.5-9	Door Close Primary Mode		3.5-22
3.5-10	Door Open Backup Mode		3.5-23
3.5-11	Door Close Backup Mode		3.5-24
3.5-12	Door-Blow Mode		3.5-25
3.6-1	Focus Detection Subsystem Elements		3.6-2
3.6-2	View Into Camera (Baffle Removed)		3.6-3
3.6-3	Focus Detection Subsystem Block Diagram		3.6-4
3.6-4	Focus Sensor Head Assembly		3.6-5
3.6-5	Focus Detection Subsystem Optics Assembly		3.6-7
3.6-6	Beam Splitter and Reticle Assembly		3.6-8
3.6-7	Typical Reticle		3.6-10
3.6-8	Signal Normalizing Module (Unit 15A3)		3.6-11
3.6-9	Instrumentation and Control Module (Unit 15A1)		3.6-13
3.6-10	Dual Photodiode Detector		3.6-14
3.6-11	Optics with Dual Detector and LED Array		3.6-16
3.6-12	Systems Operation Functional Block Diagram		3.6-17
3.6-13	Detector and Current-to-Voltage Converter		3.6-19
3.6-14	Frequency Response for Each Mode		3.6-21
3.6-15	Typical Dual Channel Amplifier		3.6-22

XLV

~~TOP SECRET~~ GHandle via **BYEMAN**
Control System Only

~~TOP SECRET~~ GBIF-008- W-C-019838-RI-80

LIST OF ILLUSTRATIONS (Continued)

VOLUME 4 <u>Figure</u>	<u>Title</u>	<u>Page</u>
3.6-16	Dual Range Amp	3.6-23
3.6-17	Typical Scaling Amplifier and Low Pass Filter	3.6-25
3.6-18	LED Oscillator and Driver	3.6-28
3.6-19	Temperature Sensor Bias Network	3.6-29
3.6-20	Power Decoupling Circuit	3.6-30
3.7-1	PPS/DP EAC Power Distribution Subsystem	3.7-2
3.7-2	SCS Power Distribution System	3.7-4
3.7-3	SCS Solar Array	3.7-6
3.7-4	Voltage/Load Relationship Due to Solar Panel Effect	3.7-7
3.7-5	PM and C Assembly	3.7-13
3.7-6	PPS/DP EAC Power Input and Filtering	3.7-15
3.7-7	9 and 5 Operational Power and Servo Power	3.7-19
3.7-8	Focus Electronics and S1-PRG Power	3.7-20
3.7-9	Focus Detection Subsystem Calibration Power	3.7-21
3.7-10	DTU 1 and 2 POWER; Instrumentation Supply and Pressure Transducer Power	3.7-22
3.7-11	5 Parking Brake Power	3.7-23
3.7-12	Environmental Branches 1, 2, 4, 5, and 6 Power	3.7-24
3.7-13	EPSM 1 and EPSM 2 Power	3.7-25
3.7-14	Standard Soft Switch Circuit	3.7-26
3.7-15	PM and C Unipoint Ground	3.7-30
3.7-16	PPS/DP EAC Instrumentation Unipoint Ground	3.7-31
3.7-17	IEU Cross-Strap Circuit Configuration	3.7-41
3.7-18	IEU Simplified Command Enable Configuration	3.7-42
3.7-19	PPS/DP EAC Pyrotechnic Subsystem Block Diagram	3.7-45
3.7-20	Arm and Safe Plugs	3.7-47
3.7-21	Command Receipt Instrumentation Digital-to-Analog Converters	3.7-50
3.7-22	Pyro Power Voltage Monitor and Instrumentation Power Power Filters	3.7-51

XLVI

~~TOP SECRET~~ GHandle via **BYEMAN**
Control System Only

~~TOP SECRET~~ GBIF-008- W-C-019838-RI-80

LIST OF ILLUSTRATIONS (Continued)

VOLUME 4		
<u>Figure</u>	<u>Title</u>	<u>Page</u>
3.7-23	Arm/Continuity Loops	3.7-53
3.7-24	Multiple Relay Logic Representation	3.7-55
3.7-25	Hatch Eject	3.7-56
3.7-26	Viewport Door Backup and Viewport Door Blow	3.7-57
3.7-27	9 Splice and Cut and 9 Roll-In Terminate	3.7-58
3.7-28	5 Splice and Cut and 5 Roll-In Terminate	3.7-59
3.7-29	Cut and Seal 1	3.7-60
3.7-30	SRV 1 Arm and Transfer	3.7-61
3.7-31	SRV 1 Separate	3.7-63
3.7-32	Spinoff Disconnect 2 and EA Separate	3.7-65
3.7-33	Cut and Seal 2	3.7-66
3.7-34	SRV 2 Arm and Transfer	3.7-67
3.7-35	SRV 2 Separate	3.7-68
3.8-1	Ground Conditioning at Launch Facility	3.8-7
3.8-2	PPS/DP EAC On-Pad Conditioning System	3.8-10
3.8-3	Floor Plan, Gantry Clean Rooms	3.8-11
3.8-4	Recommended Operating Limits for Clean Room	3.8-14
3.8-5	Film Temperature vs Timekeeping Limits	3.8-20
3.8-6	PPS/DP EAC External Thermal Control Finishes	3.8-23
3.8-7	COM Thermal Blanket Assemblies	3.8-33
3.8-8	Ground Heater Tape Locations	3.8-40
3.8-9	Ground Heater Controller Schematic	3.8-41
3.8-10	Flight Heater Branch Block Diagram	3.8-43
3.8-11	Flight Heater Tape Locations	3.8-47
3.8-12	Flight Heater Controller Schematic	3.8-49
3.8-13	COA Heater Controller Temperature Sensor Locations	3.8-50
3.8-14	EA/FA Pin-Puller Locations	3.8-53

XLVII

~~TOP SECRET~~ GHandle via BYEMAN
Control System Only

~~TOP SECRET~~ G

BIF-008- W-C-019838-RI-80

LIST OF ILLUSTRATIONS (Continued)

VOLUME 4

<u>Figure</u>	<u>Title</u>	<u>Page</u>
3.8-15	DRM Skin Temperature Instrumentation Points	3.8-67
3.8-16	Supply Electronics Module Skin Temperature Instrumentation Points	3.8-68
3.8-17	COA Structure Temperature Sensor Locations	3.8-69

XLVIII

~~TOP SECRET~~ G

Handle via **BYEMAN**
Control System Only

~~TOP SECRET~~ G

BIF-008-W-C-019838-RI-80

LIST OF ILLUSTRATIONS (Continued)

<u>VOLUME 5</u> <u>Figure</u>	<u>Title</u>	<u>Page</u>
3.9-1	Command Subsystem Block Diagram	3.9-3
3.9-2	Vehicle Communications Block Diagram	3.9-4
3.9-3	ECS Command Bit Structure	3.9-6
3.9-4	MCS Command Bit Structure	3.9-7
3.9-5	Binary-to-Octal Code Conversion	3.9-7
3.9-6	Variable Word Octal Representation	3.9-8
3.9-7	ECS 14V, 13V and 10V VSPC Octal Codes	3.9-9
3.9-8	RTC Bit Structure	3.9-10
3.9-9	Timing Signals	3.9-15
3.9-10	Timing Signal Circuit A or B Interface	3.9-16
3.9-11	Timing Signal C Circuit Interface	3.9-17
3.9-12	Extended Command Subsystem	3.9-20
3.9-13	Command Processor Assembly	3.9-27
3.9-14	OR Gating Protected Commands with Non-Protected Commands	3.9-29
3.9-15	Command Input Diode OR Gate	3.9-31
3.9-16	Latching Relay Logic Representation	3.9-31
3.9-17	Latching Relay ON/OFF Control Circuit Logic Representation	3.9-32
3.9-18	Basic Optical Isolator and Pulse Circuit	3.9-33
3.9-19	Instrumentation Digital-To-Analog Converter	3.9-34
3.9-20	Fully Redundant Processing and Outputs, Cross-Strapped Inputs	3.9-36
3.9-21	Basic CP A/B Mode Switch Circuit	3.9-37
3.9-22	Basic Servo Mode Switch Circuit	3.9-38
3.9-23	CP A Select/CP B Select	3.9-40
3.9-24	9 and 5 Operational Power ON/OFF	3.9-41

XLIX
~~TOP SECRET~~ GHandle via BYEMAN
Control System Only

~~TOP SECRET~~ G

BIF-008-W-C-019838-RI-80

LIST OF ILLUSTRATIONS (Continued)

VOLUME 5			
<u>Figure</u>		<u>Title</u>	<u>Page</u>
3.9-25		9/5 (Film Drive) ON/OFF	3.9-43
3.9-26		9 and 5 Camera Operations Counter	3.9-46
3.9-27		SRC Command Common Line	3.9-48
3.9-28		FDS and SRC Bits 1 and 2	3.9-49
3.9-29		FDS and SRC Bits 3 and 4	3.9-50
3.9-30		FDS Bits through 10	3.9-51
3.9-31		Film-Drive Speed Range High/Normal	3.9-54
3.9-32		Nominal Platen Adjust Enable/Inhibit and Mode Select	3.9-55
3.9-33		Nominal Platen Adjust Drive Control	3.9-57
3.9-34		SRC, Data Tracks, and I/F Marker Enable/Inhibit/Disable	3.9-60
3.9-35		9 and 5 Slit Drive Enable/Inhibit/Select	3.9-61
3.9-36		9 Slit Bits 1-4	3.9-62
3.9-37		5 Slit Bits 1-4	3.9-63
3.9-38		9/5 Takeup Enable/Inhibit	3.9-65
3.9-39		Heater Branches ON/OFF	3.9-67
3.9-40		5 Parking Brake ON/OFF	3.9-69
3.9-41		Crab Angle	3.9-71
3.9-42		Stereo Angle Store/Execute	3.9-73
3.9-43		Viewport Door Open/Close	3.9-75
3.9-44		DTU 1 and 2 ON/OFF	3.9-76
3.9-45		Focus Electronics Power ON/OFF	3.9-77
3.9-46		Focus Calibrate	3.9-78
3.9-47		S1-PRG Calibrate/Disable	3.9-80
3.9-48		High/Low Altitude Select FPLL Altitude Range and Focus Normal/Modify	3.9-82
3.9-49		High/Low Altitude Select SRC Common and Data Lamp Select	3.9-83
3.9-50		Camera Automatic Off Logic Diagram	3.9-84

L

~~TOP SECRET~~ GHandle via BYEMAN
Control System Only

~~TOP SECRET~~ G81F-008- W-C-019838-RI-80

LIST OF ILLUSTRATIONS (Continued)

VOLUME 5

<u>Figure</u>	<u>Title</u>	<u>Page</u>
3.10-1	PSV Telemetry Subsystem	3.10-2
3.10-2	PPS/DP EAC Instrumentation and Telemetry Subsystem	3.10-3
3.10-3	Instrumentation Processor	3.10-7
3.10-4	Instrumentation Unipoint Ground	3.10-11
3.10-5	Typical Preprocessed Analog Signal IP Circuit	3.10-13
3.10-6	Typical Signal Routine for Non-IP Generated Discrete IMP's	3.10-14
3.10-7	Typical Processing Circuit: IMP's 5013, 5076, 5235, 5236	3.10-18
3.10-8	Typical Processing Circuitry: IMP's 5099, 5110, 5113, 5115, 5120, 5150, 5155	3.10-19
3.10-9	Typical IP Processing Circuits: IMP's 5111, 5112, 5145	3.10-20
3.10-10	IMP 5114 Processing Circuit	3.10-21
3.10-11	IMP 5196 Generating Circuit	3.10-22
3.10-12	Generating Circuits: IMP's 5198 and 5200	3.10-23
3.10-13	IP Processing Circuit: IMP 5375	3.10-24
3.10-14	IP Processing Circuits: IMP's 5574 and 5575	3.10-25
3.10-15	Typical IP Processing Circuit: IMP's 5576 and 5614	3.10-26
3.10-16	Typical IP Processing Circuit: IMP's 5589 and 5590	3.10-27
3.10-17	IP Processing Circuit: BIL 8010	3.10-28
3.10-18	MDTU/DTU Interface	3.10-29
3.10-19	DTU Organization	3.10-31
3.10-20	PPS/DP EAC Slave DTU	3.10-32
3.10-21	Typical AMU and DMU Mechanical Construction	3.10-33
3.10-22	Converter Unit Mechanical Construction	3.10-34
3.10-23	DTU Power Control Logic	3.10-35

LI
~~TOP SECRET~~ GHandle via **BYEMAN**
Control System Only

~~TOP SECRET~~ GBIF-008 - W-C-019838-RI-80

LIST OF ILLUSTRATIONS (Continued)

<u>VOLUME 5</u> <u>Figure</u>	<u>Title</u>	<u>Page</u>
3.10-24	CU Block Diagram	3.10-38
3.10-25	Address Receiver Block Diagram	3.10-42
3.10-26	Timing Generator Circuit	3.10-43
3.10-27	Address Register	3.10-45
3.10-28	Analog-to-Digital Converter-Basic Elements	3.10-49
3.10-29	Analog-to-Digital Converter -Block Diagram, Sample/Encode Algorithm	3.10-50
3.10-30	NRZ Formatter	3.10-53
3.10-31	Reply Modulator	3.10-55
3.10-32	Group-Channel Address Code	3.10-56
3.10-33	AMU Block Diagram	3.10-57
3.10-34	Typical Overvoltage Protection Network	3.10-60
3.10-35	DMU Block Diagram	3.10-63
3.10-36	Simplified Analog Address/Reply Timing	3.10-67
3.10-37	Simplified Discrete Address/Reply Timing	3.10-69
3.10-38	PSV Slave and Master Telemetry Units	3.10-73
3.10-39	Remote Channel Address Signal	3.10-76
3.10-40	Serial Pulse Code Data Signal	3.10-78
3.10-41	Time Relationship: Remote Channel Address Code/Serial Pulse Code Data Reply	3.10-79
3.10-42	Remote Channel Address Generation Rate	3.10-81
3.10-43	Binary Coded Square Wave NRZL Pulse Code Train	3.10-82
3.10-44	Subframe Construction	3.10-87
3.10-45	Format Example: 10 sps and 5 sps Monitors	3.10-91
3.10-46	Format Example: 200 sps Monitor	3.10-92
3.10-47	Record Main-Frame Format: PPS/DP. EAC Allocation	3.10-97

~~TOP SECRET~~ G

~~TOP SECRET~~ G

BIF-008-W-C-019838-RI-80

LIST OF ILLUSTRATIONS (Continued)

VOLUME 5

<u>Figure</u>	<u>Title</u>	<u>Page</u>
3.10-48	Normal (Real Time) Format: PPS/DP EAC Allocation	3.10-98
3.10-49	Diagnostic 1 Main-Frame Format: PPS/DP EAC Allocation	3.10-99
3.10-50	Diagnostic 2 Main-Frame Format: PPS/DP EAC Allocation	3.10-100
3.10-51	Subroutine Construction	3.10-106
3.10-52	DC Offset Error Source	3.10-108
3.10-53	Sampling Transient Error Source	3.10-109
3.11-1	Cutter/Sealer and Splicer Mechanism Location	3.11-4
3.11-2	Cutter/Sealer Assembly (Partially Closed)	3.11-5
3.11-3	Cutter/Sealer Assembly (Open)	3.11-6
3.11-4	Cutter/Sealer Film Path Space Location	3.11-7
3.11-5	Typical Cutter/Sealer Device	3.11-8
3.11-6	Splicer Mechanism	3.11-11
3.11-7	Splicer Mechanism Components	3.11-12
3.11-8	Splicer/Cutter Device	3.11-13
3.11-9	Positive Stop Leader	3.11-15
3.11-10	Sequential Events vs Shuttle Drive Position	3.11-19

LIII
~~TOP SECRET~~ GHandle via BYEMAN
Control System Only

~~TOP SECRET~~ GBIF-008- W-C-019838-RI-80

LIST OF ILLUSTRATIONS (Continued)

VOLUME 5

<u>Figure</u>	<u>Title</u>	<u>Page</u>
3.12-1	DRM Internal Components	3.12-3
3.12-2	Powered Yaw and Pitch Maneuver	3.12-6
3.12-3	Internal Recovery Sequence Maneuvers	3.12-7
3.12-4	SRV Sequences of Events	3.12-14
3.12-5	SRV Assembly - Exploded View	3.12-20
3.12-6	Thrust Cone	3.12-24
3.12-7	SRV Heater Branches	3.12-27
3.12-8	Recoverable Capsule	3.12-28
3.12-9	Capsule Cover	3.12-29
3.12-10	SRV Temperature Sensor Locations	3.12-33
3.13-1	S1 Sensor Assembly	3.13-5
3.13-2	S1 Rod and Truss Assembly	3.13-6
3.13-3	Typical Sensor Assembly	3.13-9
3.13-4	S1-PRG Component Locations	3.13-10
3.13-5	Typical PRG Sensor Mounting	3.13-11
3.13-6	PRG Target	3.13-12
3.13-7	Slide Input-Output Position Relation	3.13-13
3.13-8	S1-PRG Sensor System Block Diagram	3.13-15
4.2-1	Initiator Subsystem (Typical)	4.2-4
4.2-2	Stereo Servo Redundancy	4.2-6
4.2-3	Crab Servo Redundancy	4.2-7
4.2-4	Instrumentation Subsystem	4.2-9
4.2-5	Focus Detection Subsystem	4.2-10
4.2-6	S1-PRG Subsystem	4.2-11
4.2-7	9 Camera Platen Drive Subsystem	4.2-14
4.2-8	NPA Subsystem (9 & 5 Identical)	4.2-16
4.2-9	SRC Subsystem (9 and 5)	4.2-17

LIV

~~TOP SECRET~~ GHandle via **BYEMAN**
Control System Only

~~TOP SECRET~~ GBIF-008- W-C-019838-RI-80

LIST OF ILLUSTRATIONS (Continued)

<u>VOLUME 5</u> <u>Figure</u>	<u>Title</u>	<u>Page</u>
4.2-10	VEM Subsystem (9 & 5 Identical)	4.2-19
4.2-11	9 Film Handling Subsystem	4.2-20
4.2-12	5 Film Handling Subsystem	4.2-22
4.2-13	Primary Mode Viewport Door Operation	4.2-25
4.2-14	Backup Mode Viewport Door Operation	4.2-26
4.3-1	Aerospace Vehicle Buildup	4.3-2
4.3-2	COA Assembly Flow	4.3-4
4.4-3	Polishing Primary Mirror	4.3-5
4.3-4	Assembling Stereo Mirror to COA	4.3-7
4.3-5	Primary Mirror Alignment	4.3-8
4.3-6	Alignment of Stereo Mirror to Optical Axis	4.3-9
4.3-7	Alignment of A&B Reference Mirrors to Optical Axis	4.3-11
4.3-8	Mating COA to Aft Barrel	4.3-14
4.3-9	Interface Alignment Gage	4.3-15
4.3-10	Optical Axis to Vehicle Axis Roll Alignment	4.3-16
4.3-11	Optical Axis to Vehicle Axis Pitch and Yaw Alignment	4.3-18
4.3-12	SEM Assembly Flow	4.3-20
4.3-13	Supply Electronics Module (-Z View)	4.3-22
4.3-14	DRM Assembly Flow	4.3-24
4.3-15	Dual Recovery Module	4.3-25
4.3-16	SEM/COM Assembly	4.3-27
4.3-17	PPS/DP EAC	4.3-28
4.4-1	On-Back Primary and Stereo Mirror Tests	4.4-2
4.4-2	Ross Match and COA Level Optical Test Set-Ups	4.4-4
4.4-3	Condition of COA for Testing	4.4-8
4.4-4	COA on Vibration Fixture	4.4-12
4.4-5	COA Assembly and Test Flow	4.4-14

LV

~~TOP SECRET~~ GHandle via **BYEMAN**
Control System Only

~~TOP SECRET~~ G

BIF-008-W-C-019838-RI-80

LIST OF ILLUSTRATIONS (Continued)

<u>VOLUME 5</u> <u>Figure</u>	<u>Title</u>	<u>Page</u>
4.4-6	CUETS System	4.4-15
4.4-7	Supply Assembly Test Set	4.4-17
4.4-8	COM Assembly and Test Flow	4.4-19
4.4-9	SEM Assembly and Test Flow	4.4-20
4.4-10	Assembly Flow and EA/FA/TSRT Test	4.4-22
4.4-11	Assembly Flow and SRV Test	4.4-24
4.4-12	Assembly Flow and DRM Test	4.4-25
4.4-13	PPS/DP EAC Assembly and Test Flow from Buildup to Shipment	{ 4.4-27 4.4-28 4.4-29
4.4-14	SEM/COM I _{xx} Measurement Equipment	4.4-45
4.4-15	General View of Assembly Area	4.4-46
4.4-16	PPS/DP EAC Assembly and Test Flow for Film Change	4.4-48

LVI

~~TOP SECRET~~ GHandle via **BYEMAN**
Control System Only

~~TOP SECRET~~ GBIF-008- W-C-019838-RI-80

LIST OF ILLUSTRATIONS (Continued)

VOLUME 6

Figure

		<u>Page</u>
4.5-1	PPS/DP EAC in Shipping Container	4.5-3
4.5-2		4.5-5
4.5-3		4.5-7
4.6-1	Gambit Organization at VAFB	4.6-2
4.6-2	Launch Site Software Block Diagram	4.6-7
4.6-3	Gambit Vehicle Launch Site (SLC 4-W)	4.6-10
4.6-4	Gantry Clean Rooms (A and B/C Rooms)	4.6-12
4.6-5	FAS Activity Block Diagram	4.6-15
4.7-1	 Organization	4.7-6
4.7-2	Dynamic Filter Block Diagram	4.7-9
4.7-3	Gambit Operational Software	4.7-16
4.7-4	Event Generator System	4.7-20
4.7-5	Optimization Algorithm	4.7-25
4.7-6	Mode Generation	4.7-43
4.7-7	Telemetry Predict Subsystem	4.7-44
4.7-8	Typical Telemetry Limits	4.7-45
4.7-9	Pass (Real Time) Data Flow	4.7-49
4.7-10	Postpass Data Flow	4.7-51
4.8-1	Factory-Field Liaison Organization for Flight Operations	4.8-2
APPENDIX C		
C-1	MSA Block Diagram	C-5
APPENDIX E		
E-1	Normalized Standard Deviation	E-2
E-2	Graph for Computation of 95%/95% Probability	E-6

25X1

LVII

~~TOP SECRET~~ GHandle via **BYEMAN**
Control System Only

~~TOP SECRET~~ GBIF-008- W-C-019838-RI-80

LIST OF TABLES

<u>VOLUME 1</u> <u>Table</u>	<u>Title</u>	<u>Page</u>
2.2-1	Pointing Error Contributors	2.2-22
2.2-2	Symbols Used in Pointing Error Equations	2.2-24
2.2-3	PPS/DP EAC Pointing Error Contributors	2.2-36
2.2-4	PSV Pointing Error Budget	2.2-37
2.4-1	9-Inch Smear Equations	2.4-18
2.4-2	Symbols Used in Smear Equations	2.4-21
2.4-3	PPS/DP EAC Linear Smear Budget (with Software)	2.4-37
2.4-4	Minimum Acceptable Modulation Transfer Function Resulting from Nonlinear Smear	2.4-39
2.4-5	Smear Contributor Budget (F/O-7)	2.4-40
2.4-6	Satellite Vehicle System, Equivalent Smear Rate ($\mu\text{R}/\text{SEC}$) * Statistical Combination (with Adaptive Bias and Software)	2.4-41
2.4-7	Smear Slit Dimensions	2.4-45
2.4-8	Smear Slit Dimensions - (EAC)	2.4-46
2.5-1	Focus Error Budget	2.5-24
2.6-1	Table of Exposure Modifier, M (Algorithm Table 2)	2.6-9
2.6-2	Table of Snow Biases to Exposure Time (Algorithm Table 3)	2.6-10
2.7-1	Thermal Properties of Film	2.7-15
2.7-2	Weight and Moisture Content, Gambit Films	2.7-19
2.7-3	Threshold Modulation Curves	2.7-32
2.7-4	Film Characteristics	2.7-33
2.8-1	Orbital Parameters	2.8-2
2.8-2	Acquisition Limits	2.8-7
2.8-3	Constraints on Target Selection	2.8-8
2.8-4	Cloud Conditions for the Months of Simulation	2.8-9
2.8-5	Weather Thresholds for Acquisitions	2.8-10
2.8-6	Weather Threshold Averages	2.8-11

*Scale table values by $\frac{90}{h}$ for other altitudes.

LVIII

~~TOP SECRET~~ GHandle via **BYEMAN**
Control System Only

~~TOP SECRET~~ GBIF-008- W-C-019838-RI-80

LIST OF TABLES (Continued)

<u>VOLUME 1</u> <u>Table</u>	<u>Title</u>	<u>Page</u>
2.8-7	Photographic Performance Model	2.8-13
2.8-8	Mission Simulation Smear Contributor Matrix	2.8-15
2.8-9	9 Plus 5 Combined Geometric Mean Ground Resolution (from Mission Simulations)	2.8-20
2.8-10	Resolution Contributors	2.8-21
2.8-11	Number of Targets with a 95% Probability of at Least One Clear Acquisition	2.8-24
2.8-12	Equipment Usage Summary	2.8-25
2.8-13	Orbital Parameters	2.8-26
2.10-1	Launch, Orbit, and Recovery Information	2.10-2
2.10-2	Time Dependent Events	2.10-8

LIX

~~TOP SECRET~~ GHandle via **BYEMAN**
Control System Only

~~TOP SECRET~~ GBIF-008- W-C-019838-RI-80

LIST OF TABLES (Continued)

VOLUME 2 <u>Table</u>	<u>Title</u>	<u>Page</u>
2.11-1	Cloud Cover Multiplier	2.11-7
2.11-2	Total Integrated Irradiance and Approximate Illumination	2.11-16
2.12-1	Ross Lens Surface Contributions to Wavefront Error	2.12-21
2.12-2	Summary of Tolerances and Distributions	2.12-24
2.12-3	Lens Inhomogeneity OQF Contribution	2.12-25
2.12-4	OQF Summary	2.12-27
2.13-1	Venting Model Parameters	2.13-4
2.13-2	Maximum Differential Pressures	2.13-6
2.14-1	COM Curvature Equations	2.14-41
2.15-1	Center of Gravity Offsets (\bar{Z})	2.15-8
2.15-2	Mass Properties (1/78 Estimate)	2.15-9
2.15-3	Distribution Parameters	2.15-10
2.15-4	Estimated Range of Miss-Distances	2.15-14
2.15-5	Analysis Result for Mass Properties	2.15-17
3.1-1	DRM Access Panels	3.1-15
3.1-2	COM Access Panels	3.1-47

LX

~~TOP SECRET~~ GHandle via **BYEMAN**
Control System Only

~~TOP SECRET~~ G

BIF-008-W-C-019838-RI-80

LIST OF TABLES (Continued)

<u>VOLUME 3</u> <u>Table</u>	<u>Title</u>	<u>Page</u>
3.2-1	Tension Arm Instrumentation Data	3.2-25
3.2-2	9 and 5 Take-up Spools Data Summary	3.2-32
3.2-3	Operational Slit Widths	3.2-56
3.2-4	Film Path Lengths	3.2-75
3.2-5	Film Handling Subsystem Instrumentation: 9 and 5	3.2-134
3.2-6	9x5 Dual Platen Camera Instrumentation	3.2-146
3.3-1	R-5 Optical Formula	3.3-6
3.3-2	R-5 Refractive Indices	3.3-7
3.3-3	Optical System Physical Characteristics Summary	3.3-8
3.3-4	Optical Properties Summary	3.3-9
3.3-5	Percent Obstruction (Vignetting)	3.3-15
3.3-6	Optical Subsystem Instrumentation	3.3-17
3.4-1	Stereo Position vs Executed Command Bit State	3.4-12
3.4-2	Crab Position vs Command Bit State	3.4-24
3.4-3	Mirror Positioning Instrumentation Summary	3.4-27

LXI
~~TOP SECRET~~ GHandle via BYEMAN
Control System Only

~~TOP SECRET~~ GBIF-008- W-C-019838-RI-80

LIST OF TABLES (Continued)

VOLUME 4 <u>Table</u>	<u>Title</u>	<u>Page</u>
3.5-1	Viewport Door Subsystem Instrumentation Summary	3.5-26
3.6-1	Focus Detection Subsystem 4V WORD Command	3.6-31
3.6-2	Focus Detection Subsystem Instrumentation	3.6-32
3.7-1	PPS/DP EAC Power Consumption	3.7-9
3.7-2	PM and C Power Distribution	3.7-16
3.7-3	Pyro-Actuated Events	3.7-38
3.7-4	Main Power Subsystem Instrumentation	3.7-73
3.7-5	Pyro Power Subsystem Instrumentation	3.7-80
3.7-6	Command Logic Summary	3.7-85
3.8-1	Clean Area and Clean Room Characteristic and Usage	3.8-4
3.8-2	Characteristics of External Thermal Control Finishes	3.8-25
3.8-3	Ground Heater System	3.8-38
3.8-4	Heater Controller Set Points	3.8-44
3.8-5	Flight Heater Tape Locations	3.8-45
3.8-6	Environmental Subsystem Instrumentation Summary	3.8-55
3.8-7	Umbilical Instrumentation Summary	3.8-70

LXII

~~TOP SECRET~~ GHandle via **BYEMAN**
Control System Only

~~TOP SECRET~~ GBIF-008-W-C-019838-RI-80

LIST OF TABLES (Continued)

<u>VOLUME 5</u> <u>Table</u>	<u>Title</u>	<u>Page</u>
3.9-1	ECS SPC Decoder Selection	3.9-10
3.9-2	Possible Simultaneous Decoder Executions in the ECS	3.9-13
3.9-3	Instrumentation Voltage Levels	3.9-35
3.9-4	Command Processor Instrumentation	3.9-86
3.10-1	IP Board and Module Assemblies	3.10-8
3.10-2	IP Processed or Generated Instrumentation and Umbilical Points	3.10-15
3.10-3	D-Type Flip-Flop Logic Table	3.10-47
3.10-4	AMU Address Recognition	3.10-59
3.10-5	DMU Address Recognition	3.10-65
3.10-6	-7 (PPS/DP EAC) Slave DTU Slice Codes	3.10-72
3.10-7	Octal Count, Decimal Count, TM Volts, and Percent Bandwidth Conversion	3.10-84
3.10-8	Overall MDTU Telemeter, Data Capabilities	3.10-89
3.10-9	Format and Mode Capability	3.10-102
3.10-10	Instrumentation and Telemetry Subsystem Instrumentation Summary	3.10-114
3.11-1	Functions Performed by Cutter/Sealer and Splicer Mechanisms	3.11-3
3.11-2	Instrumentation Summary	3.11-20
3.12-1A	Primary Mode Recovery Sequence	3.12-15
3.12-1B	Backup Mode Recovery Sequence	3.12-18
3.12-2	SRV Instrumentation	3.12-34
3.12-3	SRV Related PPS/DP EAC Instrumentation	3.12-36
3.13-1	S1-PRG Experimental System Instrumentation Summary	3.13-22
4.2-1	Reliability Qualification Tests	4.2-30
4.4-1	PPS/DP EAC Test and Assembly Flow Description	4.4-30
4.4-2	PPS/DP EAC Assembly and Test Flow for Film Change Description	4.4-49

LXIII

~~TOP SECRET~~ GHandle via **BYEMAN**
Control System Only

~~TOP SECRET~~ GBIF-008- W-C-019838-RI-80

LIST OF TABLES (Continued)

VOLUME 6 <u>Table</u>	<u>Title</u>	<u>Page</u>
4.6-1	Allowable Blanket Off Times	4.6-18
4.7-1	Event 406 Setup/Shutdown, Setup Portion	4.7-28
4.7-2	Event 406 Setup/Shutdown, Shutdown Portion	4.7-29
4.7-3	Event 400, Basic Camera Event	4.7-31
4.7-4	Modes Matrix	4.7-52
C-1	Key to Input/Output Parameters for MSA Block Diagram	C-6
G-1	PPS/DP EAC Instrumentation Listing	G-1
K-1	PPS/DP EAC Pyrotechnic Device Parts and Mechanical Data	K-3
K-2	PPS/DP EAC Pyrotechnic Device Electrical Data and Notes	K-18

LXIV

~~TOP SECRET~~ GHandle via **BYEMAN**
Control System Only

~~TOP SECRET~~ G

BIF-008- W-C-019838-RI-80

This page intentionally blank

LXV
~~TOP SECRET~~ G

Handle via BYEMAN
Control System Only

~~TOP SECRET~~ G

BIF-008-W-C-019838-RH-80

PART 1 SYSTEM OVERVIEW

1.0 THE GAMBIT RECONNAISSANCE SYSTEM

The Photographic System Reference Handbook (PSRH) has been produced by BIF-008 in accordance with Contract (Revision I dated 1 January 1979) between BIF-008 and the United States Air Force. This document is classified BYEMAN TOP SECRET and must be distributed and handled under the BYEMAN System only.

25X1

The handbook is designed to be a comprehensive reference source describing efforts by BIF-008 in support of the Gambit Reconnaissance System having Extended Altitude Capabilities (EAC). The usefulness of this handbook will be maintained by publishing updates at appropriate times.

This document replaces the earlier (1976) version of the Photographic System Reference Handbook and contains material applicable to an extended altitude mission, or to a vehicle configured for an extended altitude mission.

In order to place the activities undertaken by BIF-008 in perspective, a brief description of the Gambit Reconnaissance System as a whole is included below.

1.1 System Definition

The Gambit system is a satellite-borne, photographic reconnaissance system.

1.2 Mission Definition

The objective of a Gambit reconnaissance mission with Extended Altitude Capability (EAC) is to obtain high resolution photographs of targets selected by members of the United State intelligence community and other interested parties. In addi-

1.1-1

~~TOP SECRET~~ G

Handle via BYEMAN
Control System Only

~~TOP SECRET~~ GBIF-008- W-C-019838-RH-80

tion, the Extended Altitude Capability (EAC) allows operation at altitudes at which the larger swath provides coverage and scale commensurate with Search-mode requirements.

1.2.1 Mission Requirements

Gambit mission requirements stem from two sometimes opposing considerations: The perceived needs of the user community and the state-of-the-art technical limitations of real-world hardware. The primary Gambit mission requirement may be related to resolution (Reconnaissance-type mission) or area coverage (Search-type mission).

1.2.1.1 Image Quality. The amount of information which can be extracted from satellite photography is strongly dependent on the quality and type of acquired imagery. The user community, therefore, plays a major role in establishing basic system performance requirements in terms of the resolution necessary to obtain the desired information. The resolution requirements appropriate for a Reconnaissance Mission will differ greatly from those applicable to a Search Mission.

1.2.1.2 Multiple Film Types. Color film provides a definite spectral information gain over black-and-white film even though the image quality may not be as good. Similarly, infrared (false color) film has the unique ability to record an image which is interpretable in terms of the health of agricultural crops and the presence of camouflage materials. These considerations, among others, result in the requirement that multiple film types be useable for a Gambit mission.

1.2.1.3 Stereo Acquisition. The technical intelligence content of photography is enhanced through the use of stereoscopic pictures; i.e., pictures taken of the same target from two different angles. The capability to provide stereoscopic

1.1-2

~~TOP SECRET~~ GHandle via **BYEMAN**
Control System Only

~~TOP SECRET~~ GBIF-008- W-C-019838-RH-80

photography is a requirement for the Gambit system. A mirror, used to direct the ground scene to the primary mirror, may be set to any of three discrete positions with respect to the local vertical thereby providing appropriate stereo convergence angles.

1.2.1.4 Ground Coverage. When the Gambit vehicle is being operated in the Search mode, the community interest lies in obtaining lower resolution photography over a larger ground area. The accessible area will depend on the altitude chosen and the distribution of obliquities selected by operational software.

1.2.2 Mission Orbits

Gambit missions will have orbit parameters within the following envelope:

- (1) Launch Site: Vandenberg Air Force Base, California
(Air Force Western Test Range)
- (2) Inclination: Between 82° and 120°
- (3) Altitude: Between 68 nmi and 470 nmi

1.2.3 Mission Duration

Gambit missions may be planned for up to 120-days duration. In certain cases, contractually required orbital lifetime may be less than the planned mission duration. The duration of a given mission will be a complex function of hardware performance, consumables management, and the degree to which mission objectives have been met.

1.3 System Description

Hardware produced by various associate contractors is joined together and necessary software and supporting activities are coordinated under the overall

1.1-3

~~TOP SECRET~~ GHandle via BYEMAN
Control System Only

~~TOP SECRET~~ GBIF-008- W-C-019838-RH-80

direction of the Secretary of the Air Force for Special Projects (SAFSP).

1.3.1 Hardware

The aerospace vehicle consists of the boost vehicle and the photographic satellite vehicle (PSV). The aerospace vehicle is illustrated in Figure 1.1-1.

The photographic satellite vehicle is made up of the photographic payload section/dual platen Extended Altitude Capability (PPS/DP EAC) and the satellite control section (SCS). The PPS/DP EAC provides precision optics, a means of transporting and exposing a wide range of photographic materials, and provisions for ejecting two satellite re-entry vehicles (SRVs) in which the exposed film is spooled for return to earth. The SCS provides a stable platform, accomplishes the roll maneuvers of the PPS/DP EAC necessary for target acquisition, and includes a propulsion system for orbit maintenance and required orbit altitude changes. Power is supplied by the SCS through use of internal batteries and solar panels. Commands and telemetry are routed through subsystems within the SCS for both the PPS/DP EAC and SCS.

1.3.2 Software

Complex computer software is employed in many areas of the Gambit Reconnaissance System. Target requirements from the user community are correlated and examined by computer routines which generate target listings for a given mission. Operational software utilizes ephemeris data, weather data, and PSV status information to assemble a time-ordered list of targets which will achieve maximum satisfaction of the specified photographic requirements. Computers at the

assemble the rev-by-rev commands which direct PSV photographic activity, provide environmental control, and institute orbit-adjust maneuvers. These commands

1.1-4

~~TOP SECRET~~ GHandle via **BYEMAN**
Control System Only

~~TOP SECRET~~ G

BIF-008- W-C-019838-RH-80

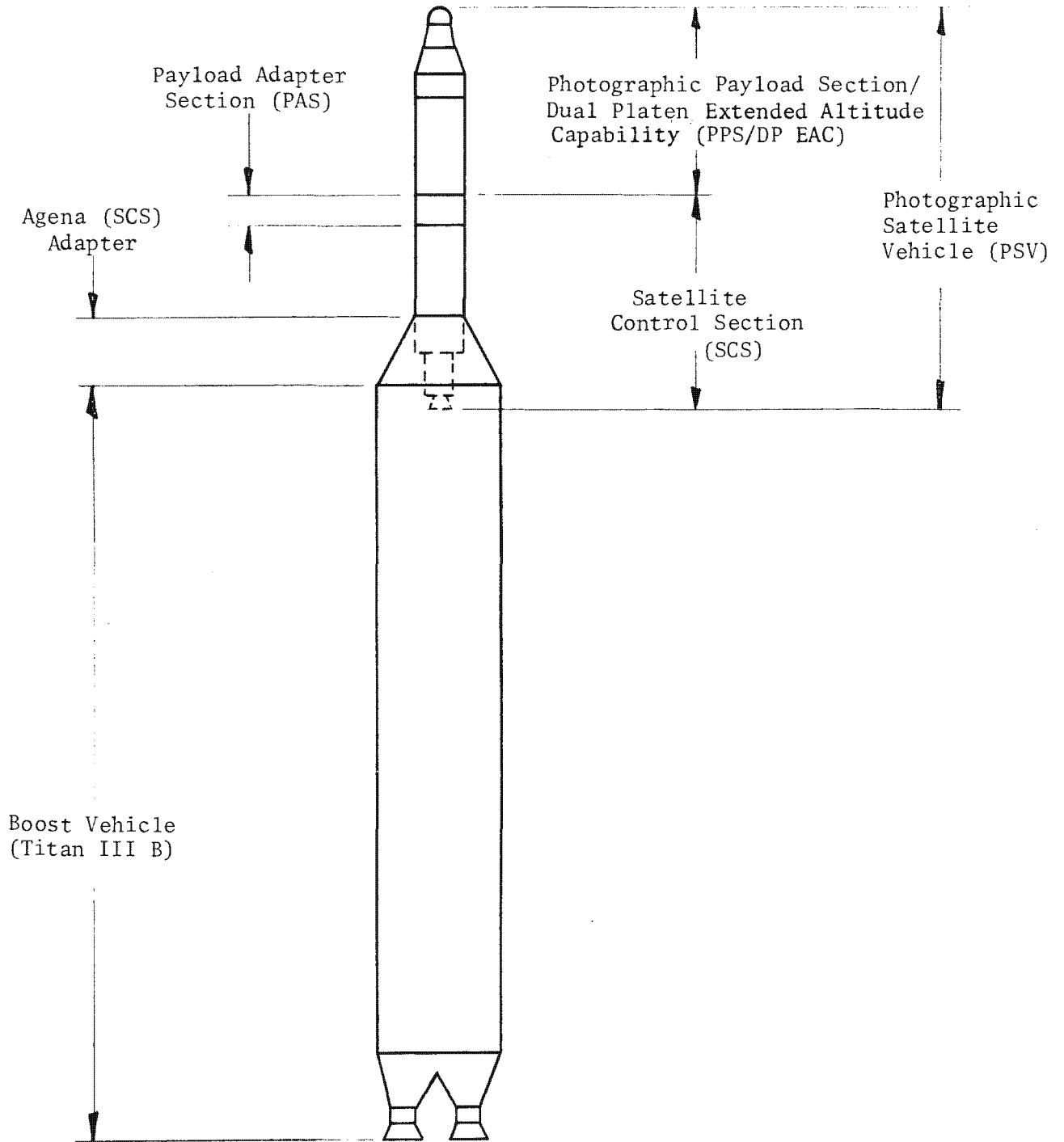


Figure 1.1-1. Gambit Aerospace Vehicle

1.1-5

~~TOP SECRET~~ G

Handle via BYEMAN
Control System Only

~~TOP SECRET~~ GBIF-008- W-C-019838-RH-80

are transmitted to the PSV by one of the remote tracking stations (RTS), and stored in the on-board command system memories for execution at the appropriate, predetermined time.

software also provides bookkeeping data and statistics to assist in mission planning and expendables management. Operational activities supported computers include prediction and reduction of telemetry data and estimates of probable success (i.e., meeting of requirements) for each photograph.

25X1

The targetting philosophy, as well as the orbital altitude, is different in a Search Mission from that in a Surveillance Mission. This results in major differences in many of the operational software routines and operational ground rules.

1.3.3 Support Activities

Activities in support of the Gambit Reconnaissance System are undertaken by all system contractors and various divisions of the United States Air Force. These activities include technical support at the launch site and at the STC, maintenance of remote tracking stations and the associated communications network, global weather monitoring and prediction, recovery support, and processing of the returned film.

1.4 Mission Description

The interaction of the various hardware and software subsystems during the operation of the PSV is shown in block form in Figure 1.1-2.

1.1-6

~~TOP SECRET~~ GHandle via **BYEMAN**
Control System Only

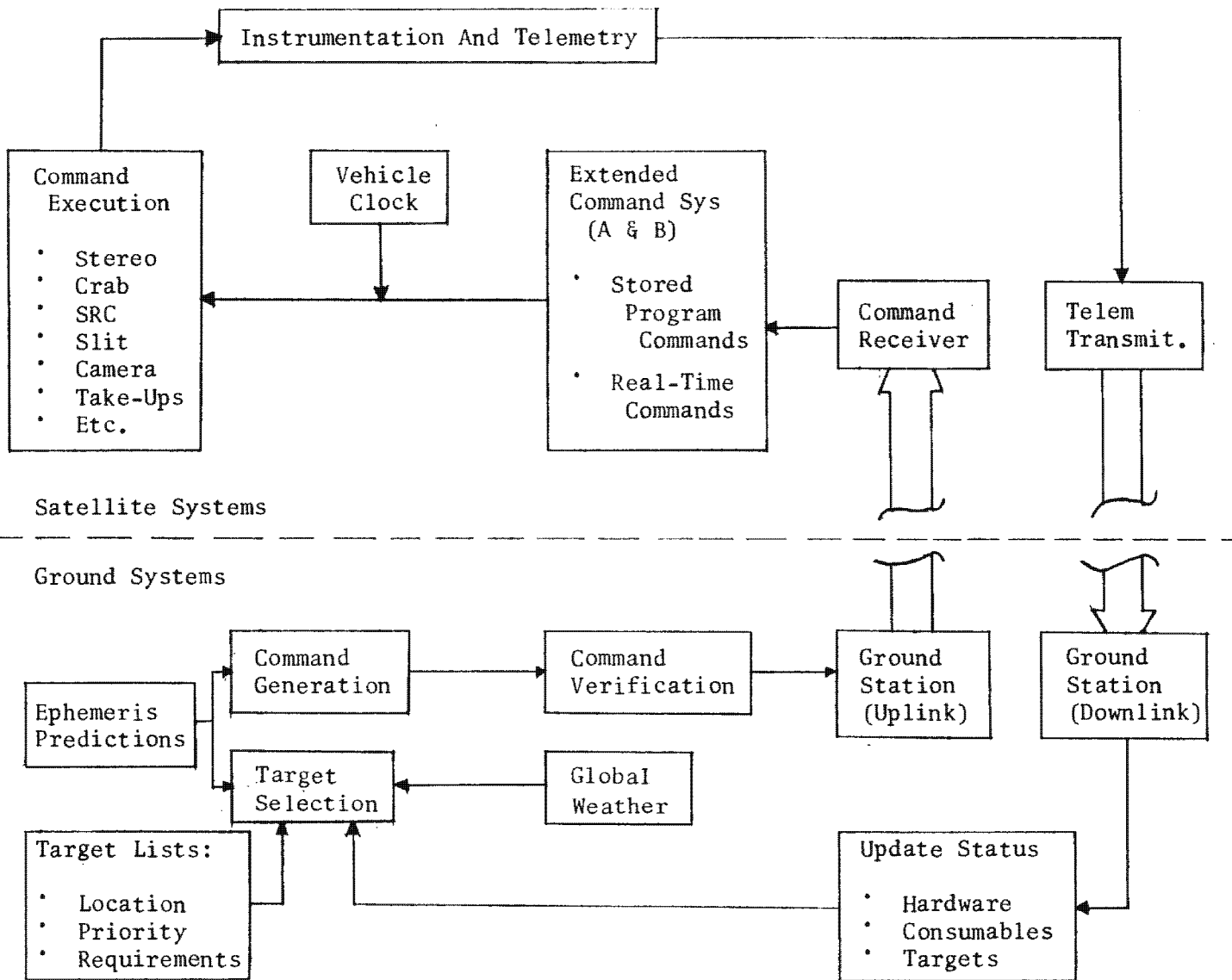


Figure 1.1-2. Gambit Reconnaissance System Operational Block Diagram

Handle via BYEMAN Control System Only

Approved for Release: 2017/02/14 C05097211

Approved for Release: 2017/02/14 C05097211

~~TOP SECRET~~ G

BIF-008-W-C-019838-RI-80

This Page Intentionally Blank

1.1-8

~~TOP SECRET~~ G

Handle via BYEMAN
Control System Only

~~TOP SECRET~~ G

BIF-008-W-C-019838-RH-80

2.0 THE BIF-008 SUBSYSTEM

As one of the associate contractors for the Gambit Reconnaissance System, BIF-008 has undertaken design, manufacturing, test and administrative tasks in response to the terms of Contract (Revision I dated 1 January 1979). This section of the Photographic System Reference Handbook (PSRH) provides an overview of these tasks in the context of the Gambit system and sets the stage for the detailed design and analytical descriptions contained in subsequent sections.

25X1

2.1 Mission

The mission of the photographic payload section dual platen Extended Altitude Capability (PPS/DP EAC) is to provide a high-quality aerial image of a distant earth-scene, record this image on 9.5-inch and/or 5-inch wide photographic film, and store the exposed film for controlled re-entry into the earth's atmosphere.

2.1.1 General Mission Description

The photographic satellite vehicle (PSV) is launched from Space-Launch Complex 4-West (SLC4-W) at Vandenberg Air Force Base by a Titan III B booster. At a specified point in the ascent trajectory, the main hatch of the PPS/DP EAC is ejected, thus exposing the viewport doors. After injection into a stable orbit having parameters commensurate with lifetime requirements, the PSV is ready to either begin photographic operations or be boosted to the high orbit associated with Search-type missions.

A break strip between the satellite control section (SCS) and the PPS/DP EAC is actuated so that the PPS/DP EAC may be rotated about the vehicle X-axis for

1.2-1

~~TOP SECRET~~ GHandle via BYEMAN
Control System Only

~~TOP SECRET~~ GBIF-008- W-C-019838-RH-80

pointing purposes while the SCS is maintained in a stable attitude with the Z-axis parallel to local vertical, the Y-axis perpendicular to local vertical, and the X-axis in the plane of the orbit. Refer to Figure 1.2-1 for an illustration of the PSV. Note that different coordinate systems are used in the PPS/DP EAC and SCS.

The momentum induced by a PPS/DP EAC roll is counteracted by the payload adapter section (PAS) portion of the SCS. A flywheel having a calibrated moment of inertia is driven in a direction opposite to that of the PPS/DP EAC roll to provide momentum compensation. Since the magnitude of the momentum impulse initiating a PPS/DP EAC roll equals the oppositely directed impulse when the PPS/DP EAC is stopped at the desired roll angle, a software technique known as Adaptive Bias may be used by Lockheed Missile and Space Company (LMSC) to decouple these impulses from the attitude control system, thereby reducing the expenditure of attitude control gas.

2.1.2 Photographic Modes of Operation

Photography may be accomplished in any of the following modes.

2.1.2.1 Strip. Strip photography is a continuous recording of the ground scene swept by the projection of the camera slit on the ground.

2.1.2.2 Stereo Pair (Full or Half). A stereo pair consists of two photographs of the same ground scene, separated by a 17.3-degree (or 8.65-degree for half) stereo convergence angle. This is accomplished by rotating the stereo mirror about an axis parallel to the vehicle Y-axis (for zero crab) between the two photographs. (See Figures 1.2-2 and 1.2-3.)

2.1.2.3 Stereo Triplet. A stereo triplet consists of three photographs of the same point separated by 8.65-degree stereo convergence angles. The stereo mirror

1.2-2

~~TOP SECRET~~ GHandle via BYEMAN
Control System Only

1.2-3

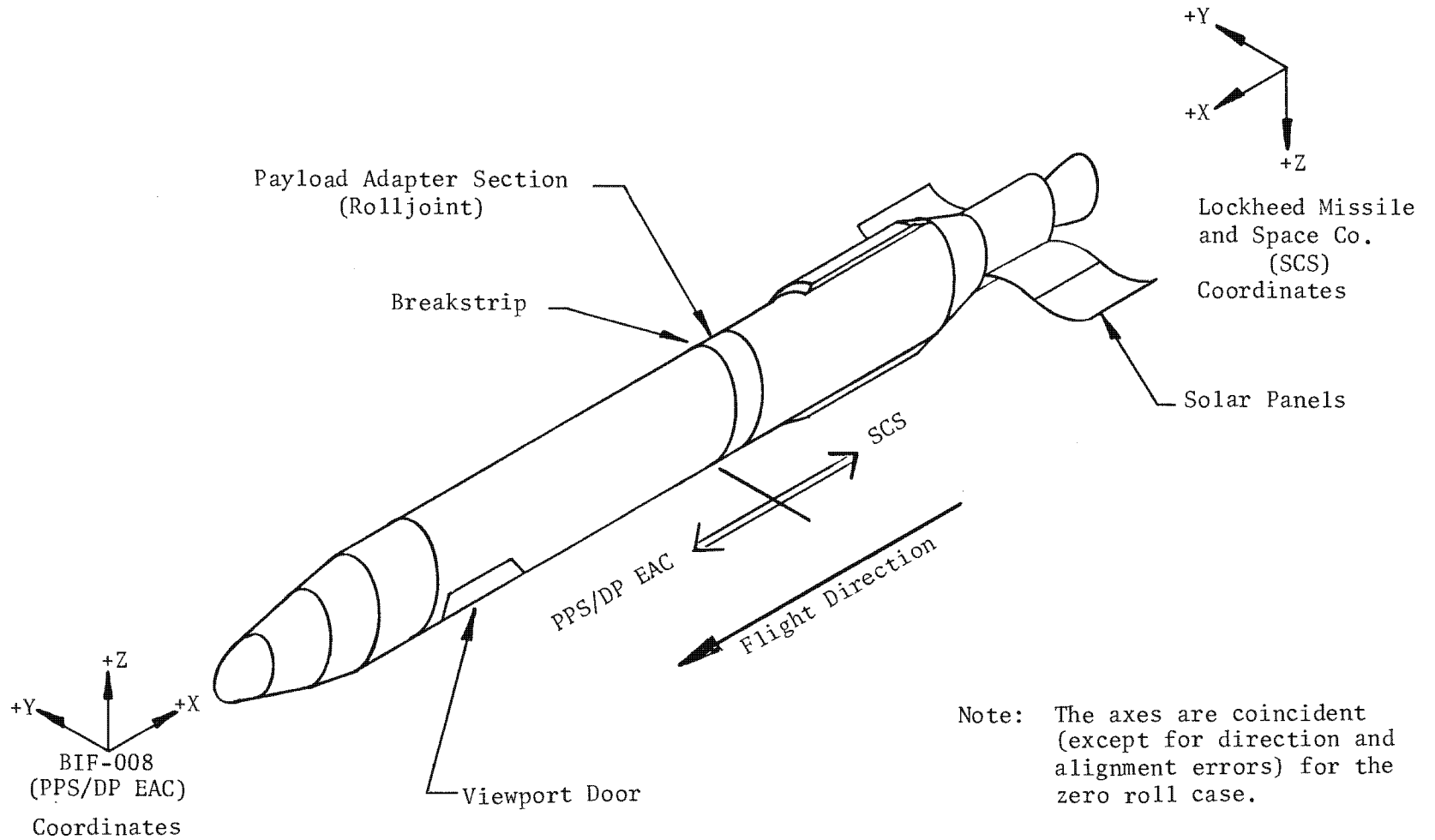
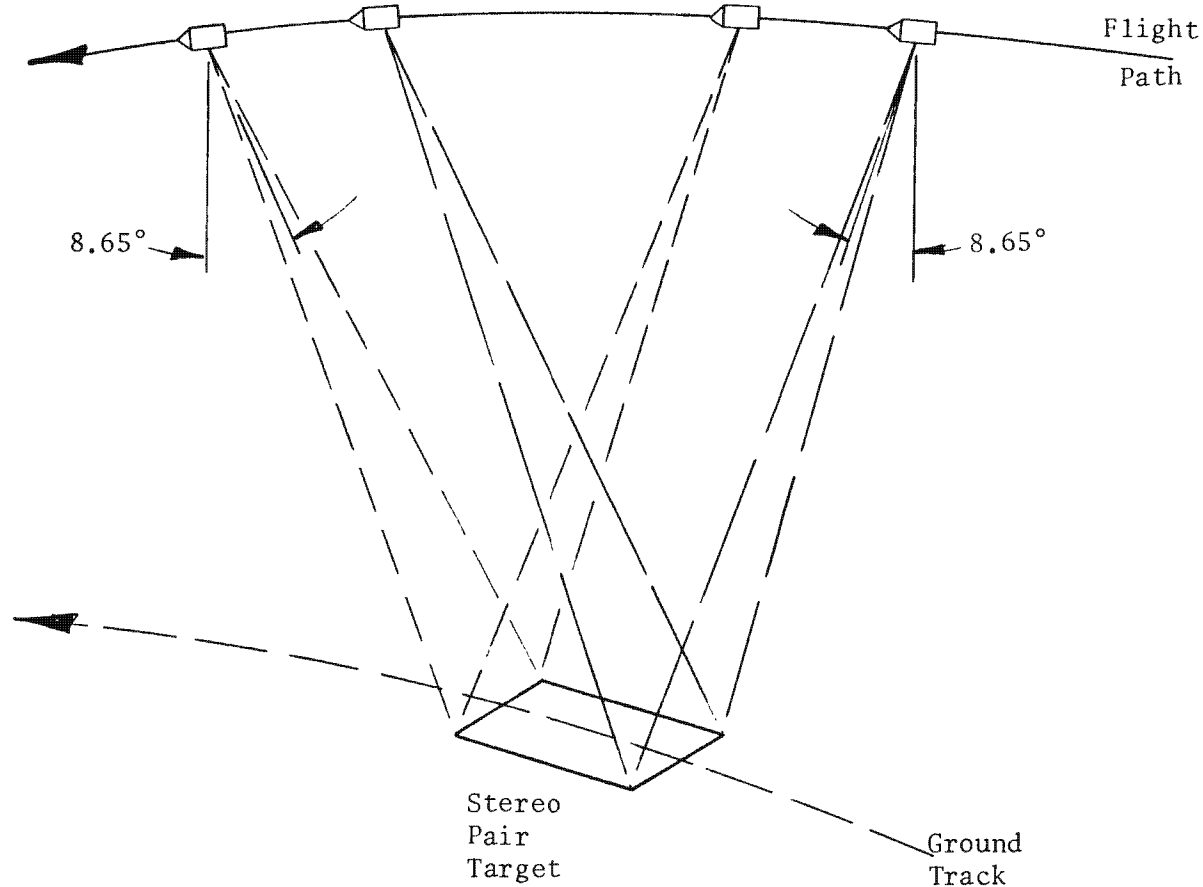


Figure 1.2-1. The Photographic Satellite Vehicle

Handle via **BYEMAN**
Control System Only

~~TOP SECRET~~ G

BI F-008- W-C-019838-RH-80



1.2-4

Figure 1.2-2. Stereo Pair Geometry

Handle via BYEMAN
Control System Only

~~TOP SECRET~~

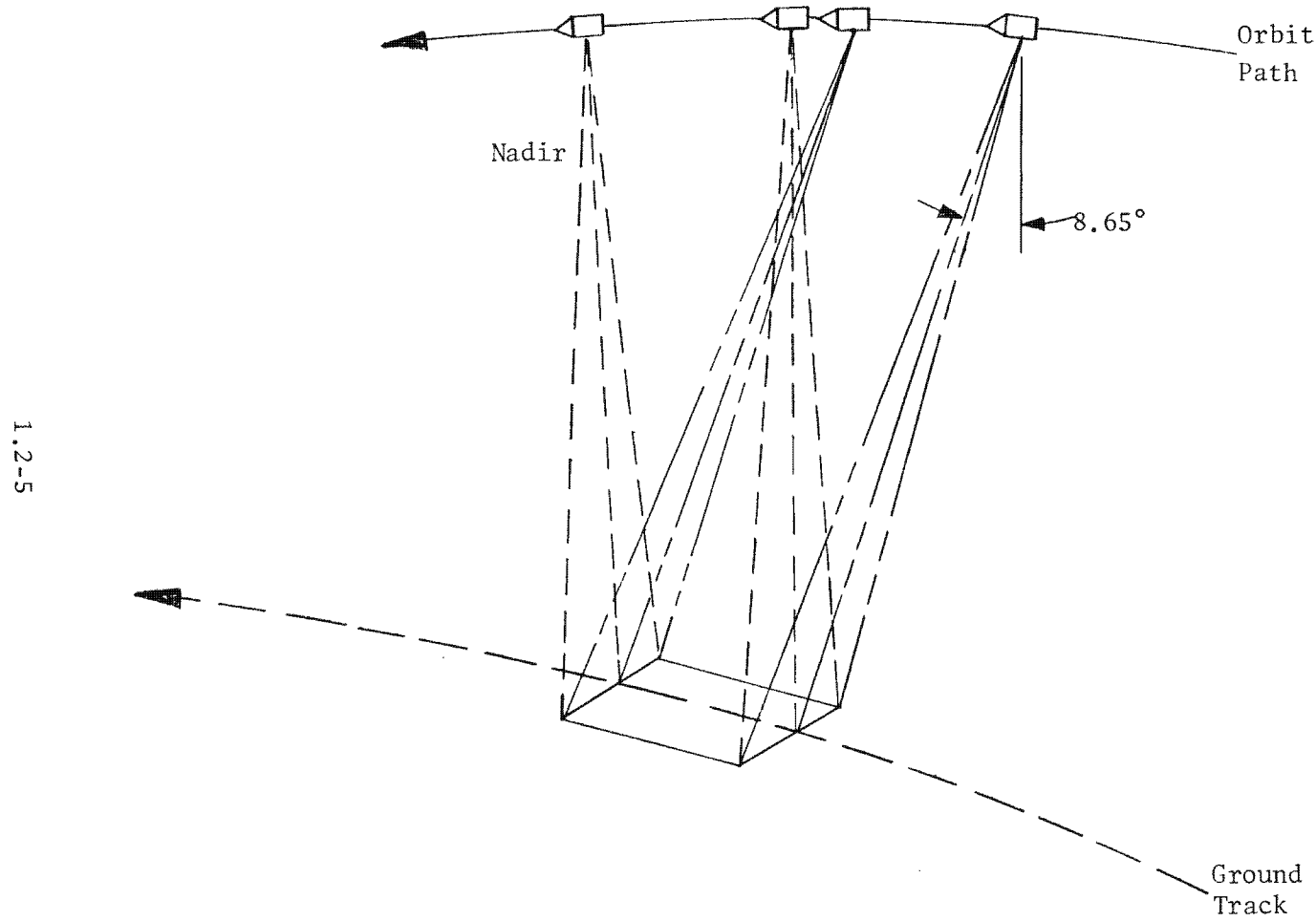


Figure 1.2-3. Half-Stereo Pair Geometry

Handle via **BYEMAN**
Control System Only

~~TOP SECRET~~ GBIF-008- W-C-019838-RH-80

is rotated about an axis parallel to the vehicle Y-axis (for zero crab) between each photograph. (See Figure 1.2-4.)

2.1.2.4 Lateral Pair. A lateral pair consists of two photographs displaced from one another in the cross-track (perpendicular to vehicle-ground-track motion) direction. A roll maneuver is employed concurrently with the movement of the stereo mirror described in Section 2.1.2.2. (See Figure 1.2-5.)

2.1.2.5 Lateral Triplet. A lateral triplet is similar to the stereo triplet described in Section 2.1.2.3 but with a roll maneuver between segments. Generally the segments of a lateral triplet will be displaced in the in-track direction also.

2.1.2.6 Monoscopic (Short-Strip). A frame taken in the strip mode may be accomplished at any of the three available stereo positions ($+8.65^\circ$, 0° or nadir, -8.65°). Those frames whose length is equivalent to one-half of a stereo pair may be termed "monoscopic" to differentiate from the longer "strip" frames.

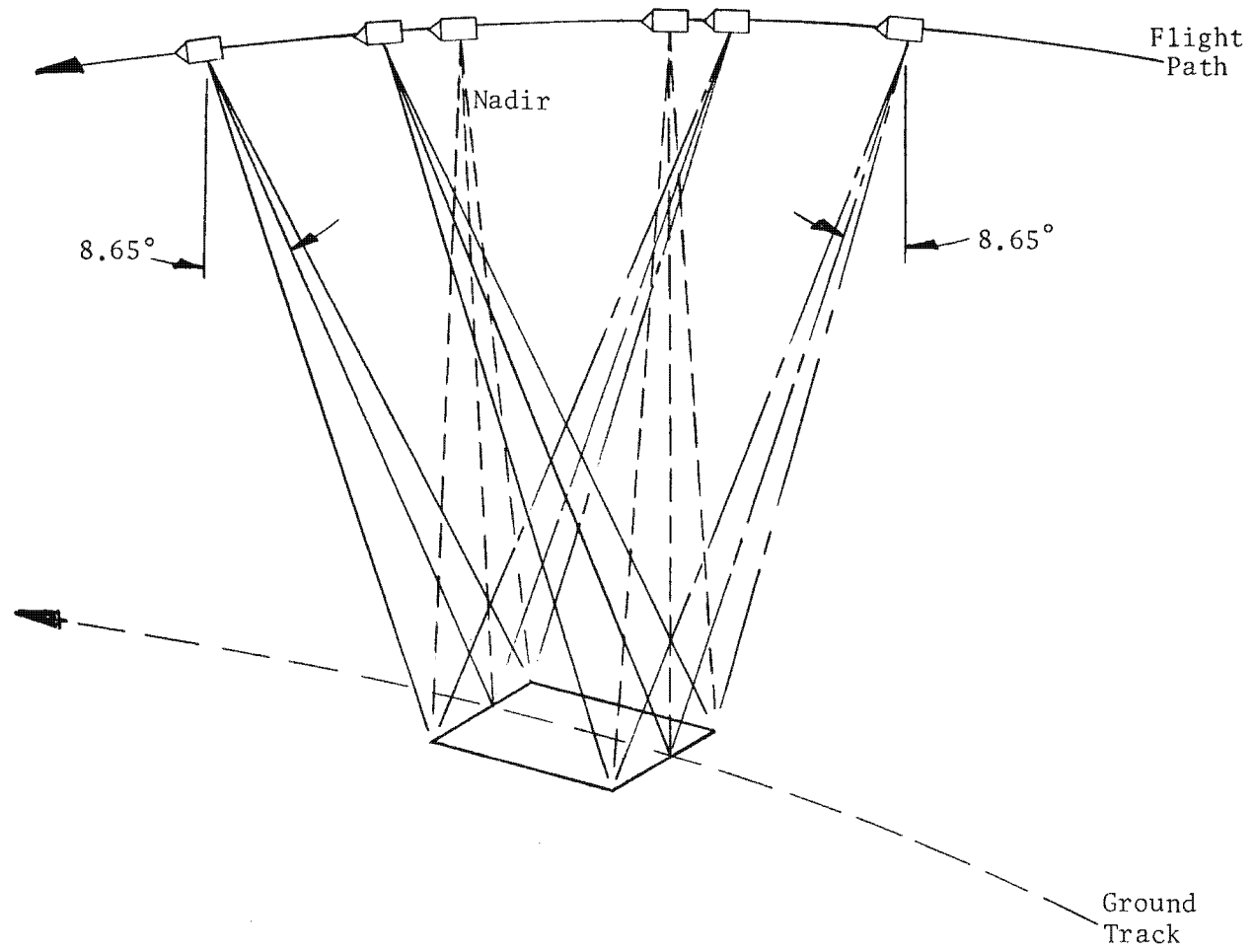
2.1.3 Image Motion Compensation

Relative motion between the ground scene and the orbiting vehicle gives rise to a corresponding motion of the image. This image motion has both magnitude and direction and is, therefore, a vector quantity. The process of aligning this vector with the film velocity vector, in both magnitude and direction, is called image motion compensation (IMC).

The apparent object (ground scene) velocity consists of two components: that resulting from the projection of the vehicle orbital motion on the ground, and that resulting from rotation of the earth. (See Figure 1.2-6.) The observed image motion arises from the resultant of these two components.

1.2-6

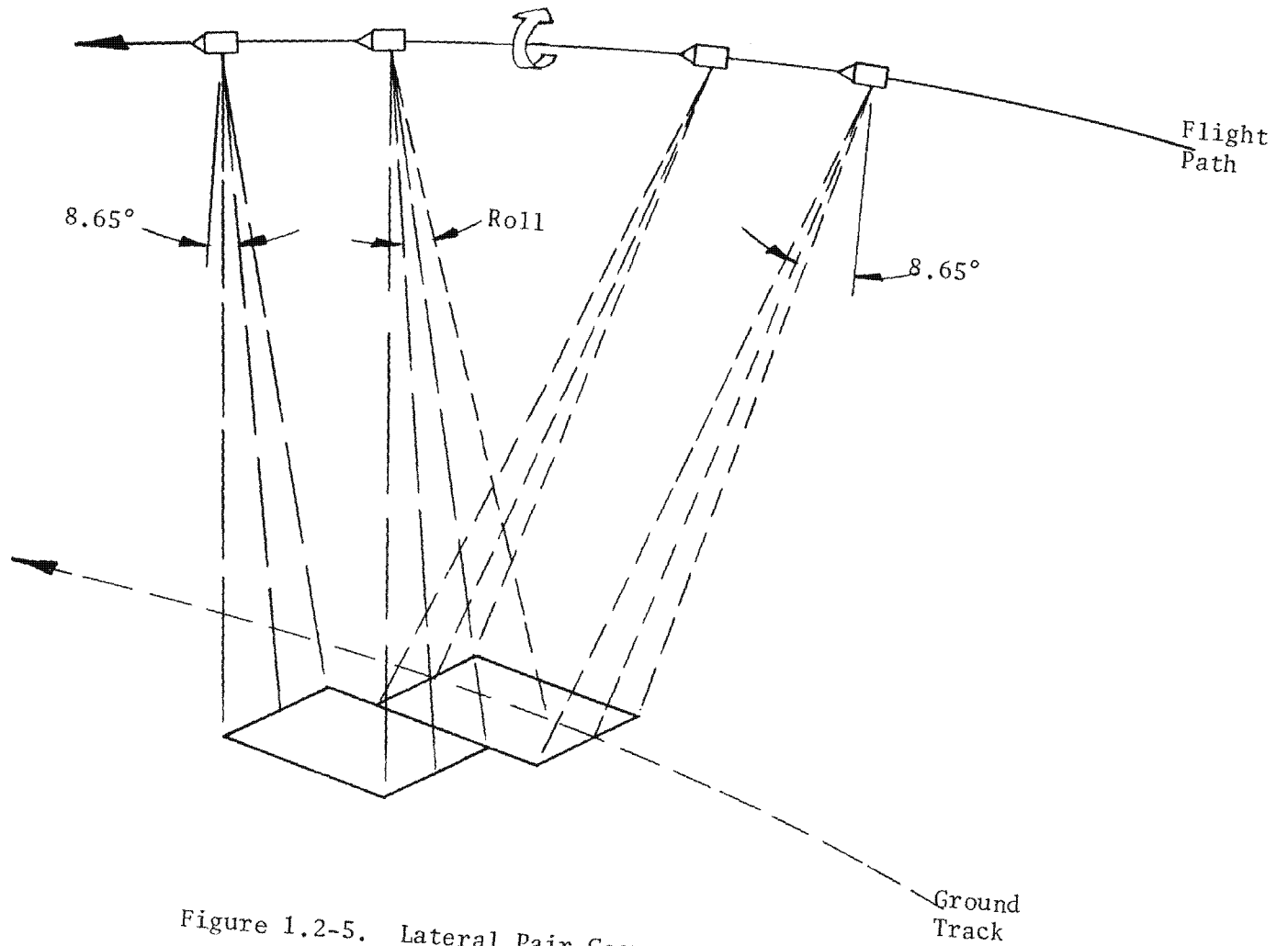
~~TOP SECRET~~ GHandle via BYEMAN
Control System Only



1.2-7

Figure 1.2-4. Stereo Triplet Geometry

Handle via **BYEMAN**
Control System Only



1.2-8

Figure 1.2-5. Lateral Pair Geometry

Handle via **BYEMAN**
Control System Only

~~TOP SECRET~~ G

BIF-008- W-C-019838-RH-80

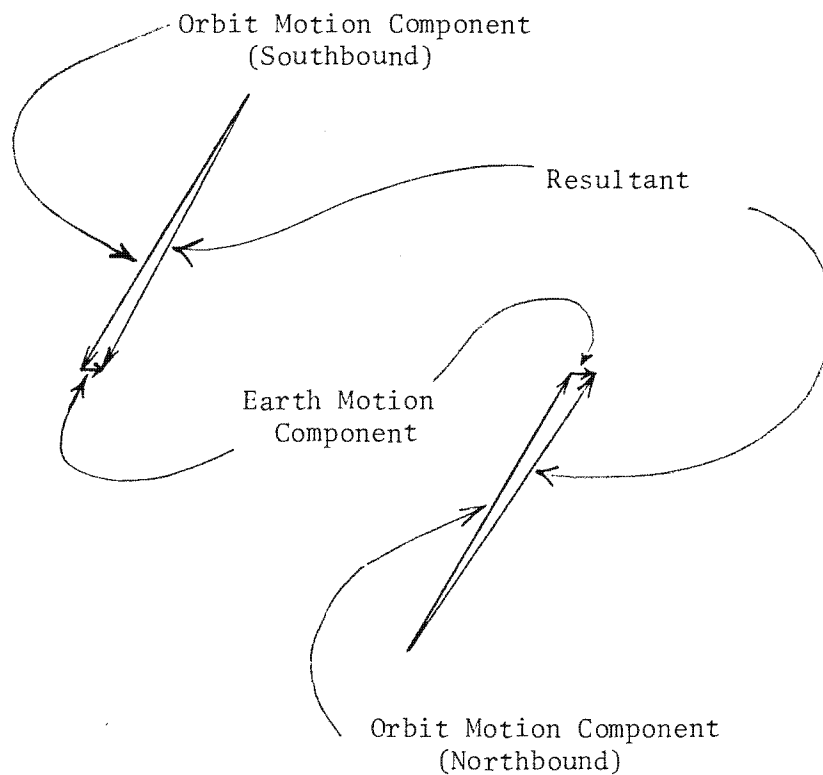


Figure 1.2-6. Object Velocity Components

1.2-9

~~TOP SECRET~~ G

Handle via **BYEMAN**
Control System Only

~~TOP SECRET~~ GBIF-008- W-C-019838-RH-80

2.1.3.1 Stereo Mirror Positioning. There are two types of mirror movement required for photography:

- (1) Stereo Movement - Three, servo-controlled positions of the stereo mirror about an axis parallel to the vehicle Y-axis (for zero crab) are provided to accomplish photography at the required stereo convergence angles.
- (2) Crab Movement - The rotation of the image vector for IMC is accomplished by placing the stereo mirror and yoke assembly in one of 23 discrete positions about an axis parallel to the vehicle X-axis. A total rotation of ± 3.85 degrees is required, resulting in positions being separated by 0.35 degree.

Both movements of the stereo mirror are shown in Figure 1.2-7. Figure 1.2-8 provides an illustration of the effect of a negative crab position. Since a non-zero crab displaces the line-of-sight (i.e., produces a roll effect equal in magnitude to the crab angle) as well as rotating the apparent motion vector, a roll maneuver must also be employed to ensure target centering.

2.1.3.2 Film-Drive Speed. The magnitude of the required film-drive speed varies inversely to vehicle-to-target distance (slant range). Discrete film-drive speeds are available to match (within granularity limits) those required by a wide range of vehicle-target geometries. The analytic equations for crab angle, film-drive speed, and roll angle for a given vehicle-target geometry are presented in Part 2, Sections 2 and 3.

2.1.4 Exposure Control

In the Gambit system, as in any strip camera, exposure time is controlled by the combination of film velocity past an exposure slit and the width of the slit. As described above, film-drive speed is uniquely determined by slant range considerations. Therefore, a variable width slit must be employed to provide for variations in exposure time needed to accommodate a wide range of film sensitivity

1.2-10

~~TOP SECRET~~ GHandle via BYEMAN
Control System Only

~~TOP SECRET~~ G

BI F-008- W-C-019838-RH-80

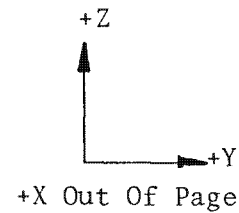
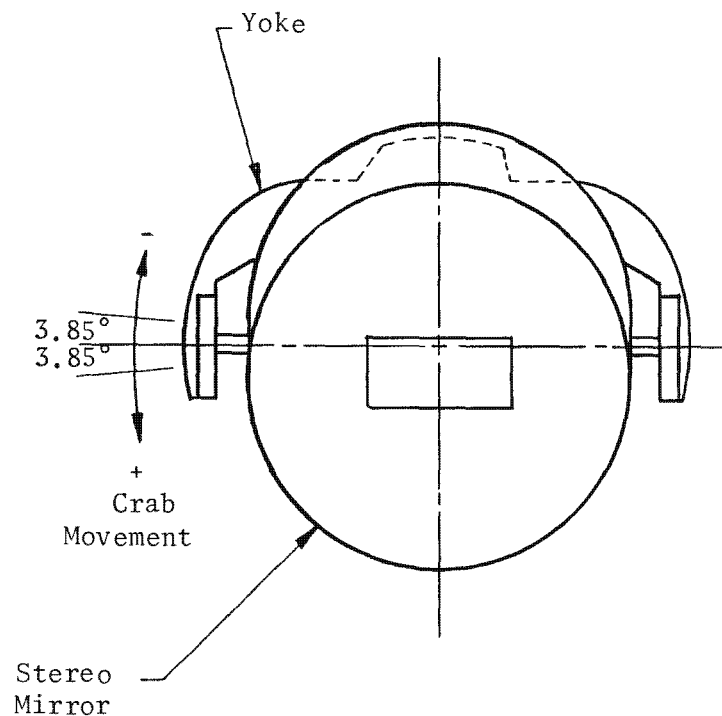
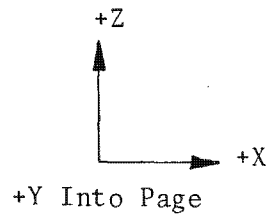
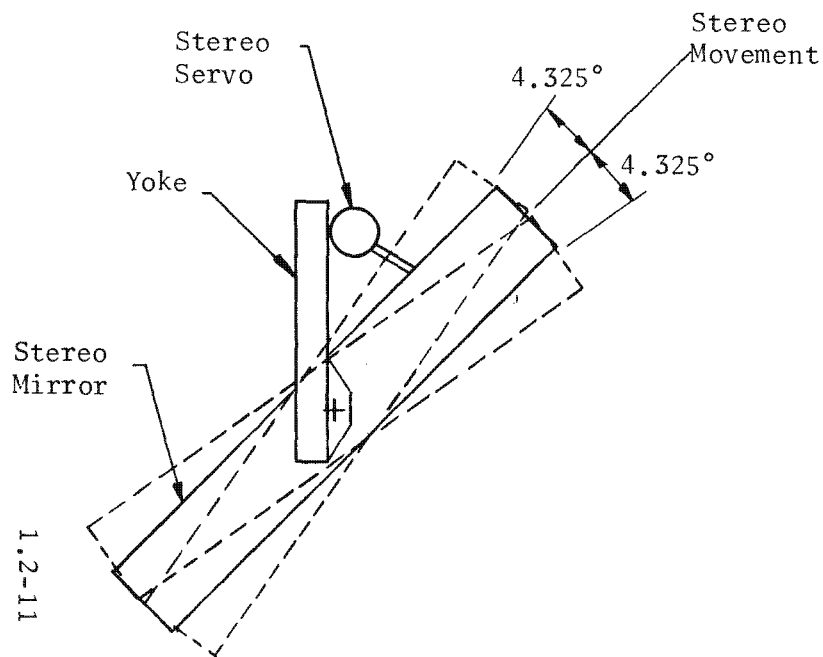


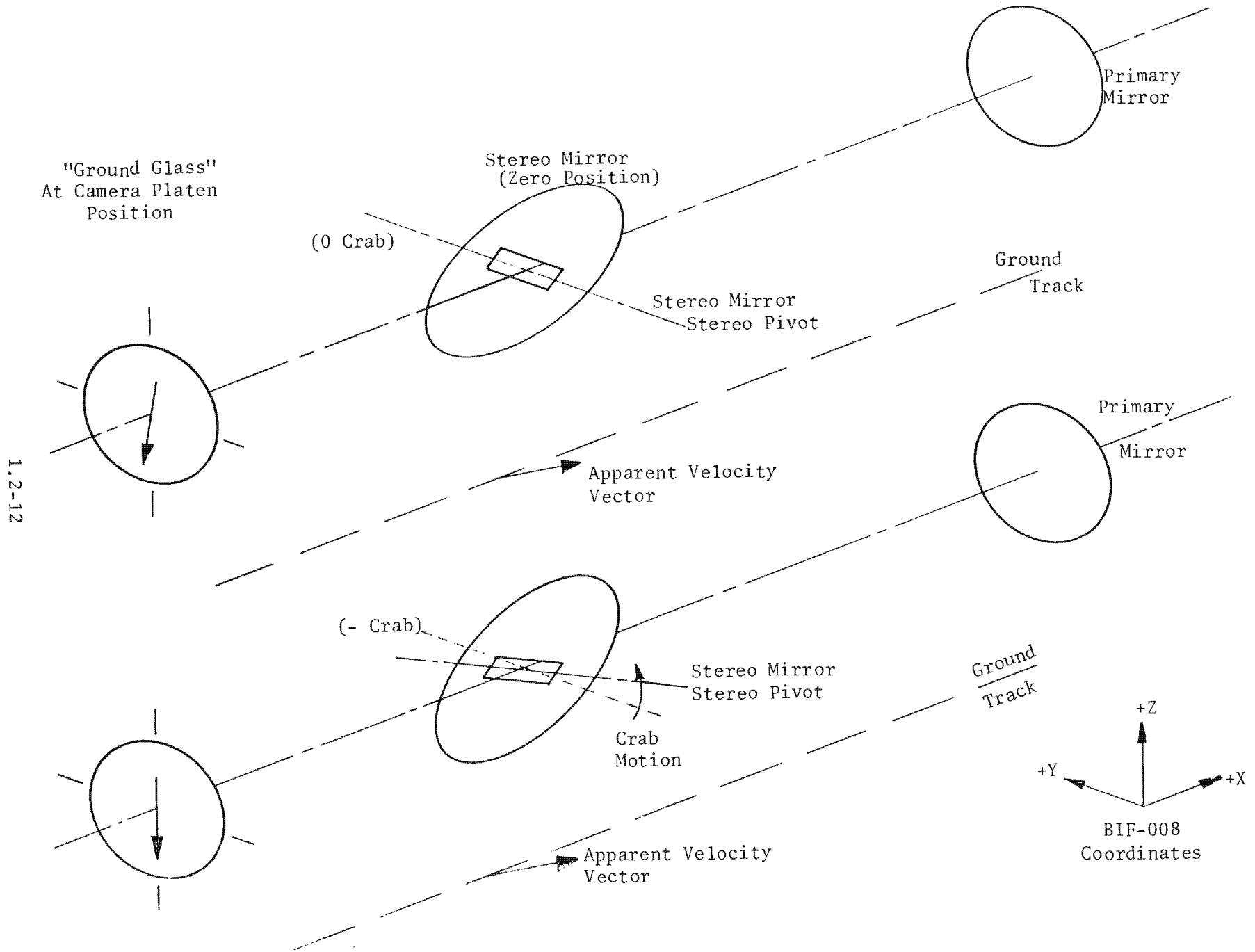
Figure 1.2-7. Mirror Movements for Stereo and IMC

Handle via **BYEMAN**
Control System Only

~~TOP SECRET~~ G

~~TOP SECRET~~ G

BIF-008- W-C-019838-RH-80



1.2-12

Handed by a BYEMAN
Control System Only

Figure 1.2-8. Illustration of the Effect of Crab

~~TOP SECRET~~ G

~~TOP SECRET~~ G

BIF-008-W-C-019838-RH-80

and target luminance. In the dual platen system, different film types may be employed in each system, hence, independent variable exposure mechanisms are provided for each. Detailed analyses of exposure requirements and the means chosen to meet them are presented in Part 2, Section 6.

2.1.5 Mission Orbits

The PPS/DP EAC is capable of fulfilling its mission while operating at target ranges between 206 and 710 nautical miles (nmi). Orbit inclination may range from 82 degrees to 120 degrees, with perigee anywhere in the orbit path. The most probable inclination for EAC missions is that providing a sun-synchronous orbit ($94.6^\circ \leq i \leq 98.5^\circ$).

2.1.6 Mission Duration

The operating lifetime of vehicles in the EAC configuration is 120 days. SRV No. 1 is normally returned at approximately mid-mission. SRV No. 2 is normally returned at mission completion.

2.1.7 Films

The PPS/DP EAC is capable of utilizing 9.5-inch wide and 5-inch wide black-and-white or color materials between 0.0015-inch and 0.0039-inch in thickness (3σ). Because of limitations imposed by mechanical clearances in some locations, films thicker than 0.0039-inch have a relatively high probability of jamming and should, therefore, be avoided.

1.2-13

~~TOP SECRET~~ GHandle via BYEMAN
Control System Only

~~TOP SECRET~~ GBIF-008-W-C-019838-RH-80

2.2 Aerospace Flight Equipment-Modular Subsystems

For the purposes of specification, manufacture, assembly, and initial testing, the BIF-008 subsystem is divided into three assembly modules. (See Figure 1.2-9.) These modules are assembled into a photographic payload section dual platen Extended Altitude Capability (PPS/DP EAC) which represents the complete, deliverable photo-optical system.

2.2.1 Supply and Electronics Module (SEM)

This cylindrical module contains the film supplies, film-handling components, and those electrical units associated with signal generation, power control, and commanding and telemetry functions.

2.2.2 Camera Optics Module (COM)

The COM is that portion of the PPS/DP EAC which contains the precision optical system including an aspheric primary mirror, a flat "stereo" mirror with a central opening, and a five-element Ross corrector. The dual-platen camera is also mounted in the COM. Commandable viewport doors are mounted to the COM and allow the entrance of energy from the scene.

2.2.3 Dual Recovery Module (DRM)

The dual recovery module contains those components associated with the mounting and on-orbit ejection of two satellite re-entry vehicles (SRVs) and an ejectable adapter (EA). Provision is also made in the DRM for enclosing the film path between the supply enclosure in the SEM and the SRVs. Sealing of film passages as necessary and redundant means for cutting film strands are also provided.

~~TOP SECRET~~ GHandle via BYEMAN
Control System Only

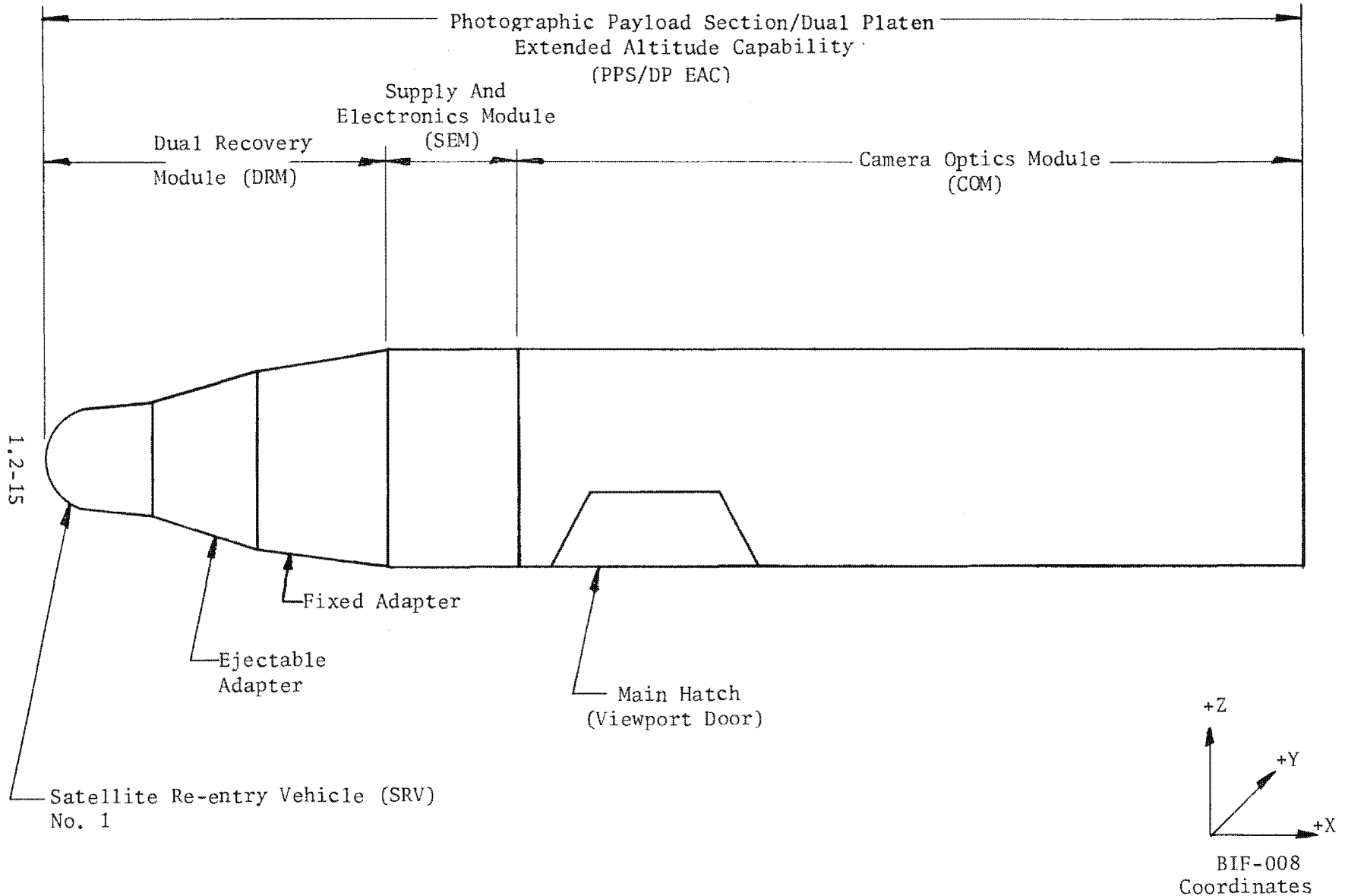


Figure 1.2-9. Photographic Payload Section/Dual Platen Extended Altitude Capability

Handle via **BYEMAN**
Control System Only

Approved for Release: 2017/02/14 C05097211

Approved for Release: 2017/02/14 C05097211

~~TOP SECRET~~ GBIF-008- W-C-019838-RH-80

2.3 Aerospace Flight Equipment-Functional Subsystems

For design, analytical, and testing purposes, the BIF-008 subsystem is divided into functional subsystems. These functional subsystems may lie in one or more modules. A listing of the subsystems, along with a brief description of the associated functions, is presented below. For a complete description of the functional subsystems, consult Part 3 of this handbook under the appropriate heading.

2.3.1 External

The external subsystem is made up of those components and structures which form the framework of the PPS/DP EAC and upon, or within, which all other components are mounted.

2.3.2 Film Handling Subsystem and Camera

This subsystem includes all components having to do with the storage of unexposed film of both sizes, the movement of the film to and through the camera past the exposure slit, and movement of the film to the take-up mechanisms in the recovery capsule.

2.3.3 Optics Subsystem

The optics subsystem includes all optical elements associated with the production of a high-quality aerial image at the focal plane.

2.3.4 Servos

This subsystem consists of the drive mechanisms which position the stereo mirror in both stereo and crab.

1.2-16

~~TOP SECRET~~ GHandle via **BYEMAN**
Control System Only

~~TOP SECRET~~ GBIF-008- W-C-019838-RH-80

2.3.5 Viewport Door Subsystem

Included in this subsystem are those motors, linkages, control circuits, and pyrotechnic devices required for the operation of the viewport doors. An ejectable cover protects the viewport doors until shortly before orbit injection.

2.3.6 Focus Detection Subsystem

The focus detection subsystem includes all those components which sense the location of the highest quality aerial image with respect to the platen and encode this information for transmission to the ground.

2.3.7 Power Subsystem

This subsystem controls and monitors the distribution of power throughout the PPS/DP EAC including main power, heater power, and pyro power.

2.3.8 Thermal Control Subsystem

The components in the thermal control subsystem include external paint patterns, vehicle heaters, and insulation blankets. Other factors influencing PPS/DP EAC temperature include thermal design techniques and such operational parameters as Beta angle* and perigee altitude.

2.3.9 Command Subsystem

The command subsystem includes those components necessary to receive commands and distribute them to the commanded units.

*Beta angle is defined as the acute angle between the earth-sun line and the projection of that line on the orbit plane.

~~TOP SECRET~~ GHandle via **BYEMAN**
Control System Only

~~TOP SECRET~~ G

BIF-008-W-C-019838-RH-80

2.3.10 Telemetry and Instrumentation Subsystem

This subsystem includes the components necessary to sense conditions or events of interest and present this data to the telemetry system in such a fashion that it may be encoded and transmitted to the ground.

2.3.11 Cutter/Sealer and Splicer Subsystem

This subsystem deals with the on-orbit transfer of film from one path to another within the PPS/DP EAC. Also included are those components whose function is to redundantly cut film and/or seal film passages.

2.3.12 Recovery Subsystem

The recovery subsystem, the responsibility of an associate contractor, includes those components necessary to achieve a controlled re-entry into the earth's atmosphere while protecting the exposed film inside against degrading environments. Also provided are a parachute to slow the descent and recovery aids to assist the airborne recovery effort.

2.4 Experimental Subsystems

Experimental subsystems include those hardware systems or special requirements which are not directed toward the fulfillment of the Gambit mission objectives, but toward system development or extended capability.

2.4.1 S-1/Platen Reference Gage

This experimental hardware provides outputs which should be correlated with structural shifts or distortions which may produce focus shifts.

1.2-18

~~TOP SECRET~~ GHandle via BYEMAN
Control System Only

~~TOP SECRET~~ G

BIF-008- W-C-019838-RH-80

2.4.2

25X1

1.2-19

~~TOP SECRET~~ G

Handle via **BYEMAN**
Control System Only

~~TOP SECRET~~ G

BIF-008-W-C-019838-RI-80

This Page Intentionally Blank

1.2-20

~~TOP SECRET~~ G

Handle via **BYEMAN**
Control System Only

~~TOP SECRET~~ GBIF-008- W-C-019838-RI-80

PART 2 ANALYSIS

1.0 REFERENCE FRAMES

Descriptions of the photographic satellite vehicle (PSV) have historically involved the use of various coordinate systems, where each system was developed for specific reasons, by different contractors. The two main coordinate systems, both approved for use by the Air Force in January of 1966, are depicted schematically in the frontispiece of each volume of the Photographic System Reference Handbook (PSRH) with the system in use throughout the handbook designated. Both are right-hand systems and differ only in that one is rotated 180 degrees about the Y axis, reversing the X and Z directions. Caution should be exercised in the use of documentation and equations when interfaces between contractors are crossed.

1.1 Coordinate System Conventions

Figure 2.1-1 depicts both the BIF-008 and the Lockheed Missiles and Space Company (LMSC) coordinate systems presently in use. All documentation produced by BIF-008 uses the vehicle and orbit coordinate system No. 1. All operational software and most associate contractors use the LMSC vehicle and orbit coordinate system No. 2. Correspondence between organizations using different coordinate systems should clearly define the convention in use to prevent confusion.

1.2 Vehicle and Orbit Coordinate Systems

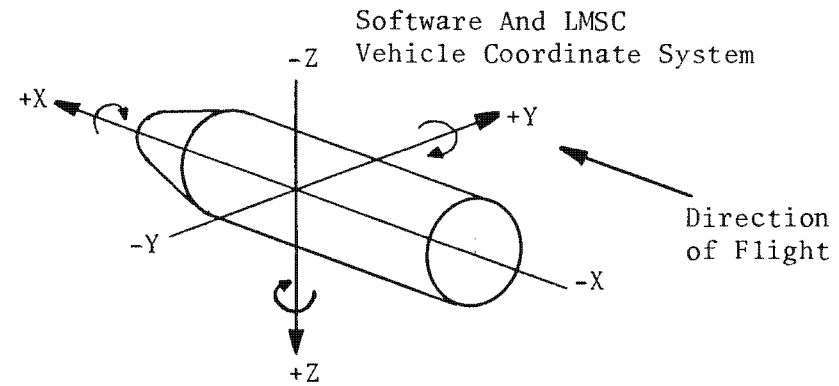
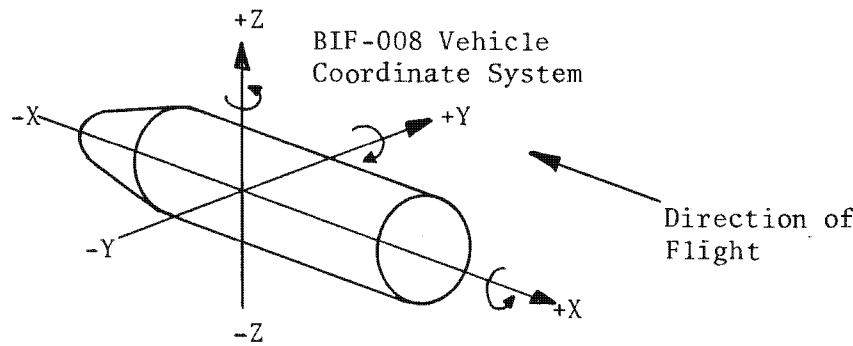
An orbit coordinate system (X, Y, Z) has the Z axis coincident with the orbit radius vector, the X axis in the plane of the orbit, and the Y axis to complete a right-handed system. The position of the vehicle relative to the orbit

2.1-1

~~TOP SECRET~~ GHandle via BYEMAN
Control System Only

~~TOP SECRET~~ G

BIF-008-W-C-019838-RI-80



Roll, Crab, Obliquity - Positive, Left Wing Down
 Yaw - Positive, Nose Left
 Pitch - Positive, Nose Up
 Stereo Angle - Positive, Principal Ray Forward
 Crab Negative Southbound, Crab Positive Northbound
 Platen Motion - Platen Plus is toward the lens, shortening the image distance.
 This coordinate system is used on all BIF-008 documentation, correspondence, and data package inputs. It is the system used throughout this document.

Roll, Crab, Obliquity - Positive, Right Wing Down
 Yaw - Positive, Nose Right
 Pitch - Positive, Nose Up
 Stereo Angle - Positive, Principal Ray Forward
 Crab Negative Northbound, Crab Positive Southbound
 Platen Motion - Platen Plus is toward the lens, shortening the image distance.
 This coordinate system is used in all software. It is the system used by associate contractors.

2.1-2

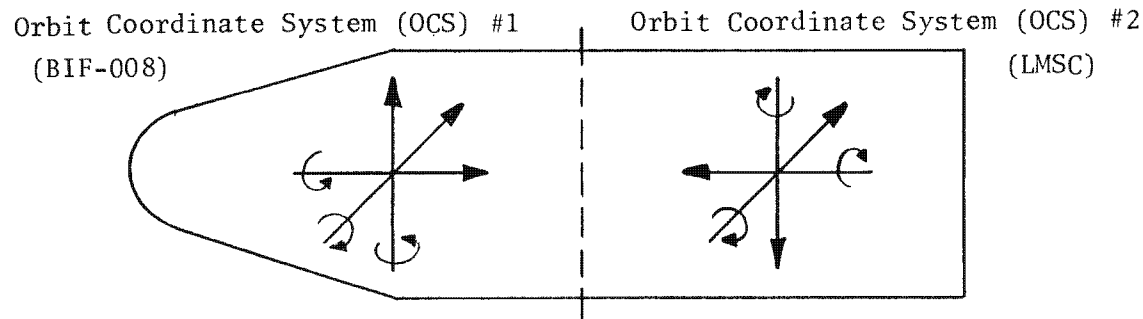


Figure 2.1-1. BIF-008 And LMSC Coordinate Systems

Handle via BYEMAN
 Control System Only

~~TOP SECRET~~ G

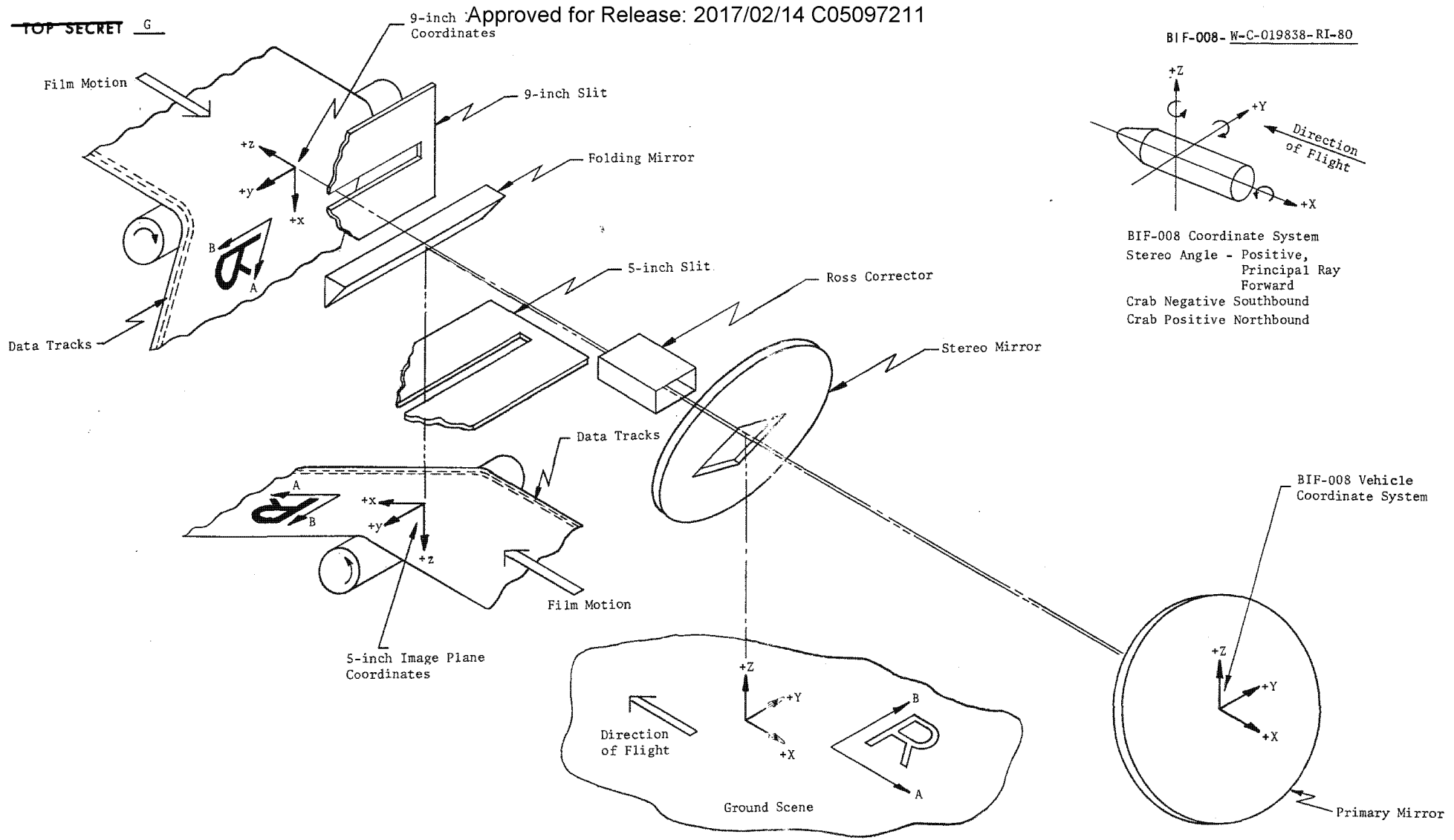


Figure 2.1-2. Simplified Schematic of Coordinate System Requirements

2.1-5/2.1-6

Handle via BYEMAN Control System Only

~~TOP SECRET~~ GBIF-008- W-C-019838-RI-80

coordinates is expressed in a vehicle coordinate system (X' , Y' , Z'). If there are no attitude displacements in yaw, pitch, and roll of the PPS/DP EAC, the (X' , Y' , Z') system is aligned with, and identical to, the orbit coordinate system, (X , Y , Z). Since attitude errors are normally small, and PPS/DP EAC roll can be as great as 45 degrees, the major difference between (X' , Y' , Z') and (X , Y , Z) is a rotation about the X axis. The (X , Y , Z) designation is often used to denote the vehicle coordinate system in applications where no confusion between the vehicle and orbit coordinate systems is anticipated.

1.3 Image Plane and Ground Coordinate Systems

A ground scene passing through the PPS/DP EAC optics is first reflected from the stereo mirror, then the primary mirror. The image then passes through the Ross corrector where it is focused on the 9-inch film plane. The incoming scene is also reflected by a folding mirror and comes to a focus on the 5-inch film plane. These relationships are graphically depicted in Figure 2.1-2. The X , Y , Z coordinates of the ground scene are translated into the image plane coordinates x , y , z by the optical system. More detailed information concerning the image plane coordinate systems and the film formats is provided in Part 2, Section 7.

1.4 PPS/DP EAC Cylindrical Coordinate System

A cylindrical coordinate system, shown in Figure 2.1-3, is frequently used to specify the location of instrumentation sensors and other components. The system in use for the PPS/DP EAC uses the parameters X , R and θ as follows:

- X = Position along the longitudinal (X) axis expressed as a station number (a number indicating the distance, in inches, from a predetermined zero point.)
- R = The distance from the vehicle centerline to the point of interest.
- θ = The angle around the longitudinal (X) axis looking toward the aft end of the vehicle, measured clockwise from the $+Z$ axis to the point of interest on R .

~~TOP SECRET~~ G

~~TOP SECRET~~ G

BIF-008-W-C-019838-RI-80

THIS PAGE INTENTIONALLY BLANK

2.1-4

~~TOP SECRET~~ G

Handle via BYEMAN
Control System Only

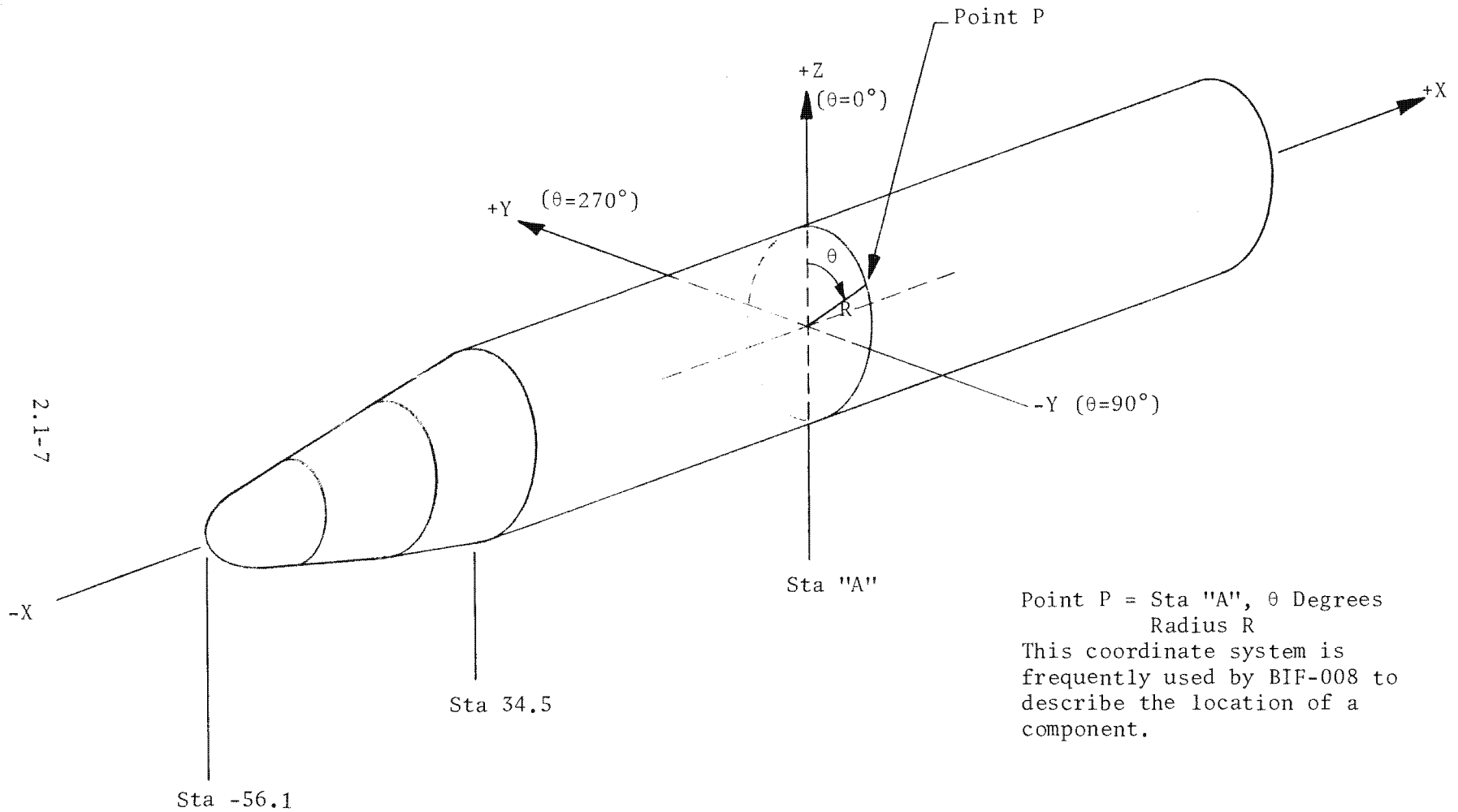


Figure 2.1-3. PPS/DP EAC Cylindrical Coordinates

Handle via **BYEMAN**
Control System Only

~~TOP SECRET~~ G

BIF-008-W-C-019838-RI-80

THIS PAGE INTENTIONALLY BLANK

2.1-8

~~TOP SECRET~~ G

Handle via **BYEMAN**
Control System Only

~~TOP SECRET~~ GBIF-008- W-C-019838-RI-80

2.0 POINTING AND TARGET ACQUISITION

The photographic satellite vehicle (PSV) is programmed to point and operate such that the centers of the camera slit areas projected onto the ground will intersect the target areas. Pointing errors, which cause the lines-of-sight (LOS) of the two camera systems to miss the target centers, result in miss-distances which have in-track (X) and cross-track (Y) components.

In-track pointing errors, which include target location uncertainty, ephemeris uncertainty, clock granularity, and pointing uncertainty, can be accommodated by programming the camera systems to operate for an appropriately longer time than is required for the zero-error condition.

Evaluation of the capability to accommodate cross-track pointing errors is more complex. The magnitude of the cross-track error which can be accommodated by a given swath, w, (which is fixed by the altitude, focal length, field angle of the lens, obliquity angle, and the stereo angle) is determined by random errors characteristic of individual frames, together with errors caused by relative motion of the earth, target location uncertainties, vehicle ephemeris uncertainties, and pointing uncertainties.

2.1 Swath Width

Swath width, making the "flat earth" assumption, is calculated according to the formula:

$$w = \frac{2h \sin \mu \cos \mu \cos \Sigma}{(\cos \Sigma \cos \Omega \cos \mu)^2 - (\sin \Omega \sin \mu)^2}$$

2.2-1

~~TOP SECRET~~ GHandle via BYEMAN
Control System Only

~~TOP SECRET~~ GBIF-008- W-C-019838-RI-80

where: w = swath width in nautical miles (nmi). This is the swath width swept out by the projection of the slit on the earth.

h = altitude of vehicle in nmi

Σ = stereo mirror angle in degrees

Ω = obliquity angle in degrees

μ = semifield angle in degrees

The "flat earth" model yields swath widths to better than 2% of the altitude used up to 300 nmi, for all obliquity and stereo angles. The R-5 (175-inch focal length) lens provides a 2.90-degree field of view for the 9-inch system and a 1.48-degree field of view for the 5-inch system. These correspond to a 4.55 nmi swath width for the 9-inch system for vertical photography from a 90 nmi altitude and a 2.32 nmi swath width for the 5-inch system under the same circumstances.

For altitudes above 300 nmi, a more complex spherical earth model must be employed. Such a model was used to generate the values shown in Figures 2.2-1 and 2.2-2.

2.2 5-Inch Pointing Biases

Positioning of the 5-inch system folding mirror approximately 0.725 inch below (-Z direction) the optical axis causes the 5-inch line-of-sight (LOS) to be directed slightly differently than the 9-inch LOS. Because the cross-track bias is extremely small (less than 0.016 degree) and varies as a function of commanded crab angle, operational software makes no attempt to compensate for the cross-track pointing error induced by the 5-inch system offset.

The in-track pointing error caused by the 0.725-inch offset causes the 5-inch LOS to be directed approximately 0.237 degree aft of the 9-inch LOS. The simplest and most direct approach to compensating for this difference is shown in Figure 2.2-3.

2.2-2

~~TOP SECRET~~ GHandle via BYEMAN
Control System Only

~~TOP SECRET~~ G

BIF-008-W-C-019838-RI-80

2.2-5

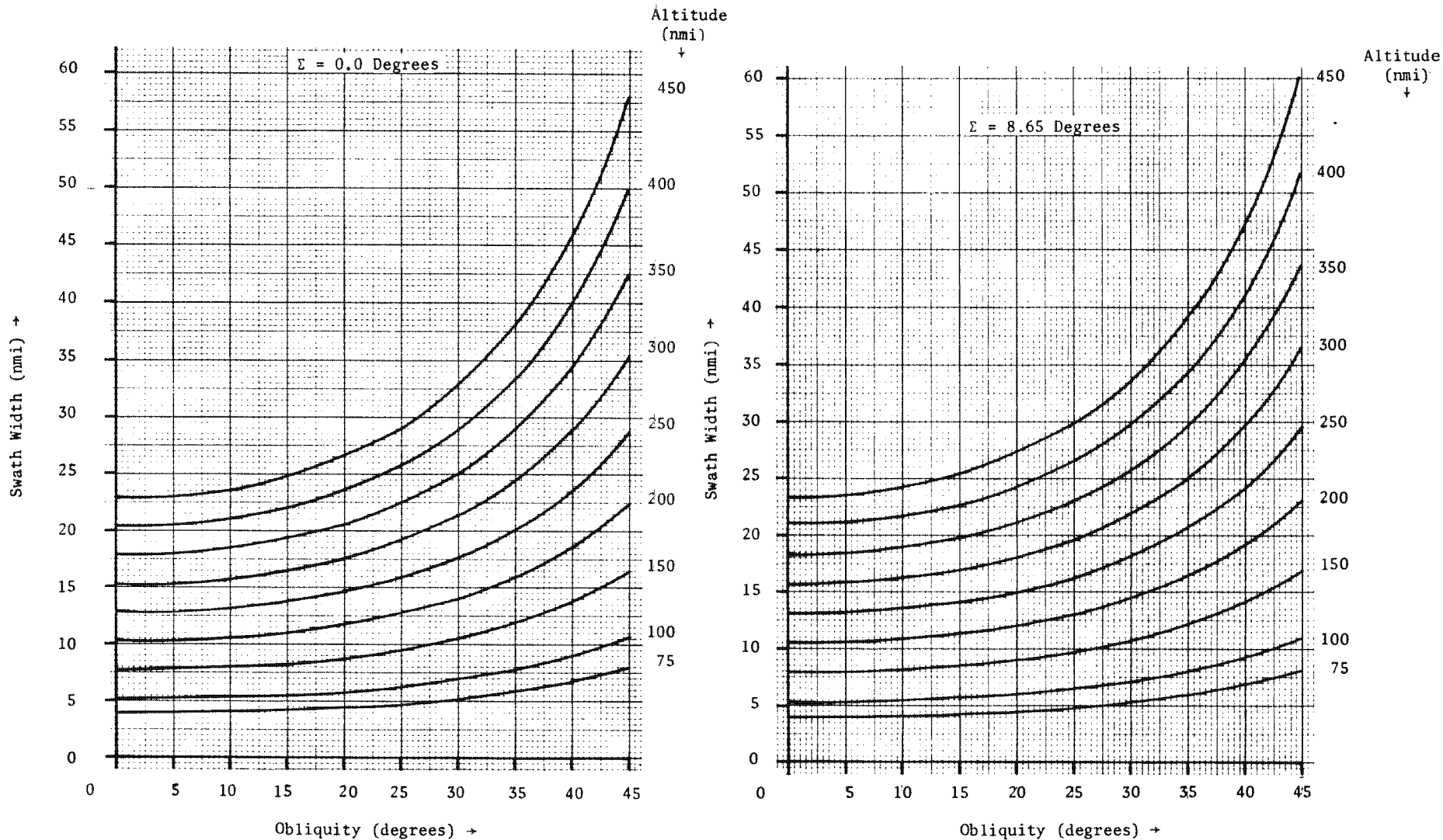


Figure 2.2-1. 9 System Swath Width vs. Obliquity

Handle via BYEMAN
Control System Only

~~TOP SECRET~~ G

~~TOP SECRET~~ G

BIF-008-W-C-019838-RI-80

2.2-4

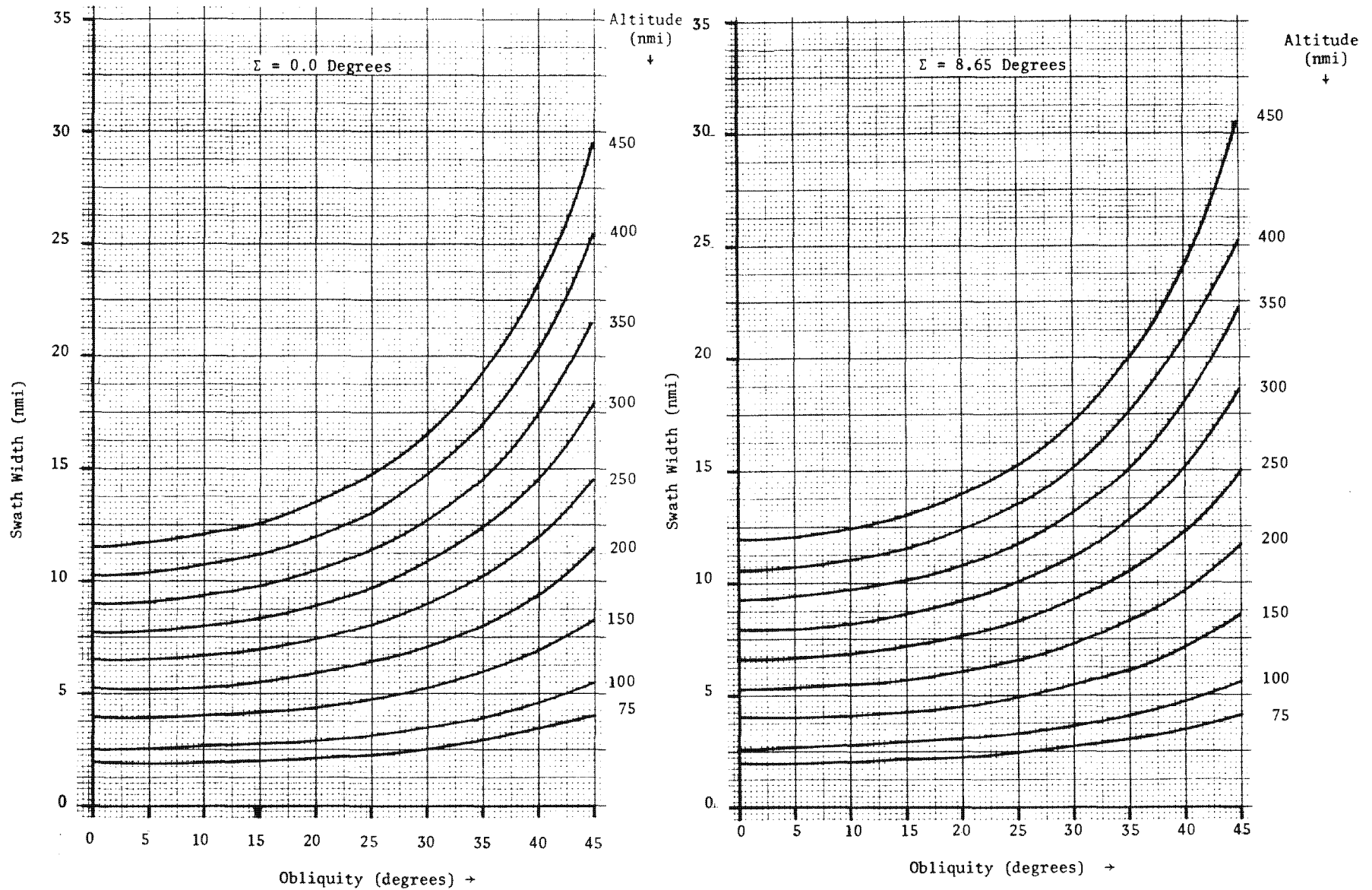


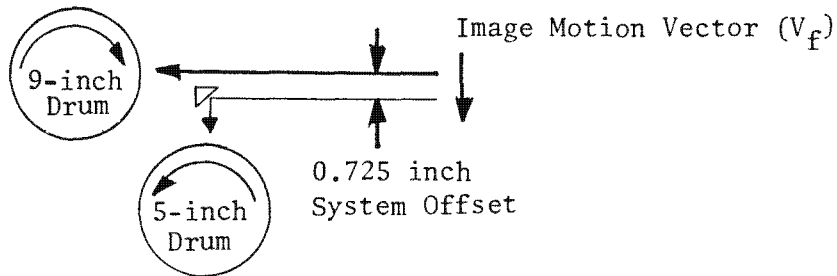
Figure 2.2-2. 5 System Swath Width vs. Obliquity

Handle via BYEMAN
Cont System Only

~~TOP SECRET~~ G

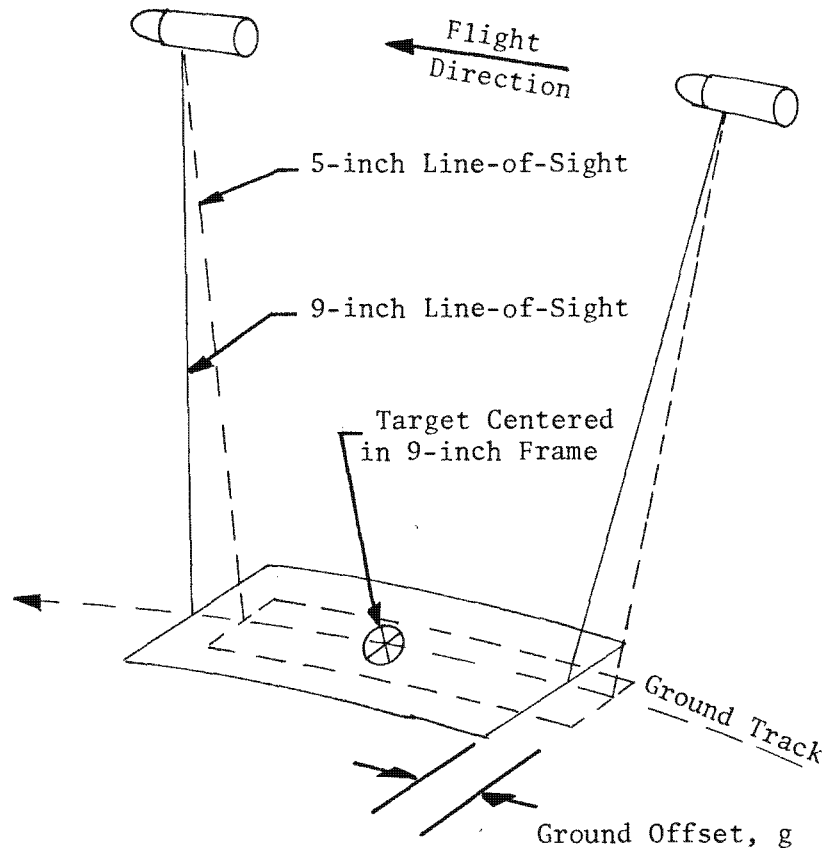
~~TOP SECRET~~ G

BIF-008-W-C-019838-RI-80



$$\Delta t (9/5) = \frac{0.725}{V_f} \quad V_f \approx \frac{745}{a}$$

$$g = V_{nx} \Delta t = 0.004136a$$



2.2-5

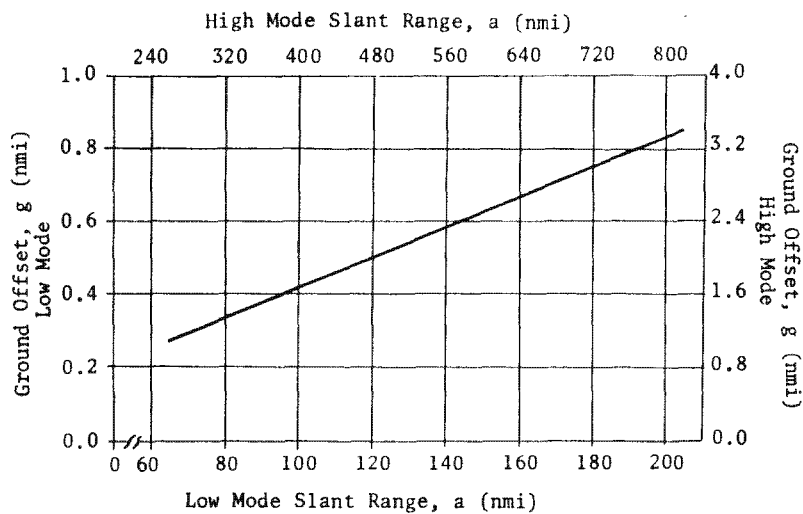


Figure 2.2-3. Effect of Offset of 5-Inch System on Pointing

Handle via **BYEMAN**
Control System Only

~~TOP SECRET~~ G

~~TOP SECRET~~ GBIF-008- W-C-019838-RI-80

All pointing and image motion compensation (IMC) parameters for a given target are calculated for the 9-inch system. The time required for the 9-inch strand to move 0.725 inch, if it is moving at the preferred (unquantized) film-drive speed (FDS), is the same as the offset in acquisition time between the 9-inch and 5-inch systems. Operational software then adds this time offset to the 9-inch CAMERA ON and CAMERA OFF times to arrive at the required CAMERA ON and CAMERA OFF times for 5-inch system photography of the same target. In equation form,

$$\Delta t = \frac{\Delta_5}{v_f}$$

where: v_f is the 9-inch preferred FDS (unquantized)

Δ_5 is the 5-inch system offset (nominally 0.725 inch)

Δt is the time bias between 9-inch and 5-inch acquisition of the same point

The 5-inch system ON and OFF commands are the only pointing parameters which are computed differently for the 9-inch and 5-inch systems. The only other targetting parameter which is treated differently for the two systems is the film-drive speed required for image motion compensation (IMC). The approach used to calculate the proper FDS is described in Part 2, Section 3.0.

2.3 Target Acquisition

For two reasons it is advantageous to aim the systems so that the targets to be photographed are near the centers of the fields-of-view of the lens. The first is to obtain highest resolution, since the optical quality factor (OQF) of the lens decreases as field angles increases. Secondly, placing the target near the

~~TOP SECRET~~ G

~~TOP SECRET~~ GBIF-008- W-C-019838-RI-80

center of the field-of-view increases the probability of covering the entire target area. (The center of field-of-view for the lens is not exactly at the center of the 9 x 5 film-image formats. The difference is about 0.04 inch for the 9-inch system and about 0.01 inch for the 5-inch system as shown in Part 3, Section 2.)

Whether a target is actually acquired in the swath recorded when a camera system is commanded to operate is determined by such variables as vehicle location (ephemeris), target location, target size, and vehicle pointing descriptors. Since each of these parameters has an associated uncertainty, probabilistic statements are most appropriate. Certain situations, however, lends themselves to a "geometric" analytic approach in which the expected, or nominal, value for one or more parameters is used. Both approaches are found in the following sections.

2.3.1 Slant Range

A knowledge of the calculation of slant range is helpful in many parts of this section. The complete equation for slant range is as follows:

$$(1) \quad a = (h + R) \cos \Sigma \cos \Omega - [(h + R)^2 \cos^2 \Sigma \cos^2 \Omega - h^2 - 2 Rh]^{1/2}$$

where: a = slant range in nautical miles
 h = vehicle nadir altitude in nautical miles
 R = radius of earth in nautical miles (\cong 3,440 nmi)
 Ω = obliquity angle in degrees
 Σ = stereo angle in degrees

For altitudes less than approximately 150 nmi, this expression may be approximated by:

2.2-7

~~TOP SECRET~~ GHandle via **BYEMAN**
Control System Only

~~TOP SECRET~~ GBIF-008- W-C-019838-RI-80

$$(2) \quad a = h \sec \Sigma \sec \Omega$$

Figure 2.2-4 is a graph of the complete equation at selected values of obliquity.

2.3.2 In-Track Acquisition

In-track target acquisition is controlled by the time at which a camera system is turned ON for photography. Timing considerations, as they influence target acquisition, are examined below for both monoscopic and stereoscopic photography. Analyses are performed for the 9-inch system with an appropriate increment assumed to apply for the 5-inch system. (See Part 2, Section 2.2.)

2.3.2.1 In-Track Monoscopic Acquisition. It is desired to turn the camera ON at such time as to cause the beginning of high-resolution photography to coincide with the leading edge of the target area. Uncertainties in timing requirements stem from target location uncertainty, vehicle location uncertainty, time uncertainty, and pointing uncertainty. These parameters may be described as follows:

$$\begin{aligned} \sigma &= \text{location uncertainty} \\ \sigma_t &= \text{time of arrival uncertainty} \\ \sigma_t &= \sigma/V_{nx} \text{ where } V_{nx} \text{ is vehicle nadir ground velocity} \\ \sigma_{tE} &= \text{ephemeris uncertainty} \\ &= \sigma_E/V_{nx} \\ \sigma_{tTL} &= \text{target location uncertainty} \\ &= \sigma_{TL}/V_{nx} \\ \sigma_{tCG} &= \text{clock granularity} \\ &= \frac{0.2}{\sqrt{12}} = 0.057735 \text{ second} \\ \sigma_{tP} &= \text{pointing uncertainty (total PPS)} \\ &= \sigma_P/V_{nx} \end{aligned}$$

~~TOP SECRET~~ G

~~TOP SECRET~~ G

①

BIF-008-W-C-019838-RI-80

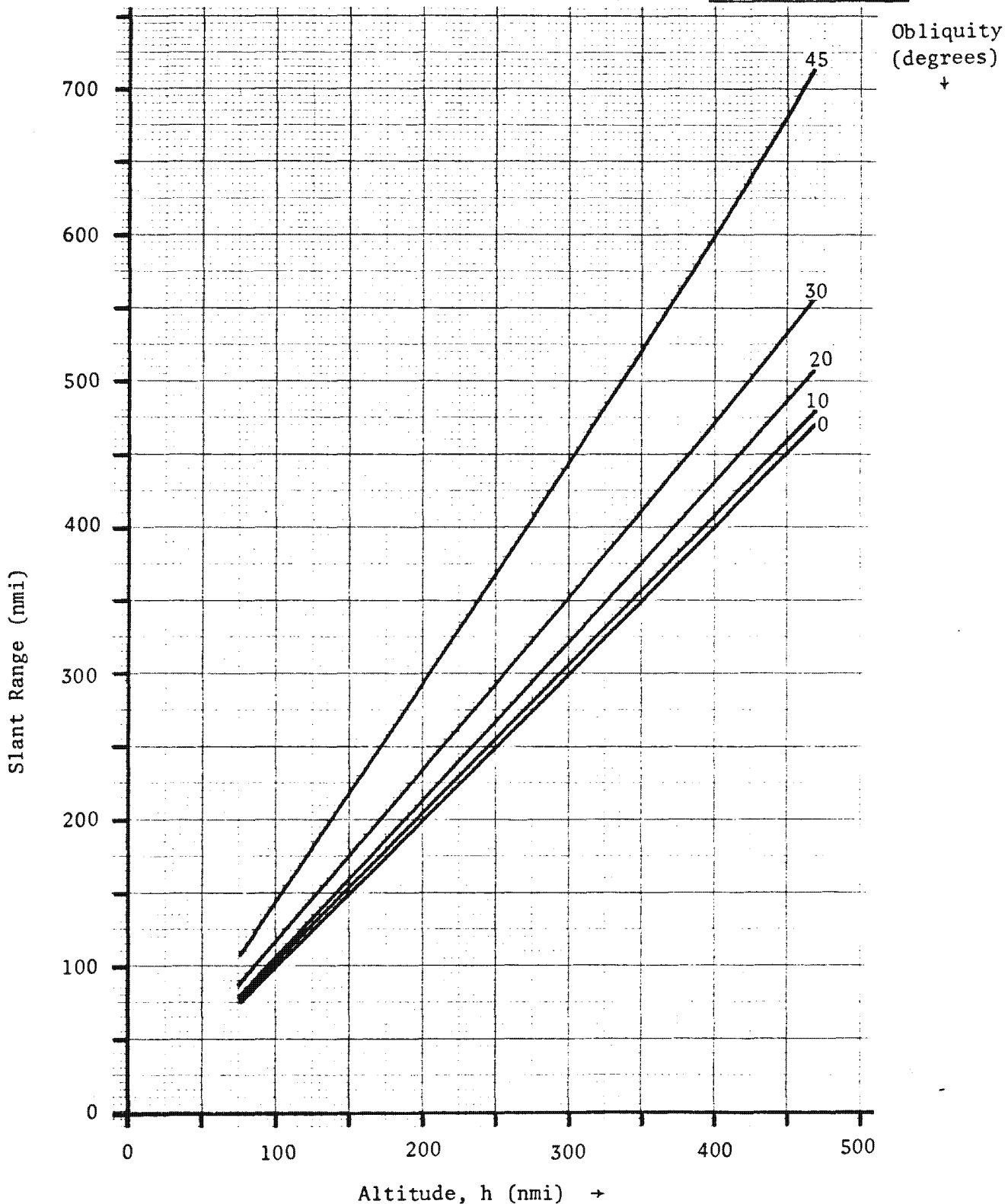


Figure 2.2-4. Slant Range vs. Altitude (Complete Equation)

2.2-9

~~TOP SECRET~~ G

Handle via BYEMAN
Control System Only

"WARNING - THIS DOCUMENT SHALL NOT BE USED AS A SOURCE FOR DERIVATIVE CLASSIFICATION"

~~TOP SECRET~~ GBIF-008- W-C-019838-RI-80

The total time of arrival uncertainty is the root-sum-squared of the four contributors.

$$\sigma_{tT} = \sqrt{\sigma_{tE}^2 + \sigma_{tTL}^2 + \sigma_{tCG}^2 + \sigma_{tP}^2}$$

Figure 2.2-5 illustrates the manner in which this parameter is applied. N is the pad multiplier which varies with target priority code. To determine the system time at which the camera should be turned ON, the software computes the time of target center, and subtracts one-half of the time required to traverse the target. A time equal to $N\sigma_{tT}$ is subtracted, resulting in the time at which high-resolution performance is desired. The data base value for camera start-up is subtracted, yielding the time at which the camera is to be turned ON. This technique results in a certain probability that high-resolution photography will be achieved before the line-of-sight (LOS) crosses the target's leading edge. This probability will vary from target-to-target depending on the value selected for N. The relationship between the value chosen for N and the probability that high-resolution photography will be achieved before the LOS crosses the target's leading edge is shown in Figure 2.2-6.

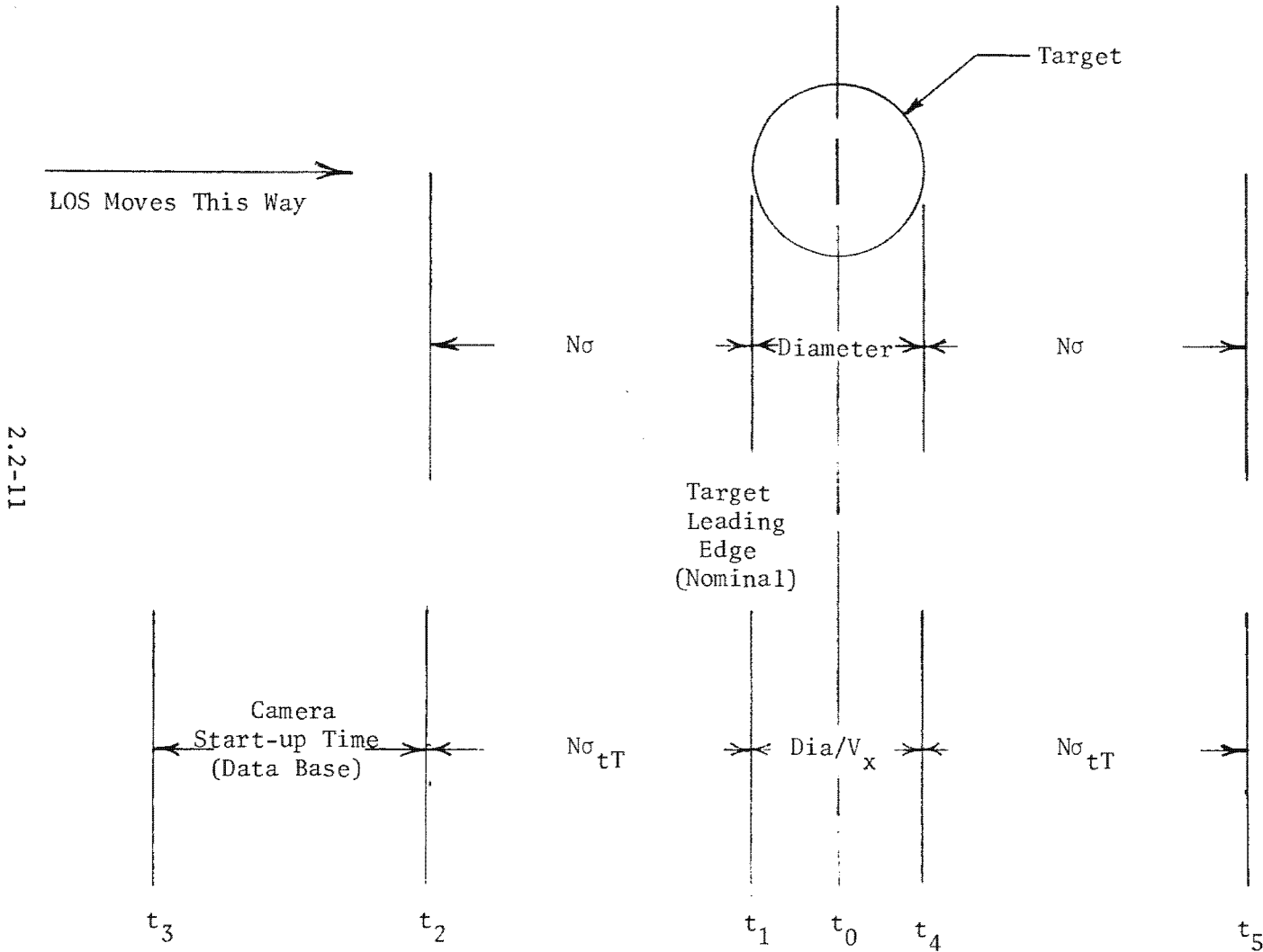
2.3.2.2 In-Track Stereoscopic Acquisition. The following discussion refers to the terminology presented in Figure 2.2-7.

The time between stereo looks ($T_7 - T_2$) at a target is approximately:

$$T_7 - T_2 = \frac{2 h \tan \Sigma \sec \Omega}{V_{nx}}$$

where: h = altitude in nautical miles
 Σ = stereo angle (8.65 degrees)
 Ω = obliquity in degrees, and
 V_{nx} = in-track vehicle nadir velocity.

~~TOP SECRET~~ G



- t_0 = Computed Time For Target Center.
- t_1 = Computed Time For Target Leading Edge.
- t_2 = Earliest Time For Target Leading Edge With Probability 1 (See Figure 2.2-6)
- t_3 = Time For Camera ON Command.
- t_4 = Target Trailing Edge
- t_5 = Latest Time For Target Trailing Edge Time For Camera Off Command.

2.2-11

Figure 2.2-5. In-Track Monoscopic Acquisition

Handle via BYEMAN Control System Only

Approved for Release: 2017/02/14 C05097211

Approved for Release: 2017/02/14 C05097211

~~TOP SECRET~~ G

BIF-008- W-C-019838-RI-80

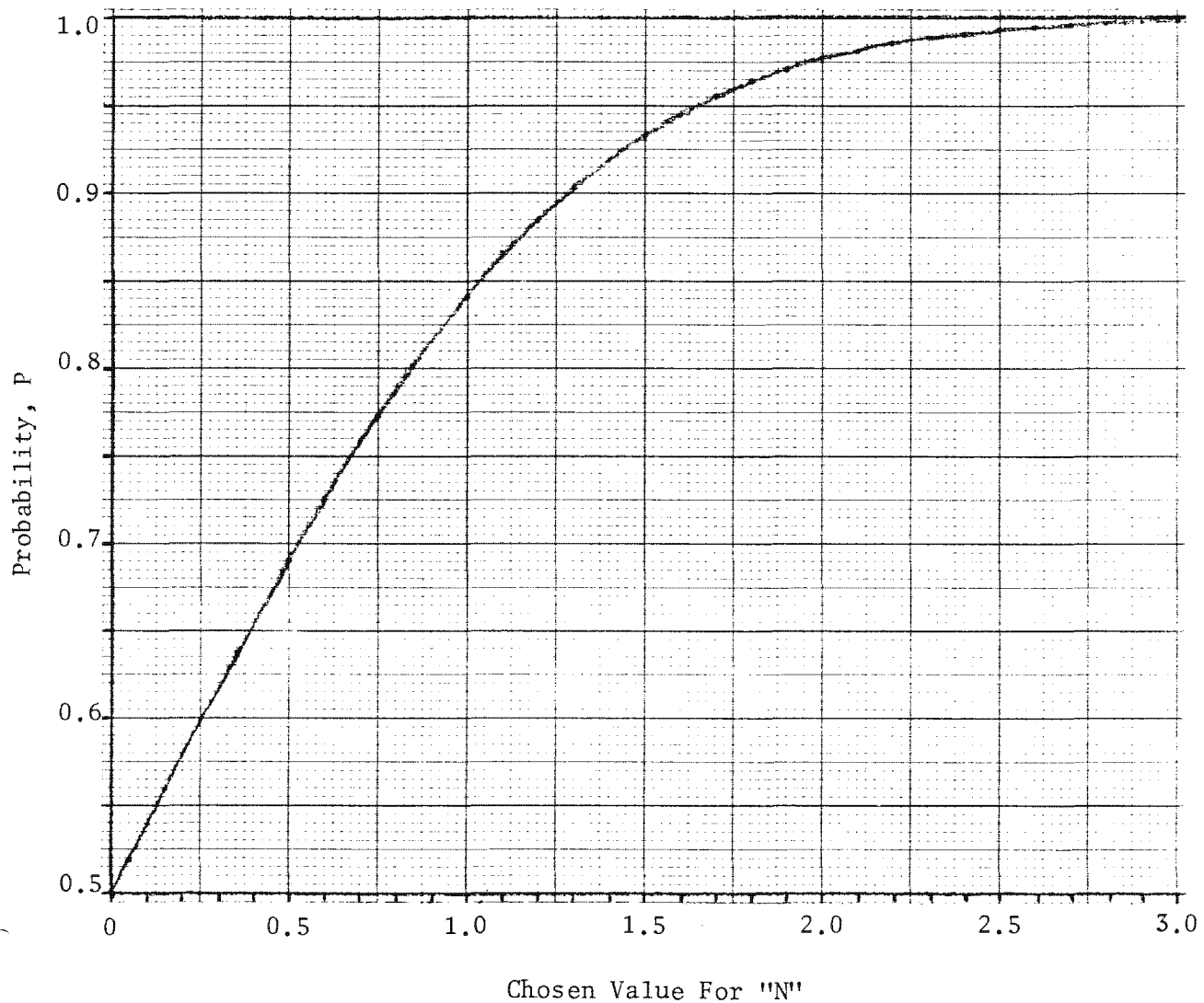


Figure 2.2-6. Probability of High Resolution Before Target Acquisition

~~TOP SECRET~~ G

Handle via **BYEMAN**
Control System Only

- T_0 = Camera ON, First Frame of Stereo Pair
- T_1 = Film Begins To Move
- T_2 = Film At Commanded Speed
(Beginning of High-Resolution Photography)
- T_3 = Camera OFF, HR Ends, Mirror Move Begins
- T_4 = Film Stopped
- T_5 = Camera ON, Second Frame
- T_6 = Film Begins To Move
- T_7 = Film At Commanded Speed, HR
Photography Begins, Mirror Stopped
- T_8 = Camera OFF, Second Frame, HR Ends
- T_9 = Film Stopped

2.2-13

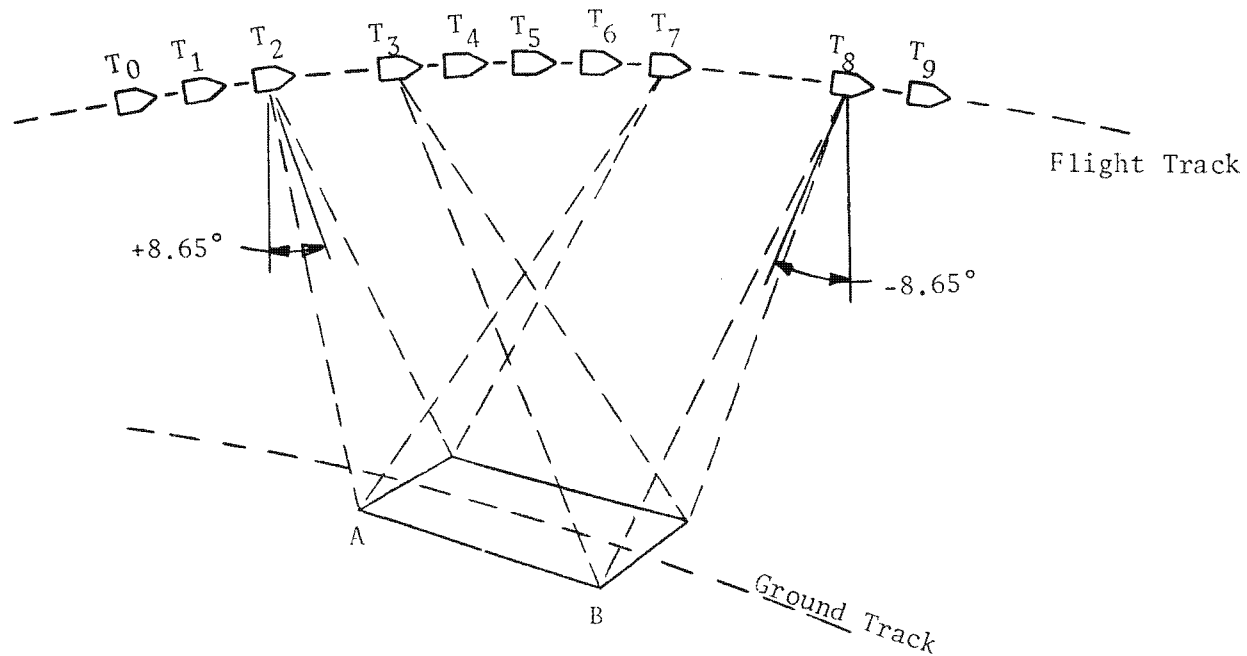


Figure 2.2-7 Stereoscopic Acquisition

Handle via **BYEMAN**
Control System Only

Approved for Release: 2017/02/14 C05097211

Approved for Release: 2017/02/14 C05097211

~~TOP SECRET~~ GBIF-008- W-C-019838-RI-80

The time allocated between the end of high-resolution photography in the first frame and the start of high-resolution photography in the second frame, $T_7 - T_3$, is a minimum of three (3) seconds based on the specified stereo mirror transition time. The maximum duration of high-resolution stereo photography is therefore (using the flat earth model):

$$T_3 - T_2 = \frac{2h \tan \Sigma \sec \Omega}{V_{nx}} - 3.0 \text{ seconds}$$

and

$$AB = 2 h \tan \Sigma \sec \Omega - 3 V_{nx} \text{ nmi}$$

where: AB is the maximum swath length on the ground for which stereo overlap is obtainable in high resolution.

To determine the maximum target length that can be acquired with a given probability, the in-track, root-sum-square contribution, ΔX , of the pointing-error contributors in Table 2.2-3 (PSV Pointing Error Budget) or Table 2.2-4 (PPS/DP Pointing Error Contributors) must be computed in a similar manner. Allowance must be made for the 0.2-second granularity in the commands to start and stop the camera. The length of target, D, which can be acquired while photographing AB is therefore:

$$\begin{aligned} D &= AB - 2\Delta X - 0.4 V_{nx} \\ &= [2h \tan \Sigma \sec \Omega - 2\Delta X - 3.4 V_{nx}] \end{aligned}$$

The probability of acquiring high-resolution stereo photography for D nautical miles, using the worst-case condition of 0.4-second granularity, is better than 95 percent if 95-percentile values are used for computing ΔX .

2.2-14
~~TOP SECRET~~ G

Handle via **BYEMAN**
Control System Only

~~TOP SECRET~~ GBIF-008- W-C-019838-RI-80

For EAC altitudes, it is necessary to invoke the spherical earth model. We note that in the previous equations for $T_3 - T_2$ and AB that $2h \tan \Sigma \sec \Omega$ may be written as $2a \sin \Sigma$. A good approximation will result if the value for a calculated by the spherical earth model is used and V_{nx} is taken to be the circular orbit ground velocity, V_{cx} .

Figure 2.2-8 shows camera ON time as a function of altitude with interframe time as a parameter for in-track stereo coverage. Obliquities of zero and 45 degrees are shown.

To find the in-track stereo coverage, in nautical miles, the camera ON time determined from Figure 2.2-8 must be multiplied by the V_{cx} value from Figure 2.3-2.

Example: An EAC vehicle is in a 360 nmi circular orbit. It is desired to take a stereo pair at 0-degree obliquity and a 10-second interframe time. What is the first frame ON time? What is the in-track ground swath?

Answer: 21.1 seconds
77.6 nmi

Example: What are the corresponding figures for 45-degree obliquity?

Answer: 37.2 seconds
136.8 nmi

~~TOP SECRET~~ G

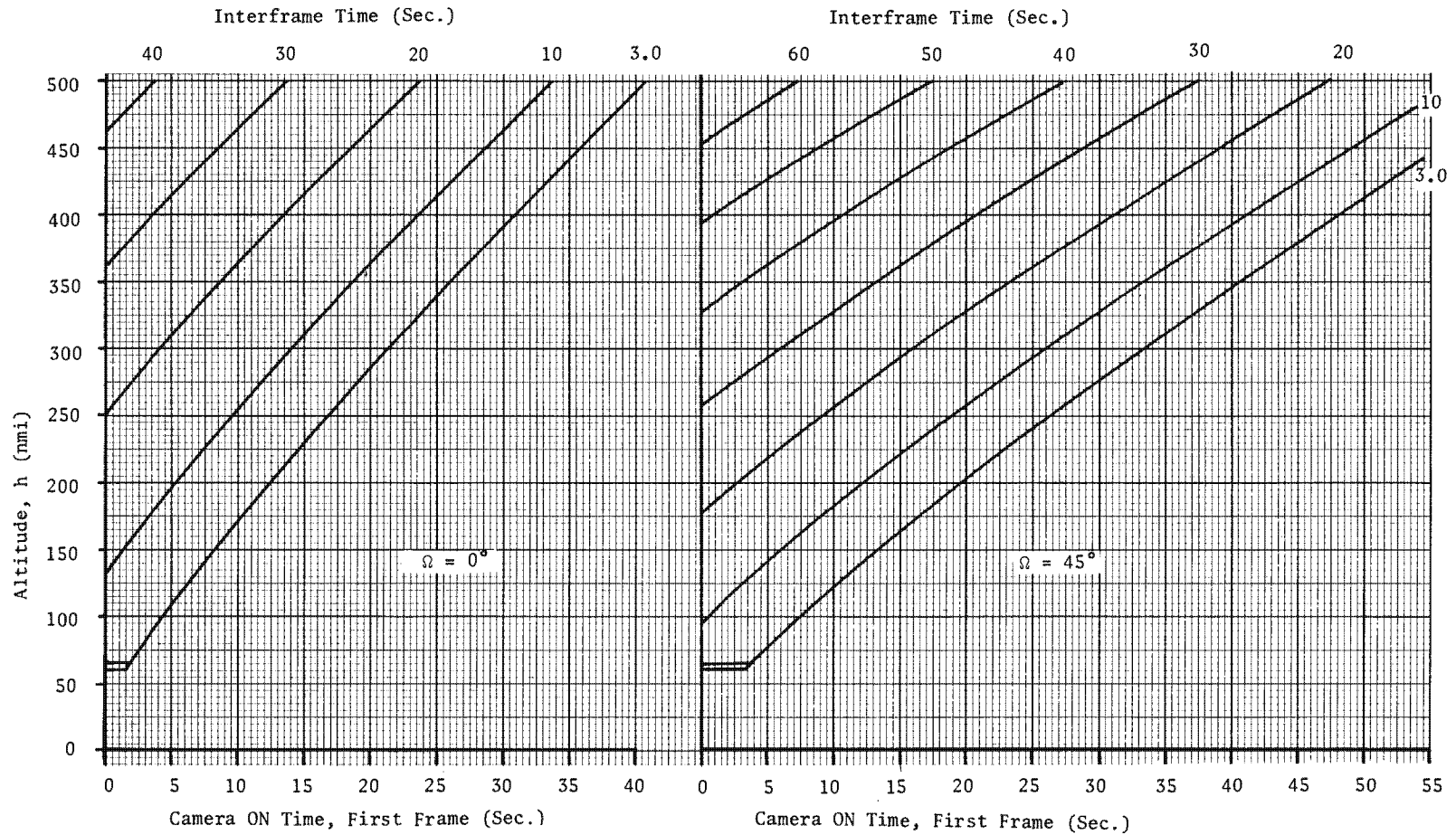


Figure 2.2-8. In-Track Stereo Coverage

~~TOP SECRET~~ GBIF-008- W-C-019838-RI-80

2.3.3 Cross-Track Target Acquisition

2.3.3.1 Cross-Track Monoscopic Acquisition. The LOS of the PPS/DP EAC is programmed to intersect the center of the target. Because of the errors in pointing, swath-width limitations, target location uncertainty, vehicle ephemeris uncertainty, earth rotation, and command granularity, the probability of obtaining the entire target within a given swath-width varies depending on target size and orbit parameters. Figure 2.2-9 shows the target-swath relationship used in deriving the appropriate probabilistic statements.

The total time-of-arrival uncertainty, as developed in section 2.3.2.1, is:

$$\sigma_{tT} = \sqrt{\sigma_{tE}^2 + \sigma_{tTL}^2 + \sigma_{tCG}^2 + \sigma_{tP}^2}$$

The cross-track velocity, V_y , acting over this time of arrival uncertainty, results in a cross-track position uncertainty, $\sigma_y(t)$.

Cross-track velocity is calculated as follows:

V_E = velocity of a point on the earth due to rotation

$$V_E = R_E (\theta) \cos \theta \eta_E$$

where: $R_E (\theta)$ = radius of earth at θ Latitude

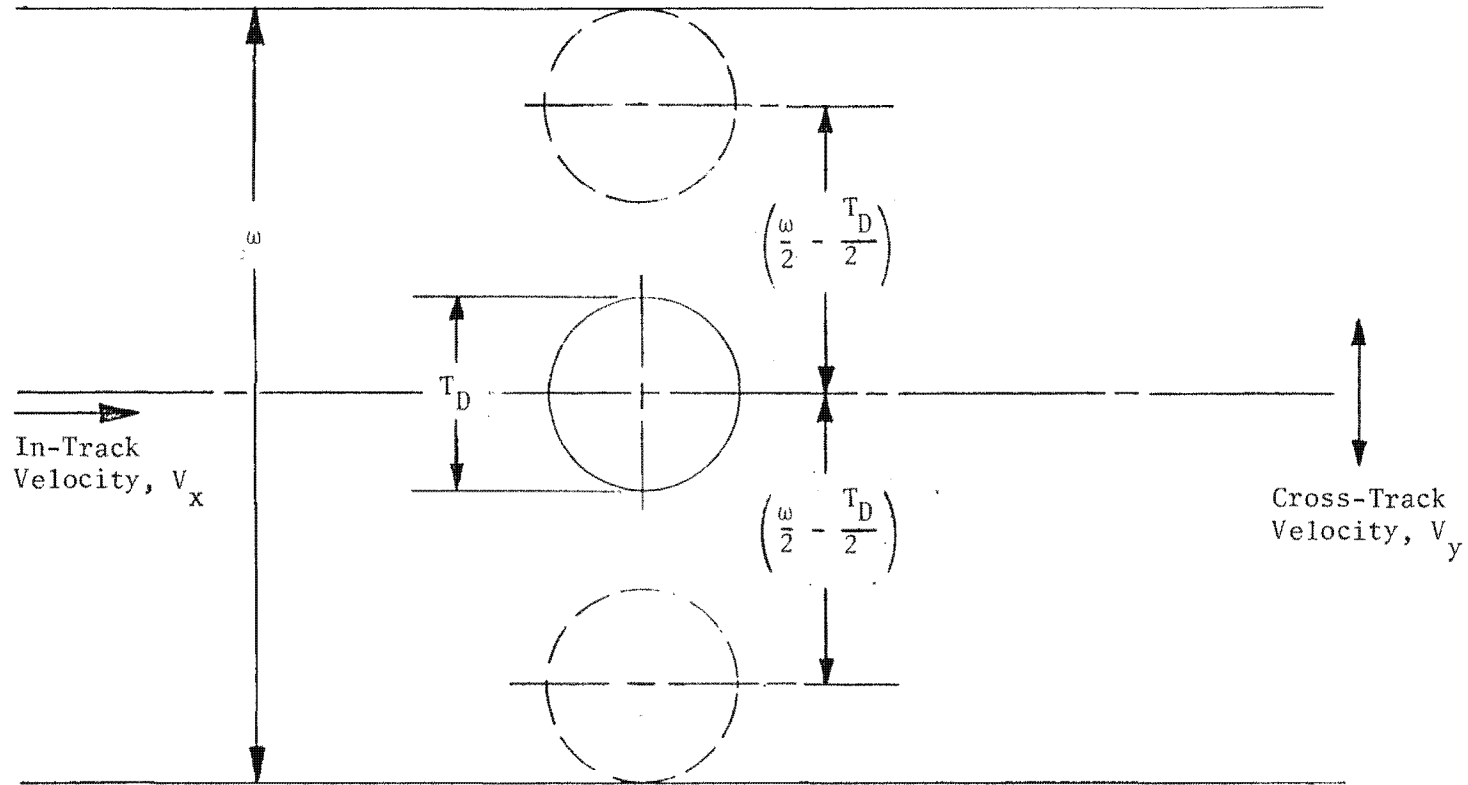
$$R_E (\theta) = R_E \left[\frac{1 - \epsilon^2}{1 - \epsilon^2 \cos^2 \theta} \right]^{1/2}$$

θ = Latitude of interest

ϵ = ellipticity of earth
= 0.08181333

and η_E = rotation rate of earth
= $7.292115855 \times 10^{-5}$ rad/sec

~~TOP SECRET~~ G



2.2-18

Figure 2.2-9. Target-Swath Relationship

~~TOP SECRET~~ GBIF-008- W-C-019838-RI-80

The apparent cross-track velocity is:

$$V_y = V_E \cos A_Z$$

where: $A_Z = \sin^{-1} \left[\frac{|\cos i|}{\cos \theta} \right]$

and, $i =$ inclination of orbit plane

The cross-track position uncertainty arising from earth rotation and time-of-arrival uncertainty is then:

$$\sigma_{y(t)} = \sigma_{tT} V_y$$

where: $\sigma_{y(t)} =$ cross-track position uncertainty

$\sigma_{tT} =$ time-of-arrival uncertainty

$V_y =$ cross track velocity

A cross-track position uncertainty also arises from the target location uncertainty in the cross-track direction. This is independent of the in-track location uncertainty used to develop the time-of-arrival uncertainty, σ_{tT} , and is equal to the target location uncertainty, σ_{TL} . The total cross-track position uncertainty is the root-sum-squared of the two contributors:

$$\sigma_{y(T)} = \sqrt{\sigma_{y(t)}^2 + \sigma_{TL}^2}$$

Examination of Figure 2.2-9 reveals that $\frac{w}{2} - \frac{T_D}{2}$ represents the largest deviation of the LOS for which the target remains completely within the swath. Since $\sigma_{y(T)}$ represents the one-sigma uncertainty, the ratio of $\frac{w}{2} - \frac{T_D}{2}$ to $\sigma_{y(T)}$ is related to the probability of the target being completely encompassed in the swath.

2.2-19
~~TOP SECRET~~ G

Handle via BYEMAN
Control System Only

~~TOP SECRET~~ GBIF-008- W-C-019838-RI-80

$$R = \frac{W - T_D}{2\sigma_y(T)}$$

The associated probability may be found by reference to Figure 2.2-10.

2.3.3.2 Cross-Track Stereoscopic Acquisition. Each separate frame, regardless of whether it is monoscopic or stereoscopic, receives the same attention with respect to aiming. Therefore, the second frame of a stereo pair has the same probability of acquiring the target as the first frame. Hence, the probability of acquiring a target in stereo is the square of the probability of acquiring it in a monoscopic mode.

2.4 Pointing Error Analysis

The pointing error for a given frame is a complex function of the pointing parameters associated with the frame, and the probabilistic errors inherent in each pointing parameter.

2.4.1 Pointing Error Contributors

Contributors to pointing error are listed in Table 2.2-1, with equations for determining the in-track and cross-track components of pointing error for each in nautical miles on the ground. The symbols used in these equations are listed in Table 2.2-2. Total pointing error at any given time is the vector sum of all 13 contributors. Note that some of the terms in this sum would tend to cancel, depending on the sign of such parameters as obliquity angle and stereo angle. (Note: Sign conventions are as shown in Figure 2.1-1.)

~~TOP SECRET~~ G

~~TOP SECRET~~ G

BIF-008- W-C-019838-RI-80

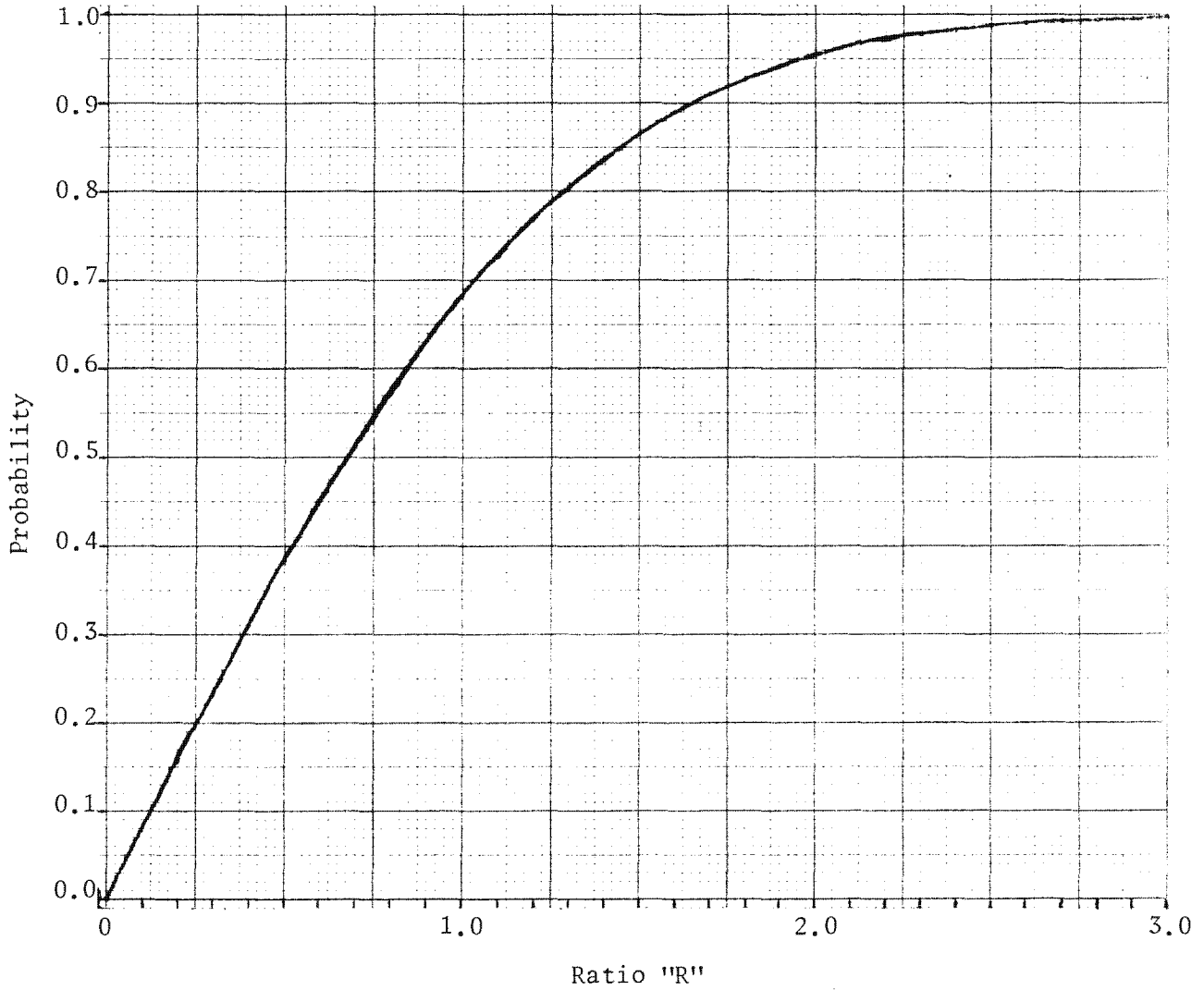


Figure 2.2-10. Probability of Target Within Swath

2.2-21

~~TOP SECRET~~ G

Handle via **BYEMAN**
Control System Only

~~TOP SECRET~~ GBIF-008- W-C-019838-RI-80

TABLE 2.2-1

POINTING ERROR CONTRIBUTORS

<u>Contributor</u>	<u>Equations</u>	<u>Applicable Graphs</u>
1. Pitch attitude and alignment	$X_1 = -h (1 + \tan^2 \Sigma \sec^2 \Omega) A_y$ $Y_1 = h (\tan \Omega \tan \Sigma \sec \Omega) A_y$	2.2-11 2.2-12
2. Roll attitude and alignment	$X_2 = -h (\tan \Omega \tan \Sigma \sec \Omega) A_x$ $Y_2 = h (\sec^2 \Omega) A_x$	2.2-12 2.2-13
3. Yaw attitude and alignment	$X_3 = -h (\tan \Omega) A_z$ $Y_3 = -h (\tan \Sigma \sec \Omega) A_z$	2.2-14 2.2-15
4. Stereo servo	$X_4 = -2h (\Delta \Sigma \sec \Omega \sec^2 \Sigma)$ $Y_4 = 0$	2.2-16 --
5. Crab servo	$X_5 = -h (\tan \Omega \tan \Sigma \sec \Omega) E(5)$ $Y_5 = h (\sec^2 \Omega) E(5)$	2.2-12 2.2-13
6. Altitude	$X_6 = (-\tan \Sigma \sec \Omega) \Delta h$ $Y_6 = \Delta h (\tan \Omega)$	2.2-15 2.2-14
7. Discreteness of roll step	$X_7 = -h (\tan \Omega \tan \Sigma \sec \Omega) E(7)$ $Y_7 = h (\sec^2 \Omega) E(7)$	2.2-12 2.2-13
8. Discreteness of crab step	$X_8 = -h (\tan \Omega \tan \Sigma \sec \Omega) E(8)$ $Y_8 = h (\sec^2 \Omega) E(8)$	2.2-12 2.2-13
9. Target position	$X_9 = E(9)$ $Y_9 = E(9)$	-- --
10. Vehicle nadir position (in-track)	$X_{10} = E(10)$ $Y_{10} = 0$	-- --

2.2-22

~~TOP SECRET~~ GHandle via **BYEMAN**
Control System Only

~~TOP SECRET~~ GBIF-008- W-C-019838-RI-80

TABLE 2.2-1 (Continued)

<u>Contributor</u>	<u>Equations</u>	<u>Applicable Graphs</u>
11. Vehicle nadir position (cross-track)	$X_{11} = 0$	--
	$Y_{11} = E (11)$	--
12. Stereo mirror alignment (stereo)	$X_{12} = -2h (\sec \Omega \sec^2 \Sigma) M_s$	2.2-16
	$Y_{12} = 0$	--
13. Stereo mirror alignment (crab)	$X_{13} = -h (\tan \Omega \tan \Sigma \sec \Omega) M_c$	2.2-12
	$Y_{13} = h (\sec^2 \Omega) M_c$	2.2-13

~~TOP SECRET~~ G

~~TOP SECRET~~ GBIF-008- W-C-019838-RI-80

TABLE 2.2-2

SYMBOLS USED IN POINTING ERROR EQUATIONS

<u>SYMBOL</u>	<u>DEFINITION</u>	<u>UNITS</u>
A_x	Combined roll attitude and alignment errors	Radians
A_y	Combined pitch attitude and alignment errors	Radians
A_z	Combined yaw attitude and alignment errors	Radians
M_c	Angular error in stereo mirror crab alignment	Radians
M_s	Angular error in stereo mirror stereo alignment	Radians
h	Altitude above geoid	Nautical miles
X_i	In-track aiming error due to i^{th} contributor	Nautical miles
Y_i	Cross-track aiming error due to i^{th} contributor	Nautical miles
E(5)	Crab servo error	Radians
E(7)	Discreteness of roll step	Radians
E(8)	Discreteness of crab step	Radians
E(9)	Target position error	Nautical miles
E(10)	Vehicle nadir position error (in-track)	Nautical miles

2.2-24
~~TOP SECRET~~ GHandle via **BYEMAN**
Control System Only

~~TOP SECRET~~ GBIF-008- W-C-019838-RI-80

TABLE 2.2-2 (Continued)

<u>SYMBOL</u>	<u>DEFINITION</u>	<u>UNITS</u>
E(11)	Vehicle nadir position error (cross-track)	Nautical miles
Δh	Uncertainty in knowledge of altitude	Nautical miles
$\Delta \Sigma$	Uncertainty in stereo mirror angle due to positioning mechanism errors	Radians
Σ	Stereo angle of the line of sight	Degrees
Ω	Obliquity angle of the line-of-sight	Degrees

2.2-25

~~TOP SECRET~~ GHandle via **BYEMAN**
Control System Only

~~TOP SECRET~~ GBIF-008- W-C-019838-RI-80

The pointing error equations presented in Table 2.2-1 are plotted in Figures 2.2-11 through 2.2-16 for conventional (Surveillance) altitudes. The figures containing the graphs appropriate to each contributor are identified in the column at the right of Table 2.2-1. The "X" printed in the small matrix in each figure indicates the function covered by that figure. For example, Figure 2.2-11 can be used for finding the in-track component of pointing error due to pitch attitude and alignment (X_1). An example is given below to explain the use of these graphs.

Example: Find the approximate range in pointing error at an 80 nmi altitude due to a crab servo error of -0.01 radian.

- Step 1: Figure 2.2-12 is used for finding the in-track component, X_5 . Place a straightedge on the graph parallel to the lines labeled 206 or 65 (these are the plots of the function at an altitude of 206 nmi and 65 nmi respectively). The straightedge should be positioned to intersect the altitude scale at 80.
- Step 2: The straightedge now represents the function for an obliquity of 45 degrees and stereo angle of ± 8.65 degrees and is seen to intersect the 0.01 radian ordinate at approximately 0.17 nmi on the pointing error scale.
- Step 3: To find the pointing error at other obliquity angles, slide the straightedge down and to the right along the obliquity scale, maintaining the parallel relationship with the plotted functions. The marks on the obliquity scale represent the lateral distance to move the straightedge from a reference obliquity to some other obliquity angle. For example, for an obliquity of 5 degrees the straightedge is moved from its position in step 2 down along the obliquity scale line a distance equal to that between the 45-degree and 5-degree marks. This is seen to result in pointing error of approximately 0.011 nmi for the 5-degree case. As indicated in the note, the pointing error is zero for zero obliquity, and zero for all obliquities at the zero stereo angle position.
- Step 4: Figure 2.2-13 is used for finding the cross-track component, Y_5 . As before, place a straightedge on the graph parallel to the plotted lines and intersecting the altitude scale at 80 nmi. This represents the function for an obliquity of 45 degrees and all stereo angles, and is seen to intersect the 0.01 radian ordinate at approximately 1.6 nmi on the pointing error scale.

~~TOP SECRET~~ G

~~TOP SECRET~~ G

BIF-008- W-C-019838-RI-80

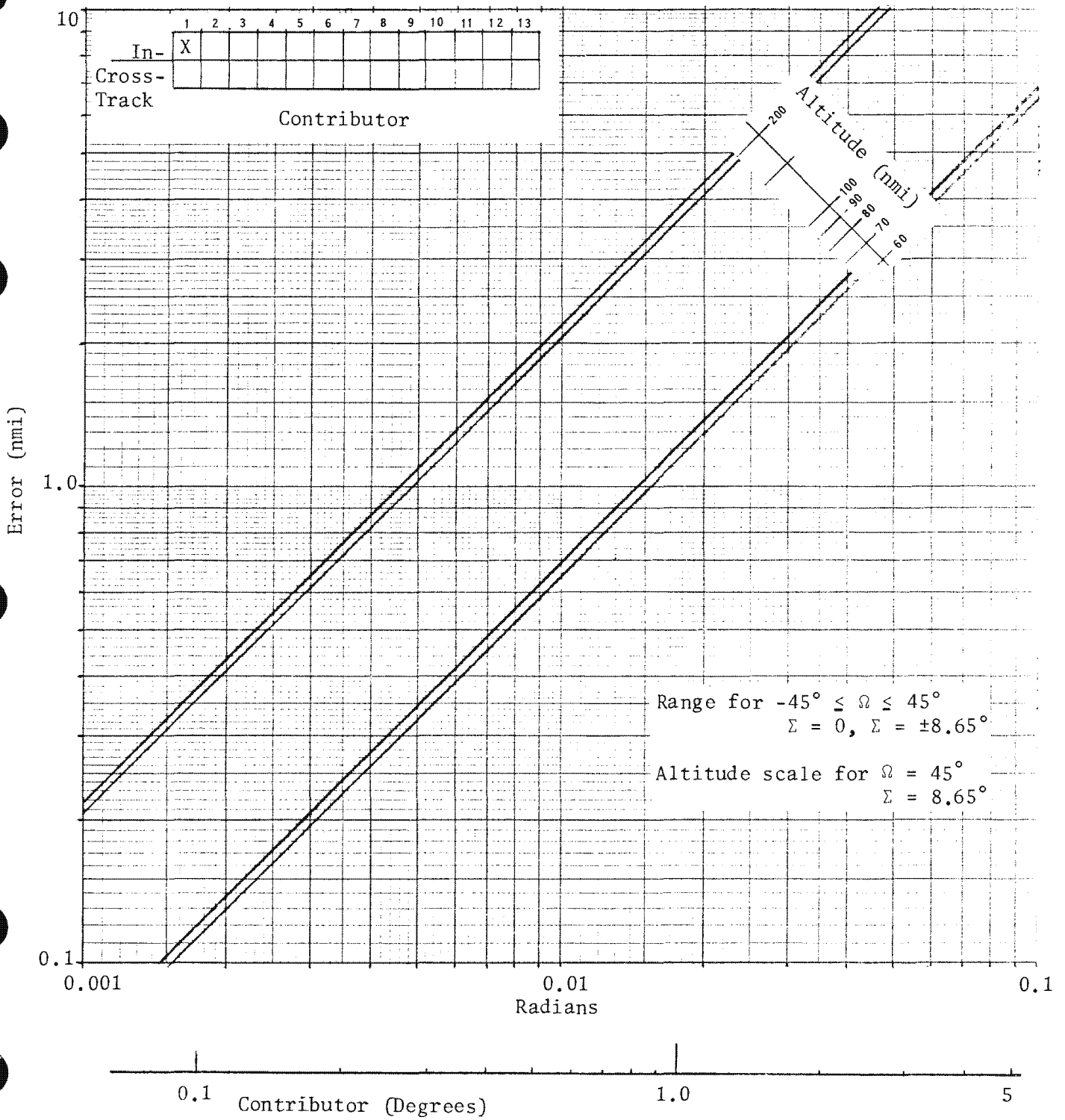


Figure 2.2-11. Pointing Error vs Error Contributor

2.2-27

~~TOP SECRET~~ G

Handle via BYEMAN
Control System Only

~~TOP SECRET~~ G

BIF-008- W-C-019838-RI-80

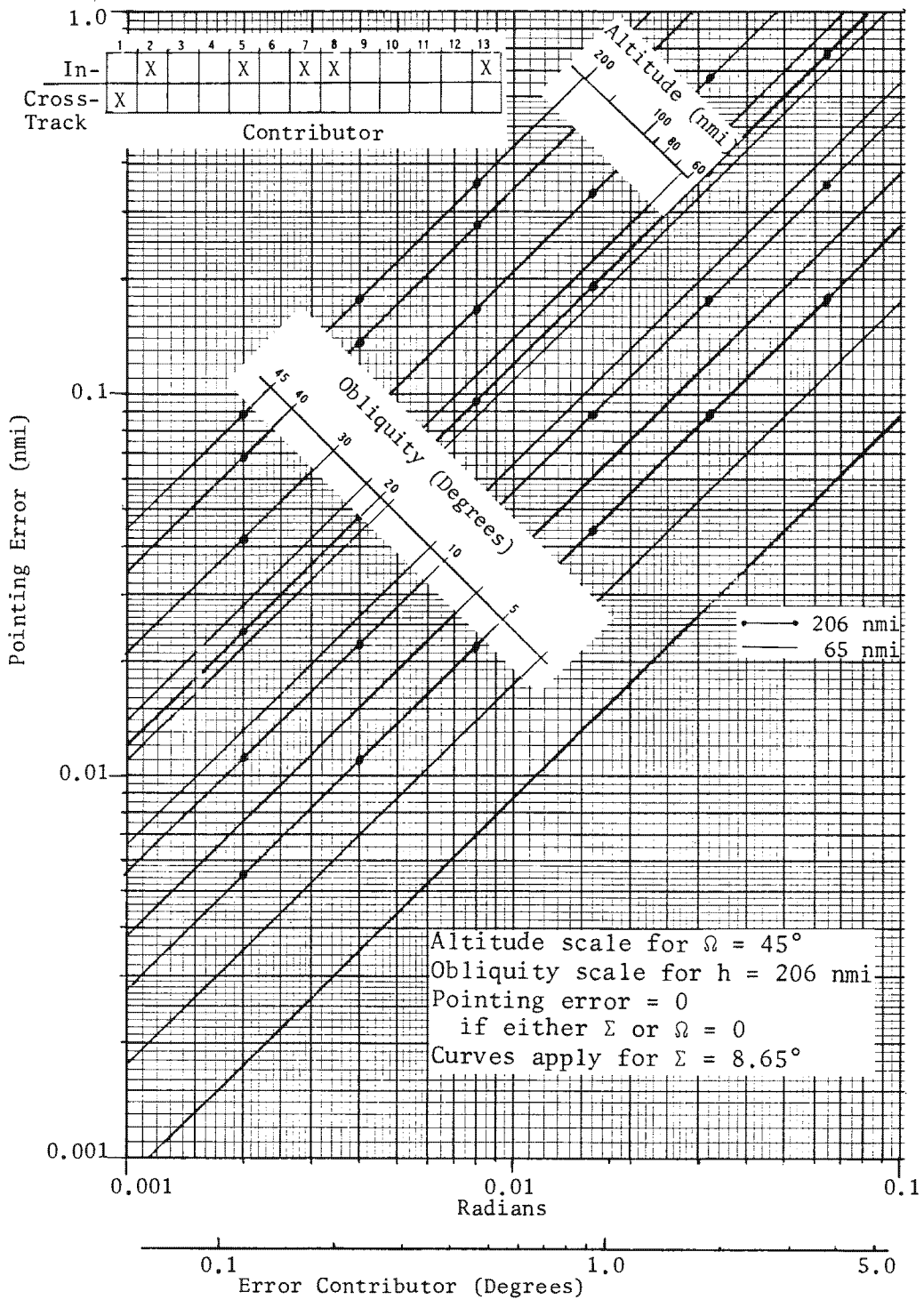


Figure 2.2-12. Pointing Error vs Contributor

2.2-28

~~TOP SECRET~~ G

Handle via BYEMAN
Control System Only

~~TOP SECRET~~ G

BIF-008-W-C-019838-RI-80

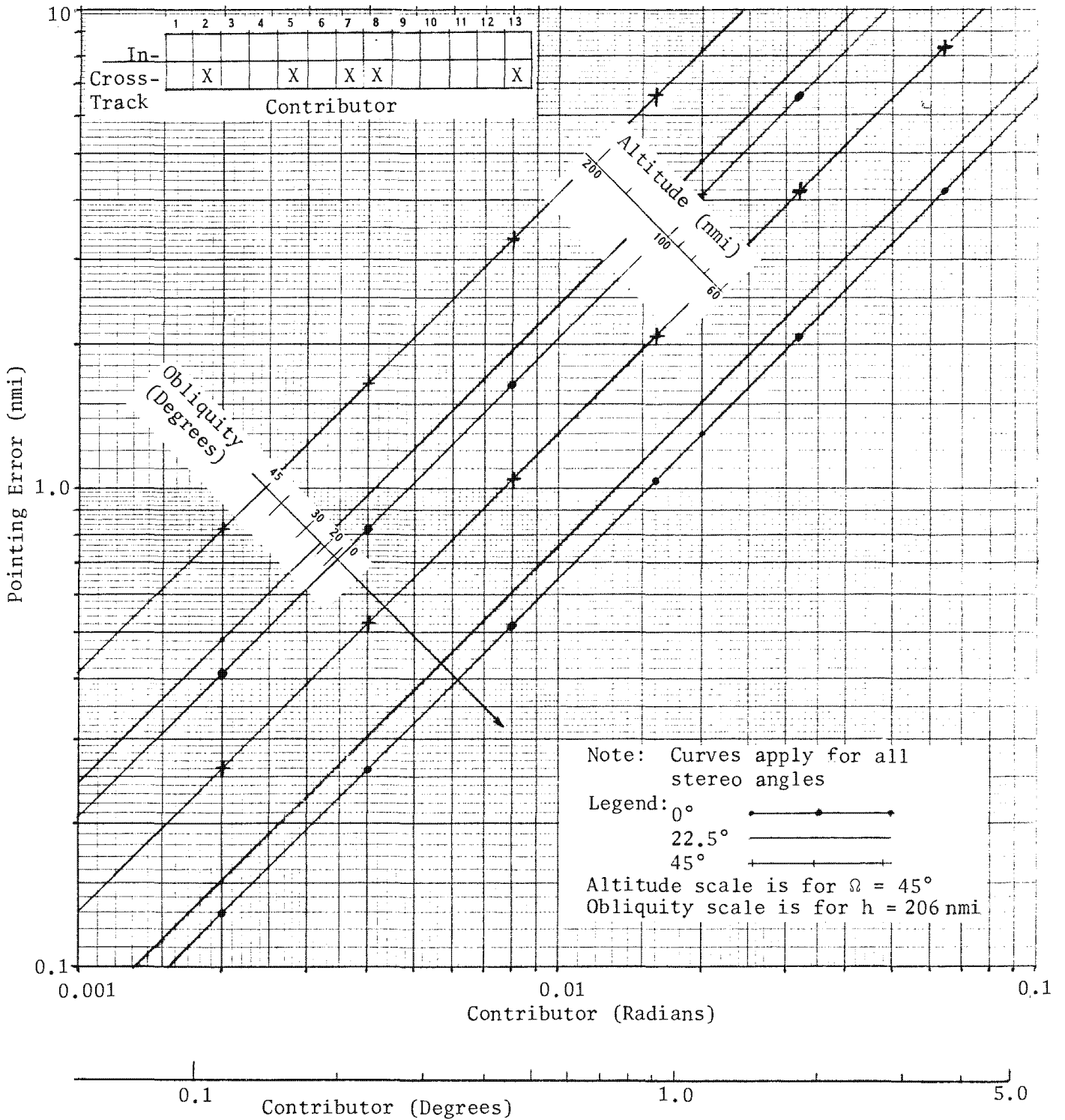


Figure 2.2-13. Pointing Error vs Contributor

2.2-29

~~TOP SECRET~~ G

Handle via BYEMAN
Control System Only

~~TOP SECRET~~ G

BIF-008- W-C-019838-RI-80

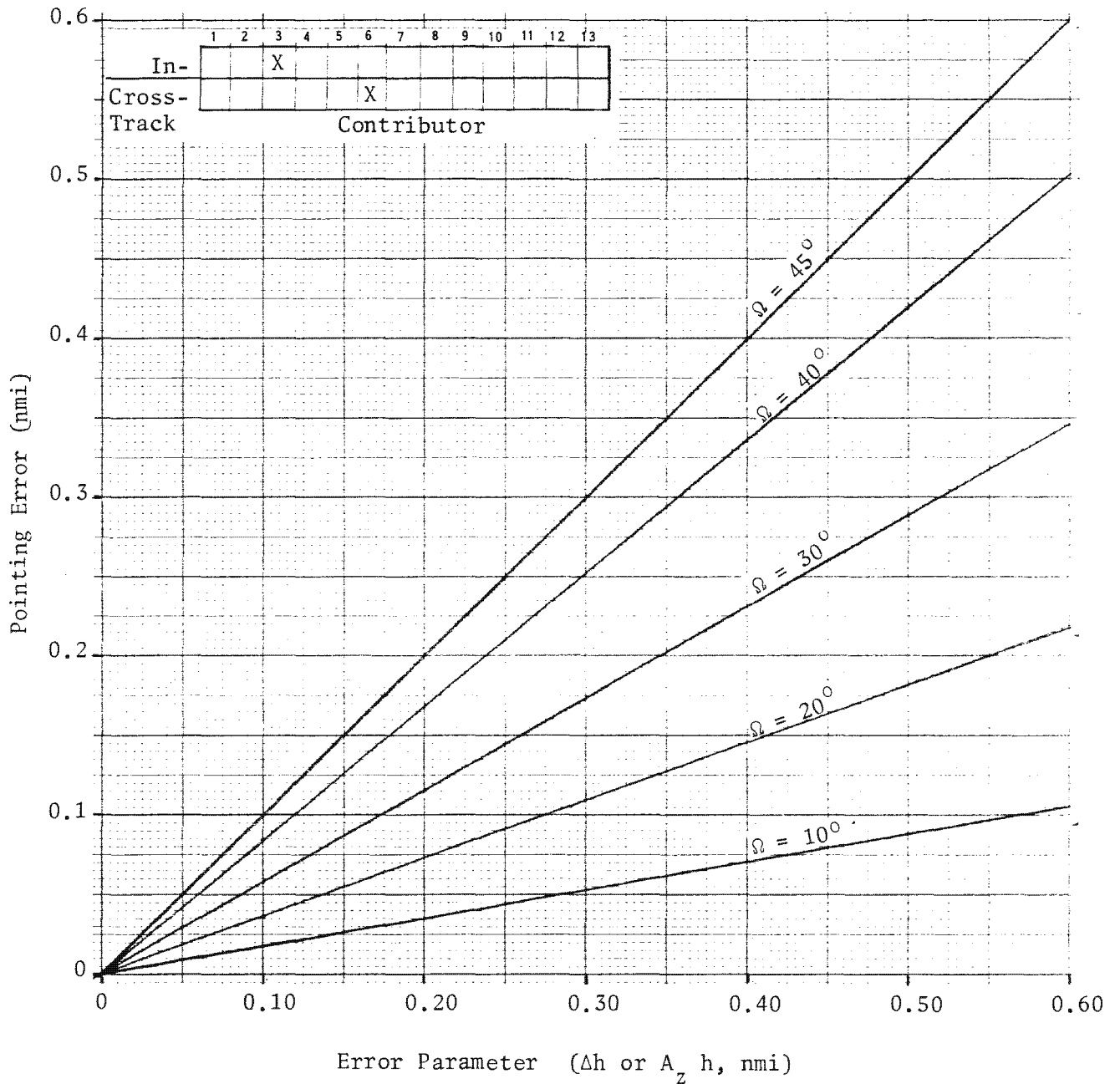


Figure 2.2-14. Error Parameter vs Pointing Error

2.2-30

~~TOP SECRET~~ G

Handle via **BYEMAN**
Control System Only

~~TOP SECRET~~ G

BIF-008- W-C-019838-RI-80

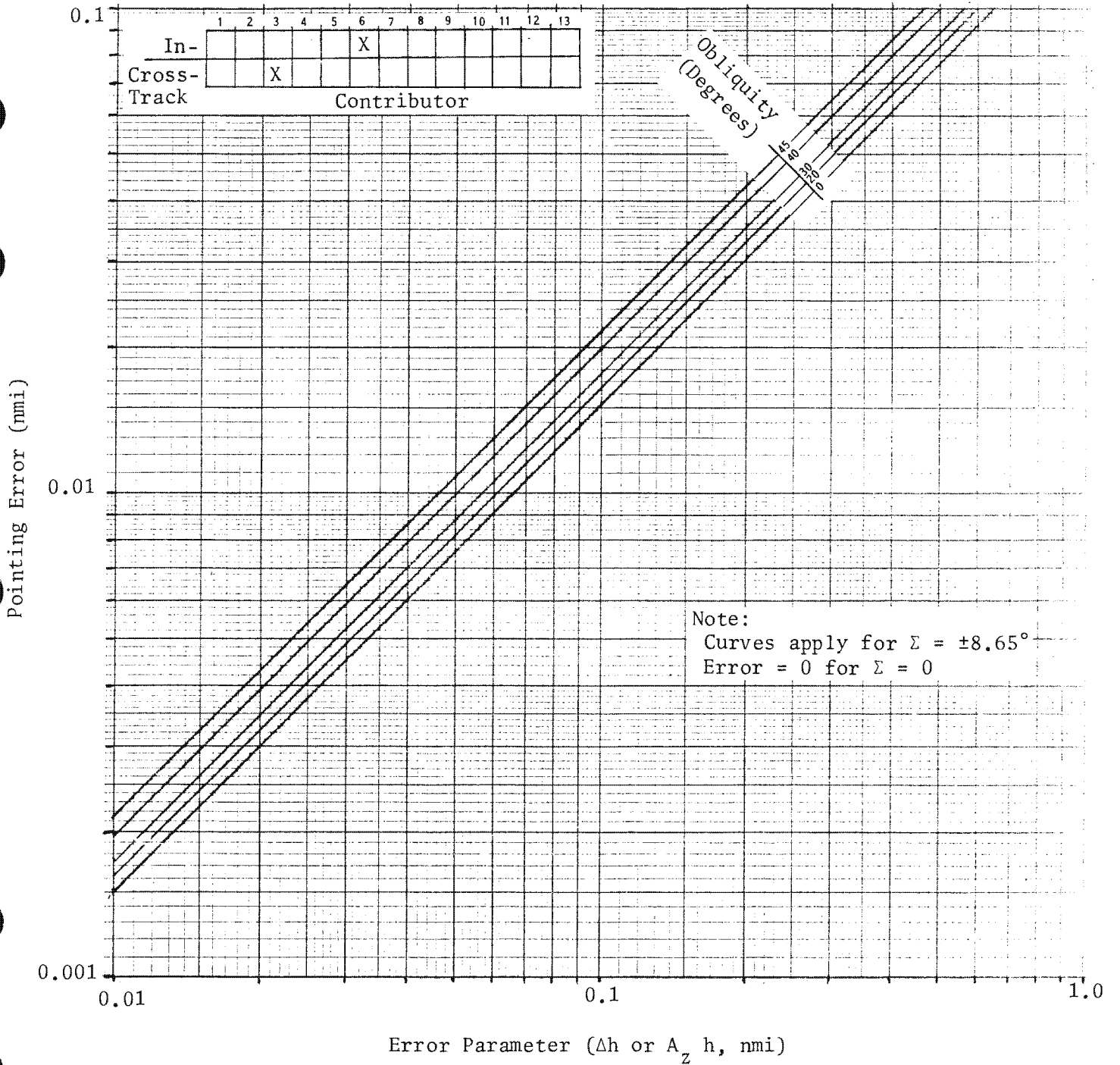


Figure 2.2-15. Error Parameter vs Pointing Error

2.2-31

~~TOP SECRET~~ G

Handle via BYEMAN
Control System Only

~~TOP SECRET~~ G

BIF-008- W-C-019838- RI-80

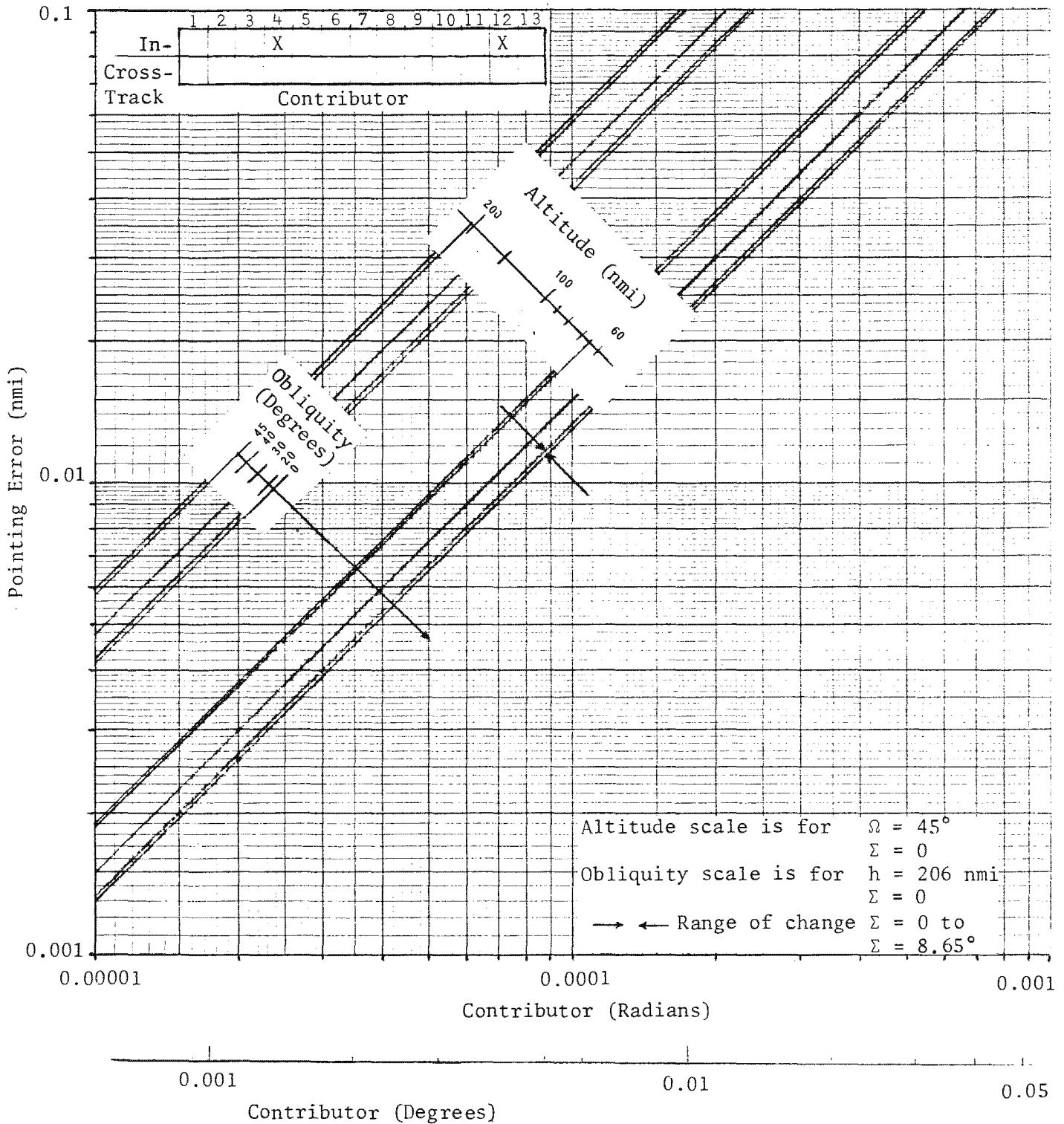


Figure 2.2-16. Pointing Error vs Contributor
2.2-32

~~TOP SECRET~~ G

Handle via BYEMAN
Control System Only

~~TOP SECRET~~ GBIF-008- W-C-019838-RI-80

Step 5: To find the pointing error at other obliquity angles, slide the straightedge down and to the right along the obliquity scale, maintaining the parallel relationship with the plotted functions. The marks on the obliquity scale represent the lateral distance to move the straightedge from a reference obliquity to some other obliquity angle. For example, for an obliquity of 20 degrees the straightedge is moved from its position in step 4 down along the obliquity scale line a distance equal to that between the 45-degree and 20-degree marks. This is seen to result in a pointing error of approximately 1.0 nmi for the 20-degree case.

Step 6: If the sign of the error is desired, inspection of the terms of the equations can be made, remembering that the tangent of a negative angle of 90 degrees or less is negative, and the secant of a negative angle of 90 degrees or less is positive.

Figures 2.2-14 and 2.2-15 are entered with the uncertainty in altitude, Δh , in nautical miles or with the product of the combined yaw attitude and alignment errors, A_z , and the altitude. For the latter case, altitude is in nautical miles and the yaw error in radians.

The pointing errors derived from the plots given may be extended to EAC altitude ranges through scaling by slant range. Figure 2.2-17 is provided to assist the reader in this scaling. To estimate pointing errors for the EAC operating range, (1) find the pointing error, in nautical miles, from the appropriate figure using an altitude of 200 nmi, an obliquity of 30 degrees and a stereo angle of 8.65 degrees. Next, (2) find the slant range for the case in question from either the slant-range equation, (1), page 2.2-7, or Figure 2.2-4. Then (3) enter Figure 2.2-17 at the appropriate slant-range and obtain multiplier. Finally, (4) multiply the multiplier obtained above by the pointing error derived in step one (1).

~~TOP SECRET~~ G

~~TOP SECRET~~ G

BIF-008-W-C-019838-RI-80

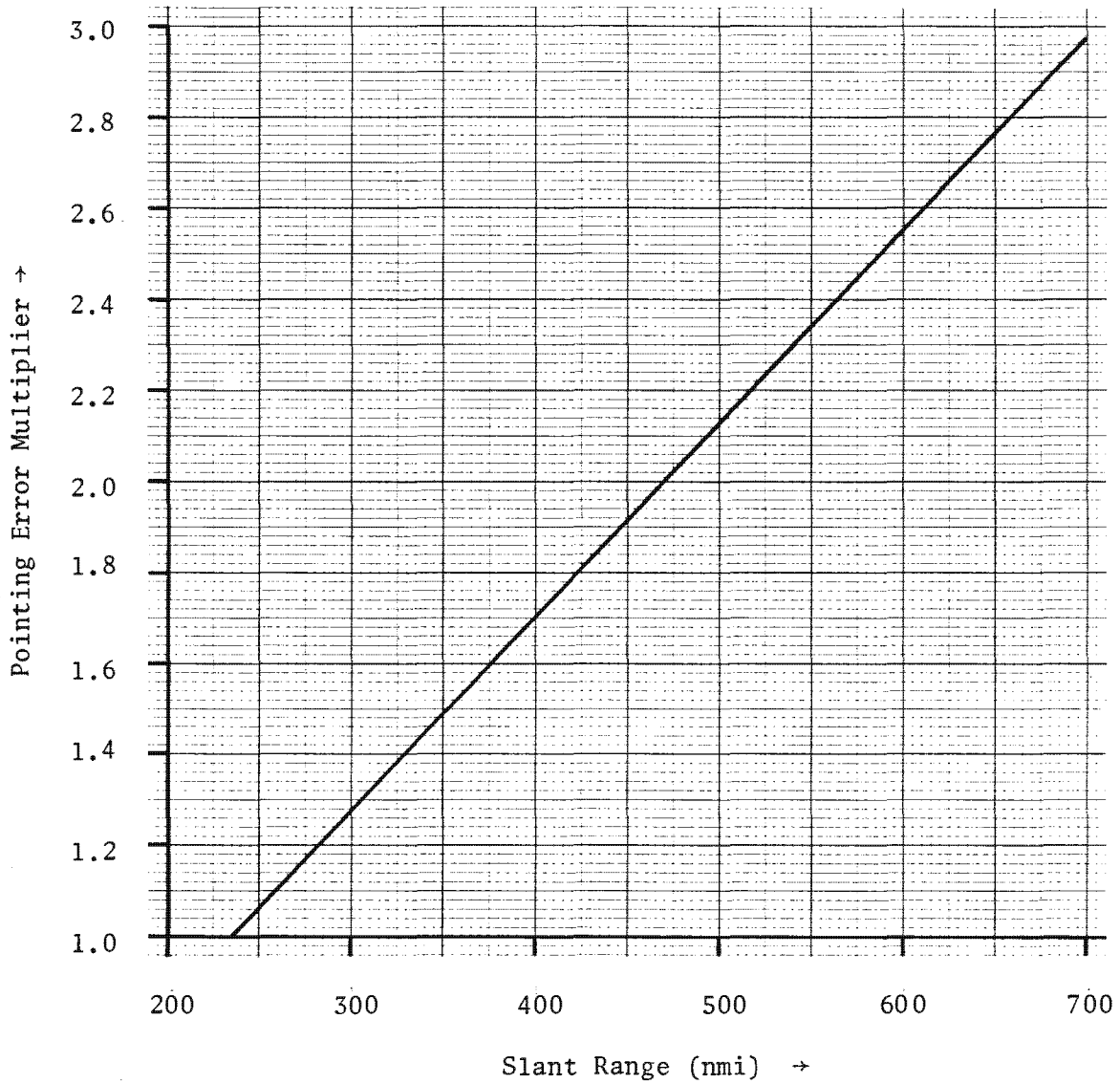


Figure 2.2-17. Pointing Error Multiplier vs. Slant Range
(Based on 200 nmi altitude, $\Omega = 30^\circ$, $\Sigma = 8.65^\circ$)

2.2-34

~~TOP SECRET~~ G

Handle via BYEMAN
Control System Only

~~TOP SECRET~~ GBIF-008- W-C-019838-RI-80

2.4.2 Pointing Error Limits

Sources of PSV pointing error are summarized in Tables 2.2-3 and 2.2-4. The tolerances, distributions, 95-percent bias error and 95/95-percent error are taken from values in the General System Specification. The pointing errors, (95-percent bias error and 95/95-percent error) were calculated using the criteria of Appendix E of this document for combining means and standard deviations. Note that Table 2.2-4 combines errors for the PSV and that Table 2.2-3 details those contributors allocated and attributable to the PPS/DP EAC. Cross-track pointing errors are shown for two different conditions: 8.65-degree stereo angle, 0-degree obliquity and at 90 nmi or 65 nmi altitude.

The values in these tables reflect an error reducing software technique called adaptive bias. Adaptive biasing corrects the pointing for predictable error contributors such as thermal hotdogging and roll attitude. (It is not intended to fully explain adaptive biasing here, as it is a LMSC responsibility, but merely to point out that errors reported herein do take into consideration this adaptive biasing capability.)

2.2-35

~~TOP SECRET~~ GHandle via BYEMAN
Control System Only

TABLE 2.2-3

PPS/DP EAC POINTING ERROR CONTRIBUTORS*

<u>Contributor</u>	<u>Tolerance</u>	<u>Distribution</u>	<u>Standard Deviation</u>				
			<u>Between Mission</u>	<u>Within Mission</u>	<u>95% Bias Error</u>	<u>95%/95% Error</u>	
<u>Roll Attitude and Alignment</u>						0.170	0.176
Between Mission:							
LOS to mechanical interface	± 0.018	Normal	0.006	0.000			
Crab Positioning	± 0.15	Uniform	0.087	0.000			
Within Mission:							
Crab LOS reproducibility	± 0.010	Normal	0.000	0.0033			
<u>Pitch Attitude and Alignment</u>						0.170	0.176
Between Mission:							
LOS to mechanical interface	± 0.019	Normal	0.006	0.000			
Stereo Positioning	± 0.15	Uniform	0.087	0.000			
Within Mission:							
Stereo LOS reproducibility	± 0.010	Normal	0.000	0.0033			
<u>Yaw Attitude and Alignment</u>						0.012	0.012
Between Mission:							
LOS to mechanical interface	± 0.019	Normal	0.006	0.000			

* All figures are in degrees.

Graph does not include hotdog errors and crab granularity which are included in SCS budget.

Approved for Release: 2017/02/14 C05097211

2.2-36

Approved for Release: 2017/02/14 C05097211

TABLE 2.2-4

PSV POINTING ERROR BUDGET*

<u>PSV Contributors</u>	<u>Mean Bias Error</u>	<u>Between Mission Standard Dev</u>	<u>Within Mission Standard Dev</u>	<u>95% Bias Error</u>	<u>95%/95%</u>	<u>95%/95% Error (nmi), Cross-Track</u>	
						$\Sigma = 8.65^\circ, \Omega = 0^\circ, X = 0^\circ$	$h = 90 \text{ nmi} \quad h = 400 \text{ nmi}$
<u>Roll Attitude & Alignment:</u>							
SCS	0.011	0.060	0.167	0.119	0.395		
PPS/DP	0.000	0.087	0.003	0.170	0.176		
Total	0.011	0.106	0.167	0.209	0.489	0.678 nmi	3.349 nmi
<u>Pitch Attitude & Alignment:</u>							
SCS	0.033	0.086	0.098	0.180	0.341		
PPS/DP	0.004	0.087	0.014	0.170	0.193		
Total	0.037	0.122	0.099	0.251	0.414	0.000 nmi	0.000 nmi
<u>Yaw Attitude & Alignment:</u>							
SCS	0.026	0.074	0.111	0.154	0.336		
PPS/DP	0.044	0.009	0.015	0.059	0.083		
Total	0.070	0.075	0.112	0.194	0.379	0.091 nmi	0.450 nmi
Target Location Uncertainty**	(One σ value, nmi)			0.214			
Ephemeris Uncertainty**	(One σ value, nmi)			0.083			

* With adaptive bias and software (includes residual hotdog error assuming 75% correction)

** Best estimate supplied by LMSC as of 12/75.

Note: All figures are in degrees except where otherwise noted.

2.2-37

Approved for Release: 2017/02/14 C05097211

Approved for Release: 2017/02/14 C05097211

~~TOP SECRET~~ G

BIF-008-W-C-019838-RI-80

This Page Intentionally Blank

2-2-38

~~TOP SECRET~~ G

Handle via **BYEMAN**
Control System Only

~~TOP SECRET~~ GBIF-008- W-C-019838-RI-80

3.0 IMAGE MOTION COMPENSATION (IMC)

The 9 x 5 photographic payload section/dual platen extended altitude capability (PPS/DP EAC) employs two means which attempt to eliminate relative image motion during photography. First, the stereo mirror is positioned (within granularity limits) to a preferred crab angle,* χ , which has the effect of reducing cross-track axial image velocity, \dot{s}_{y_0} , to near zero (neglecting perturbations). Second, the photographic film is driven (within granularity limits) at a preferred velocity, V_f , which matches the in-track axial image velocity, \dot{s}_{x_0} , for the crabbed system. The equations for crab angle and film velocity are discussed in this section.

A comprehensive document on image motion compensation for a photographic system employing a two-gimballed mirror was prepared in 1971 for this program. This document derived the transformation equations (in matrix form) which describe the image vector of the 9 x 5 photographic system. Due to the complexity and magnitude of this derivation, no attempt is made to reproduce it here and interested readers are referred to BIF-008 document K-085772-RH, dated 9-3-71, for the detailed analysis. Image motion compensation equations discussed herein are reproduced from this referenced document.

*Crab about roll axis only.

~~TOP SECRET~~ G

~~TOP SECRET~~ GBIF-008- W-C-019838-RI-803.1 Crab

3.1.1 Nine-Inch System

Directional alignment of the image velocity vector with the film-drive velocity vector is achieved by rotating the stereo mirror about the roll (X) axis. Because of the orientation of the stereo mirror at 45 degrees (± 8.65 degrees) to the X -axis, a rotation with respect to the platen axis also occurs. This rotation of the stereo mirror relative to the platen axis, termed "crabbing," produces the desired rotation of the image velocity vector and a concomitant deviation of the line-of-sight in the cross-track direction (see Part 2, Section 2). Crabbing is performed as a set-up operation prior to photography.

Selection of the crab angle for each frame is based on both image velocity vector alignment and pointing considerations. The obliquity angle (Ω) is equal to the sum of the vehicle roll angle (Ω_V) and the crab angle (χ) for a crab-about-roll system (see Figure 2.3-1).

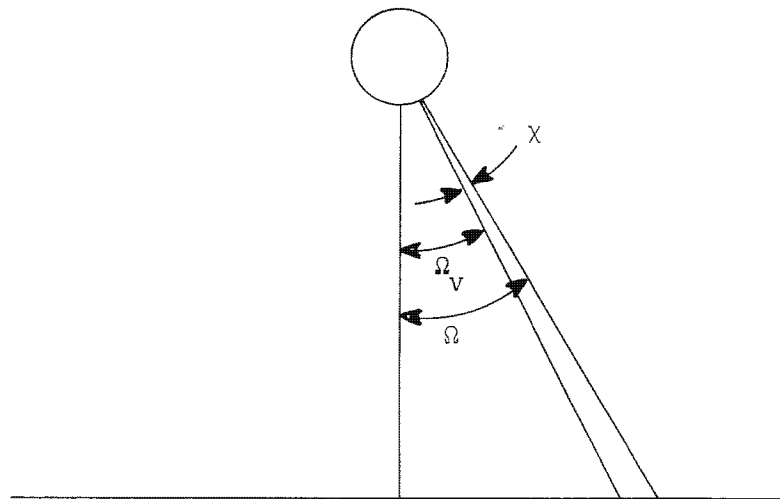


Figure 2.3-1. Roll, Crab and Obliquity

2.3-2

~~TOP SECRET~~ GHandle via BYEMAN
Control System Only

~~TOP SECRET~~ GBIF-008- W-C-019838-RI-80

Twenty-three different crab angles are selectable by command.* These crab angles range from -3.85 degrees to +3.85 degrees and are spaced at 0.35-degree intervals. This range covers worst cases (encountered on most probable missions) which occur at or near the equator where the earth rotation velocity is highest. In general, for southbound photography, negative crab angles (BIF-008 sign convention) are required, for northbound passes, positive angles are necessary. Pointing considerations for photographs at higher latitudes may dictate an occasional reversal of this generality.

The equation for the crab angle is:

$$\chi = \tan^{-1} \left[\frac{V_y \cos \Omega + V_z \sin \Omega}{V_x \cos \Sigma + V_y \sin \Sigma \sin \Omega - V_z \sin \Sigma \cos \Omega} \right]$$

where:

- V_x = in-track component of vehicle-target relative velocity measured in the target plane, nmi/sec
- V_y = cross-track component of vehicle-target relative velocity measured in the target plane, nmi/sec
- V_z = vertical component of vehicle-target relative velocity measured with respect to the target plane, nmi/sec
- Σ = stereo angle, degrees
- Ω = obliquity angle, degrees

*These angles include eleven in each direction and zero. Each commanded angle (except for the extremes) actually results in a slightly different position depending on the direction from which the position is approached. Crab step selection software is configured to make use of this effect to optimize crab angle whenever time permits.

~~TOP SECRET~~ G

~~TOP SECRET~~ GBIF-008-W-C-019838-RI-80

3.1.2 Five-Inch System

Differences in crab angle between the nine-inch system and the five-inch system are negligible and therefore the crab angle calculated for the nine-inch system is used for the five-inch system.

3.2. Film-Drive Speed

3.2.1 Nine-Inch System

Film-drive speed (FDS) is determined from the following equation:

$$V_f = \frac{F}{a} [V_x \cos \Sigma \cos \chi + V_y (\sin \chi \cos \Omega + \sin \Sigma \cos \chi \sin \Omega) + V_z (\sin \chi \sin \Omega - \sin \Sigma \cos \chi \cos \Omega)]$$

where: V_f = film velocity, inches per second (in a plane parallel to the Z-Y plane and tangent to the 9-inch platen)
 F = lens focal length, inches
 a = slant range, nmi.

Slant range is determined from the following equation:

$$a = (h + R_E) \cos \Sigma \cos \Omega - [(h + R_E)^2 \cos^2 \Sigma \cos^2 \Omega - h^2 - 2R_E h]^{1/2}$$

where: h = height of vehicle over assumed spherical earth
 R_E = spherical earth radius (3438.15 nmi.)
 Σ = stereo angle
 Ω = obliquity angle

2.3-4
~~TOP SECRET~~ GHandle via BYEMAN
Control System Only

~~TOP SECRET~~ GBIF-008- W-C-019838-RI-80

A good first approximation for film velocity is:

$$V_f = V_{cx} \frac{F}{a} \cos \Sigma,$$

where: F = focal length, inches

a = slant range, nmi.

Σ = stereo angle, degrees

V_{cx} = in-track ground velocity of a satellite in circular orbit, nmi/sec

The parameter V_{cx} may be calculated from:

$$V_{cx} = R_E \cdot \dot{\theta} = R_E \left[\frac{\mu}{(R_E + h)^3} \right]^{\frac{1}{2}}$$

In which:

R_E = mean earth radius, 3438.15 nmi.

h = vehicle altitude over the geoid

μ = gravitational parameter, $62750.59172 \frac{(\text{nmi})^3}{\text{sec}^2}$

$\dot{\theta}$ = angular velocity of a vector from earth center to the vehicle

Figure 2.3-2 shows V_{cx} as a function of circular orbit altitude. For eccentric orbits, at altitudes below the mean altitude, the in-track ground velocity is greater than the circular velocity for that altitude. The values from Figure 2.3-2 may therefore be considered lower limits when eccentric orbits are being considered.

Calculations of limiting cases (film-drive speeds of 0.8425 and 11.8 in./sec) show that it is possible to obtain photographs with correct film-drive velocities with slant ranges varying from 65 nmi to about 710 nmi. To meet smear-limitation requirements, the calculated film velocity for each frame must be provided

2.3-5

~~TOP SECRET~~ GHandle via BYEMAN
Control System Only

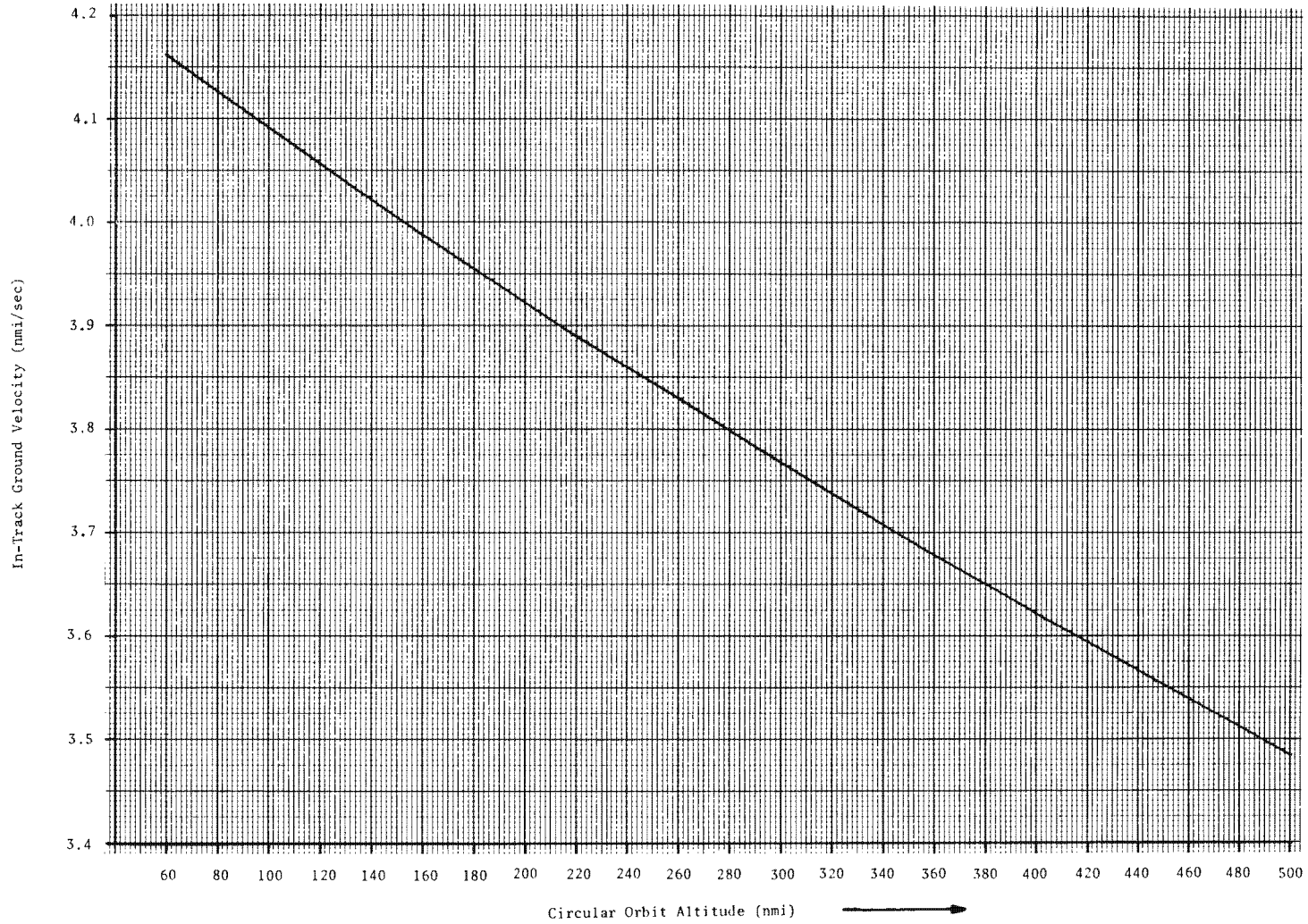


Figure 2.3-2. Ground Velocity for Circular Orbit (V_{CX})

Handle via **BYEMAN**
Control System Only

Approved for Release: 2017/02/14 C05097211

Approved for Release: 2017/02/14 C05097211

2-3-6

~~TOP SECRET~~ GBIF-008- W-C-019838-RI-80

within 0.086 percent, 95 percent of the time. Figure 2.3-3 shows plots of the required film-drive speeds versus altitude as a function of obliquity angle and stereo angle.

3.2.2 Five-Inch System

The line-of-sight (LOS) of the 5-inch system trails that of the 9-inch system due to the location of the 5-inch folding mirror, 0.725 inch below (-Z direction) the optical axis. This location difference results in a difference in the film-drive speeds required by the two systems for image motion compensation. A rigorous analysis yields the following expression:

$$\Delta V_f = - \frac{0.725}{h_T} \left\{ \begin{aligned} &[-\sin \chi \sin \Omega + \sin \Sigma \cos \chi \cos \Omega] [(-\cos \Sigma \cos \chi) V_x - \\ &(\sin \chi \cos \Omega + \sin \Sigma \cos \chi \sin \Omega) V_y + (-\sin \chi \sin \Omega + \sin \Sigma \\ &\cos \chi \cos \Omega) V_z] + [\cos \Sigma \cos \Omega] [(-\sin \Sigma) V_x + (\cos \Sigma \sin \Omega) V_y \\ &+ (-\cos \Sigma \cos \Omega) V_z] \end{aligned} \right\}$$

Although the expression is theoretically correct, it is somewhat cumbersome and inefficient for operational usage. The software contractor shortened the equation considerably by factoring out the crab angle (χ) dependency:

$$\Delta V_f = \frac{0.725}{h_T} \left[\begin{aligned} &(\cos \Omega \sin 2 \Sigma) V_x \\ &- (\cos^2 \Sigma \sin 2 \Omega) V_y \\ &+ (\cos^2 \Omega \cos^2 \Sigma - \sin^2 \Omega) V_z \end{aligned} \right]$$

The approximate film-drive speed (FDS) bias (ΔV_f) from the 9-inch FDS required for image motion compensation in the center of the 5-inch format is indicated as a function of slant range and stereo angle in Figure 2.3-4.

2.3-7

~~TOP SECRET~~ GHandle via **BYEMAN**
Control System Only

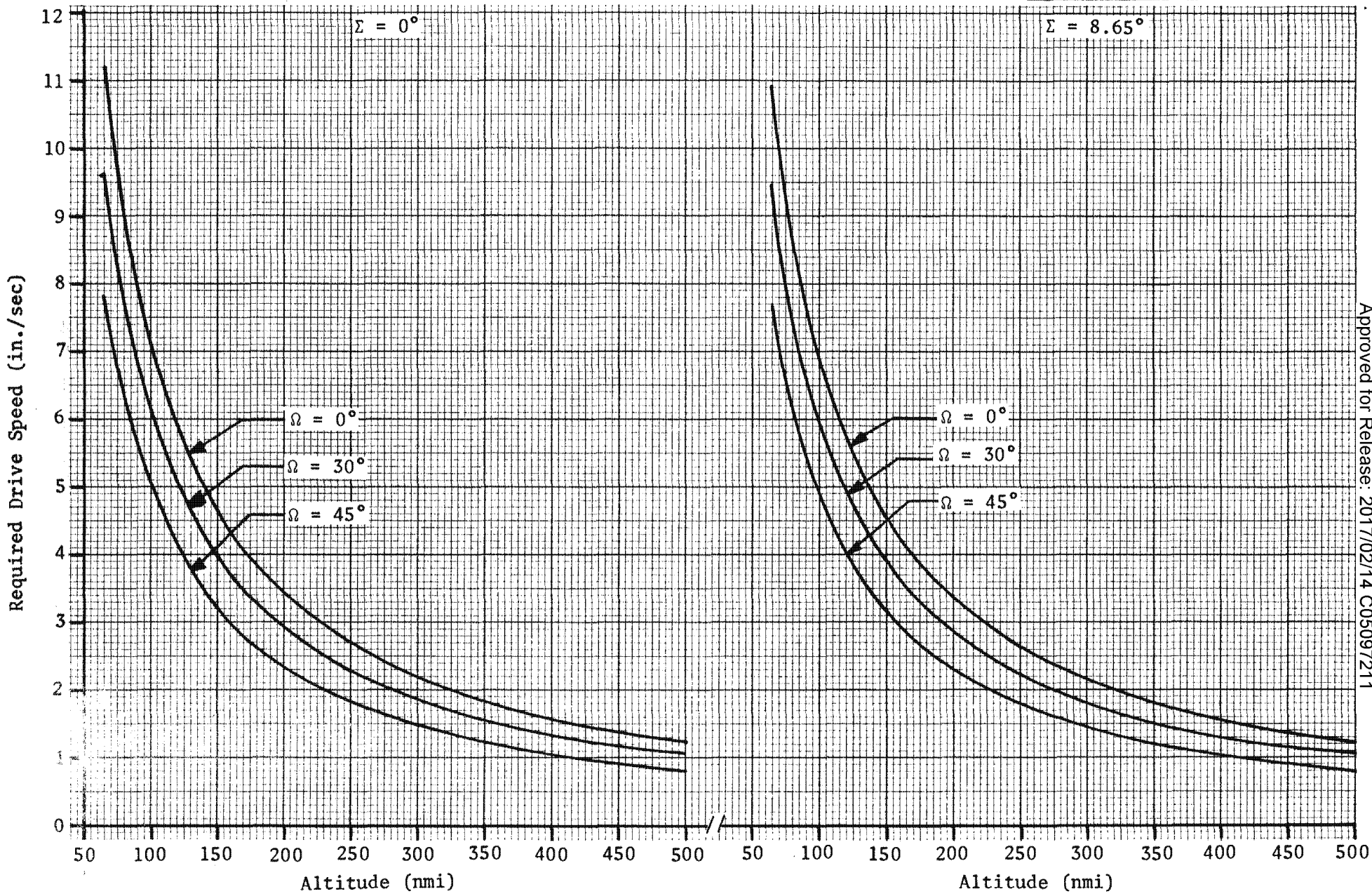


Figure 2.3-3. Required Film Velocity vs. Altitude

Handle via BYEMAN
Control System Only

Approved for Release: 2017/02/14 C05097211

2.3-8

Approved for Release: 2017/02/14 C05097211

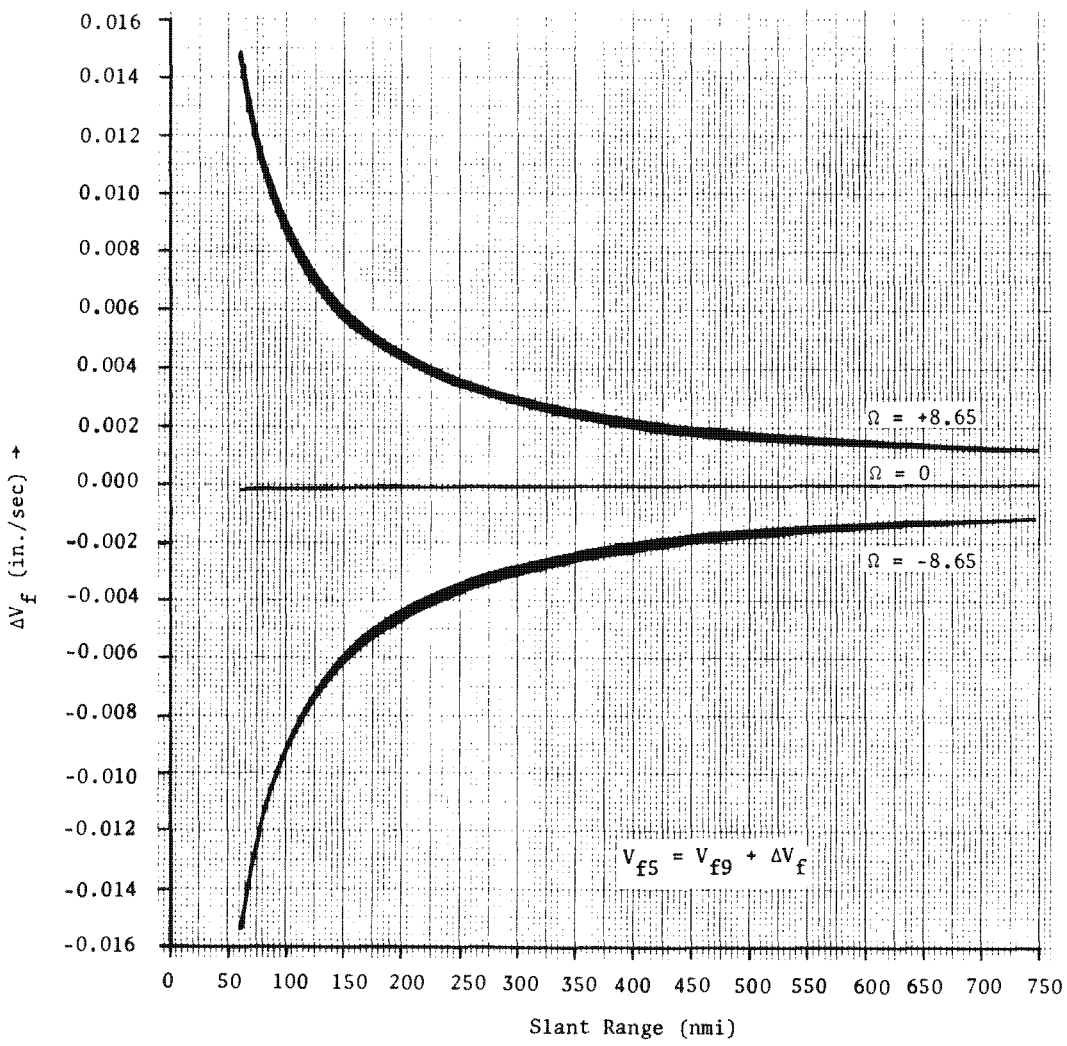


Figure 2.3-4. Film-Drive Speed Bias Approximation

Approved for Release: 2017/02/14 C05097211

2.3-9

Approved for Release: 2017/02/14 C05097211

~~TOP SECRET~~ GBIF-008- W-C-019838-RI-80

In actual practice, targeting is accomplished as if all photography will occur using the 9-inch system. After the required parameters have been calculated, i.e., stereo angle (Σ), crab angle (χ), obliquity angle (Ω), camera ON and OFF times, and FDS (V_f), the latter two are biased if the photograph is to be taken by the 5-inch system. The required camera ON and OFF times are computed as described in Part 2, Section 2. The required FDS for the 5-inch system (V_5) is computed by adding the FDS bias to the unquantized 9-inch FDS:

$$V_5 = V_f + \Delta V_f$$

Because there is only one FDS memory in the command processor (CP), only one FDS step may be commanded at any given time. This presents a conflict in cases where both the 9-inch and 5-inch systems will be operating simultaneously with different FDS steps required for each. The operational software chooses which system to optimize in such cases (normally the 9-inch system is preferred), and the other system must be operated at the less-than-optimum FDS. Some image degradation (smear) may result from improper IMC in conflict cases.

2.3-10

~~TOP SECRET~~ GHandle via BYEMAN
Control System Only

~~TOP SECRET~~ GBIF-008- W-C-019838-RI-80

4.0 IMAGE SMEAR

Smear occurs when an aerial image moves relative to the recording medium during exposure. Vehicle velocity, earth rotation, and terrain variations combine to produce considerable motion between an orbiting vehicle and a scene to be photographed. A strip-camera system attempts to compensate for this motion by moving the film at precisely the same rate as the scene translates during an exposure. Perfect image motion compensation (IMC) would reduce the smear to zero by matching the image-motion vector to the film-motion vector in both magnitude and direction (see Part 2, Section 3). In general however, there are residual IMC errors resulting from pointing uncertainties and hardware tolerances. For the Gambit system, there are additional errors introduced because of the stepwise progression of crab angles, roll angles, and film-drive speeds. Smear can be tolerated to the extent that its effect on performance does not decrease quality below the design goal. This section describes the effects of smear and identifies known smear contributors and their specified tolerances. A technique used to measure smear from PPS/DP EAC photography is also described.

4.1 Effects of Smear

The presence of smear results in decreased photographic performance. The amount of degradation is a function of the magnitude of smear. As image smear increases, the size of the smallest detail which can be resolved also increases. In theoretical analyses, scenes are often considered to be composed of sinusoidal variations in light intensity. This approach permits quantification of information in terms of spatial frequency in cycles or lines per millimeter (cpmm or lpmm). The frequency response of a recording system will

2.4-1

~~TOP SECRET~~ GHandle via BYEMAN
Control System Only

~~TOP SECRET~~ GBIF-008-W-C-019838-RI-80

then provide an indication of its theoretical performance (See Part 2, Section 12).

4.1.1 Smear Descriptors

There are three related methods used to express the magnitude of smear. These methods are described below as is the basic resolution-limiting effect of smear.

4.1.1.1 Smear Rate. Angular motion in microradians/second ($\mu\text{rad}/\text{sec}$) at the image plane is used to express the smear rate. The smear rate has the same effect as a vehicle attitude rate, though the source of the smear may not be a rate but rather a fixed offset. The effect of any smear source, however, can be completely described as an equivalent smear rate. This method is attractive because it is independent of the time of exposure and permits comparisons between PPS/DP EAC and SCS smear contributors.

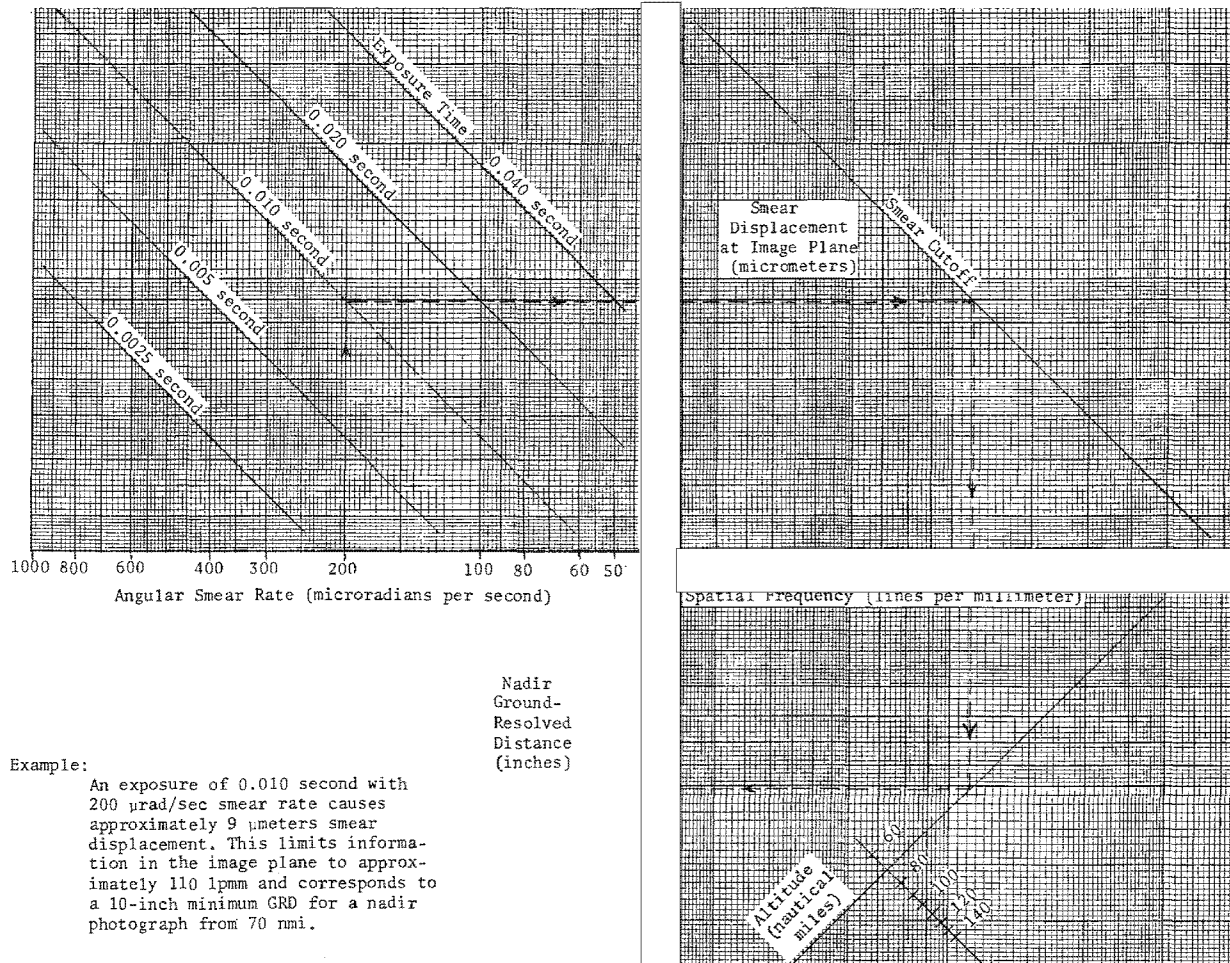
4.1.1.2 Image Plane Smear. A given smear rate will result in translation of the image of a theoretical point target during a film exposure interval. The displacement is normally expressed in micrometers (μm) and is a function of the exposure-time, smear rate, and optical-system focal length.

4.1.1.3 Ground Smear. A measured displacement on the film may be theoretically projected back through the system and expressed as displacement on the ground. Ground smear is usually expressed in inches (in.).

4.1.1.4 Resolution-Limiting Effect of Smear. The above smear descriptors are vector quantities with both magnitude and direction. Section 4.2 outlines the conventions utilized in applying smear descriptors and demonstrates conversions between the various descriptors. Figure 2.4-1 provides an indication of the resolution-limiting effect of smear on the system. The plots indicate how smear displacement increases as a function of exposure time. This

2.4-2

~~TOP SECRET~~ GHandle via BYEMAN
Control System Only



$$x_i = v_x F t_e (0.0254)$$

$$v = \frac{1}{x_i} (1000.0)$$

$$GRD = \frac{x_i h}{F} (2.8706)$$

Where:

x_i = smear displacement at image plane (umeters)

μ = smear rate (urad/sec)

F = focal length (in.)

t_e = exposure time (sec)

v = spatial frequency (lpmm)

GRD = distance resolved on ground (in.)

h = altitude (nmi)

Units Conversion Factors are:

$$0.0254 = \frac{m}{in.}$$

$$1000.0 = \frac{\mu m}{mm}$$

$$2.8706 = \frac{in.^2}{(\mu m)(nmi)}$$

2.4-3/2.4-4

Figure 2.4-1. Limiting Effect of Smear

Handle via BYEMAN
Control System Only

~~TOP SECRET~~ GBIF-008-W-C-019838-RI-80

shows why resolution is not as dramatically improved by finer grain films as might be expected. Finer grain films are normally slower, requiring longer exposures, hence, it is more severely impacted by a given rate of smear. The same relationship also explains why intentionally overexposing a frame can result in increased degradation from image smear. Figure 2.4-1 does not indicate losses due to film and lens response, but only losses related to image smear.

4.1.2 Modulation Transfer Function (MTF)

The effects of smear on photography can be quantified by calculating the transfer function of the image motion. An MTF plot represents the ratio of output modulation to input modulation at each spatial frequency. Utilization of MTF techniques is useful in performance prediction, since the MTF of each element of the system can be multiplied by the MTF of every other element to produce a system MTF. Intersection with the threshold modulation (TM) curve for the appropriate film, process, and contrast leads directly to estimates of limiting resolution. Section 4.1.3 demonstrates this application.

4.1.2.1 Smear MTF. The smear MTF (SMTF) as a function of spatial frequency, SMTF (ν), has the general form of the Fourier transform of the shutter function and the image displacement function averaged over the exposure interval:

$$\text{SMTF } (\nu) = \phi(\nu) = \frac{1}{T} \int_{-\infty}^{\infty} [S(t) \exp - (2\pi i \nu \mu(t))] dt$$

Where: SMTF (ν) = smear transfer function as a function of spatial frequency

T = exposure time

S(t) = shutter function

i = $\sqrt{-1}$

ν = spatial frequency

$\mu(t)$ = image displacement as a function of time

~~TOP SECRET~~ G

~~TOP SECRET~~ GBIF-008- W-C-019838-RI-80

4.1.2.2 Image Displacement. If complex image motion which includes both linear and sinusoidal components is considered, image displacement $\mu(t)$ can be described as follows:

$$\mu(t) = vt + \sum_i A_i \sin (2\pi f_i t + \phi_i)$$

Where: v = constant uncompensated image velocity (linear smear)

t = time of exposure

A_i = amplitude of the i^{th} component of sinusoidal image motion

f_i = temporal frequency of the i^{th} component of sinusoidal image motion

ϕ_i = phase angle of the i^{th} component of sinusoidal image motion

Image displacement resulting from all types of uncompensated image motion (linear, sinusoidal, and complex) can be indicated by the expression for $\mu(t)$. Techniques such as those employing a digital velocity measuring sensor (DVMS) allow the evaluation of image displacement when complex motion is present.

4.1.2.2.1 Linear Smear. The component vt of the image displacement represents the amplitude of smear due to linear contributors.

4.1.2.2.2 Nonlinear Smear. The summation component, \sum_i , of the image displacement represents the amplitude of smear due to sinusoidal contributors. Spectral analysis techniques are advantageous for evaluation of nonlinear smear.

~~TOP SECRET~~ G

~~TOP SECRET~~ GBIF-008-W-C-019838-RI-80

4.1.2.3 Shutter Function. The shutter function of a theoretical strip camera is shown as a step function in Figure 2.4-2:

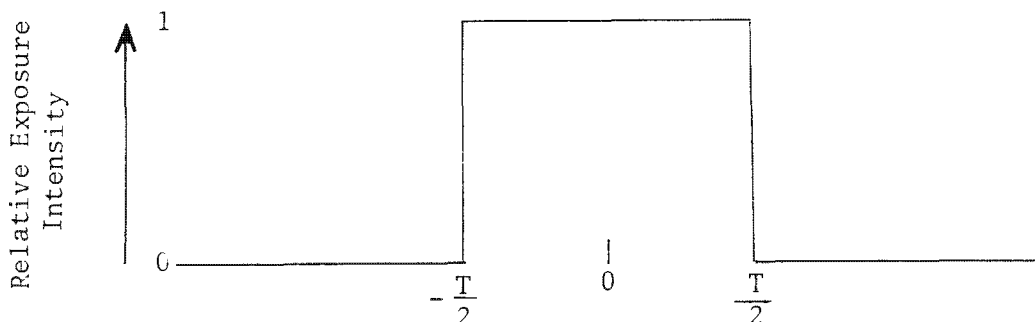


Figure 2.4-2. Ideal Shutter Function

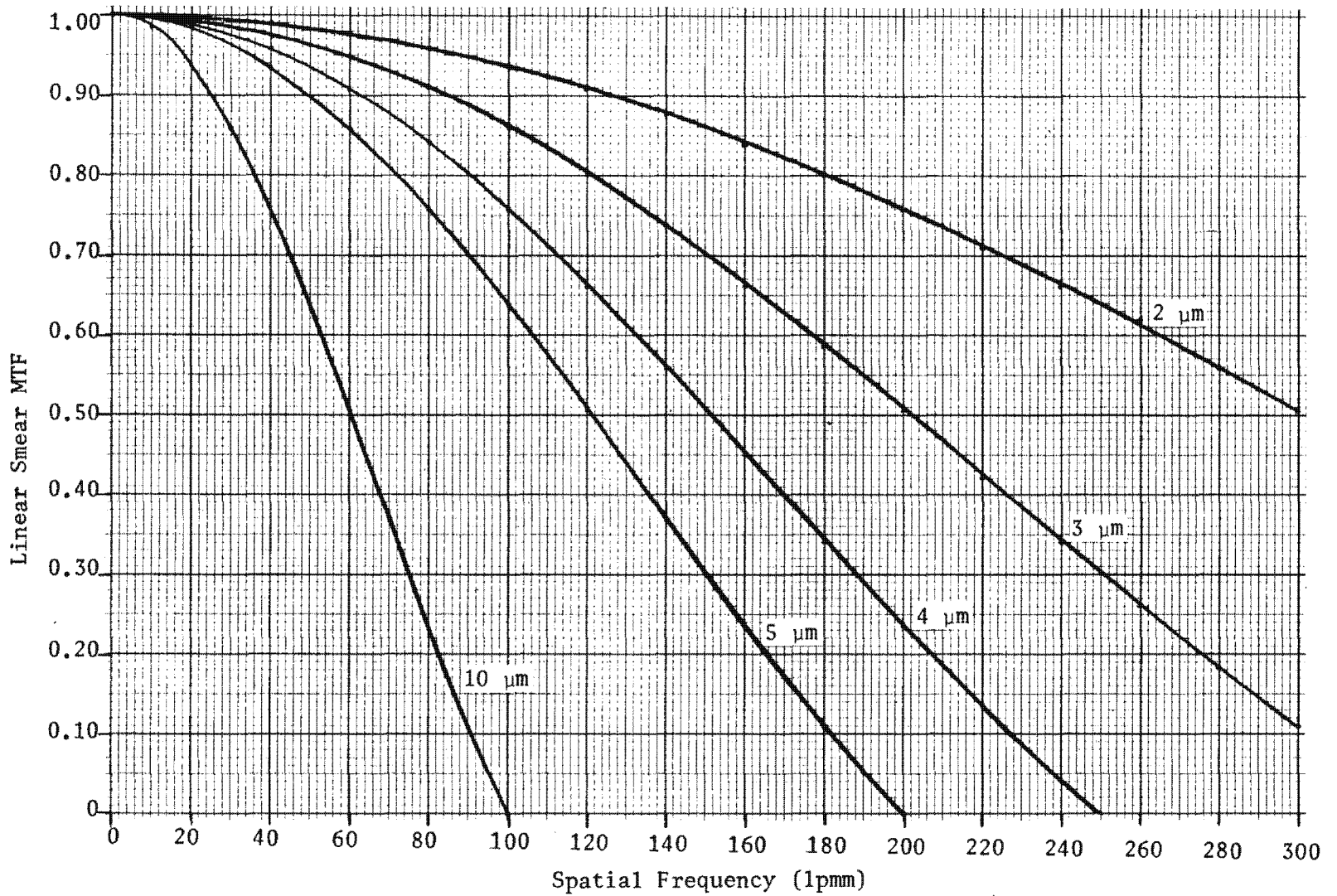
For such a perfect camera, the shutter function, $S(t)$, is 1 for the time of exposure ($-\frac{T}{2}$ to $\frac{T}{2}$), and 0 for all other times. The smear MTF can then be rewritten as:

$$\text{SMTF}(\nu) = \Phi(\nu) = \frac{1}{T} \int_{-\frac{T}{2}}^{\frac{T}{2}} [S(t) \exp - (2\pi i \nu \mu(t))] dt$$

Evaluation of the smear MTF for several values of linear smear with the theoretical shutter function leads to Figure 2.4-3, depicting the linear smear modulation transfer function at various levels of smear. With $S(t) = 1$, the MTF becomes $\frac{\sin(\pi \mu(t) \nu)}{(\pi \mu(t) \nu)}$.

~~TOP SECRET~~ G

Handle via BYEMAN
Control System Only



2.4-8

Figure 2.4-3. Linear Smear MTF

Handle via BYEMAN
Control System Only

Approved for Release: 2017/02/14 C05097211

Approved for Release: 2017/02/14 C05097211

~~TOP SECRET~~ GBIF-008-W-C-019838-RI-80

The plot shows that the modulation decreases with increasing spatial frequency. Thus, the higher frequency image content and limiting resolution are most adversely impacted by smear.

The actual strip-camera shutter function is not the step function shown in Figure 2.4-2 but can be represented by a trapezoidal function. This geometry is shown in Figure 2.4-4.

If the slit-to-emulsion distance could be reduced to zero, the shutter efficiency would be 100%. When the efficiency is less than 100%, there are two effects:

- (1) The total smear is slightly greater
- (2) Edges of imagery are less-sharp

Shutter efficiency in the Gambit system varies from 66% to 99% depending on slit width and generally has a negligible effect on performance estimates.

4.1.3 SMTF Application

Figure 2.4-5 shows the application of MTF techniques in the generation of limiting resolution estimates for the Gambit system (see also Part 2, Section 12). The MTF for each element to be considered is plotted. The example shows the static MTF for the lens, the linear SMTF, and the complex SMTF. By cascading (multiplying) the curves together at each spatial frequency the dynamic MTF of the system may be expressed. The intersection of the threshold modulation (TM) curve for a selected film process and contrast with the combined dynamic MTF curve indicates that one can expect to record information up to lpmm with the system as constituted. The curves also indicate the expected loss of 28 lpmm because of smear, 24 lpmm due to linear contributors, and 4 lpmm due to nonlinear contributors. Figure 2.4-6 indicates an additional form of the dynamic MTF which has

25X1

2.4-9

~~TOP SECRET~~ GHandle via BYEMAN
Control System Only

~~TOP SECRET~~ G

BIF-008-W-C-019838-RI-80

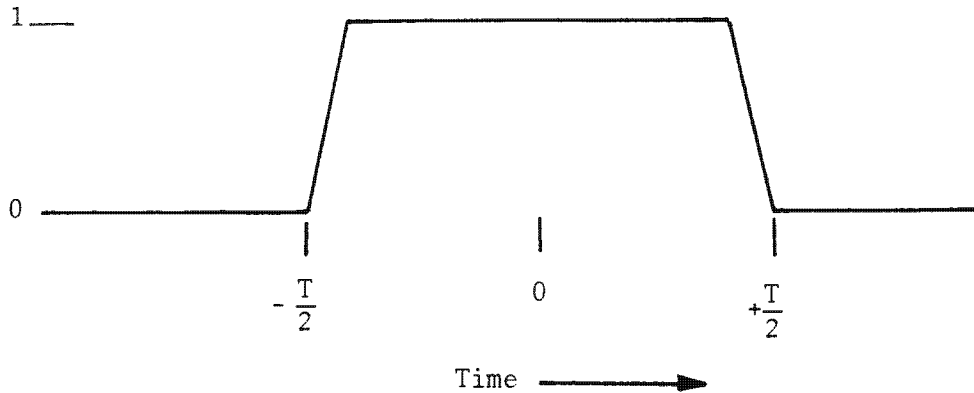
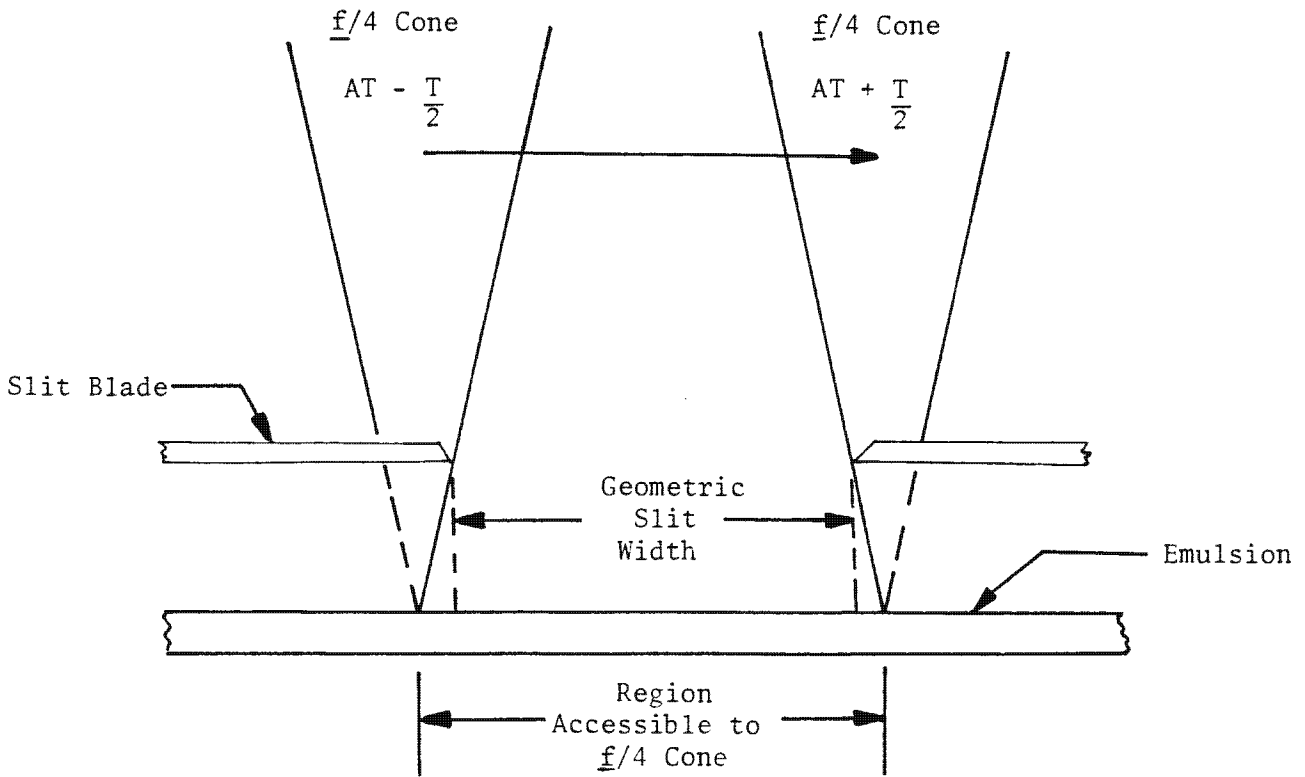
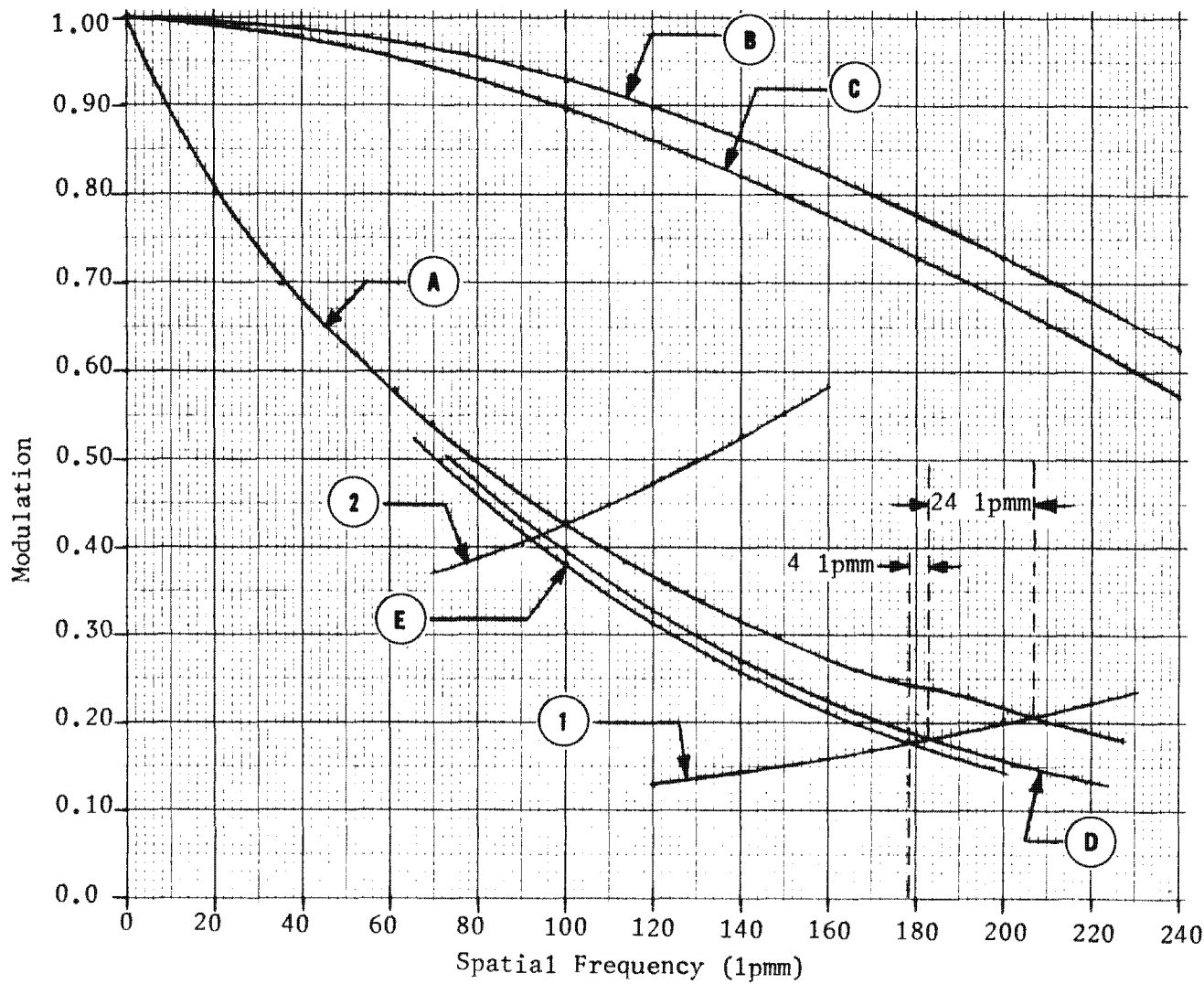


Figure 2.4-4. Strip Camera Shutter Function

2.4-10

~~TOP SECRET~~ G

Handle via **BYEMAN**
Control System Only



- (A) R-5 Lens MTF, 85% OQF, +0.0005-inch Defocus In-track
- (B) Linear Smear MTF (SMTF)
- (C) Complex SMTF (0.937 at 180 lpmm)
- (D) Lens With Linear Smear
- (E) Dynamic MTF (Lens With Complex Smear)
- (1) Film TM Type 124-102 2.0:1 Contrast
- (2) Film TM Type 124-102 1.2:1 Contrast

Figure 2.4-5. Application of MTF Techniques

2.4-11

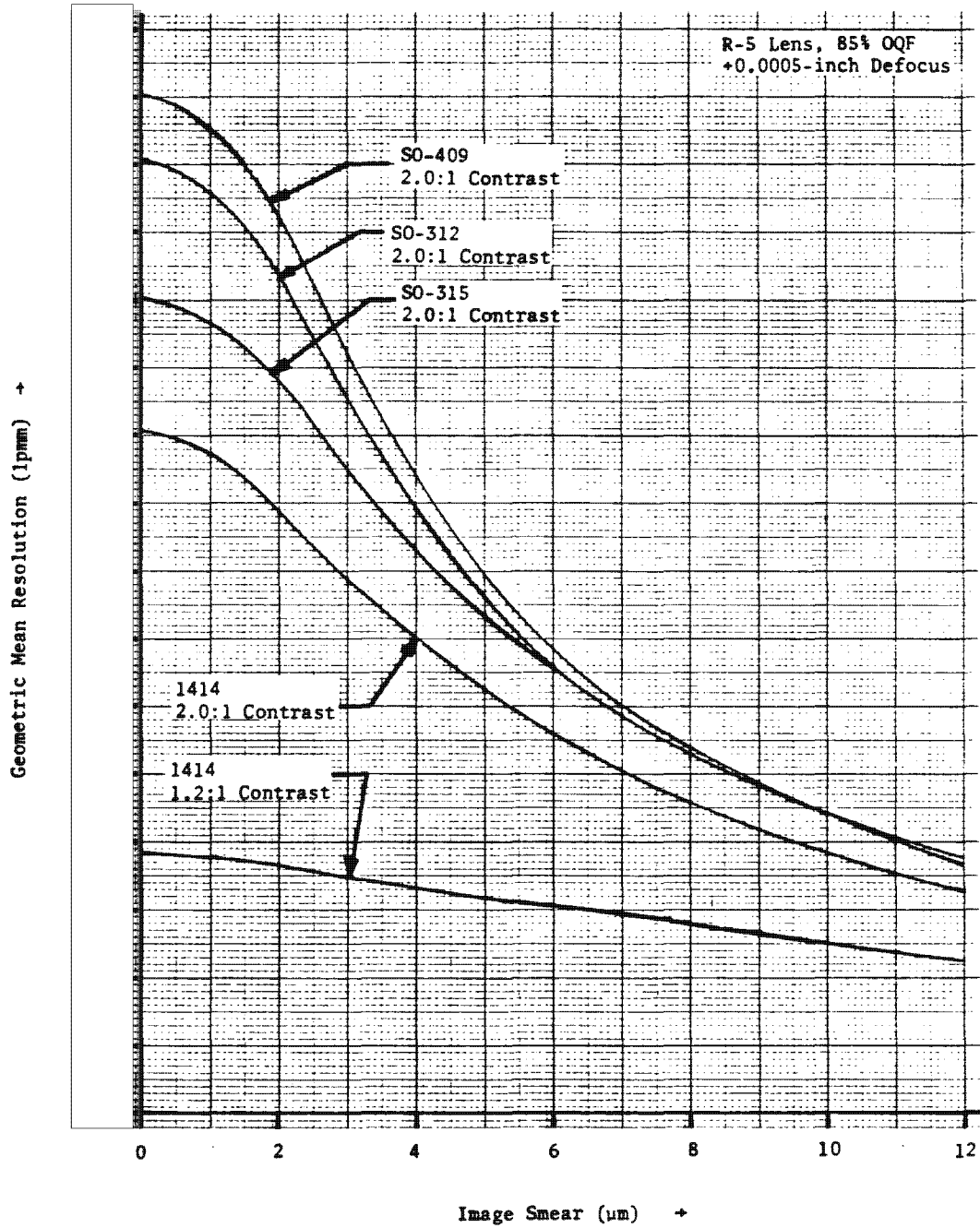
Approved for Release: 2017/02/14 C05097211

Approved for Release: 2017/02/14 C05097211

~~TOP SECRET~~ G

BIF-008-W-C-019838-RI-80

①



25X1

Figure 2.4-6. Geometric Mean Resolution given Smear and Film Type

"WARNING - THIS DOCUMENT SHALL NOT BE USED AS A SOURCE FOR DERIVATIVE CLASSIFICATION"

2.4-12

~~TOP SECRET~~ G

Handle via BYEMAN
Control System Only

~~TOP SECRET~~ GBIF-008- W-C-019838-RI-80

proven useful in performance prediction. The geometric mean resolution in lpmm can be found if the film type, target contrast, and magnitude of smear are known.

4.2 Conventions and Coordinate Systems

The expression of smear and smear rates requires the use of standard conventions and an image plane coordinate system.

4.2.1 Image Plane Coordinate System

The BIF-008 image plane coordinate system is illustrated in Figure 2.4-7. This is the same system shown in Part 2, Figure 2.1-2. It is a right-hand system with the axes denoted by the lower case letters, x, y, and z. The utility of the image plane coordinate system is that a translation of the ground scene with respect to the X, Y or Z axes results in an identical translation of the image of the ground scene with respect to the x, y or z axes. For example, with the optics in the indicated position (stereo and crab angles equal to zero), the in-track ground motion is in the +X direction relative to the vehicle. The required image motion is then, in the +x direction. To compensate for the image motion the film must be driven in the +x direction. Likewise, a decrease of vehicle altitude is equivalent to displacing the ground scene in a +Z direction. By definition this produces a focus shift in the +z direction which can be compensated for by moving the platen away from the Ross Corrector lenses. The above examples presume a nadir, zero crab situation, but they serve to most simply illustrate the relationships between the coordinate systems. Operational activity requires the use of equations involving the stereo, crab, and obliquity angles to make transformations between the ground scene and the image plane.

~~TOP SECRET~~ GHandle via BYEMAN
Control System Only

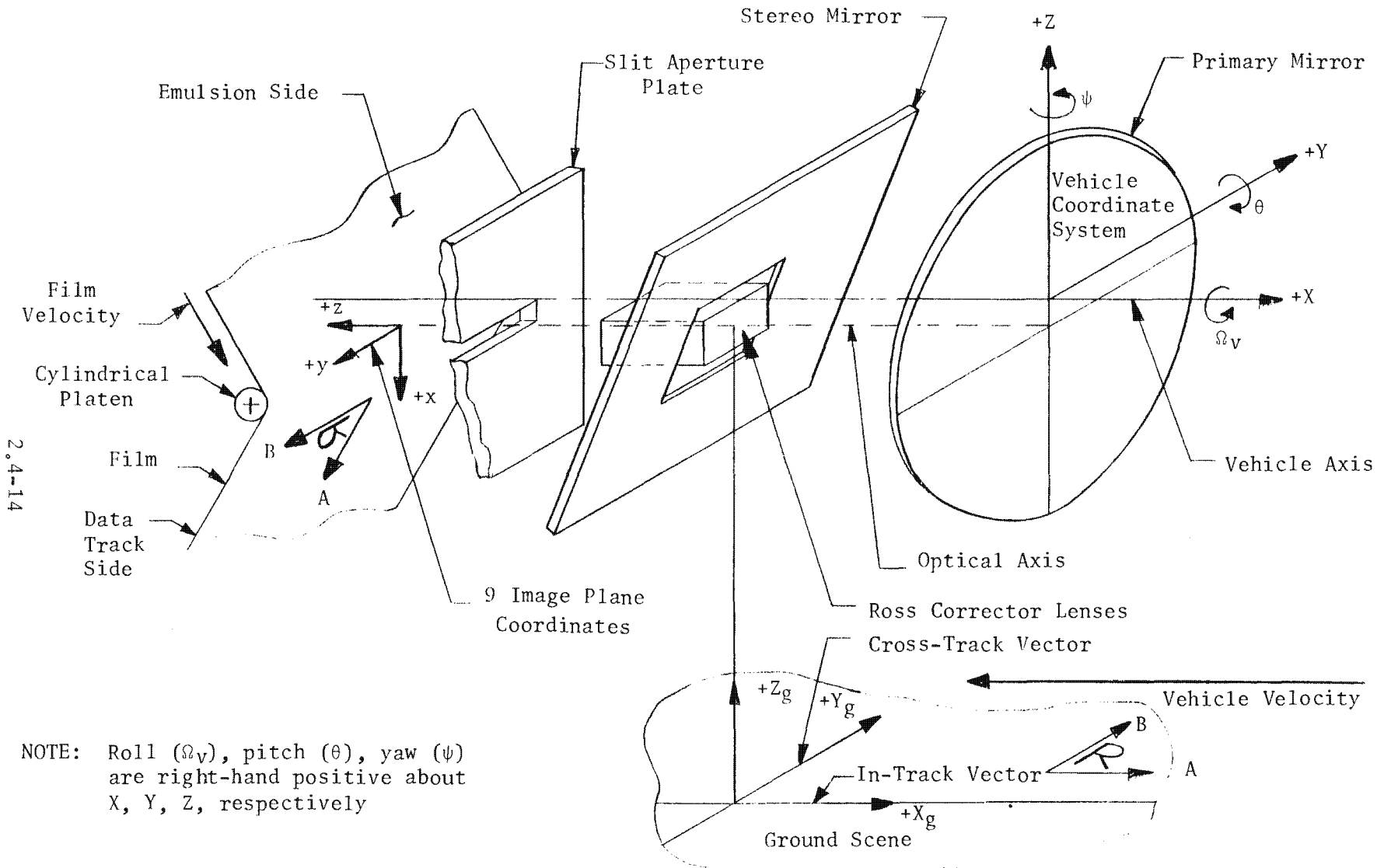


Figure 2.4-7. 9-Inch Image Plane Coordinate System

Handle via **BYEMAN**
Control System Only

Approved for Release: 2017/02/14 C05097211

Approved for Release: 2017/02/14 C05097211

~~TOP SECRET~~ GBIF-008-W-C-019838-RI-80

4.2.2 Transformation of Smear Rates

The relationships between the various smear descriptors are shown by the equations in the following sections.

4.2.2.1 Smear Rate to Image Plane. Angular smear rate in-track components (μ_{x_i}) and cross-track components (μ_{y_i}) are transformed into image plane in-track (x_i) and cross-track (y_i) smear displacements by:

$$x_i = (2.54 \times 10^{-2}) \mu_{x_i} Ft_e \quad \text{or} \quad x_i = (2.54 \times 10^{-2}) \mu_{x_i} F \left(\frac{w}{V_f} \right)$$

$$y_i = (2.54 \times 10^{-2}) \mu_{y_i} Ft_e \quad \text{or} \quad y_i = (2.54 \times 10^{-2}) \mu_{y_i} F \left(\frac{w}{V_f} \right)$$

Where: x_i = in-track image smear displacement (μm)

μ_{x_i} = in-track smear rate ($\mu\text{rad}/\text{sec}$)

F = focal length (inches)

t_e = exposure time (seconds)

w = slit width (inches)

V_f = film-drive speed (inches/second)

2.54×10^{-2} = conversion factor, inches to meters

y_i = cross-track image smear displacement (μm)

μ_{y_i} = cross-track smear rate ($\mu\text{rad}/\text{sec}$)

~~TOP SECRET~~ G

~~TOP SECRET~~ GBIF-008- W-C-019838-RI-80

4.2.2.2 Image Plane to Ground. Image-plane smear displacement (x_i, y_i) is transformed to ground smear displacement (X_i, Y_i) by:

$$X_i = x_i (2.8705) \left(\frac{h}{F \cos^2 \Sigma \cos \Omega} \right)$$

$$Y_i = y_i (2.8705) \left(\frac{h}{F \cos \Sigma \cos^2 \Omega} \right)$$

Where: X_i = in-track ground smear displacement (inches)

Y_i = cross-track ground smear displacement (inches)

h = height above target plane (nautical miles)

F = focal length (inches)

Σ = stereo angle (from nadir, +forward) (degrees)

Ω = obliquity (degrees)

x_i = in-track image smear displacement (μm)

y_i = cross-track image smear displacement (μm)

2.8705 = combined conversion factor

4.2.2.3 Example. To illustrate the use of the above equations, the following example is provided.

Given: $\mu_{x_i} = 200 \mu\text{rad/sec}$

$h = 65 \text{ nmi}$

$\Sigma = 0$

$\Omega = 0$

$F = 175 \text{ inches}$

$V_f = 10 \text{ inches/sec}$

$w = 0.100 \text{ inch}$

2.4-16

~~TOP SECRET~~ GHandle via BYEMAN
Control System

~~TOP SECRET~~ GBIF-008- W-C-019838-RI-80

Find: In-track image plane and ground smear

$$\begin{aligned}
 \text{Solution: } x_i &= (2.54 \times 10^{-2}) \mu_{x_i} F \left(\frac{w}{V_f} \right) \\
 &= (2.54 \times 10^{-2}) (200) (175) \left(\frac{0.100}{10} \right) \\
 &= 8.9 \mu\text{m} = \text{in-track image plane smear} \\
 X_i &= x_i (2.8705) \left(\frac{h}{F \cos^2 \Sigma \cos \Omega} \right) \\
 &= 8.9 (2.8705) \left(\frac{65}{175} \right) \\
 &= 9.5 \text{ inches} = \text{in-track ground smear}
 \end{aligned}$$

4.3 Smear Contributors

The contributors to image smear may be categorized as being caused by, or under the control of, the PPS/DP EAC, the SCS, or the telemetry, tracking and command system (TT and C). A short discussion of each contributor is provided and equations for determining the in-track and cross-track components of angular smear rate and ground smear are listed in Table 2.4-1. The symbols used in these equations follow in Table 2.4-2.

4.3.1 PPS/DP EAC Contributors

Design trade-offs and manufacturing tolerances during the assembly of the PPS/DP EAC can result in errors which may cause image smear. Each contributor is described below and the 3σ limits are indicated for known error-producing sources.

4.3.1.1 Film-Drive Speed (FDS). If the FDS executed for a frame differs from the required value, in-track smear results. Known PPS/DP EAC error sources are:

~~TOP SECRET~~ G

TABLE 2.4-1
9-INCH SMEAR EQUATIONS

2.4-18

	<u>Smear on Ground (nmi)</u>	<u>Smear Rate (microradians/second)</u>
Knowledge of altitude	$X_1^{**} = -\frac{w \Delta h}{F} \sec^2 \Sigma \sec \Omega$	$\mu_{X_1} = -\frac{V_f \Delta h (10^6)^*}{Fh}$
	$Y_1 = 0$	$\mu_{Y_1} = 0$
Roll attitude and alignment	$X_2 = -\frac{wh}{F} A_x \sec^2 \Sigma \tan \Omega \sec \Omega$	$\mu_{X_2} = -\frac{V_f}{F} A_x \tan \Omega (10^6)$
	$Y_2 = \frac{wh}{F} A_x \sec \Sigma \sec^2 \Omega \tan \Omega \tan \chi$	$\mu_{Y_2} = \frac{V_f}{F} A_x \tan \chi \tan \Omega (10^6)$
Pitch attitude and alignment	$X_3 = -\frac{wh}{F} A_y \sec^3 \Sigma (\sin \Sigma + \sin \Sigma \sec^2 \Omega - \tan \Omega \tan \chi)$	$\mu_{X_3} = -\frac{V_f}{F} A_y (\tan \Sigma \cos \Omega + \tan \Sigma \sec \Omega - \sec \Sigma \tan \chi \sin \Omega) (10^6)$
	$Y_3 = \frac{wh}{F} A_y \sec^2 \Sigma \sec^2 \Omega \sin \Omega$	$\mu_{Y_3} = \frac{V_f}{F} A_y \sec \Sigma \sin \Omega (10^6)$
Yaw attitude and alignment	$X_4 = -\frac{wh}{F} A_z \sec^3 \Sigma (\sin \Sigma \tan \Omega + \tan \chi)$	$\mu_{X_4} = \frac{V_f}{F} A_z (\tan \Sigma \sin \Omega + \sec \Sigma \tan \chi \cos \Omega) (10^6)$
	$Y_4 = -\frac{wh}{F} A_z \sec^2 \Sigma \sec \Omega$	$\mu_{Y_4} = -\frac{V_f}{F} A_z \sec \Sigma \cos \Omega (10^6)$

* 10^6 is the conversion factor between radians and microradians
 ** The subscripted number of the variable is that equation number
 i.e., X_1 is equation number 1

Approved for Release: 2017/02/14 C05097211

Approved for Release: 2017/02/14 C05097211

TABLE 2.4-1 (CONTINUED)

	<u>Smear on Ground (nmi)</u>	<u>Smear Rate (microradians/second)</u>
Roll rate	$X_5^{**} = - \frac{wh^2}{FV_x} \dot{A}_x \sec^3 \Sigma \sec^2 \Omega \tan \chi^*$	$\mu_{x_5} = - \frac{hV_f}{FV_x} \dot{A}_x \tan \chi \sec \Sigma \sec \Omega (10^6)$
	$Y_5 = - \frac{wh^2}{FV_x} \dot{A}_x \sec^2 \Sigma \sec^3 \Omega$	$\mu_{y_5} = - \frac{hV_f}{FV_x} \dot{A}_x \sec \Sigma \sec \Omega (10^6)$
Pitch Rate	$X_6 = \frac{wh^2}{FV_x} \dot{A}_y \sec^4 \Sigma \sec \Omega$	$\mu_{x_6} = \frac{hV_f}{FV_x} \dot{A}_y \sec^2 \Sigma (10^6)$
	$Y_6 = - \frac{wh^2}{FV_x} \dot{A}_y \sec \Sigma \sec^2 \Omega (\tan \Sigma \sec \Sigma \tan \Omega + \sec \Omega \tan \chi)$	$\mu_{y_6} = - \frac{hV_f}{FV_x} \dot{A}_y (\tan \Sigma \sec \Sigma \tan \Omega + \tan \chi \sec \Omega) (10^6)$
Yaw rate	$X_7 = \frac{wh^2}{FV_x} \dot{A}_z \sec^2 \Sigma \sec \Omega \tan \Omega$	$\mu_{x_7} = \frac{hV_f}{FV_x} \dot{A}_z \tan \Omega (10^6)$
	$Y_7 = \frac{wh^2}{FV_x} \dot{A}_z \sec \Sigma \sec^2 \Omega (\tan \Sigma \sec \Sigma - \tan \Omega \tan \chi)$	$\mu_{y_7} = \frac{hV_f}{FV_x} \dot{A}_z (\tan \Sigma \sec \Sigma - \tan \chi \tan \Omega) (10^6)$
Crab granularity	$X_8 = - \frac{wh}{F} \Delta \chi \sec^2 \Sigma \sec \Omega \tan \Omega$	$\mu_{x_8} = - \frac{V_f}{F} \Delta \chi \tan \Omega (10^6)$
	$Y_8 = - \frac{wh}{F} \Delta \chi \sec \Sigma \sec^2 \Omega$	$\mu_{y_8} = - \frac{V_f}{F} \Delta \chi (10^6)$
Crab line-of-sight reproducibility	$X_9 = - \frac{wh}{F} M_c \sec^2 \Sigma \sec \Omega \tan \Omega$	$\mu_{x_9} = - \frac{V_f}{F} M_c \tan \Omega (10^6)$
	$Y_9 = - \frac{wh}{F} M_c \sec \Sigma \sec^2 \Omega$	$\mu_{y_9} = - \frac{V_f}{F} M_c (10^6)$

* A dot (·) over a quantity denotes the time derivative of the quantity.

** The subscripted number of the variable is that equation number i.e., X_5 is equation number 5

Approved for Release: 2017/02/14 C05097211

2.4-19

Approved for Release: 2017/02/14 C05097211

2.4-20

	<u>Smear on Ground (nmi)</u>	<u>Smear Rate (microradians/second)</u>
Stereo line-of-sight reproducibility	$X_{10}^{**} = - \frac{2wh}{F} M_s \sec^2 \Sigma \tan \Sigma \sec \Omega$	$\mu_{x_{10}} = - \frac{2V_f}{F} M_s \tan \Sigma (10^6)$
	$Y_{10} = \frac{2wh}{F} M_s \sec \Sigma \tan \Sigma \sec^2 \Omega \tan \chi$	$\mu_{y_{10}} = \frac{2V_f}{F} M_s \tan \Sigma \tan \chi (10^6)$
Film-drive granularity	$X_{11} = - \frac{wh}{FV_f} \Delta V_f \sec^2 \Sigma \sec \Omega$	$\mu_{x_{11}} = - \frac{\Delta V_f}{F} (10^6)$
	$Y_{11} = 0$	$\mu_{y_{11}} = 0$
Film-drive drift	$X_{12} = - \frac{wh}{FV_f} \Delta V_f \sec^2 \Sigma \sec \Omega$	$\mu_{x_{12}} = - \frac{\Delta V_f}{F} (10^6)$
	$Y_{12} = 0$	$\mu_{y_{12}} = 0$
Knowledge of focal length	$X_{13} = \frac{wh}{F^2} \Delta F \sec^2 \Sigma$	$\mu_{x_{13}} = \frac{V_f}{F^2} \Delta F (10^6)$
	$Y_{13} = 0$	$\mu_{y_{13}} = 0$
K Distortion	$X_{14} = \frac{wh}{F} (\%D)^* \sec^2 \Sigma \sec \Omega$	$\mu_{x_{14}} = \frac{V_f}{F} (\%D)^* (10^4)$
	$Y_{14} = 0$	$\mu_{y_{14}} = 0$
Off-axis geometry	$X_{15} = - \frac{wh}{F} \sec^3 \Sigma \tan \Omega \cos \Omega \tan \mu$	$\mu_{x_{15}} = - \frac{V_f}{F} \sec \Sigma \tan \Omega \tan \mu (10^6)$
	$Y_{15} = \frac{wh}{F} \frac{(\tan \Sigma + \sin \chi \tan \Omega) \tan \mu}{\sec \Sigma \sec^2 \Omega}$	$\mu_{y_{15}} = \frac{V_f}{F} [\tan \Sigma + \sin \chi \tan \Omega] \tan \mu (10^6)$

* %D = 0.218 μ^2 where μ is semi-field angle in degrees.

** The subscripted number of the variable is that equation number i.e., X_{10} is equation number 10

Handle via **BYEMAN**
Control System Only

Approved for Release: 2017/02/14 C05097211

Approved for Release: 2017/02/14 C05097211

~~TOP SECRET~~ GBIF-008- W-C-019838-RI-80

TABLE 2.4-2

SYMBOLS USED IN SMEAR EQUATIONS

<u>Symbol</u>	<u>Definition</u>	<u>Units</u>
A_x	Roll attitude and alignment errors	radians
A_y	Pitch attitude and alignment errors	radians
A_z	Yaw attitude and alignment errors	radians
\dot{A}_x	Roll-rate error	radians/second
\dot{A}_y	Pitch-rate error	radians/second
\dot{A}_z	Yaw-rate error	radians/second
F	Focal length	inches
M_c	Angular error in stereo mirror crab alignment	radians
M_s	Angular error in stereo mirror stereo alignment	radians
V_x	In-track component of nadir velocity	nmi/second
V_y	Cross-track component of nadir velocity	nmi/second
a	Slant range	nmi
h	Altitude above geoid	nmi
X_i	In-track smear on ground	nmi
Y_i	Cross-track smear on ground	nmi
μ_{X_i}	In-track smear rate due to the i^{th} contributor (image plane)	microradians/second

2.4-21

~~TOP SECRET~~ GHandle via **BYEMAN**
Control System Only

~~TOP SECRET~~ GBIF-008- W-C-019838-RI-80

TABLE 2.4-2 (Cont'd)

<u>Symbol</u>	<u>Definition</u>	<u>Units</u>
μ_{y_i}	Cross-track smear rate due to the <u>i</u> th contributor (image plane)	microradians/ second
V_f	Film-drive speed (FDS)	inches/second
w	Slit width	inches
ΔV_f	Amplitude of the linear velocity error of the platen; actual film velocity minus commanded film velocity	inches/second
$\Delta \chi$	Error in crab compensation, true crab minus commanded crab	radians
Σ	Stereo angle of the line-of-sight	degrees
χ	Crab angle of stereo mirror	degrees
Ω	Obliquity angle of the line-of-sight	degrees
ΔF	Error in focal length; true focal length minus data-base focal length	inches
% D	Percent distortion	
Δh	Error in altitude; true altitude minus assumed altitude	nmi
μ	Semi-field angle	degrees

2.4-22

~~TOP SECRET~~ GHandle via BYEMAN
Control System Only

~~TOP SECRET~~ GBIF-008- W-C-019838-RI-80

- (1) Granularity (0.008 in./sec between steps, or 0.004 in./sec error) of the commandable FDS values ($3 \sigma = \pm 0.122\%$)
- (2) Drift in the FPLL servo (executed FDS differs from the commanded FDS) ($3 \sigma = \pm 0.100\%$)
- (3) Malfunction of the film-drive system (random)

Figure 2.4-8 can be used to estimate the equivalent smear rate due to an FDS error.

4.3.1.2 Crab Angle. Crab position error is a contributor to in-track and cross-track smear. Known error sources are:

- (1) Granularity (± 0.35 degree between steps) of commandable crab angles ($3 \sigma = \pm 0.175$ degree)
- (2) Crab reproducibility due to mirror mounting and servo errors ($3 \sigma = \pm 0.01$ degree)

Smear due to a crab angle error can be estimated by using Figure 2.4-9.

4.3.1.3 Stereo Angle. The stereo line-of-sight (LOS) accuracy impacts the slant range. Any error in stereo mirror angle will, therefore, result in an incorrect FDS and the attendant linear image smear. The inability to reproduce the commanded stereo LOS is the result of mirror mounting errors and servo inaccuracy ($3 \sigma = \pm 0.01$ degree). A stereo LOS error primarily affects pointing. Since the smear effect is slight, no plot is included for this contributor.

4.3.1.4 Knowledge of Focal Length. Uncertainty in the measurement of focal length for a given unit will result in a bias in FDS determination. This bias will be reflected as linear smear. Present capability for measurement of the focal length (3σ) is assumed to be ± 0.3 inch. No plot is included for

~~TOP SECRET~~ GHandle via BYEMAN
Control System Only

~~TOP SECRET~~ G

BIF-008- W-C-019838-RI-80

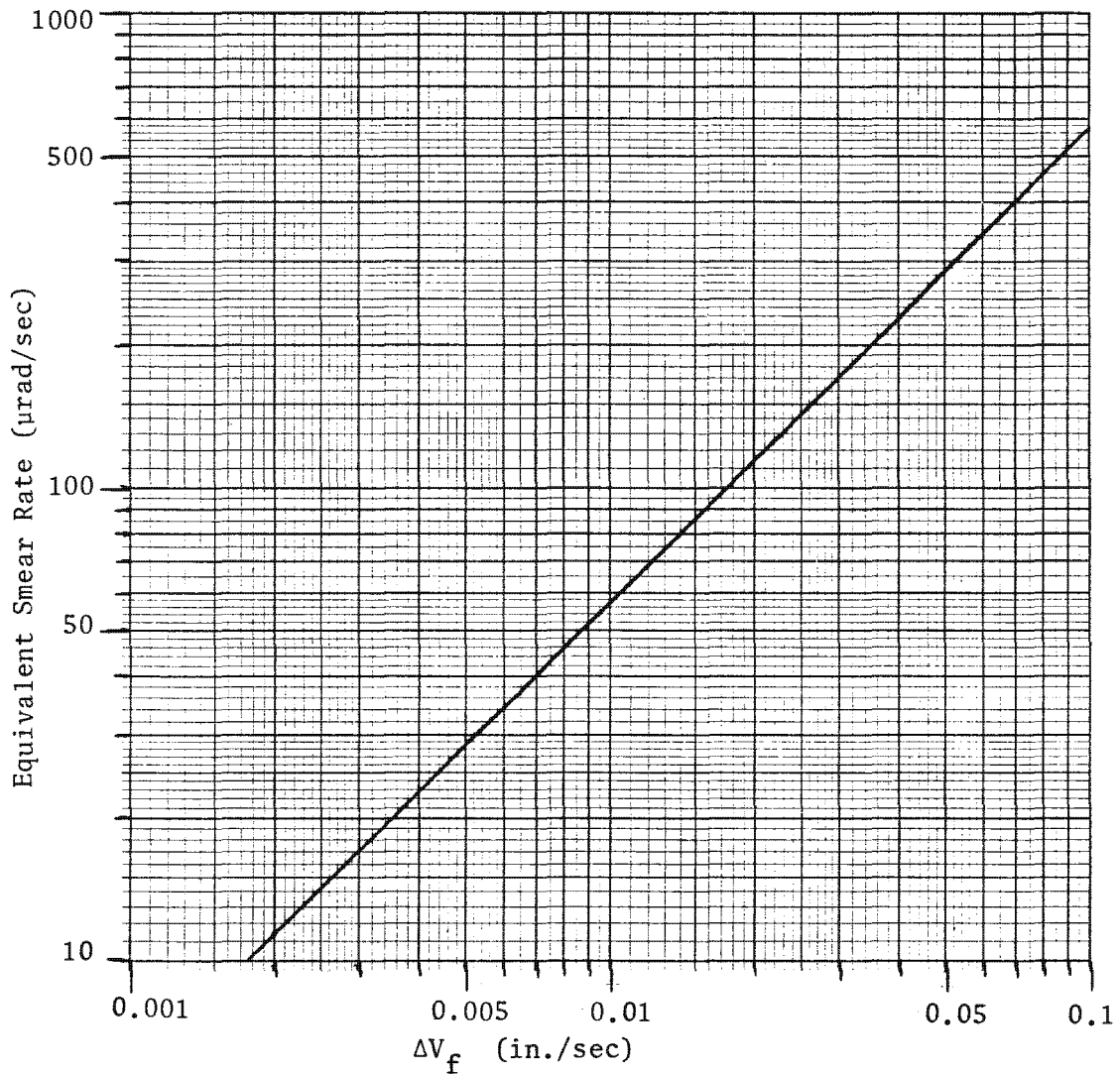


Figure 2.4-8. Equivalent Smear Rate Due to Film-Drive Speed Error

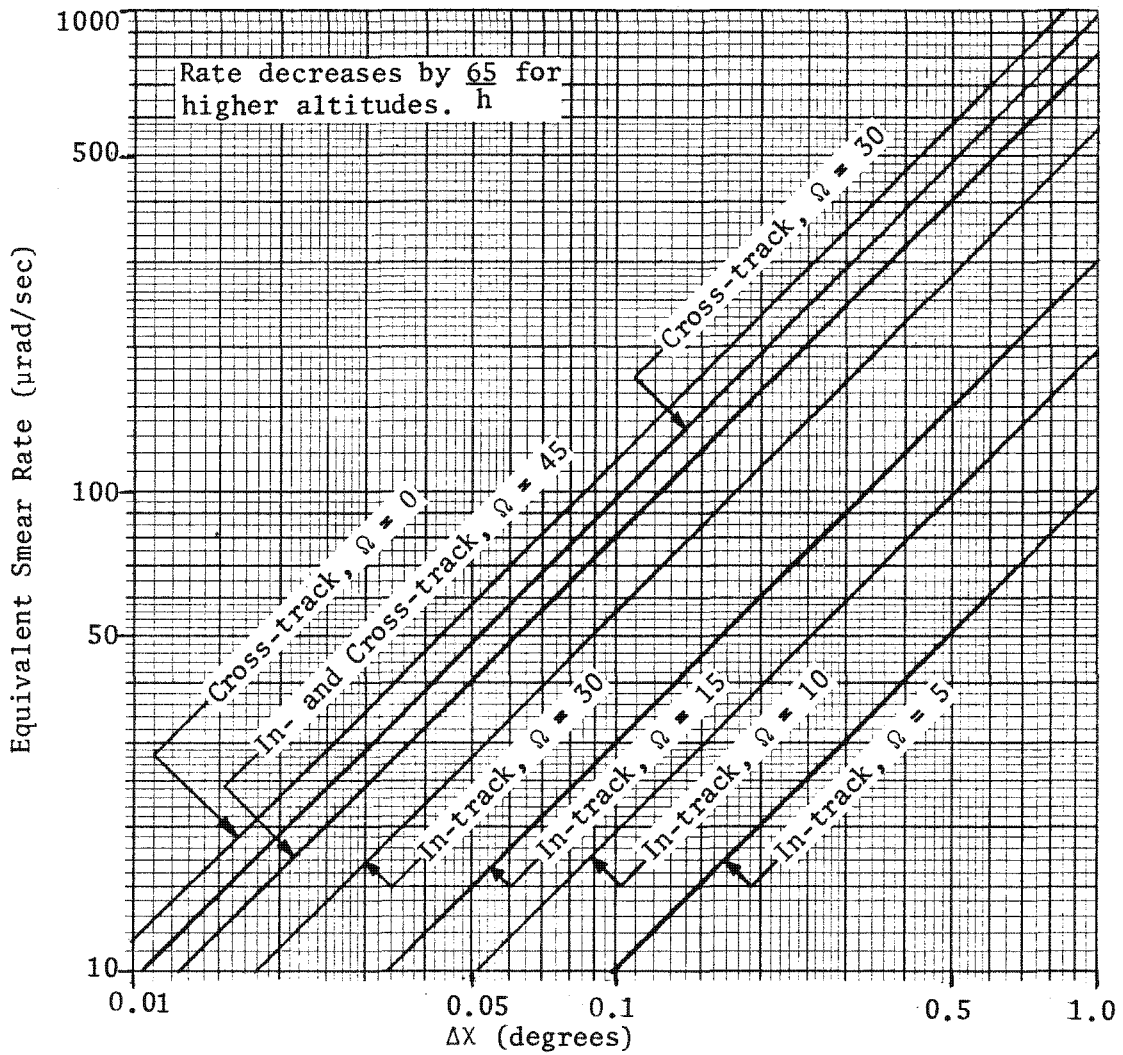
2.4-24

~~TOP SECRET~~ G

Handle via BYEMAN
Control System Only

~~TOP SECRET~~ G

BI F-008- W-C-019838-RI-80



Conditions: $h = 65$ nmi
 $\Sigma = 0$ degrees
 $F = 175$ inches

Figure 2.4-9. Crab Angle Error Contributor

2.4-25

~~TOP SECRET~~ G

Handle via BYEMAN
 Control System Only

~~TOP SECRET~~ GBIF-008- W-C-019838-RI-80

smear due to errors in the knowledge of the focal length because the smear effects are relatively minor.

4.3.1.5 Field Effects. The PPS/DP EAC is designed and operated to optimize photographic quality in the center of the field. Off-axis photography suffers degradation from the sources described below.

4.3.1.5.1 Geometric Smear. The slant range to the target plane is different at off-axis positions than it is on-axis (see Figure 2.4-10). This causes a differential image velocity across the film format. Because the preferred FDS is calculated for an on-axis position, there is differential, uncompensated motion at other points across the field. Hence, the geometric smear is zero on-axis and becomes progressively more severe toward the edges of the format. The magnitude of the geometric smear across the format increases and becomes nonsymmetrical for non-zero obliquities.

4.3.1.5.2 Lens Distortion. Distortion (pincushion or barrel) is caused by a variation of the effective focal length at different field positions. Distortion in the R-5 lens design is minimized on-axis and increases progressively toward the edges of the field. The distortion tolerance (3σ) is $\pm 0.65\%$ at points near the edges of the field. The effect on smear is the same as an error in the knowledge of the focal length.

4.3.1.5.3 Across Format, Combined Smear. Both geometric smear and lens distortion combine to produce varying smear across the format. Figure 2.4-11 shows the combined effect of geometric smear and lens distortion across the field. The plot is calculated for an altitude of 65 nautical miles and the slant ranges resulting from the indicated obliquity angles. Multiplication of smear rates by a factor of $\frac{65}{h}$ will permit use of the plot for altitudes other than 65 nautical miles. The use of Figure 2.4-11 is illustrated in

2.4-26

~~TOP SECRET~~ _____Handle via BYEMAN
Control System Only

2.4-27

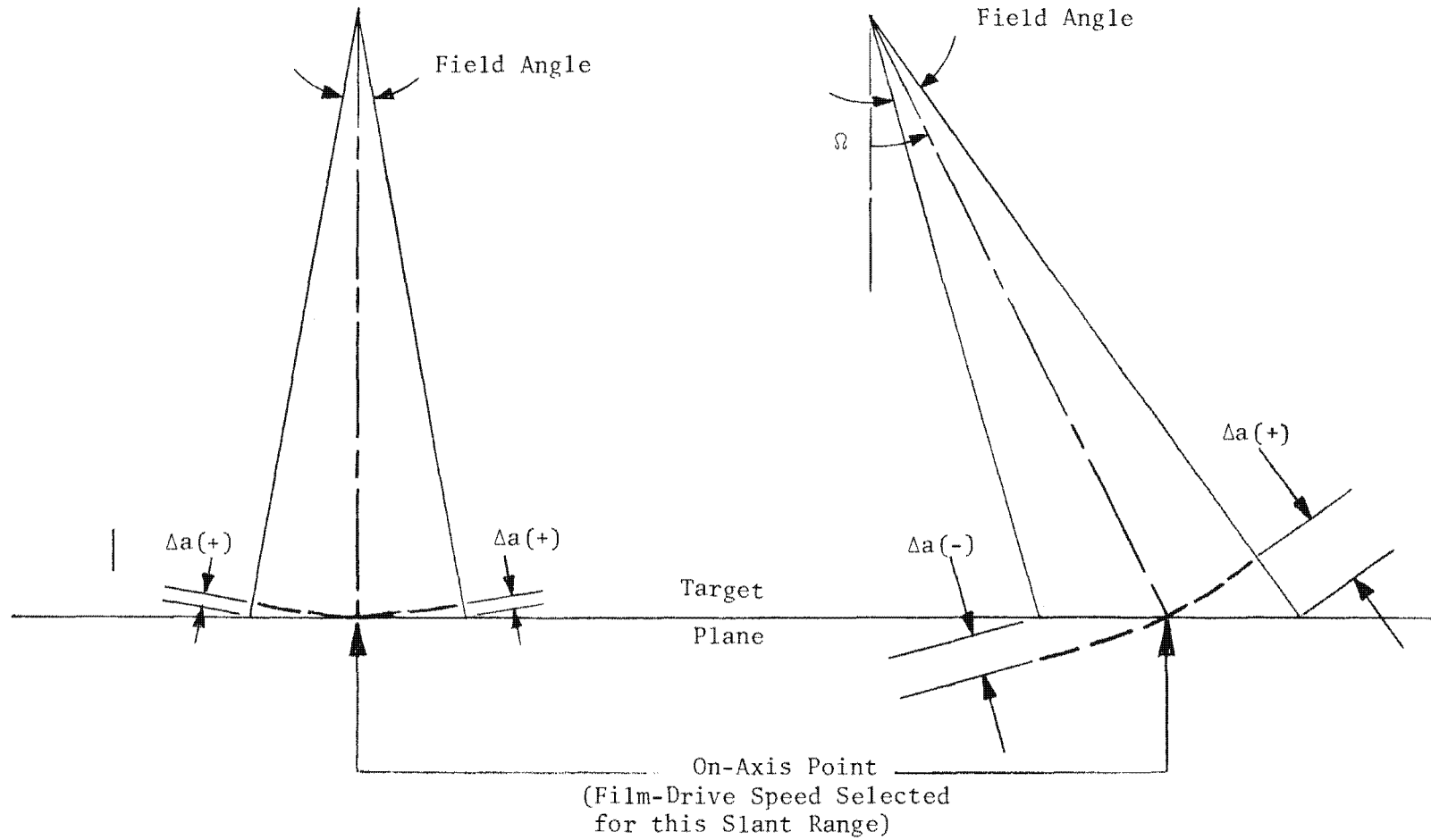
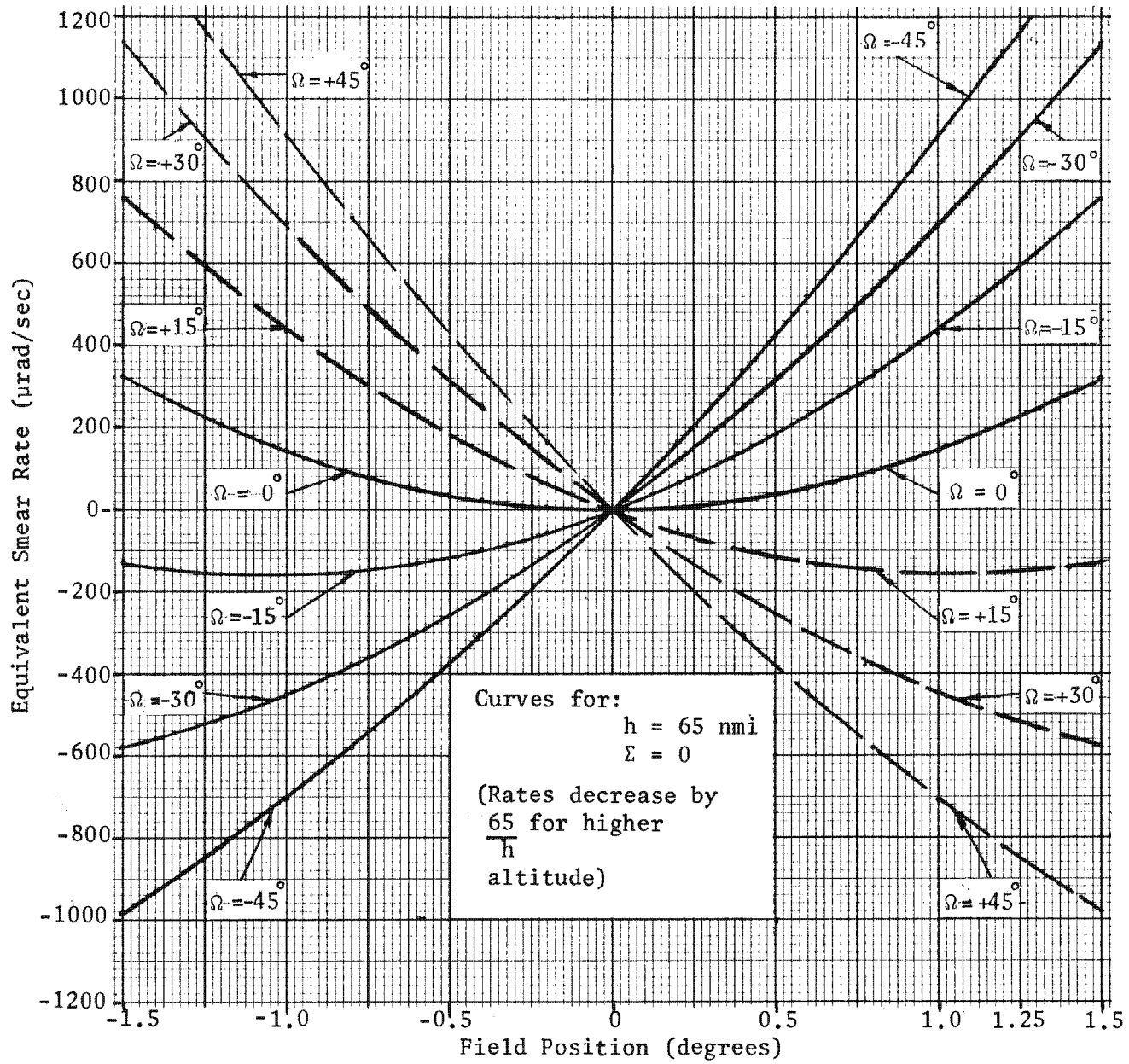


Figure 2.4-10. Geometric Smear Source



2.4-28

Figure 2.4-11. Off-Axis Smear Rates

Handle via BYEMAN
Control System Only

Approved for Release: 2017/02/14 C05097211

Approved for Release: 2017/02/14 C05097211

~~TOP SECRET~~ GBIF-008- W-C-019838-RI-80

the following example:

Given: $\Omega = 30^\circ$

$h = 119$ nmi

Field position = 1.25°

$V_f = 5.25$ in./sec

$w = 0.022$ inch

Find: Combined in-track geometric and distortion-induced smear in the image plane.

Solution: From Figure 2.4-11, the equivalent smear rate is -520 μ rad/sec for 65 nmi which yields -284 μ rad/sec for 119 nmi

$$\begin{aligned} x_i &= (2.54 \times 10^{-2}) \mu_{x_i} F\left(\frac{w}{V_f}\right) \\ &= (2.54 \times 10^{-2}) (-284) (175) \left(\frac{0.022}{5.25}\right) \\ &= -5.3 \mu\text{m} \end{aligned}$$

4.3.1.6 Misalignment. Reference mirrors (often referred to as "lollipops") are used to facilitate accurate alignment of the PPS/DP EAC to the SCS. There are two sources of error which have been identified for this method:

- (1) Optical axis to reference mirror alignment tolerances
 - (3 σ roll = ± 0.0083 degree)
 - (3 σ pitch = ± 0.0091 degree)
 - (3 σ yaw = ± 0.0091 degree)
- (2) Reference mirror to mechanical interface alignment tolerances
 - (3 σ roll = ± 0.0175 degree)
 - (3 σ pitch = ± 0.0171 degree)
 - (3 σ yaw = ± 0.0171 degree)

2.4-29

~~TOP SECRET~~ G

Handle via BYEMAN
Control System Only

~~TOP SECRET~~ GBIF-008- W-C-019838-RI-80

4.3.1.7 Thermal Bending ("Hotdogging"). Part 2, Section 14.6.2 of this document describes how the asymmetrical thermal inputs cause the PPS/DP EAC external structure to bend. Although the structures are designed to minimize coupling of this bending into the internal structure and optics, the LOS is affected to some extent. Pitch and yaw variations primarily affect pointing, but linear smear is also induced by "hotdogging". Operational software has been designed to model the thermal bending and is assumed, for budgeting purposes, to compensate for 75% of the "hotdogging" effects. The effect of the uncompensated "hotdogging" may be evaluated by treating the offsets as misalignments between PPS/DP EAC and SCS.

4.3.1.8 Nonlinear PPS/DP EAC Contributors. The sources of nonlinear smear have been classified within three major categories as described below.

4.3.1.8.1 Stereo LOS Settling. Angular oscillation of the LOS arises following a change in stereo mirror position. Nonlinear smear occurs due to this oscillation prior to completion of settling. Analyses of settling tests show that the oscillations are in the form of a damped sinusoid:

$$\theta = \theta_0 \exp(-at) \cos 2\pi ft$$

Where:

- θ = angular displacement of the LOS from the commanded position at time t
- θ_0 = the maximum angular displacement from the commanded position
- a = damping constant
- f = frequency of oscillations
- t = time

~~TOP SECRET~~ GHandle via BYEMAN
Control System Only

~~TOP SECRET~~ GBIF-008- W-C-019838-RI-80

Although this is a transient disturbance, the MTF at each spatial frequency of interest can be calculated as a function of time. Immediately after stereo mirror slew, the modulation transfer function will be quite low. After some time period, the MTF will increase to a point where it is at an acceptable level. The time at which this state is reached is defined as the settling time. In normal operation, high-resolution photography does not start until this smear source has settled to a tolerable level.

4.3.1.8.2 Film Wander. Translation of the film in a direction parallel to the longitudinal axis of the platen is called film wander. Film wander causes a low frequency (approximately 15 Hz) sinusoidal, cross-track smear.

4.3.1.8.3 Platen Vibration. Platen vibration is the term used to describe any periodic in-track variations in the FDS. Such oscillations may be due to platen runout (any effect which results in the platen surface being nonconcentric with the platen axis) or FPLL responses to unidentified electrical or mechanical perturbations and resonances. The result of platen vibration is sinusoidal, in-track image smear. In this case multiple frequency perturbations are present and spectral analysis techniques described in Part 2 Section 4.1.2 are useful. Generally, perturbations of this nature are a complex combination of linear and nonlinear dynamic functions which may often be represented by sinusoidal smear combinations.

4.3.2 SCS Contributors

The PPS/DP EAC is mounted to the SCS and depends upon the attitude control system to provide a stable and accurate platform for orbital operations. The orbiting PSV may be considered to be in continuous drift within a deadband region, with the drift, or attitude rates, under the control of the SCS. Errors in attitude (roll, pitch, and yaw) and the presence of attitude rates (roll, pitch, and yaw) can cause smear.

~~TOP SECRET~~ GHandle via BYEMAN
Control System Only

~~TOP SECRET~~ GBIF-008- W-C-019838-RI-80

As the SCS smear contributors are under the control of the SCS contractor, we assume that rates are controlled to within the values specified in the General System Specification.

4.3.3. Telemetry, Tracking, and Command (TT and C) Contributors

The telemetry, tracking, and command system (also the responsibility of another contractor) is responsible for calculation of the satellite location and velocity with respect to the target at the precise moment of an intended photograph. Any errors in this complex prediction process will contribute to image smear. Contributors to TT and C related errors are described below.

4.3.3.1 Target Location Uncertainty. The targetting procedure is based upon expressing the latitude and longitude of a desired target. Various error sources combine to hamper the capability to accurately specify the location of a target. This uncertainty introduces errors in the computation of pointing, FDS, and crab angle parameters, consequently producing image smear. The specified system requirement is to be capable of accurately specifying the location of a target within ± 0.642 nautical mile (3σ).

4.3.3.2 Ephemeris Uncertainty. Gravitational variations, aerodynamic drag, magnetic moments, system-clock drift and many other effects combine to produce inaccuracies in the knowledge of the exact vehicle location at any given instant. Ephemeris uncertainty can produce smear analogous to target uncertainty. Present state-of-the-art capability, using real-time bias techniques, results in a ± 0.246 nautical mile tolerance (3σ) for this parameter.

4.3.3.3 Knowledge of Altitude. The determination of the FDS required for IMC is, in part, a function of altitude (See Part 2, Section 3.2). Any inaccuracy in the knowledge of the altitude from the vehicle to the target is

~~TOP SECRET~~ GHandle via BYEMAN
Control System Only

~~TOP SECRET~~ G

BIF-008- W-C-019838-RI-80

reflected as a linear smear component. This uncertainty can be due to errors in knowledge of target elevation and/or ephemeris errors in specifying the height of the vehicle above the geoid. The specified system requirement allows ± 0.30 nmi tolerance (3σ) for the knowledge of vehicle altitude.

4.3.4 9-Inch Smear Equations

Table 2.4-1 lists equations for determining the expected ground smear and angular smear rate for the 9-inch system. Symbols used in these equations are described in Table 2.4-2. The equations have been derived for a flat earth model. Equations for a round earth model have been found to differ by less than 0.5 percent from those of the flat earth model. Flat earth equations are therefore considered adequate. Root-sum-square (RSS) techniques should be used to estimate the effects of several individual contributors.

4.3.5 5-Inch System Smear

The center of the 5-inch system does not coincide with the optical axis as shown in Figure 2.4-12.

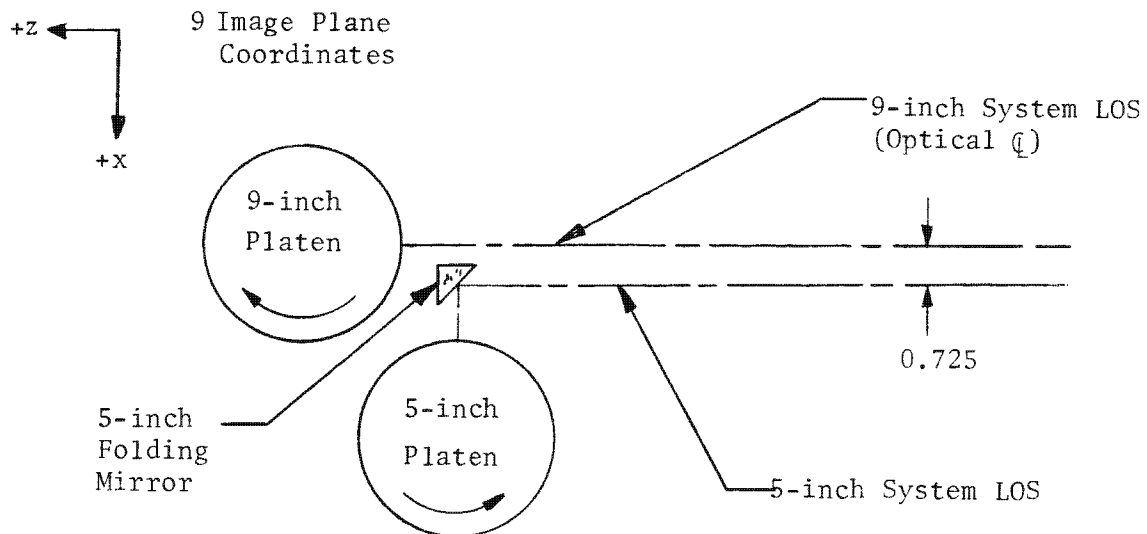


Figure 2.4-12. Five-Inch System Offset

2.4-33

~~TOP SECRET~~ G

Handle via BYEMAN
Control System Only

~~TOP SECRET~~ GBIF-008- W-C-019838-RI-80

For purposes of image motion compensation, the 5-inch folding mirror may be disregarded and the center of the 5-inch system may be considered to be a point in the 9-inch field (nominally, $x = 0.725''$, $y = 0.0''$). The effect on expected smear in a 5-inch frame as a result of this offset can be calculated. Matrix techniques have been used to evaluate the image motion vector (at $(0.725''$, $0.0''$) in the field.

Unfortunately, the matrix for the $(0.725''$, $0.0''$) point cannot be conveniently reduced to simplified smear prediction equations as was done for the $(0.0''$, $0.0''$) center of the 9-inch format. Part 2, Section 3.2.2 describes how the quantitative effect of the 5-inch offset may be described in terms of $\Delta\Sigma$ and $\Delta\Omega$ increments to the line-of-sight (LOS) of the 9-inch system. This approach can also be used to approximate the predicted smear in the 5-inch system. The equations for the 5-inch LOS are:

$$\Sigma_5 = \Sigma - \tan^{-1} \left(\frac{0.725}{F} \cos \chi \right)$$

$$\Omega_5 = \Omega + \tan^{-1} \left(\frac{0.725}{F} \sin \chi \right)$$

Where:

- Σ_5 = 5-inch stereo LOS angle
- Σ = 9-inch stereo LOS angle
- Ω_5 = 5-inch obliquity LOS angle
- Ω = 9-inch obliquity LOS angle
- χ = commanded crab angle
- F = focal length (175 in. nominal)

Smear in the 5-inch system may be predicted by using the 9-inch smear equations shown in Table 2.4-1, but substituting the 5-inch LOS angles, Σ_5 and Ω_5 , for the Σ and Ω variables. The distortion (% D) value used should be the distortion at the point in the lens field where the target would appear.

2.4-34

~~TOP SECRET~~ GHandle via BYEMAN
Control System Only

~~TOP SECRET~~ GBIF-008- W-C-019838-RI-80

The following example illustrates a case where the image is photographed 0.35° off-axis in the $-Y$ direction. Figure 2.4-13 illustrates the appropriate geometry.

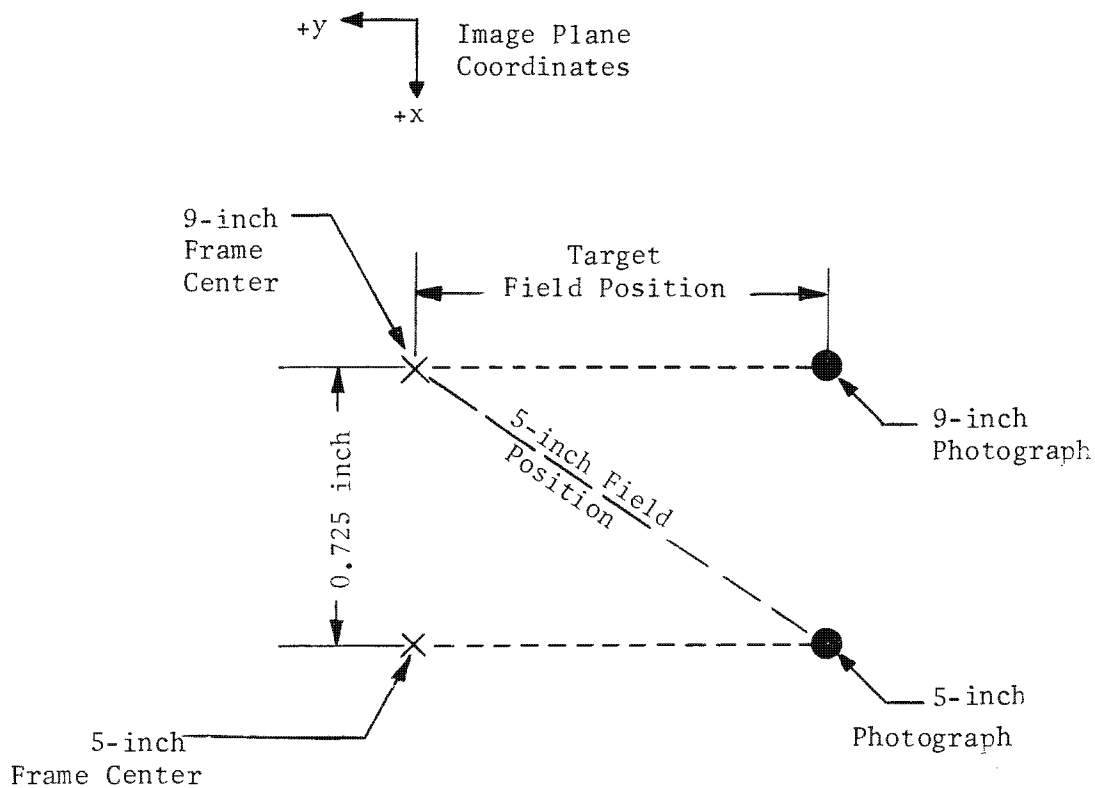


Figure 2.4-13. Five-Inch Field Position

Given: $\Sigma = -8.65$ degrees $\Omega = 30$ degrees $\chi = -3.30$ degreestarget field position = 0.35° (1.07 inches)

focal length = 175 inches

Find: Σ_5 , Ω_5 , and μ_5

2.4-35

~~TOP SECRET~~ GHandle via **BYEMAN**
Control System Only

~~TOP SECRET~~ GBIF-008- W-C-019838-RI-80

Solution:

$$\Sigma_5 = -8.65 - \tan^{-1} \left[\frac{0.725}{175} \cos(-3.30) \right]$$

$$= -8.89 \text{ degrees}$$

$$\Omega_5 = 30^\circ + \tan^{-1} \left[\frac{0.725}{175} \sin(-3.30) \right]$$

$$\Omega_5 = 29.99 \text{ degrees}$$

$$\text{5-inch field position} = \sqrt{(0.725)^2 + (1.07)^2}$$

$$= 1.292 \text{ inches}$$

$$\mu_5 = \tan^{-1} \left(\frac{\text{5-inch field position}}{\text{focal length}} \right)$$

$$= \tan^{-1} \left(\frac{1.292}{175} \right)$$

$$= 0.42 \text{ degree}$$

The 5-inch field angle, μ_5 , should be used in equation 14 to calculate the smear due to lens distortion. The 5-inch platen will normally be driven to the preferred 5-inch FDS as calculated in Part 2 Section 3.2.2. However, if the 9-inch and 5-inch systems are used simultaneously, the FDS can be optimum for only one system. In such a case, the smear due to the improper FDS may be calculated using equation 11.

4.4 Smear Budgeting

A smear budget was established early in the design phase to identify and control magnitudes of smear contributors. The tables included in this section show the tolerance permitted for each contributor and indicate the smear attributable to each. Many contributors have between-mission (unit-to-unit) and within-mission (variable for a given unit) values.

4.4.1 Between-Mission and Within-Mission Linear Smear Contributors

Table 2.4.3 lists all PPS/DP EAC between-mission and within-mission linear smear contributors. The mean and one sigma (1σ) error values are listed to facilitate the use of standard, statistical analysis techniques. The resultant

~~TOP SECRET~~ GHandle via BYEMAN
Control System Only

TABLE 2.4-3

PPS/DP EAC LINEAR SMEAR BUDGET (WITH SOFTWARE)

	PPS/DP EAC Error (degrees except where noted)		Equivalent Smear Rates (μradians/second)			
			In-Track		Cross-Track	
	μ	σ_{β}	μ	σ_{β}	μ	σ_{β}
<u>Between-Mission Contributor</u>						
Optical-axis-to-Reference Mirror (Pitch)		0.0030				
Optical-axis-to-Reference Mirror (Yaw)		0.0030			2.4	
Optical-axis-to-Reference Mirror (Roll)		0.0023				
Reference Mirror to Mechanical Interfaces (Pitch)		0.0057				
Reference Mirror to Mechanical Interfaces (Yaw)		0.0057			4.6	
Reference Mirror to Mechanical Interfaces (Roll)		0.0058				
Focal Length		0.1000 (inches)	26.4			
PPS/DP EAC Hotdogging (Pitch)	0.0041	0.0018				
PPS/DP EAC Hotdogging (Yaw)	-0.0444	0.0059			35.8	4.8
Crab Positioning (Roll)		0.0866				69.9
Stereo Positioning (Pitch)		0.0866				
			26.4		35.8	70.3
<u>Within-Mission Contributor</u>						
Crab Granularity (Roll)		0.1010				81.5
Crab Reproducibility (Roll)		0.0033				2.7
Stereo Reproducibility (Pitch)		0.0033				
Film-Drive Speed Granularity		0.0024 (inches/second)	13.9			
Film-Drive Speed Drift		0.0667 (percent)	30.9			
PPS/DP EAC Hotdogging (Pitch)		0.0139				
PPS/DP EAC Hotdogging (Yaw)		0.0147				11.9
			33.9			82.42

Conditions:

$\Omega = \epsilon = \chi = 0$ degrees $V_f = 8.1$ inches/second $h = 90$ nautical miles

Software corrections assumes 75% back-out of hotdogging errors.

μ = mean value

σ_{β} = one sigma value

* Scale rates by $\frac{90}{h}$ for other altitudes

2.4-37

Approved for Release: 2017/02/14 C05097211

Approved for Release: 2017/02/14 C05097211

~~TOP SECRET~~ GBIF-008- W-C-019838-RI-80

smear rates are calculated for a representative case. These linear smear rates represent PPS/DP EAC capability using software correction techniques to minimize on-orbit smear. Software correction for PPS/DP EAC contributors refers to the capability of the operational software to compensate for known and predicted thermal bending. Computation of statistical totals utilizes RSS techniques.

4.4.2 Nonlinear Smear Contributors

Table 2.4-4 lists the PPS/DP EAC contributors to nonlinear smear. These values are expressed as the minimum permissible MTF arising solely from the stated contributor. These values then represent the maximum acceptable degradation resulting from each contributor.

4.4.3 Smear Contributors for the PSV

Table 2.4-5 lists all known smear contributors for the entire PSV. This includes PPS/DP EAC, SCS, and TT and C contributors. The contributors are listed as either a bias or as random variables. The distributions and one sigma (1σ) values are listed for the random variables to facilitate the application of statistical combination techniques.

4.4.4 Smear Rate Statistical Combination

Table 2.4-6 shows an overall statistical combination for the entire PSV. These linear smear rates represent system capability using software correction of "hotdogging" errors and adaptive bias. Adaptive bias is a method of reducing attitude rates by decoupling the SCS attitude thrusters during periods of PPS/DP EAC induced momentum changes. The 95%/95% criteria (see Appendix E) yields the smear rates of 119 μ rad/sec in-track and 425.3 μ rad/sec cross-track for the representative case shown. The 95%/95% describes the 95th percentile performance for a 95-percent bias mission.

2.4-38

~~TOP SECRET~~ GHandle with Care
Controlled Document

TABLE 2.4-4

MINIMUM ACCEPTABLE MODULATION TRANSFER FUNCTION
RESULTING FROM NONLINEAR SMEAR

Conditions: R-5 formula lens
85% OQF
On-axis
Exposure time = 0.003 second

<u>Contributor</u>	<u>Direction</u>	<u>Minimum Transfer Function at 180 lines/millimeter</u>
Platen Vibration	In-Track	0.937
Stereo Settling *	In-Track	0.912
Film Wander **	Cross-Track	0.950

* Worst case: 3.0 seconds after execution of move command (+ to - move).

** Has been acknowledged as a legitimate requirement. No technique currently exists to adequately test for compliance.

2.4-39

Approved for Release: 2017/02/14 C05097211

Approved for Release: 2017/02/14 C05097211

~~TOP SECRET~~ GBIF-008- W-C-019838-RI-80

TABLE 2.4-5

SMEAR CONTRIBUTOR BUDGET (F/0-7)

<u>Between-Mission Bias</u>	<u>μ</u>		<u>Units</u>
Roll attitude bias	0.0000	-	deg
Pitch attitude bias	+0.0041	-	deg
Yaw attitude bias	-0.0444	-	deg
Roll rate bias	0.0000	-	deg/sec
Pitch rate bias	0.0000	-	deg/sec
Yaw rate bias	0.0000	-	deg/sec
<u>Random Error Contributor</u>	<u>One-Sigma Tolerance</u>	<u>Distribution</u>	<u>Units</u>
Knowledge of altitude	0.1000	Normal	nmi
Roll attitude	0.1228	Normal	deg
Pitch attitude	0.1143	Normal	deg
Yaw attitude	0.0788	Normal	deg
Roll rate	0.0026	Normal	deg/sec
Pitch rate	0.0010	Normal	deg/sec
Yaw rate	0.0010	Normal	deg/sec
Crab granularity	0.1750	Uniform	deg
Crab reproducibility	0.0033	Normal	deg
Stereo reproducibility	0.0033	Normal	deg
FDS granularity	0.0440	Uniform	%
FDS drift	0.0330	Normal	%
Focal length error	0.1000	Normal	inches
Knowledge of altitude	0.1000	Normal	nmi
Target location uncertainty	0.2140	Normal	nmi
Ephemeris uncertainty	0.0820	Normal	nmi
Geometric distortion*	-	-	-
Lens distortion*	-	-	-

* Function of field position: zero (0) on-axis

2.4-40

~~TOP SECRET~~ GHandle via **BYEMAN**
Control System Only

TABLE 2.4-6

SATELLITE VEHICLE SYSTEM, EQUIVALENT SMEAR RATE (μ R/SEC) *
STATISTICAL COMBINATION (WITH ADAPTIVE BIAS AND SOFTWARE)

	Mean Bias	Between Mission Variability	Within Mission Variability	μ_{95}	95/95
	μ	σ_B	σ_R		
<u>In-Track</u>					
SCS	0	11.0	18.0	22.0	52.0
PPS	0	26.4	33.9	51.2	107.4
Requirement	0	28.6	38.4	56.3	119.4
<u>Cross-Track</u>					
SCS	21.0	60.0	101.0	125.0	290.0
PPS	35.8	70.3	82.4	153.9	288.2
Requirement	56.8	92.4	130.3	210.4	425.3

$\Omega = \Sigma = \chi = 0$ degrees

$V_f = 8.1$ inches/second

$h = 90$ nautical miles

*Scale table values by $\frac{90}{h}$ for other altitudes.

Handle via **BYEMAN**
Control System Only

Approved for Release: 2017/02/14 C05097211

2.4-41

Approved for Release: 2017/02/14 C05097211

~~TOP SECRET~~ GBIF-008-W-C-019838-RI-80

4.5 Smear Detection and Measurement

Smear slits are provided as an aid in detection and measurement of the uncompensated image motion which produces smear.

4.5.1 Smear Slit Theory

Smear arises from uncompensated image motion such that the image moves relative to the film during the exposure interval. Smear is reported in length units, usually micrometers, and represents the image movement observed.

Smear slits consist of two slits, separated by a known amount, at the end of the exposure slit. If uncompensated image motion exists, the image will move relative to the film between the exposures through the two slits. This will result in a double exposure. The magnitude and direction of the image motion occurring in the time required for the film to travel between the two smear slits may be measured. The two slits are of different widths so the sign of the smear may also be determined since one image will have greater exposure.

4.5.2 Smear Slit Design

The smear slit configuration is shown in Figure 2.4-14.

4.5.3 Smear Slit Operation

Smear, although a vector quantity, is usually specified by in-track (x) and cross-track (y) components, since there are generally different contributors for in-track and cross-track smear, and measurements are most easily made in these directions.

2.4-42

~~TOP SECRET~~ GHandle via BYEMAN
Control System Only

~~TOP SECRET~~ G

BIF-008-W-C-019838-RI-80

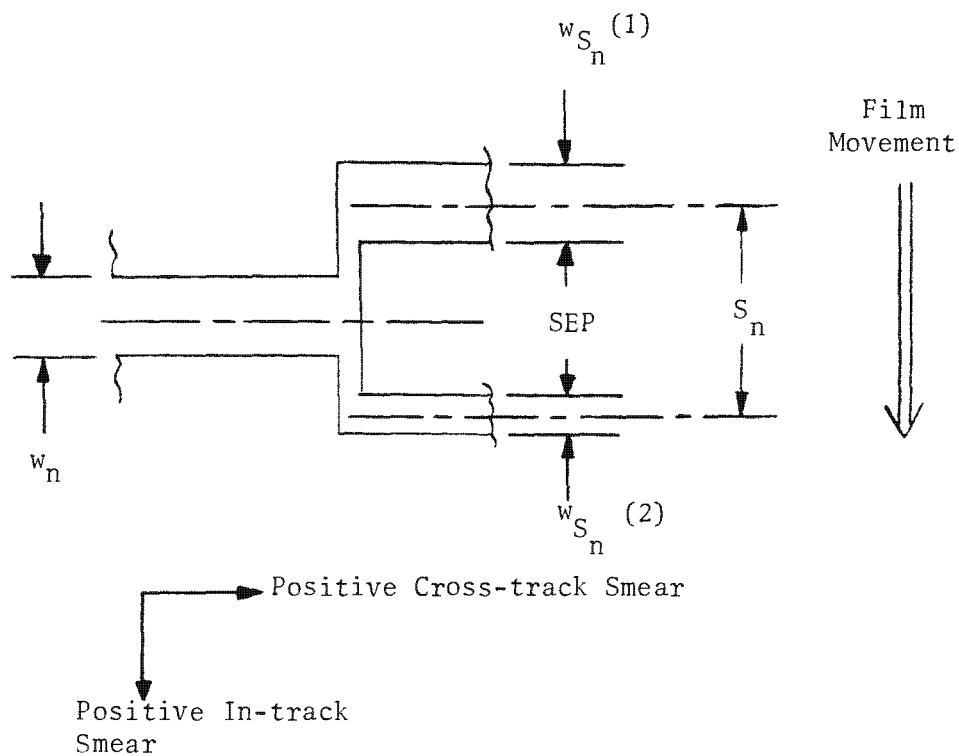


Figure 2.4-14. Smear Slit Configuration

2.4-43

~~TOP SECRET~~ G

Handle via BYEMAN
Control System Only

~~TOP SECRET~~ GBIF-008- W-C-019838-RI-80

The components of the smear (mismatch) velocity are given by:

$$V_{S(x)} = V_{i(x)} - V_f$$

$$V_{S(y)} = V_{i(y)}$$

The sign of the smear velocity is taken relative to the BIF-008, image plane coordinates.

The smear (displacement) observed in the smear slit area, in micrometers is given by:

$$S_{x_n} = \frac{S_n}{V_f} (V_{i(x)} - V_f) (2.54 \times 10^4)$$

$$S_{y_n} = \frac{S_n}{V_f} V_{i(y)} (2.54 \times 10^4)$$

Where: S_n is in inches

V_f , $V_{i(x)}$ and $V_{i(y)}$ are in in./sec at the film

The smear observed in the smear slit area differs from that in the main image area by a factor, denoted k_n , equal to the ratio of smear slit separation to slit width. Table 2.4-7 presents nominal values for the various dimensions shown in Figure 2.4-14 and for k_n . An Extended Altitude Capability (EAC) smear slit will complement the current 9-system smear slit. This was necessary to optimize smear image displacements to ensure reading accuracy when system operation occurs at EAC altitudes. These values are given in Table 2.4-8.

~~TOP SECRET~~ GHandle via BYEMAN
Control System Only

~~TOP SECRET~~ GBIF-008- W-C-019838-RI-80

TABLE 2.4-7

SMEAR SLIT DIMENSIONS
SEP = 0.0855"

<u>n</u>	<u>w_n</u>	<u>w_{S_n} (1)</u>	<u>w_{S_n} (2)</u>	<u>S_n</u>	<u>k_n</u>
1	0.0040	0.0170	0.0020	0.0950	23.75
2	0.0054	0.0177	0.0027	0.0957	17.72
3	0.0072	0.0186	0.0036	0.0966	13.42
4	0.0094	0.0197	0.0047	0.0977	10.39
5	0.0126	0.0213	0.0063	0.0993	7.88
6	0.0168	0.0234	0.0084	0.1014	6.04
7	0.0224	0.0262	0.0112	0.1042	4.65
8	0.0300	0.0300	0.0150	0.1080	3.60
9	0.0400	0.0350	0.0200	0.1130	2.83
10	0.0534	0.0417	0.0267	0.1197	2.24
11	0.0712	0.0506	0.0356	0.1286	1.81
12	0.0948	0.0624	0.0474	0.1404	1.48
13	0.1266	0.0783	0.0633	0.1563	1.23
14	0.1686	0.0993	0.0843	0.1773	1.05
15	0.2250	0.1275	0.1125	0.2055	0.91
16	0.3000	0.1650	0.1500	0.2430	0.81

$$w_{S_n} (1) = \frac{w_n + w_8}{2}$$

$$k_n = \frac{S_n}{w_n}$$

$$w_{S_n} (2) = \frac{w_n}{2}$$

$$S_n = 0.0855 + \left(\frac{w_{S_n} (1) + w_{S_n} (2)}{2} \right)$$

2.4-45

~~TOP SECRET~~ GHandle via BYEMAN
Control System Only

~~TOP SECRET G~~

BIF-008-W-C-019838-RI-80

TABLE 2.4-8

SMEAR SLIT DIMENSIONS (EAC)
SEP = 0.0214"

<u>n</u>	<u>w_n</u>	<u>w_{S_n}⁽¹⁾</u>	<u>w_{S_n}⁽²⁾</u>	<u>S_n</u>	<u>k_n</u>
1	0.0040	0.0164	0.0050	0.0321	8.03
2	0.0054	0.0171	0.0057	0.0328	6.07
3	0.0072	0.0180	0.0066	0.0337	4.68
4	0.0094	0.0191	0.0077	0.0348	3.70
5	0.0126	0.0207	0.0093	0.0364	2.89
6	0.0168	0.0228	0.0114	0.0385	2.29
7	0.0224	0.0256	0.0142	0.0413	1.84
8	0.0300	0.0294	0.0180	0.0451	1.50
9	0.0400	0.0344	0.0230	0.0501	1.25
10	0.0534	0.0411	0.0297	0.0568	1.06
11	0.0712	0.0500	0.0386	0.0657	0.92
12	0.0948	0.0618	0.0504	0.0775	0.82
13	0.1266	0.0777	0.0663	0.0934	0.74
14	0.1686	0.0987	0.0873	0.1144	0.68
15	0.2250	0.1269	0.1155	0.1426	0.63
16	0.3000	0.1644	0.1530	0.1801	0.60

$$w_{S_n}^{(1)} = w_{S_2}^{(1)} + \frac{(w_n - w_2)}{2} \quad S_n = 0.0214 + \left(\frac{w_{S_n}^{(1)} + w_{S_n}^{(2)}}{2} \right)$$

$$w_{S_2}^{(2)} = w_{S_2}^{(2)} + \frac{(w_n - w_2)}{2} \quad k_n = \frac{S_n}{w_n}$$

2.4-46

~~TOP SECRET G~~Handle via BYEMAN
Control System Only

~~TOP SECRET~~ GBIF-008- W-C-019838-RI-80

Smear measured in the smear slits may be converted to on-axis values by dividing by k_n from Table 2.4-7.

$$S_x \text{ (on-axis)} = \frac{S_{x_n}}{k_n}$$

$$S_y \text{ (on-axis)} = \frac{S_{y_n}}{k_n}$$

The equivalent smear rate may be obtained by:

$$\mu_x = \frac{S_{x_n} V_f}{S_n F} \quad (39.37)$$

$$\mu_y = \frac{S_{y_n} V_f}{S_n F} \quad (39.37)$$

Where: μ_x and μ_y are the in-track and cross-track smear rate respectively ($\mu\text{rad}/\text{sec}$)

S_{x_n} = the observed in-track smear, in the smear slit for slit n (μm)

V_f = film-drive speed (in./sec)

S_n = separation of the smear slits, slit n (inches)

F = focal length (inches)

39.37 = conversion; μm to μinch

The following example will serve to illustrate the use of these equations.

Given: An in-track image separation of $15 \mu\text{m}$ is observed in smear slit ($n = 6$)
6. The frame was exposed at a film-drive speed of 5.6 in./sec.

2.4-47

~~TOP SECRET~~ GHandle via BYEMAN
Control System Only

~~TOP SECRET~~ G

BIF-008- W-C-019838-RI-80

Find: Equivalent smear rate

Solution: From Table 2.4-7, S_n for smear slit 6 is 0.1014

$$\mu_x = \frac{(15) (5.6) (39.37)}{(0.1014) (175)}$$

$$= 186 \mu\text{rad/sec}$$

2.4-48

~~TOP SECRET~~ G

Handle via BYEMAN
Control System Only

~~TOP SECRET~~ GBIF-008- W-C-019838-RI-80

5.0 FOCUS

For optimal performance (resolution, image quality) it is mandatory that the photographic emulsion plane coincide with the plane containing the highest quality image (best photographic focus (BPF)). This section describes the precision and accuracy of the Gambit system when determining the degree of coincidence of these two planes. BPF, in reality, represents a compromise location when potential aberrations, such as astigmatism, are considered. However, it can be assumed that factory through-focus testing, using interferometric techniques, will yield a practical optimal BPF plane.

5.1 Focus Requirement

The required accuracy in placing the film at BPF can be estimated using the Rayleigh Criterion limit for allowable optical wavefront degradation. The limit states: "If the optical path difference between any axial ray and a marginal ray is one-quarter wavelength or less, the optical instrument will not have a quality noticeably short of a perfect system." When applied to focus error, this implies that a well-corrected lens has a depth of focus on either side of exact geometric focus over which the maximum optical path difference (OPD) does not exceed one-quarter wavelength. In vacuum, the depth of focus for this condition is stated:

$$\Delta F = \pm 2 C \lambda (\underline{f}/\#)^2$$

where: ΔF = depth of focus in inches
 λ = wavelength in nanometers
 $\underline{f}/\#$ = lens \underline{f} -number
 C = conversion, nanometers to inches
 $= 3.937 \times 10^{-8}$ inches/nanometer

2.5-1

~~TOP SECRET~~ GHandle via **BYEMAN**
Control System Only

~~TOP SECRET~~ GBIF-008- W-C-019838-RI-80

For the $f/4.02$ optical system used in the PPS/DP EAC, and for a wavelength of 571 nm, the calculated depth of focus is ± 0.00073 inch. Since focus errors are described by statistically derived tolerances, a statistical confidence level is assigned to the maintenance of the film plane within the calculated depth of focus. With 95 percent statistics used in budget development it is expected that the film plane will be within the bounds of the calculated depth of focus 95 percent of the time.

5.2 Focus Maintenance

There are two aspects of focus maintenance into which errors may fall:

- (1) uncertainty in the location of the plane of highest aerial image quality with respect to some arbitrary, mechanical benchmark, and,
- (2) accuracy with which the film plane may be placed at a desired location, also with respect to some arbitrary, mechanical benchmark.

Some error contributors may influence both aspects of focus maintenance but are assumed to apply to one or the other for the purposes of analysis.

5.2.1 Focus Detection Subsystem

The focus detection subsystem (see Figure 2.5-1) is designed to reduce the uncertainty in the location of the plane of highest aerial image quality by examining a portion of the incoming wavefront and generating a signal related to the amount of defocus relative to the 9-inch image plane at 14 lpmm

2.5-2

~~TOP SECRET~~ GHandle via BYEMAN
Control System Only

~~TOP SECRET~~ G

BIF-008- W-C-019838-RI-80

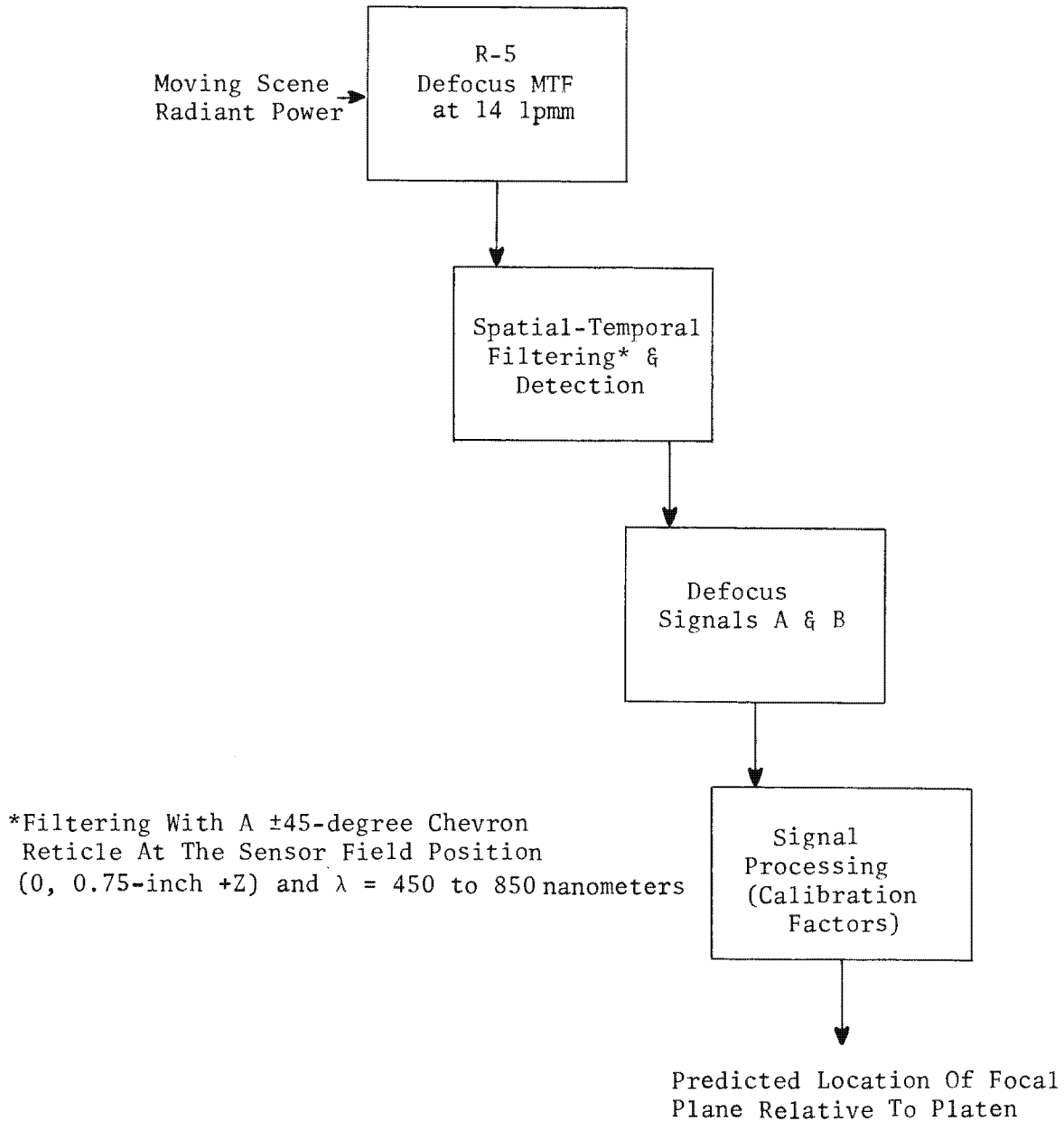


Figure 2.5-1. Focus Detection Subsystem Functional Block Diagram

2.5-3

~~TOP SECRET~~ G

Handle via BYEMAN
Control System Only

~~TOP SECRET~~ G

BIF-008-W-C-019838-RI-80

(± 45 degrees). The basic theory of operation of this system is developed in the following sections. Where applicable, the differences in operation between the low and high altitude modes are specifically delineated. Detailed hardware and operation descriptions are found in Part 3, Section 6.

5.2.1.1 Defocus MTF. The focus detection subsystem responds to the ± 45 -degree heterochromatic modulation transfer function (MTF) of the complete (R-5 and focus system) optical system at a spatial frequency of 14 lpmm. A chevron reticle is used to spatially filter the modulation to the 14-lpmm frequency level. The average heterochromatic through-focus MTF for the R-5 system at 14 lpmm is shown in Figure 2.5-2.

5.2.1.2 Scene Input and Reticle. The radiant power of a scene, expressed as a function of spatial frequency, is termed the Wiener spectrum of the scene. The approximate average Wiener spectrum of the earth as viewed from an altitude of 75 and 710 nmi through the Gambit system optics is shown in Figure 2.5-3.

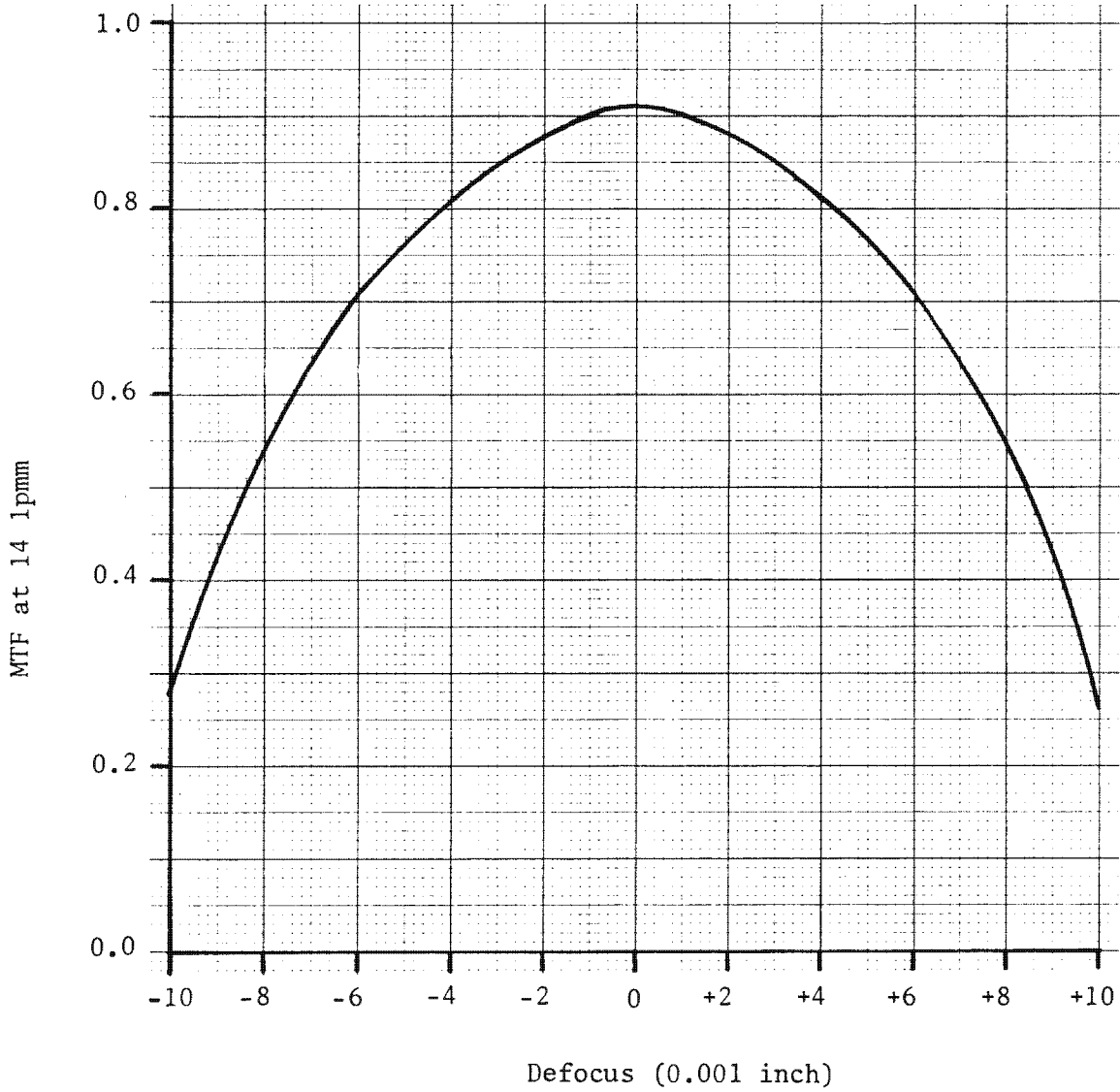
The scene power is spatially filtered by a chevron reticle having a 14-lpmm pitch and a ± 45 -degree orientation. The orthogonal relationship is required to sense mean* focus and ± 45 -degree orientation is needed to produce a common temporal frequency. The reticle width, 0.16 inch, is determined by longitudinal color considerations and a "vignetting" (apodization) mask is used to improve stop-band suppression. (The stop band is that region from the dc peak at $\nu = 0$ to the first peak at $\nu = 14$ lpmm.) A typical chevron reticle is shown in Figure 2.5-4.

*Because of the small amount of astigmatism present in the Gambit optics, focus may vary slightly between in-track and cross-track directions. Focus system models have shown that the focus indication based on the 45-degree MTF is comparable to the average of the in-track and the cross-track focus positions. Factory tests have shown the design to be insensitive to astigmatism orientation for magnitudes up to about 0.002 inch.

~~TOP SECRET~~ G

~~TOP SECRET~~ G

BIF-008-W-C-019838-RI-80



Conditions:

- Average for ± 45 degrees
- R-5 Lens
- 400-900 nm wavelength
- 9-inch Platen

Figure 2.5-2. Heterochromatic, 14 lpmm through Focus MTF

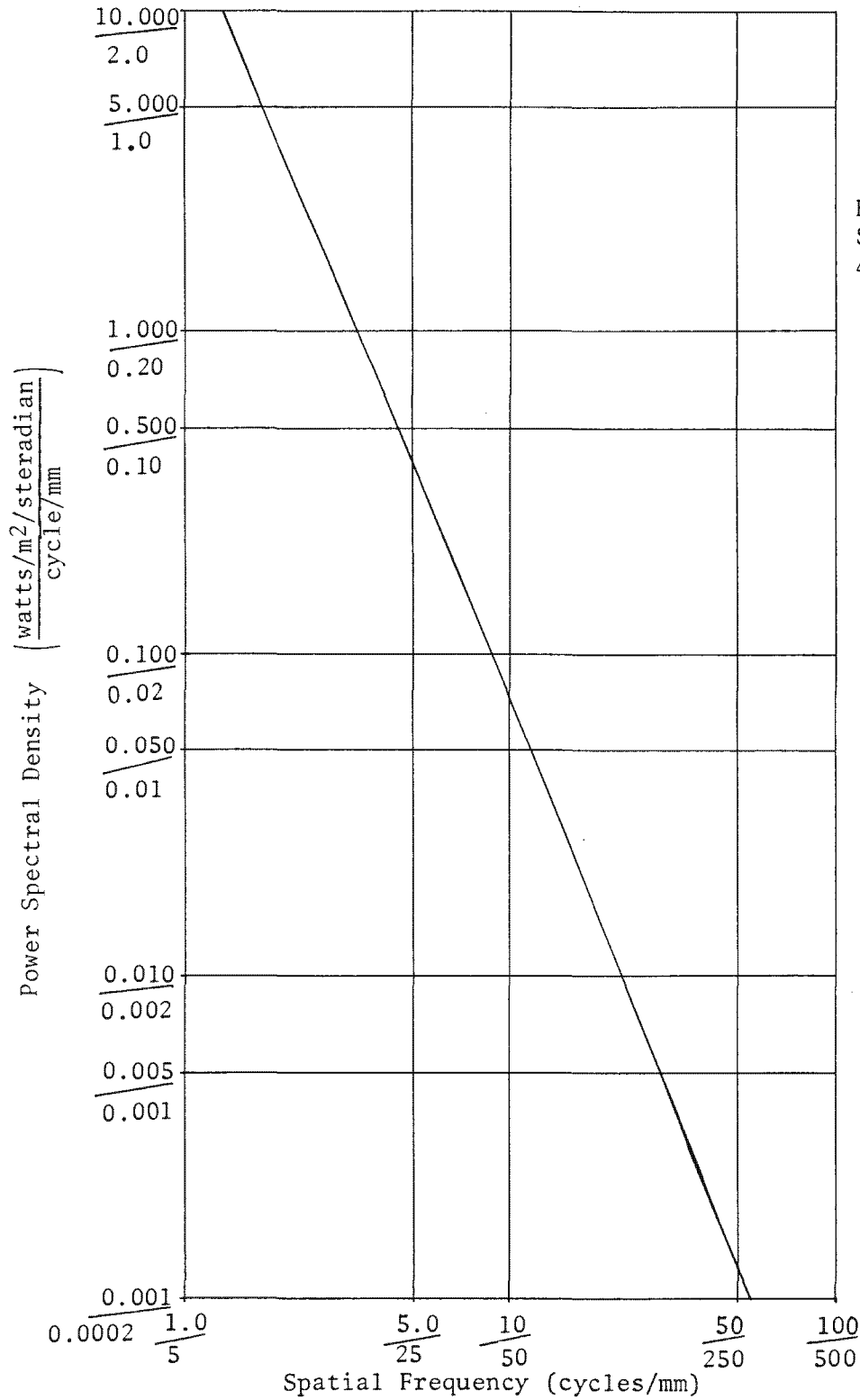
2.5-5

~~TOP SECRET~~ G

Handle via BYEMAN
Control System Only

~~TOP SECRET~~ G

BIF-008- W-C-019838-RI-80

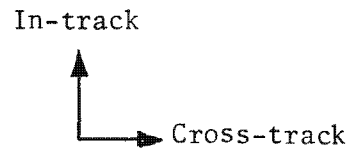


NOTE:
 Top Scale =
 75 nmi.
 Bottom
 Scale =
 450 nmi.

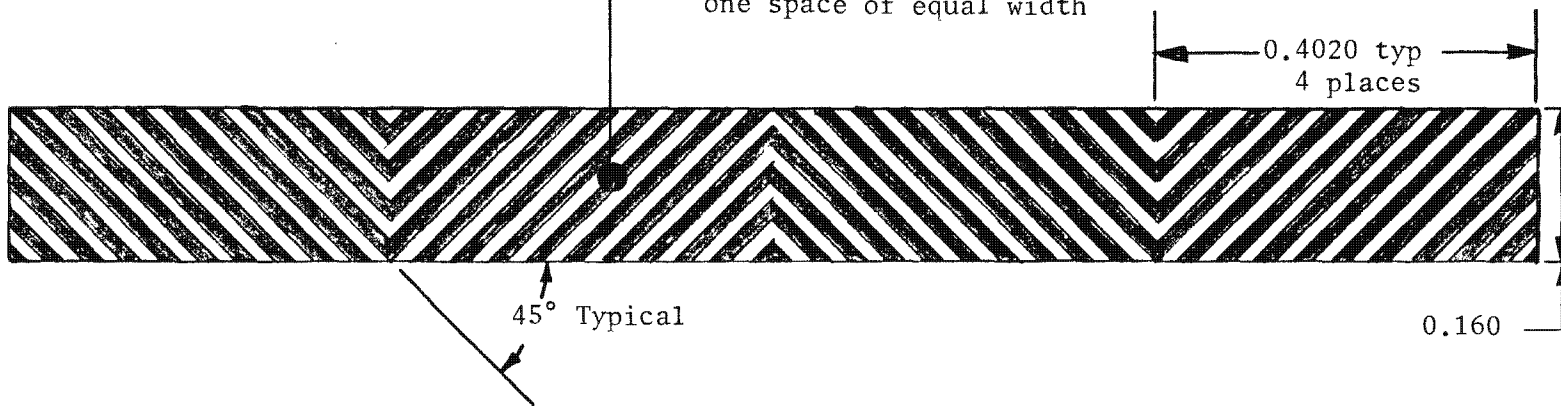
Figure 2.5-3 Earth's Wiener Spectrum
 (With 175-inch FL, 85% OQF Optics)

2.5-6
~~TOP SECRET~~ G

Handle via BYEMAN
 Control System Only



Spatial Frequency = 14 lpmm \perp bars (10 lpmm Cross-track and In-track)
1 lpmm = 1 line and one space of equal width



Dimensions are in inches unless otherwise noted.

Figure 2.5-4. Typical Chevron Reticle

Approved for Release: 2017/02/14 C05097211

Approved for Release: 2017/02/14 C05097211

~~TOP SECRET G~~BIF-008- W-C-019838-RI-80

The transfer function of the reticle is:

$$T(\nu) = \frac{\sin N\pi \nu/\nu_0}{N \pi \nu/\nu_0} \times \frac{1}{\cos \pi \nu/2\nu_0}$$

Power transfer peak amplitudes are:

$$|T(\nu_0)|^2 = \frac{4}{(2n+1)^2 \pi^2}$$

where: ν = spatial frequency (lpmm)
 n = number of bars \perp in reticle
 ν_0 = fundamental frequency of peak
 n = harmonic

Figure 2.5-5 shows the transfer function of the reticle from 0 to 0.5 lpmm and from 13.5 to 14.6 lpmm. The transfer function also peaks at multiples of the base frequency, but since the Wiener spectrum decreases as $\frac{1}{\nu^n}$ ($1 < n < 4$), and electronic filtering further reduces the effect of the higher frequencies, they present no problem. The transfer function of the reticle between 0.5 and 135 lpmm remains below 0.001.

The 14 lpmm component of scene power varies with time since the scene image is moving across the spatial filter. The range of temporal frequencies resulting from this "scan" is determined by the range of image velocities and ranges from 211 Hz (0.84 in./sec) to 2967 Hz (11.8 in./sec).

2.5-8

~~TOP SECRET G~~Handle via BYEMAN
Control System Only

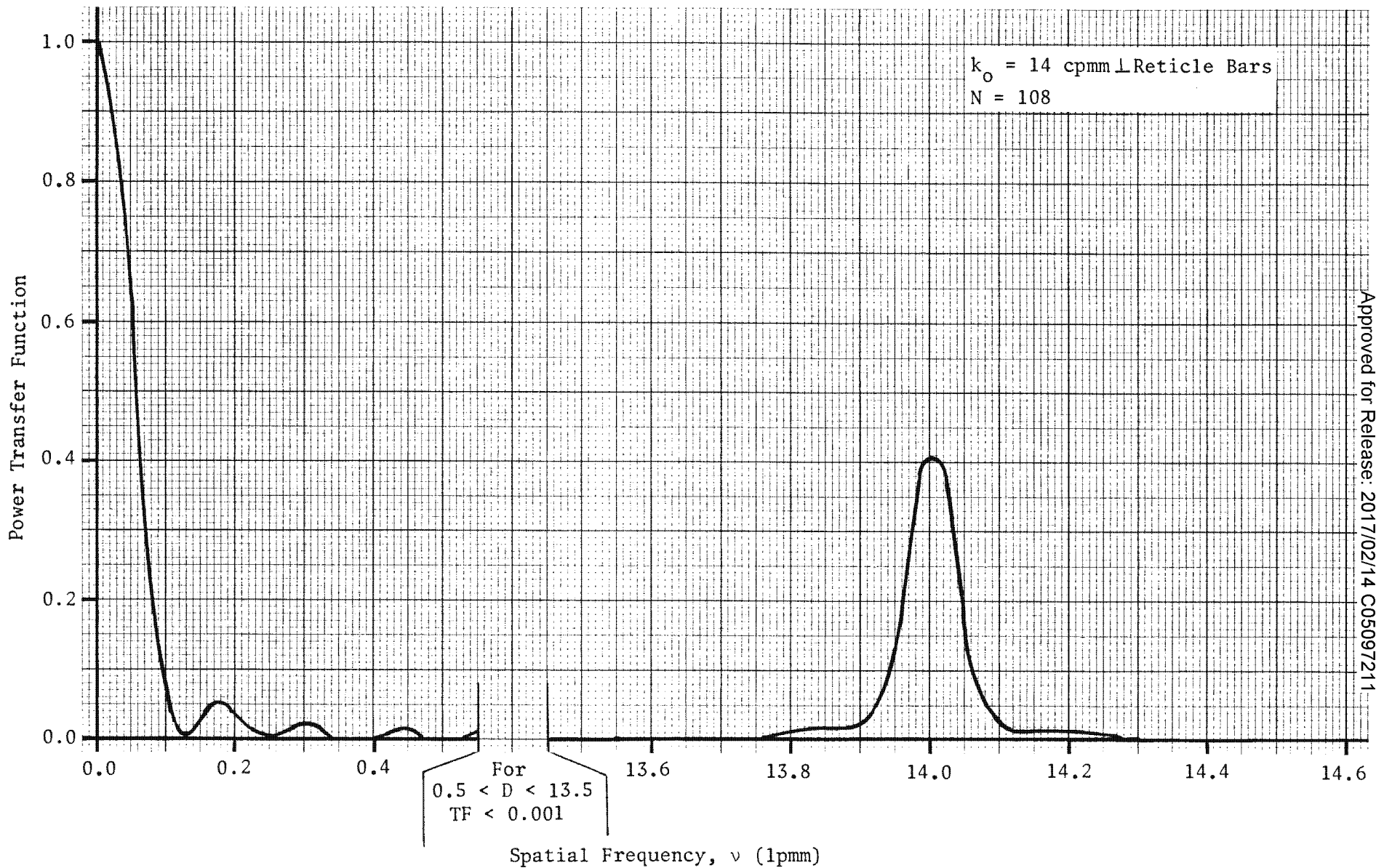


Figure 2.5-5. Reticule Transfer Function

~~TOP SECRET~~ GBIF-008- W-C-019838-RI-80

5.2.1.3 Focus Signal. A system which sees only constant input scene power could be made to work with one of the reticles described earlier, positioned optically conjugate to the film plane. Best focus would then be indicated by a maximum in the AC signal corresponding to 14-lpmm spatial frequency. This configuration would be useful as a focus sensor only if the input scene power were constant, since the focus indication would then be a function of the AC signal level (which changes when the input level changes). In practice, of course, the Wiener spectrum is not constant (see Figure 2.5-3).

The focus system design bases the focus indication on signals obtained from 2 channels derived from reticles displaced equal distances (0.015 inch) in front of (channel A) and behind (channel B) the image plane conjugate. The physical layout of this system is shown in Figure 2.5-8, Focus System, Physical Layout. The particular function of the channel A and B signals chosen to monitor the focus condition is the difference between the channel A and B signals normalized by the average signal strength $\frac{(A + B)}{2}$; that is, defocus is proportional to $\frac{2(A - B)}{A + B}$.

Figure 2.5-6 depicts the source of the channel A and channel B signals. The shape of the MTF curve, combined with the positions of the reticles, is such that a 0.17 change in signal $\left(\frac{2(A - B)}{A + B}\right)$ is related to a nominal change in position of 0.001. This results in the relationship between normalized signal and defocus shown in Figure 2.5-7. Graphs are shown relative to the 9-inch platen.

The normalization procedure effectively removes dependence on signal strength; as can be seen from the following argument. If the input scene energy is denoted E, the form of the scene energy functions contributing to channels A and B can be obtained by inspection of Figure 2.5-8, wherein:

2.5-10

~~TOP SECRET~~ GHandle via **BYEMAN**
Control System Only

~~TOP SECRET~~ G

BIF-008-W-C-019838-RI-80

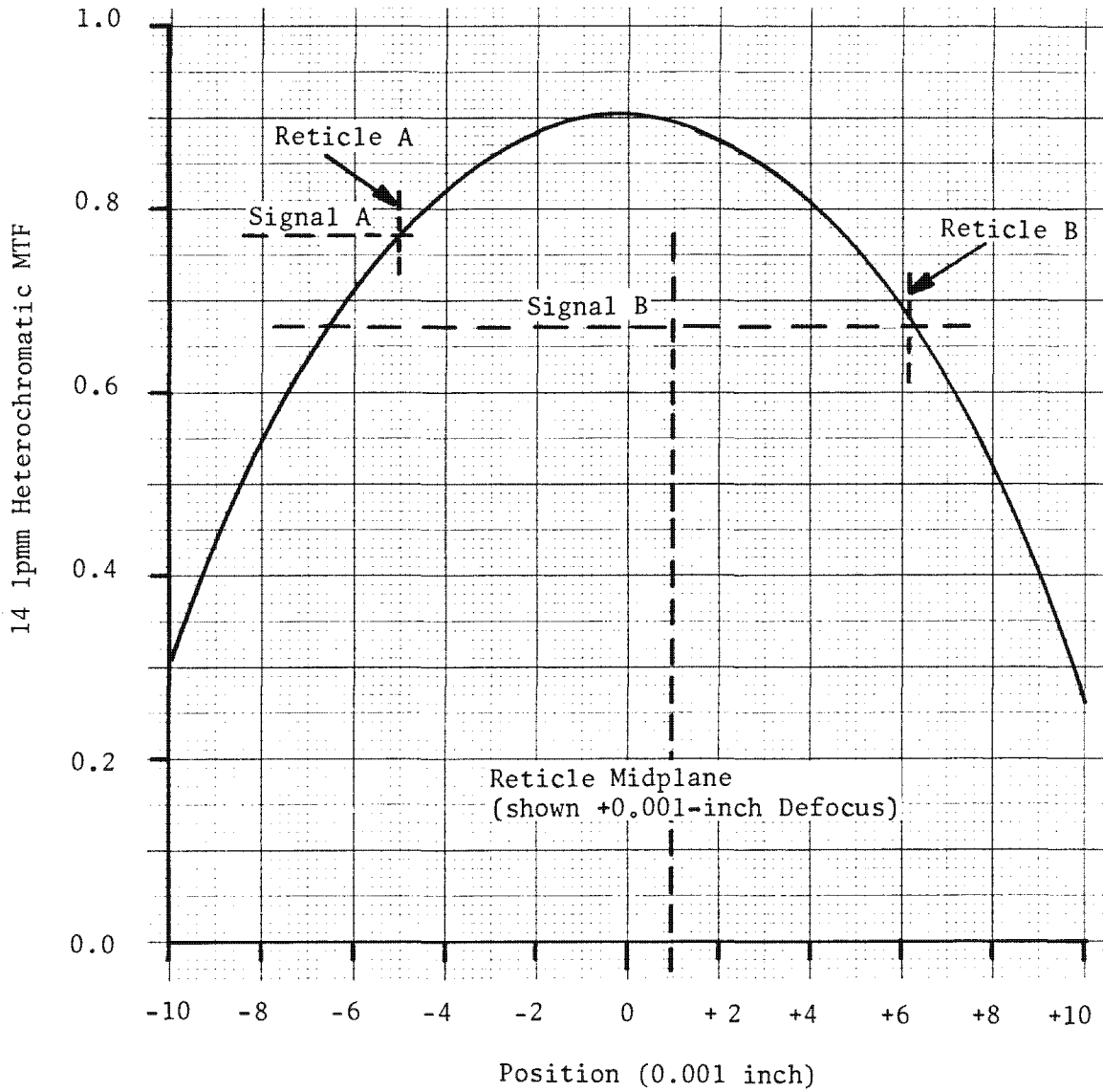


Figure 2.5-6. Channel A and B Signals

2.5-11

~~TOP SECRET~~ G

Handle via BYEMAN
Control System Only

~~TOP SECRET~~ G

BIF-008-W-C-019838-RI-80

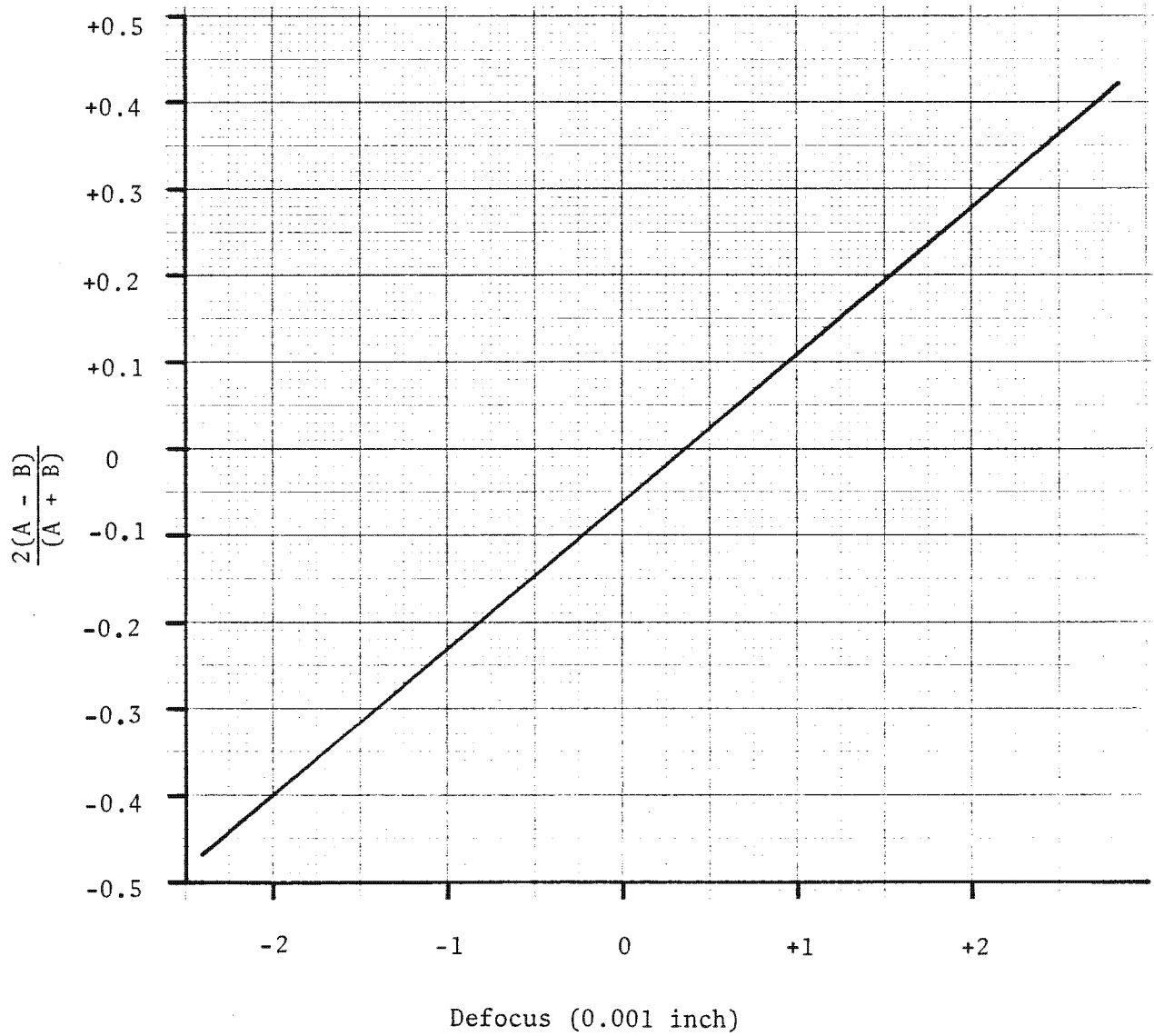
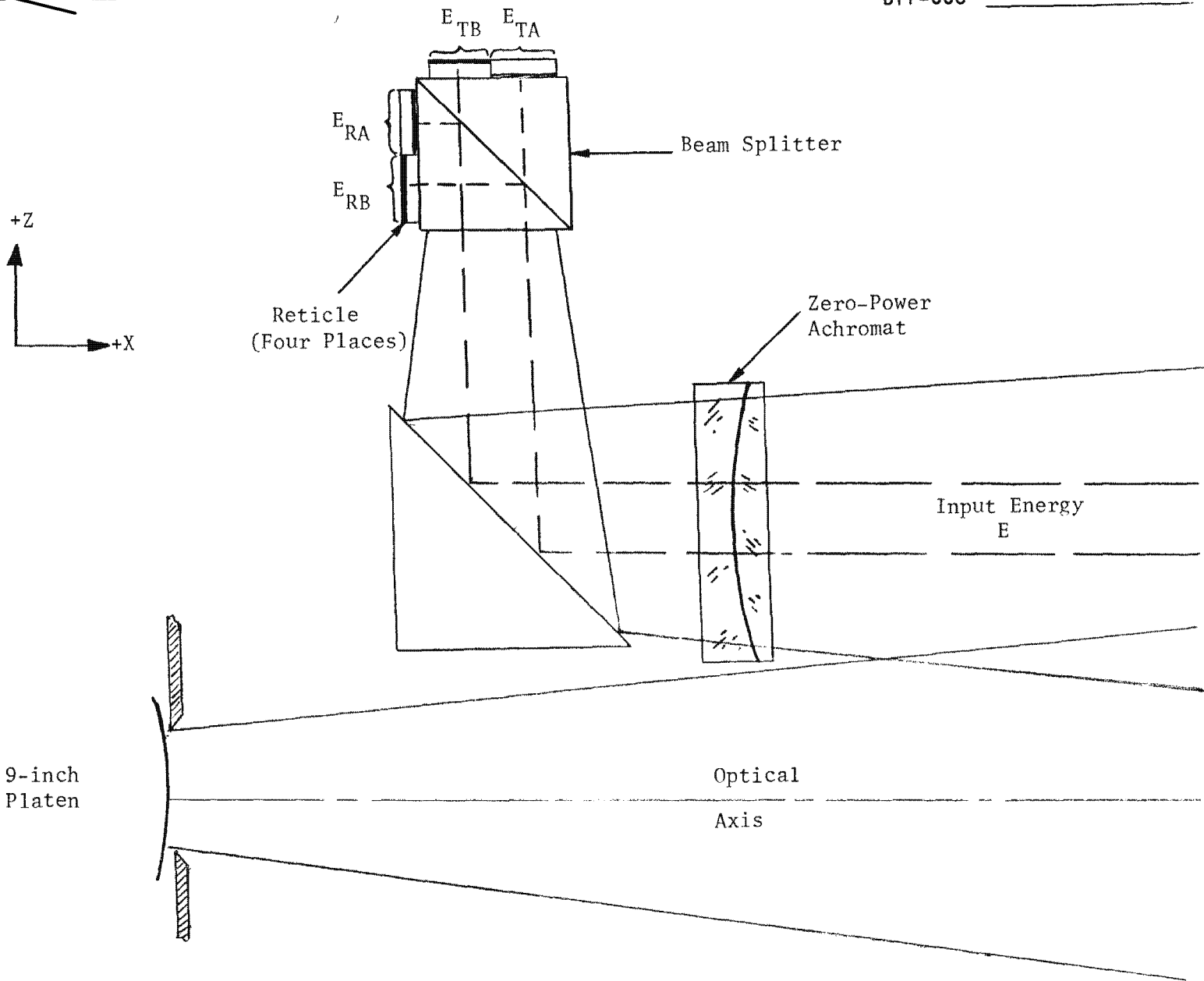


Figure 2.5-7. Signal vs. Defocus

2.5-12

~~TOP SECRET~~ G

Handle via BYEMAN
Control System Only



2.5-13

Figure 2.5-8. Focus System, Physical Layout

Approved for Release: 2017/02/14 C05097211

Approved for Release: 2017/02/14 C05097211

~~TOP SECRET~~ GBIF-008- W-C-019838-RI-80

$$E_A = (T_A + R_A + \alpha_A) E$$

$$E_B = (R_B + T_B + \alpha_B) E$$

where: T_A , T_B and R_A , R_B are transmittances and reflectances of channel A and channel B respectively.
 α is the absorption in the optical path.

Since the absorption is equal for both channels (no channel-specific glass inhomogeneity in the beam splitter or reticle plates), $\alpha_A = \alpha_B = \alpha$ and

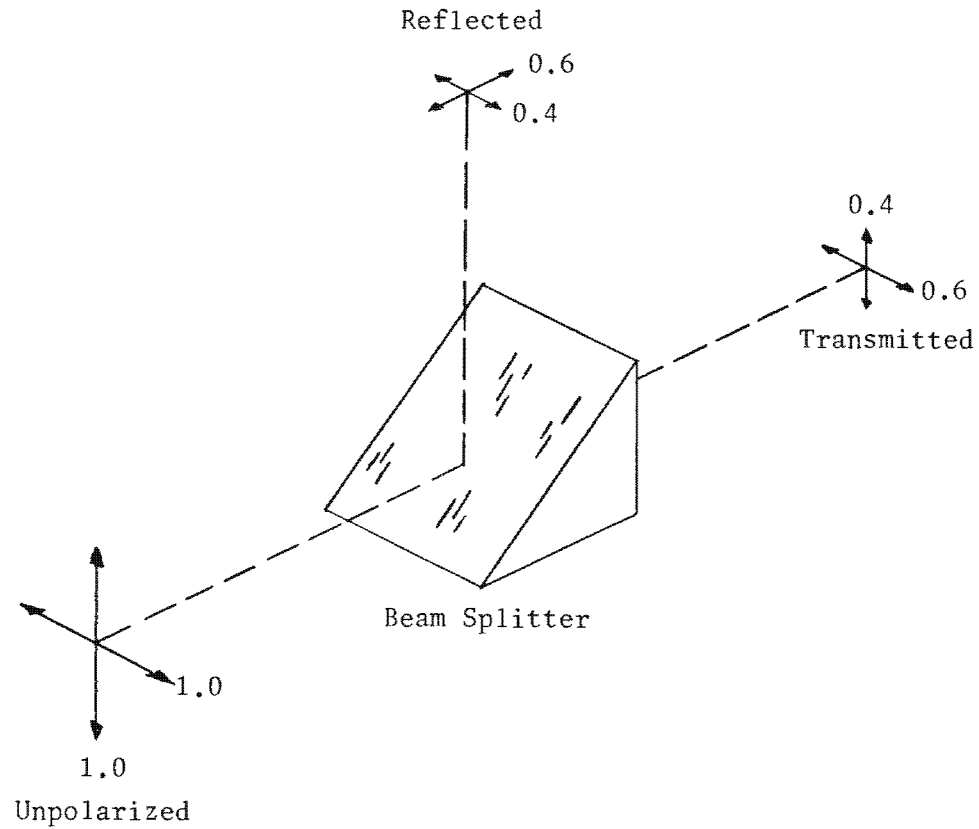
$$\frac{E_A - E_B}{E_A + E_B} = \frac{T_A - T_B + R_A - R_B}{T_A + T_B + R_A + R_B + 2\alpha}$$

All dependence on input energy, E , has disappeared.

The reflectance and transmittance values for the inconel (45-degree) beam splitter depend on the state of polarization of the incoming scene energy. Figure 2.5-9 illustrates this phenomenon. Significant changes in the state of polarization of the input energy cause changes in R_A , R_B , T_A , and T_B which result in apparent focus changes. The so-called "T+R" design, as just described, minimizes such polarization effects since both channels contain an R component and a T component and therefore both channels are affected similarly. (The polarization effect is certainly much reduced compared to a system in which channel A or B alone results from purely reflected or purely transmitted contributions.)

System calculations and available atmospheric data indicate that for realistic conditions the polarization induced focus error is probably small, and is correlated with sun angle. This has been demonstrated in factory tests where 100-percent linearly polarized light caused negligible shifts in the focus indication upon 90-degree rotation of the plane of polarization.

~~TOP SECRET~~ G



2.5-15

Figure 2.5-9. Polarization Effect

Handle via **BYEMAN**
Control System Only

Approved for Release: 2017/02/14 C05097211

Approved for Release: 2017/02/14 C05097211

~~TOP SECRET~~ GBIF-008- W-C-019838-RI-80

5.2.1.4 On-Board Signal Processing. The broad-band scene power, spatially filtered to a narrow band about 14 lpmm and varying temporally due to scene movement across the reticles, then falls on photodiodes placed behind the reticles. These photodiodes integrate and transfer linearly the incoming irradiance fluctuations into current fluctuations. The RMS signal at the photodiodes is in the picowatt range and the resulting current is in the nanoampere range. The linearity is a function of photodiode uniformity over the image blur circle.

The current signal at the photodiodes is converted to a voltage signal by a current-to-voltage converter. The virtual ground thus obtained is required to obtain the desired frequency response with the large shunt capacity resulting from the large area photodiodes.* The load resistor associated with this stage (100 k Ω) is sized to maximize the signal-to-noise ratio while not allowing system saturation at high-input light levels. The voltage gain of each channel varies from 840 at 211 Hz to 7560 at 2967 Hz with the peak gain of 9500 occurring at 2000 Hz. In order to operate with two orders of magnitude signal variation spread over more than a frequency decade, two passbands, switchable from one to the other, are incorporated into the four-stage channel amplifier and filter section. The switchover from one bandpass to the other is made at 741 Hz (2.95 inches/second) corresponding with the FPLLE speed range changeover. The RMS voltage in the 211- to 2967-Hz range is converted to a dc signal proportional to the true RMS signal. These signals are logically summed to obtain A - B and A + B levels, which are then presented to a divider to obtain $\frac{(A - B)}{(A + B)}$. This signal is scaled to correspond to $\frac{1 \text{ volt}}{17\% \Delta \text{ MTF}}$ and $\frac{0.5 \text{ volt}}{17\% \Delta \text{ MTF}}$.

The total system response is then:

*Space limitations preclude the use of condenser optics to provide a smaller exit pupil, thereby allowing smaller photodiodes, and less dependency on photodiode linearity.

~~TOP SECRET~~ G

~~TOP SECRET~~ G

BIF-008-W-C-019838-RI-80

$$\frac{17\% \Delta \text{ MTF}}{0.001\text{-inch defocus}} \frac{1 \text{ volt}}{17\% \Delta \text{ MTF}} = \frac{1.0 \text{ volt}}{0.001\text{-inch defocus}} \quad (\text{Fine})$$

$$\frac{17\% \Delta \text{ MTF}}{0.001\text{-inch defocus}} \frac{0.5 \text{ volt}}{17\% \Delta \text{ MTF}} = \frac{0.5 \text{ volt}}{0.001\text{-inch defocus}} \quad (\text{Coarse})$$

5.2.1.5 Ground Signal Processing (Dynamic Filter). The focus detection subsystem provides seven output signals which are carried by telemetry to the ground. These include:

Focus correction signal, coarse (IMP 5107)	2.5 volts = 0 correction; slope = 0.5 volt/mil of platen movement
Focus correction signal, fine (IMP 5067)	2.5 volts = 0 correction; slope = 1.0 volt/mil of platen movement
Average irradiation level, channel A (IMP 5231)	2.5 volts = 78 ft-candles; slope = 0.052 volt/ft-candle
Average irradiation level, channel B (IMP 5105)	2.5 volts = 78 ft-candles; slope = 0.052 volt/ft-candle
Focus difference signal (A - B) (IMP 5108)	2.5 volts = 0-volt output; slope = 0.033 volt/percent difference A and B
Focus signal strength (A + B (IMP 5059)	3.75 volts = 1.75-volt output; 4.75 volts = 10-volt output (for instrumentation voltage <3.75: slope = 5 volts/volt; for instrumentation >3.75: slope = 0.235 volts/volt)
Focus sensor head temperature (IMP 5058)	2.5 volts = 70F; slope = -5F/volt

2.5-17

~~TOP SECRET~~ GHandle via BYEMAN
Control System Only

~~TOP SECRET~~ GBIF-008-W-C-019838-RI-80

A data reduction and recursive filter software package is applied to the telemetered data. Further details on this "Dynamic Filter" software package are found in Appendix C. The equation and required telemetry data and calibration values are listed below.

$$BEF = \frac{L_R}{L_P} \left[\frac{V_{\text{sensor}} - \text{Null} - \Delta\text{Bal}}{S_F} + \text{ABS} \right] - \text{SRC}_I + e_{\text{cal}}$$

- where:
- BEF = focus system prediction of the plane of best geometric mean focus
 - L_P = distance from pivot point to platen centerline
= 5.080 inches
 - L_R = distance from pivot point to reticle centerline
= 4.330 inches
 - V_{sensor} = sensor correction signal in volts (IMP 5067)
(image relative to reticle midplane)
 - Null = sensor readout for equal electrical input signals
(factory calibration)
 - ΔBal = sensor readout for equal electrical input signals
(on-orbit calibration, see Section 5.3.3)
 - S_F = platen sensitivity in volts/mil of image displacement
 - ABS = absolute platen position during readout as determined from platen position instrumentation
= $\text{NPA} + \text{SRC}_A$ (the actual SRC step in use when focus data was taken)
 - SRC_I = correct SRC step for the conditions when focus data was taken

~~TOP SECRET~~ G

~~TOP SECRET~~ GBIF-008-W-C-019838-RI-80

e_{cal} = calibration factors required in converting sensor readout to image displacement from platen; consists of:

B_v = spatial frequency bias; difference between the high-frequency (180 lpmm) GM focal plane and the low-frequency (14 lpmm) mean focal plane

B_{ct} = field curvature and tilt bias; difference in image location at the platen axial position and reticle field position due to field curvature and mounting tilt in the Z direction

B_{RP} = reticle placement bias; difference in actual reticle midplane placement after shimming from calculated midplane position

5.2.2 Platen Adjustment Subsystems

The uncertainty in the location of the platen arises from mechanical tolerances during buildup of the camera, the accuracy with which platen adjustment subsystems move the platen, and other factors such as thermal hotdogging, test equipment error, etc. Platen movements are required to respond to systematic image movements resulting from slant-range changes and other nonsystematic changes resulting from thermal or other influences.

5.2.2.1 Slant Range Compensation (SRC). The position of the image along the optical axis varies with the vehicle-to-target distance (slant range) by the relationship:

$$\frac{1}{F} = \frac{1}{O} + \frac{1}{I}$$

where: F = focal length
O = object distance from the primary principal plane
I = image distance from the primary principal plane

2.5-19

~~TOP SECRET~~ GHandle via BYEMAN
Control System Only

~~TOP SECRET~~ GBIF-008- W-C-019838-RI-80

It has been shown (Part 2, Section 3) that the required film-drive speed also varies with slant range. The calculated slant range for a given frame then uniquely defines both film-drive speed and image location (focus). In the low-mode, the four most significant bits of the film-drive speed command are therefore used to command the platen adjustment subsystem over a range of +0.0018 to -0.0027 inch (see Part 3, Section 2), in 16 steps (64 film-drive speeds make up one SRC step).

The maximum altitude consideration for PPS/DP EAC is 470 nmi which results in a maximum slant range of 710 nmi using a spherical earth model. When the vehicle is in the high mode, SRC will be disabled at step 1. Changes in focus position will then be accomplished with platen adjustment by NPA. Figure 2.5-10 shows focus position as a function of slant range from 40 to 710 nmi. Also indicated are the SRC step positions in both platen locations and slant range.

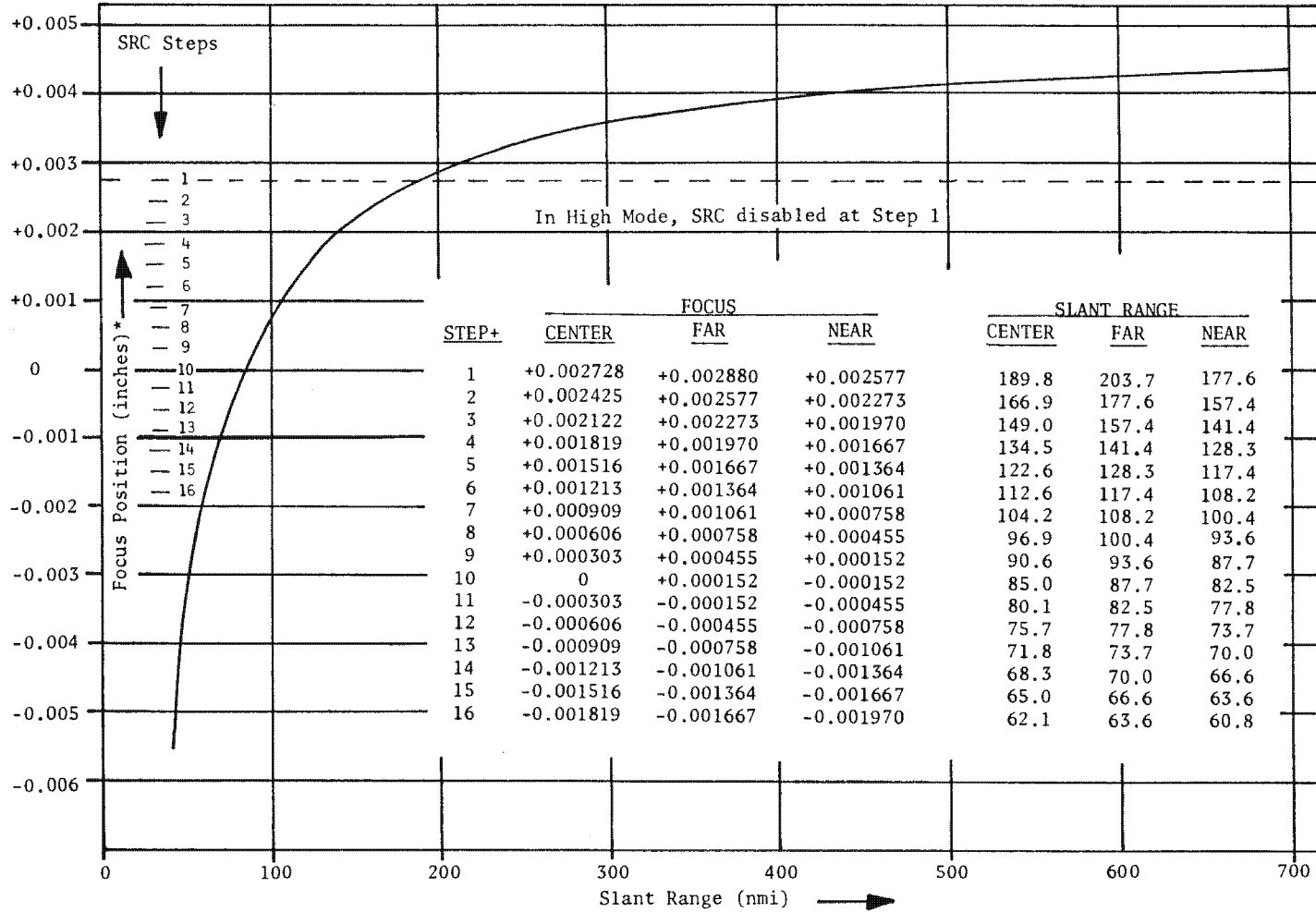
5.2.2.2 Nominal Platen Adjust (NPA). The location of the plane of best focus may differ from the factory-set platen position because of factors such as thermal hotdogging, mirror thermal distortions, and mechanical relaxation of launch-induced stresses. Provisions have been made to accomplish adjustments in platen position by an explicitly commanded movement called nominal platen adjust (see Part 3, Section 2).

5.3 Error Contributors

The accuracy with which the relative position of the high-quality aerial image and film plane is known is dependent upon the accuracy with which each position is known individually. Each of the known sources of error in each system has been assigned a statistical error. The combination of these errors results in a system where the platen and the plane of best focus will be within 0.000537 inch 95-percent of the time (based on calculations using specification values and best engineering judgement).

2.5-20

~~TOP SECRET~~ GHandle via BYEMAN
Control System Only



* Position is relative to Factory zero

Figure 2.5-10. Focus Position vs. Slant Range

2.5-21

Approved for Release: 2017/02/14 C05097211

Approved for Release: 2017/02/14 C05097211

~~TOP SECRET~~ GBIF-008- W-C-019838-RI-80

5.3.1 Error Sources

The sources of error in the location of the plane of best focus by means of the focus detection system, and the sources of error in the placement of the platen at this position are summarized as follows.

5.3.1.1 Focus Detection Subsystem. The focus detection subsystem errors are:

color aberration	the variation of focus as a function of scene spectral content
electronic channel balance	the variation of photocell and amplifier parameters
data reduction	variation arising from processing telemetry data
spatial frequency bias	difference between best focus at low and high spatial frequencies remaining after calibration
signal correlation	scene differences between reticle pairs, reticle offsets, and alignments
polarization	variation in focus due to polarization of incoming scene irradiance
residual error	errors from all other sources
air-to-vacuum bias	difference in refractive index between air and vacuum.

5.3.1.2 Camera and Optical System. Focus errors associated with the camera or optical system are:

platen setting	precision in the setting of the platen to best photographic focus for orbital conditions
platen/reticle mechanical stability	mechanical stability between platen/Y-axis plane and reticle plane

~~TOP SECRET~~ G

~~TOP SECRET~~ GBIF-008- W-C-019838-RI-80

platen/camera mechanical stability	mechanical stability of platen to camera mounting plane coordinates
platen/reticle thermal stability	thermal stability between platen/Y-axis plane and reticle plane
platen/camera thermal stability	thermal stability of platen to camera mounting plane
platen reticle alignment	initial precision in setting platen/Y-axis plane to reticle plane (remaining after calibration)
image plane tilt	uncertainty in the measurement of image plane tilt at focus sensor axial location
platen runout	eccentricity of platen
film tension	variation in platen position due to film tension excursions
film thickness	variability in film thickness within a given film type
SRC/NPA granularity	variability resulting from discrete SRC step width
SRC/NPA reproducibility	hardware imprecision due to slant-range within-step reproducibility
optical assembly, mechanical stability	stability of optical assembly to transient mechanical loads
optical assembly, thermal stability	stability of optical assembly to on-orbit temperature variations

5.3.2 Error Budget

Table 2.5-1 summarizes the budget values for the various defocus contributors.

~~TOP SECRET~~ G

TABLE 2.5-1 FOCUS ERROR BUDGET

(1σ Values, in mils)

<u>Contributor</u>	<u>Between-Mission Variability</u>	<u>Within-Mission Variability</u>
Focus Detection System		
Color Aberration	-	0.04
Electronic Channel Balance*	0.05	-
Data Reduction	-	0.05
Spatial Frequency Bias	0.05	-
Signal Correlation	-	0.05
Polarization	0.05	0.08
Residual Errors	0.05	-
Camera/Optical System		
Platen Setting	(1)	(1)
Platen/Reticle Mechanical Stability	0.06	-
Platen/Camera Mechanical Stability	(1)	(1)
Platen/Reticle Thermal Stability	0.05(2)	-
Platen/Camera Thermal Stability	(1)	(1)
Platen/Reticle Alignment	0.033	-
Image-Plane Tilt	0.06	-
Platen Runout	-	0.033
Film Tension	-	0.020
Film Thickness	-	0.033
SRC/NPA Granularity	-	0.092
SRC/NPA Reproducibility	-	0.038
Optical Assy; Mechanical Stability	(1)	(1)
Optical Assy; Thermal Stability	(1)	0.170(3)
Total 1σ by RSS	<u>0.1442</u>	<u>0.2332</u>
Total Combined 1σ error by RSS = 0.2742		
95% = 0.5374 mil		

*System uncertainty using on-board calibration (1) assumes that the focus detection subsystem will correct for this contributor to within accuracy indicated by budget, (2) includes both static and dynamic thermal environments, (3) includes error in door-open-light (DOL) model prediction of BEF.

2.5-24

Approved for Release: 2017/02/14 C05097211

Approved for Release: 2017/02/14 C05097211

Handle via BYEMAN
Control System Only

~~TOP SECRET~~ GBIF-008- W-C-019838-RI-805.4 Calibration

In addition to the usual mechanical calibration factors developed during assembly and testing, an electronic, on-orbit calibration of the focus detector may be accomplished. This is done through light-emitting diodes (LEDs) placed on the beam splitter in such a way that the photodiode detectors are illuminated. The LEDs are pulsed at frequencies of 300 Hz and 850 Hz when the high mode is selected and 1025 Hz and 1600 Hz when low mode is selected. The result of pulsing the LEDs should be a "NULL" or zero focus error indication.

~~TOP SECRET~~ GHandle via BYEMAN
Control System Only

~~TOP SECRET~~ G

BIF-008-W-C-019838-RI-80

This page intentionally blank

2.5-26

~~TOP SECRET~~ G

Handle via **BYEMAN**
Control System Only

~~TOP SECRET~~ GBIF-008- W-C-019838-RI-80

6.0 EXPOSURE

Exposure, the amount or quantity of light received by the photographic emulsion over a given time period, is defined by:

$$E = It$$

where: E = exposure
 I = illuminance, flux of light
 received by the emulsion surface,
 usually expressed in meter-candles
 t = exposure time

The units of exposure are therefore meter-candles-seconds (mcs).

6.1 Spectral Dependency

All of the major influences on the amount of light energy received by the photographic emulsion and the response of that emulsion to the light received vary to a greater or lesser extent with the wavelength of the light. Since all "natural" illumination is traceable to sunlight, film response, target reflectances, optical transmission values, etc. are based on daylight quality illuminant. Daylight quality illuminant is said to have a spectral distribution similar to a black-body at a temperature of 5800 °K. In the following discussions, when single numbers are given for quantities having a spectral dependence, it may be assumed that the figures given are for daylight quality illuminant.

2.6-1

~~TOP SECRET~~ GHandle via BYEMAN
Control System Only

~~TOP SECRET~~ GBIF-008- W-C-019838-RI-806.2 Exposure Determination

The exposure for a given frame is a function of vehicle-target geometry and the commanded slit width.

6.2.1 Geometric Considerations

In a frame camera, the illuminance, I , is controlled by (but not uniquely determined by) the lens aperture, while the exposure time, t , is controlled by the shutter speed. With a strip camera, I is controlled by (but again not uniquely determined by) the entrance pupil aperture, while the exposure time is controlled by the film drive speed, V_f , and slit width, w . However, a strip camera used in an application characterized by relative motion between the camera and the subject (as in satellite reconnaissance systems) is subject to the constraint that the image velocity vector and the film drive speed vector be matched. The physical implementation of this requirement is called image motion compensation (IMC), and results in an explicit film drive speed for a given camera-target geometry.

6.2.2 Slit-Width

With film drive speed determined by camera-target geometry, the only remaining means of exposure control for a strip camera is the slit width, w .

$$t = w/V_f$$

6.3 Slit Selection, Graphical Approximation

In practice, once the geometrical target acquisition conditions are known, V_f is determined to meet IMC requirements. Software is then utilized to find the proper slit width based on local target sun angle, target mean reflectance,

~~TOP SECRET~~ GHandle via **BYEMAN**
Control System Only

~~TOP SECRET~~ GBIF-008- W-C-019838-RI-80

film type in use, etc. A graphical portrayal of the interaction between the major parameters involved in slit selection appears in Figure 2.6-1, and 2.6-2.

To make use of these figures, the required film drive speed is found from Figure 2.6-1, or through the use of the appropriate equations found in Part 2, Section 3 of this document. A vertical line is then drawn on the right-hand graph of Figure 2.6-2 corresponding to this film drive speed. The required exposure time is determined from the left-hand graph of Figure 2.6-2 by finding the intersection of sun angle with the appropriate film curve. A horizontal line is drawn from this point on the left-hand graph to intersect the vertical line previously drawn on the right-hand graph. The curved line closest to this intersection point represents the slit which would be selected.

Example:

Given: Altitude = 105 nmi
 Ω = 30°
 Σ = 0°
 Sun Angle = 30°
 Film Type = SO-312

Find: Nominal Slit

The exposure time is found to be 5.05×10^{-3} sec.

The required slit is slit 8.

6.4 Slit Selection Operational Software

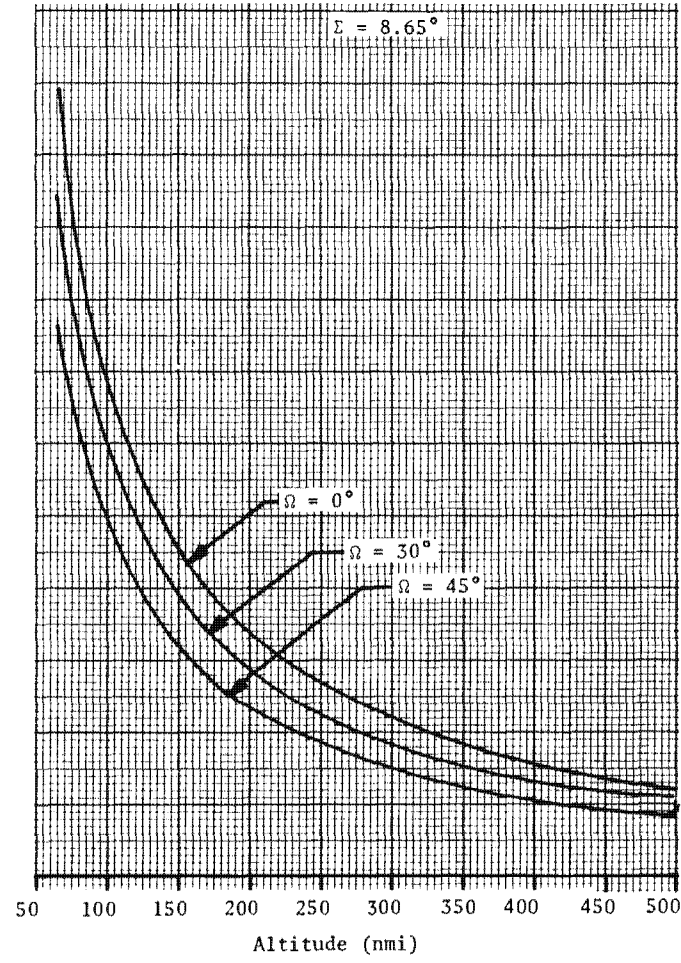
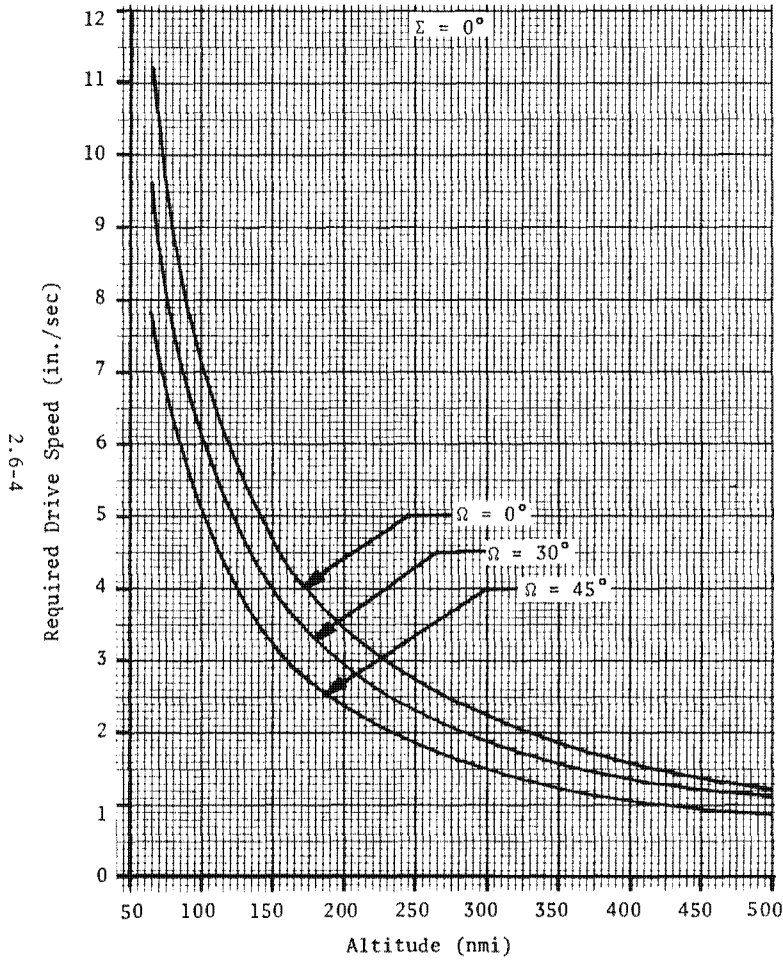
The operational software exposure algorithm which calculates the required slit width for each photograph takes account of the following acquisition dependent quantities (assuming V_f has already been fixed):

Exposing Optical System: Spectral transmittance; T-number

2.6-3

~~TOP SECRET~~ G

Handle via BYEMAN
 Control System Only



Σ = Stereo Angle; Ω = Obliquity

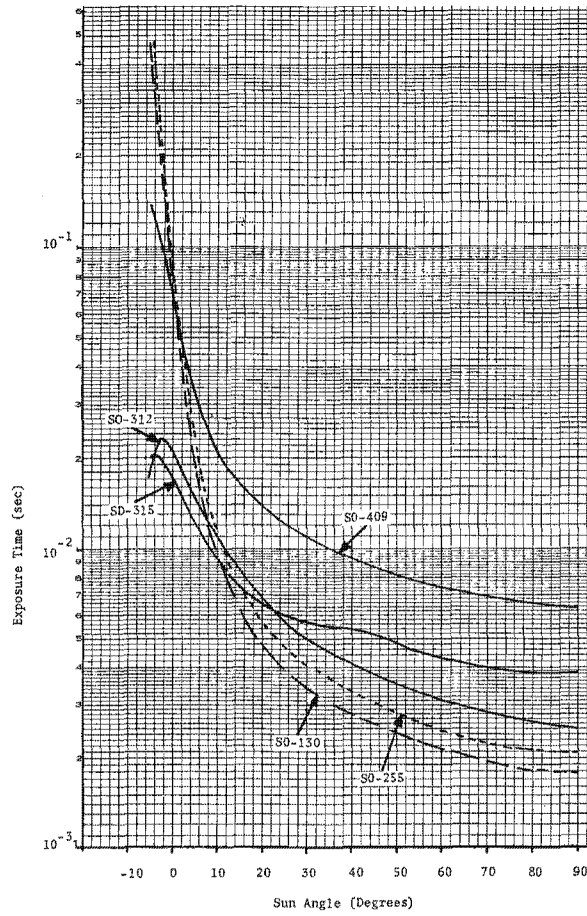
Figure 2.6-1. Exposure Model, Graph 1

Handle via BYEMAN
Control System On

Approved for Release: 2017/02/14 C05097211

2.6-4

Approved for Release: 2017/02/14 C05097211



NOTE:

Films shown are those currently available for use in the Gambit Vehicle having Extended Altitude Capabilities. Because of normal emulsion improvements and batch-to-batch variability, the GEAFS* of material for a given load may vary from that shown below.

*GEAFS = Gambit Equivalent Film Speeds

Film Type	GEAFS
SO-312	4.7
SO-315	9.3
SO-409	1.2
SO-130	9.5
SO-255	10.7

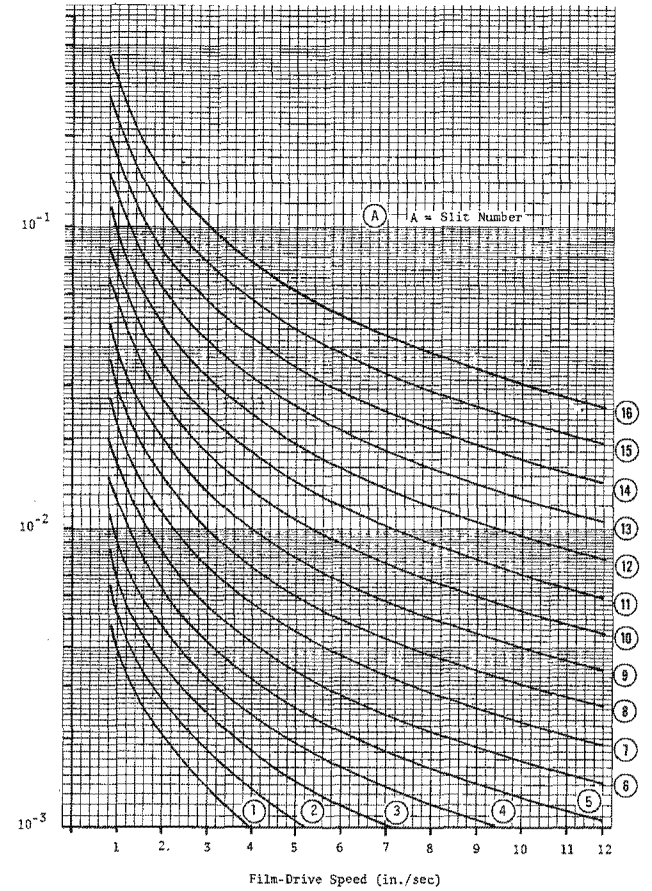


Figure 2.6-2. Exposure Model, Graph 2

2.6-5/2.6-6

Handle via **BYEMAN**
Control System Only

~~TOP SECRET~~ GBIF-008- W-C-019838-RI-80

Scene Parameters: Target mean reflectance; distribution of scene spectral reflectances; atmospheric parameters (e.g. water vapor content, dust content, percent ozone, etc., based on seasonal atmospheric models).

Acquisition Conditions: Local sun angle; target geographic location; time of year; local weather conditions (if snow is present, its estimated age and depth).

Film Characteristics: Response (D-log E) curve shape (important in placing highlight and shadow illuminances for desired tone reproduction); reciprocity characteristics; spectral character of the laboratory sensitometer illuminant used to determine film spectral sensitivity.

6.4.1 Slit Selection Algorithm Inputs

The slit selection algorithm utilizes six input variables and three internal tables in the selection of the slit which will provide optimum exposure.

6.4.1.1 Mission Correlation Data (MCD) Inputs. Mission correlation data (MCD) inputs are parameters computed by the operational software or obtained from external sources. They include: the solar altitude at the target in degrees ($-10^\circ < SA \leq 90^\circ$), film type ($F = 1, 2, \dots, n$), and forecast snow depth in inches ($SN = 0'', 4'', 10''$, with default value = $0''$).

6.4.1.2 Target Card Inputs. Target card inputs include those parameters read from the target deck which are unique to the specific target to be acquired. They are the mean reflectance of the target complex, MR, in percent ($0\% \leq MR \leq 100\%$ with default value = 12%), initial exposure bias, B_0 , deter-

~~TOP SECRET~~ GHandle via **BYEMAN**
Control System Only

~~TOP SECRET~~ GBIF-008- W-C-019838-RI-80

mined on an R & D basis for special investigations ($B_o = -9, -8, \dots 0 \dots +8, +9$; default value = 0. B_o is used internally to generate the multiplicative bias, m_o where $m_o = 10^{0.1B_o}$) and a safety flag, L , to insure no exposure modification beyond the predetermined m_o . ($L= 1$ causes inhibition of all other biases, while the default value $L= 0$ removes the flag and permits additional biasing).

6.4.1.3 Table 1. Slit selection algorithm Table 1 is exposure time in seconds (t) versus solar altitude (SA) for each film type (F) assuming a nominal scene mean reflectance of 12%.

The source of the exposure time versus solar altitude data of Table 1 is the computer program KALEIDOSCOPE. Basically KSCOPE mathematically models solar spectral irradiance incident on the scene, spectral reflectance from the scene for a range of local solar altitudes, spectral transmittance of the atmosphere, spectral radiance attributable to atmospheric haze, spectral transmittance of the R-5 lens system including any filter coatings, R-5 lens obstruction and focal ratio, film spectral sensitivity, and the sensitometric effects peculiar to the processing method used. The required exposure time (t) is then found by dividing the exposure necessary to produce negative density 1.1 with a radiometrically calibrated (daylight + wratten E2) sensitometer (in watts-sec/m²) by the effective spectral irradiance at the image plane (in watts/m²).

6.4.1.4 Table 2. Slit selection algorithm Table 2, reproduced here as Table 2.6-1, lists the exposure modifiers (M) that adjust the basic KSCOPE recommendation for a mean reflectance (MR) of other than 12%. The change in exposure required outside the atmosphere for given change in target reflectance varies with solar altitude. The table is quantized for both solar altitude and reflectance cells corresponding to 0.10 log E exposure units change ($0.250 \leq M \leq 2.000$, with default value = 1.000 implying no adjustment necessary).

2.6-8

~~TOP SECRET~~ GHandle via BYEMAN
Control System Only

~~TOP SECRET~~ GBIF-008- W-C-019838-RI-80

TABLE 2.6-1

TABLE OF EXPOSURE MODIFIER, M
(Algorithm Table 2)

<u>Percent Mean Reflectance (MR)</u>	<u>M, Exposure Modifier</u>		
	<u>SA < 9°</u>	<u>Solar Altitude (SA) 9° ≤ SA ≤ 25°</u>	<u>SA > 25°</u>
MR < 4	1.259	1.585	2.000
4 ≤ MR < 7	1.259	1.259	1.585
7 ≤ MR < 10	1.000	1.259	1.259
10 ≤ MR < 14	1.000	1.000	1.000
14 ≤ MR < 17	1.000	1.000	0.794
17 ≤ MR < 20	0.794	0.794	0.794
20 ≤ MR < 23	0.794	0.794	0.631
23 ≤ MR < 27	0.794	0.631	0.631
27 ≤ MR < 32	0.631	0.631	0.500
32 ≤ MR < 35	0.631	0.500	0.500
35 ≤ MR < 40	0.631	0.500	0.398
40 ≤ MR < 45	0.500	0.500	0.398
45 ≤ MR < 58	0.500	0.398	0.316
MR ≥ 58	0.398	0.316	0.250

2.6-9

~~TOP SECRET~~ GHandle via **BYEMAN**
Control System Only

~~TOP SECRET~~ GBIF-008- W-C-019838-RI-80

6.4.1.5 Table 3. Slit selection algorithm contains the multiplicative snow bias factors (N) to be applied when snow is forecast for a particular target. The bias so applied is a function of snow depth (SN). The default value N= 1.000 implies no snow bias needed. Table 2.6-2 shows the values for snow bias (N) for the three ranges of snow depth forecast for the target.

TABLE 2.6-2
TABLE OF SNOW BIASES TO EXPOSURE TIME (ALGORITHM TABLE 3)

(1 November through 31 March only)

<u>Inches of Snow Forecast</u>	<u>Value of SN</u>	<u>Snow Bias (N)</u>
less than 4"	0	1.000
4" to 10"	4	0.794
10" or more	10	0.631

6.4.2 Slit Selection Algorithm

The slit selection algorithm is shown in Figure 2.6-3. Operation of the algorithm is largely self-explanatory, but the following points deserve emphasis. Once the basic 12% MR exposure time (t) is obtained from the KSCOPE table and the appropriate modifiers M (for target MR \neq 12%) and N (snow bias) selected, a test is made for the presence of the safety flag (L= 1). Sequencing then proceeds as follows:

(A) Flag ON (L=1)

Ignore N and calculate adjusted exposure time:

$$t' = tMm_0$$

2.6-10

~~TOP SECRET~~ G

Handle via **BYEMAN**
Control System Only

~~TOP SECRET~~ G

BIF-008- W-C-019838-RI-80

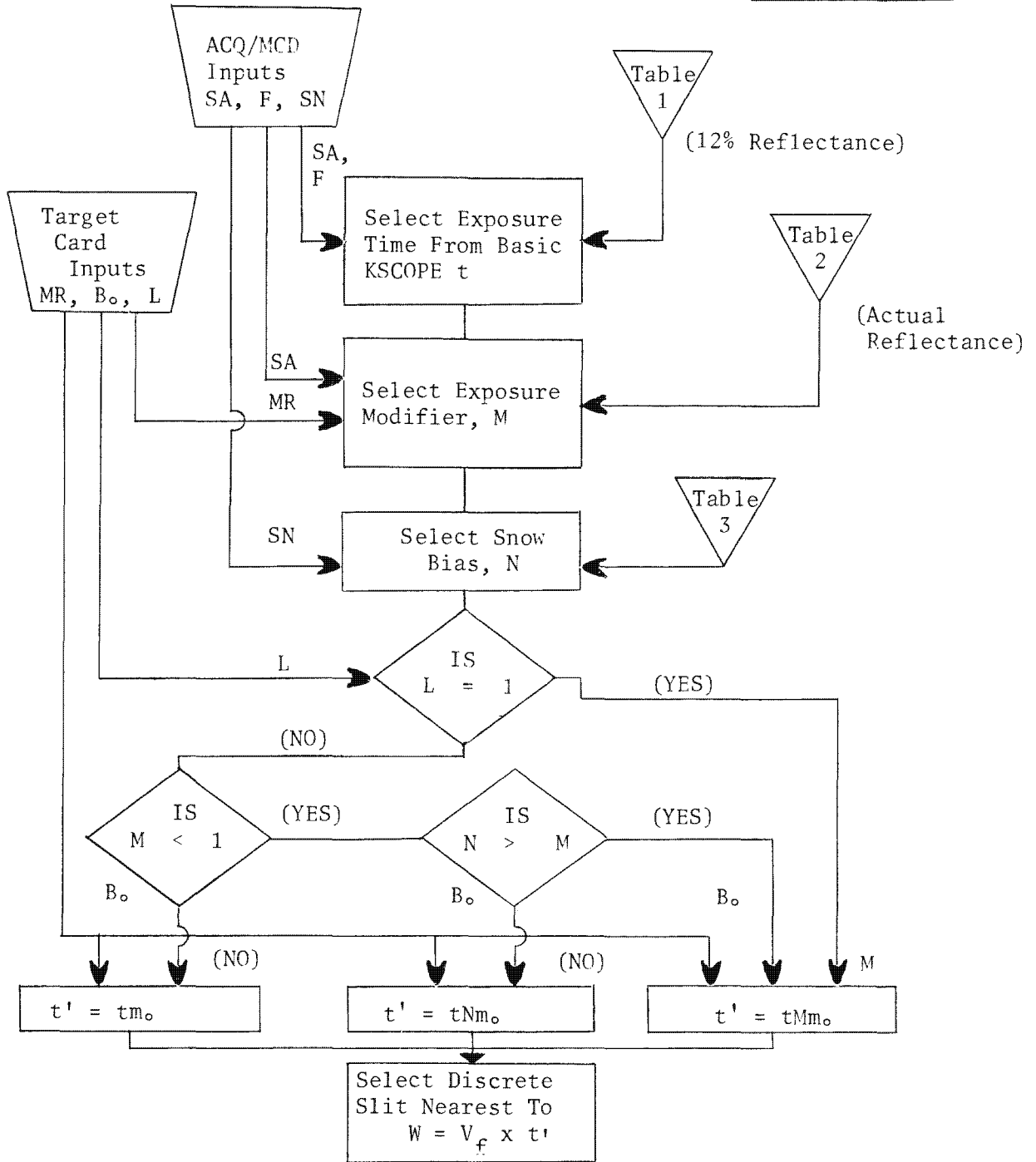


Figure 2.6-3. Slit Selection Algorithm

~~TOP SECRET~~ G

Handle via **BYEMAN**
Control System Only

~~TOP SECRET~~ GBIF-008- W-C-019838-RJ-80

(B) Flag OFF (L=0)

1. $M < 1$

This implies that the actual $MR > 12\%$ so that a reduction in t is called for.

a. $N > M$

The snow bias, N , alone would reduce t less than, the exposure modifier M . Then:

$$t' = tMm_0$$

and the snow bias is ignored. When both contributors call for an exposure change in the same direction, the strongest one takes precedence.

b. $N \leq M$

The snow bias, N , alone would reduce t more than the exposure modifier, M . Then:

$$t' = tNm_0$$

and again the strongest contributor (N) takes precedence since both N and M call for reduced exposure.

2. $M \geq 1$

This implies that the actual $MR \leq 12\%$ so either no change in t results from the application of M or t must be increased.

$$t' = tm_0$$

In this case N calls for less exposure while M calls for more exposure. Experience under such circumstances has shown no advantage in allowing the two factors to interact (by writing $t' = tNMm_0$), so N and M are considered mutually compensating.

2.6-12

~~TOP SECRET~~ GHandle via BYEMAN
Control System Only

~~TOP SECRET~~ G

BIF-008- W-C-019838-RI-80

Note that in all cases the opportunity exists (through m_0) for additional exposure biasing in steps of 0.1 log E units. It is intended that such biasing be done on a purely experimental basis so that should the results indicate continued preference for a specific m_0 , the target MR bias factor M would be appropriately changed ($\text{new } M = \text{old } M \times m_0$).

2.6-13

~~TOP SECRET~~ G

Handle via **BYEMAN**
Control System Only

~~TOP SECRET~~ G

BIF-008-W-C-019838-RI-80

This Page Intentionally Blank

2.6-14

~~TOP SECRET~~ G

Handle via **BYEMAN**
Control System Only

~~TOP SECRET~~ GBIF-008- W-C-019838-RI-80

7.0 FILM CHARACTERISTICS

In the Gambit Reconnaissance System, the medium upon which the high-quality aerial image is recorded is photographic film. The system has been designed to utilize films having a range of physical and sensitometric properties. This section discusses many of the physical and sensitometric properties of photographic films as they relate to use in the Gambit system.

Photographic film used in the Gambit system is supplied to BIF-008 by the Air Force as "Government Furnished Equipment" (GFE). Although nothing in the design of the PPS/DP EAC mandates the use of film from any given vendor, films manufactured by Eastman Kodak Company have been used in the past.

Typical cross-sections of a black-and-white and color film are shown in Figure 2.7-1. Each of the dimensions shown may vary with different film types. Some features may not be employed in a given film type, but the basic structure will be as shown. The emulsion may consist of a complex of layers including the photosensitive layer, dye layers and gelatin pads to produce the desired photographic and physical characteristics.

7.1 Physical Characteristics

Physical parameters of interest for the various film layers and coatings include: material, physical dimensions, strength, optical properties, and frictional characteristics. Parameters of interest for the film as a whole are: splice configuration, curl, electrical (static) properties, response to environmental conditions, and spectral transmission.

7.1.1 Base

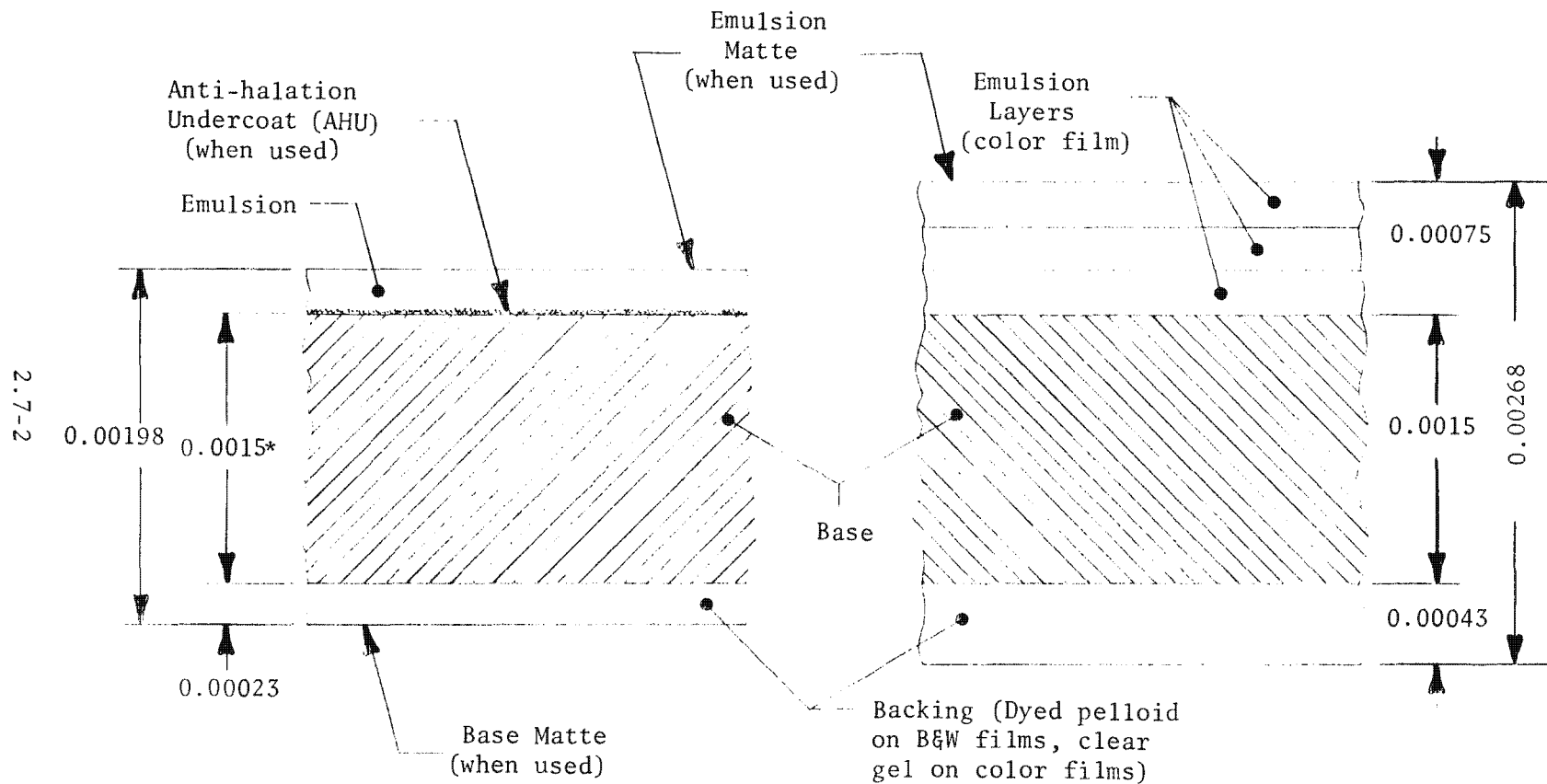
At the present time, all Kodak aerial films have an ESTAR base. ESTAR is a polymer of the polyester type; meltcast, stretched and heat-set poly-

2.7-1

~~TOP SECRET~~ GHandle via **BYEMAN**
Control System Only

Black-and-White Film

Color Film



NOTE: Dimensions are in inches

*Many aerial films are available with a base thickness of 0.0012".

Figure 2.7-1. Typical Film Cross-Section

Handle via **BYEMAN**
Control System Only

~~TOP SECRET~~ GBIF-008-W-C-019838-RI-80

terephthalate. It is an excellent base material because it is tough, stable, flexible and nearly uniaxial.

7.1.1.1 Base Thickness. The standard base thicknesses and tolerances are as follows:

ESTAR Ultra-Ultra Thin Base*	1.2 ± 0.10 mils
ESTAR Ultra Thin Base	1.5 ± 0.10 mils
ESTAR Thin Base	2.5 ± 0.10 mils
ESTAR Base	4.0 ± 0.20 mils

7.1.1.2 Tensile Strength. The strength of aerial films is almost wholly dependent upon the properties of the base material. For ESTAR base, the properties vary less than 15 percent with direction and are nominally as shown below at 70F and 50 percent relative humidity.

Yield strength	13,500 psi
Yield elongation	5.5 percent
Break strength	25,600 psi
Break elongation	115 percent
Toughness	21,500 in.-lb/cu in.
Young's Modulus	6.8 x 10 ⁵ psi

Tensile strength properties vary with the environment. As the films become drier and colder, tensile strength increases.

*Most films on 1.2-mil base have a total thickness outside the range for which Gambit system operation is required by specification. An extensive factory testing program has not revealed any significant problems associated with the use of 1.2 mil base film in the Gambit system.

~~TOP SECRET~~ G

~~TOP SECRET~~ GBIF-008- W-C-019838-RI-80

7.1.1.3 Tear Strength. It is extremely difficult to tear ESTAR base films, provided no nicks or edge-defects are present. The force required to propagate a tear, once started, is several orders of magnitude lower than the force necessary to initiate the tear. If edge integrity is maintained, tear is not a practical problem in ESTAR base films.

7.1.1.4 Brittleness. Brittle fracture of film starts with weakness of the emulsion layer under tension. Bending (such as occurs at a small diameter roller) can cause fracture in the layer on the outside of the bend. Generally, in ESTAR base aerial films, the fracture will not continue through the base causing a film break, but will cause only minor photographic defects. Brittleness is greater at the low temperatures and humidities encountered in the Gambit application.

7.1.2 Emulsion

The emulsion is an organic binder, or gel, in which particles of photo-reactive materials are suspended.

7.1.2.1 Gel. Gel, or gelatin, is a colloidal protein obtained from the rendering of certain animal tissues. In the highly purified form used in emulsion making, the gelatin provides an optically clear vehicle having an index of refraction of about 1.5.

7.1.2.2 Photoreactive Materials. The photoreactive materials in a photographic emulsion are crystals of silver halide (chloride, bromide). When a photon of sufficient energy interacts with a silver halide crystal, a latent image center is formed. Subsequent treatment with appropriate developing agents converts the latent image centers into metallic silver particles. For color films, the products of development in an emulsion layer react with dye-couplers to form appropriate colored dyes within that layer.

~~TOP SECRET~~ G

~~TOP SECRET~~ GBIF-008- W-C-019838-RI-80

7.1.3 Backing

Gelatin, either dyed or clear, is also placed on the side of the base away from the photoreactive layer. Addition of the gel backing reduces the tendency of the film to bend under the influence of unbalanced expansion between emulsion and base (curl). A dye is included in some backing layers to reduce the effect of light passing through the film and reflecting from the platen. Small matte particles are added to the backing to influence the frictional and other physical characteristics of the film-backing.

7.1.4 Anti-Halation Undercoat (AHU)

The AHU is a coating placed on the base material which diffuses into the emulsion. The AHU functions to reduce the amount of light scattered within the emulsion as well as the amount of light reflected at the emulsion-base interface thereby reducing the exposure from the reflected or scattered light. (See Figure 2.7-2.)

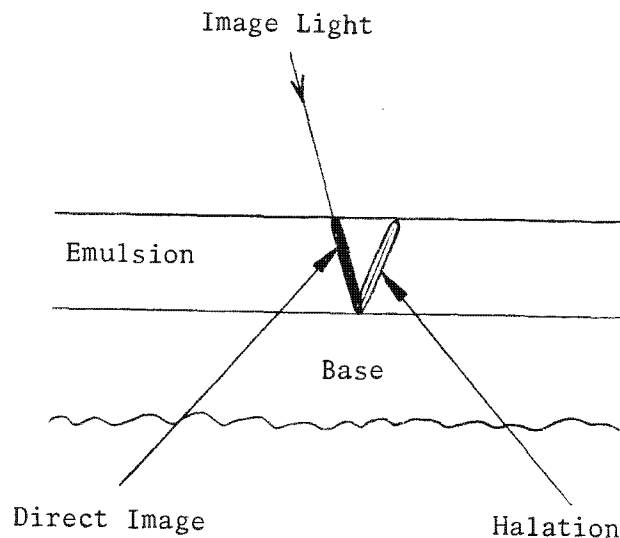


Figure 2.7-2. Halation

2.7-5

~~TOP SECRET~~ GHandle via **BYEMAN**
Control System Only

~~TOP SECRET~~ GBIF-008- W-C-019838-RI-80

7.1.5 Dye Layers

Dye layers are used to prevent light in a selected wavelength band from reaching a layer sensitive to that wavelength. Examples include the yellow layer in some color films which blocks blue light from the emulsion layers designed to be sensitive to the green or red spectral region, and the cover layer of some infrared films which blocks the shorter, visible wavelengths.

7.1.6 Emulsion Matte

A matte coating is sometimes included on the emulsion side of some films. It was originally designed to increase surface roughness and thereby reduce the occurrence of Newton's rings on duplicating film. A matte coating is now sometimes found on acquisition films whose origins are in duplicating applications.

It is expected that the use of emulsion matte coatings on black-and-white acquisition films will be discontinued in the near future. Emulsion matte coatings will continue to be employed in color applications to maintain handling and duplicating characteristics.

7.1.7 Total Film Properties

Some physical properties of the film as a whole as received from the vendor are described below.

2.7-6

~~TOP SECRET~~ GHandle via BYEMAN
Control System Only

~~TOP SECRET~~ GBIF-008- W-C-019838-RI-80

7.1.7.1 Film Splices. All vendor splices are of the ultrasonic-weld type. Splice thickness is constrained to 0.0062 inch by hardware design tolerances. Since the thickness of an ultrasonic splice is approximately the sum of the thicknesses of the films being spliced, this thickness limit may be exceeded when relatively thick films are spliced.

In some instances, especially when films of different types are spliced together, the splice strength may be less than the desired safety margins. In these cases (thick or understrength splices) a short segment of clear base material is spliced between the two film segments. This is called a window splice and is shown in Figure 2.7-3. Figure 2.7-4 illustrates a standard ultrasonic-weld splice.

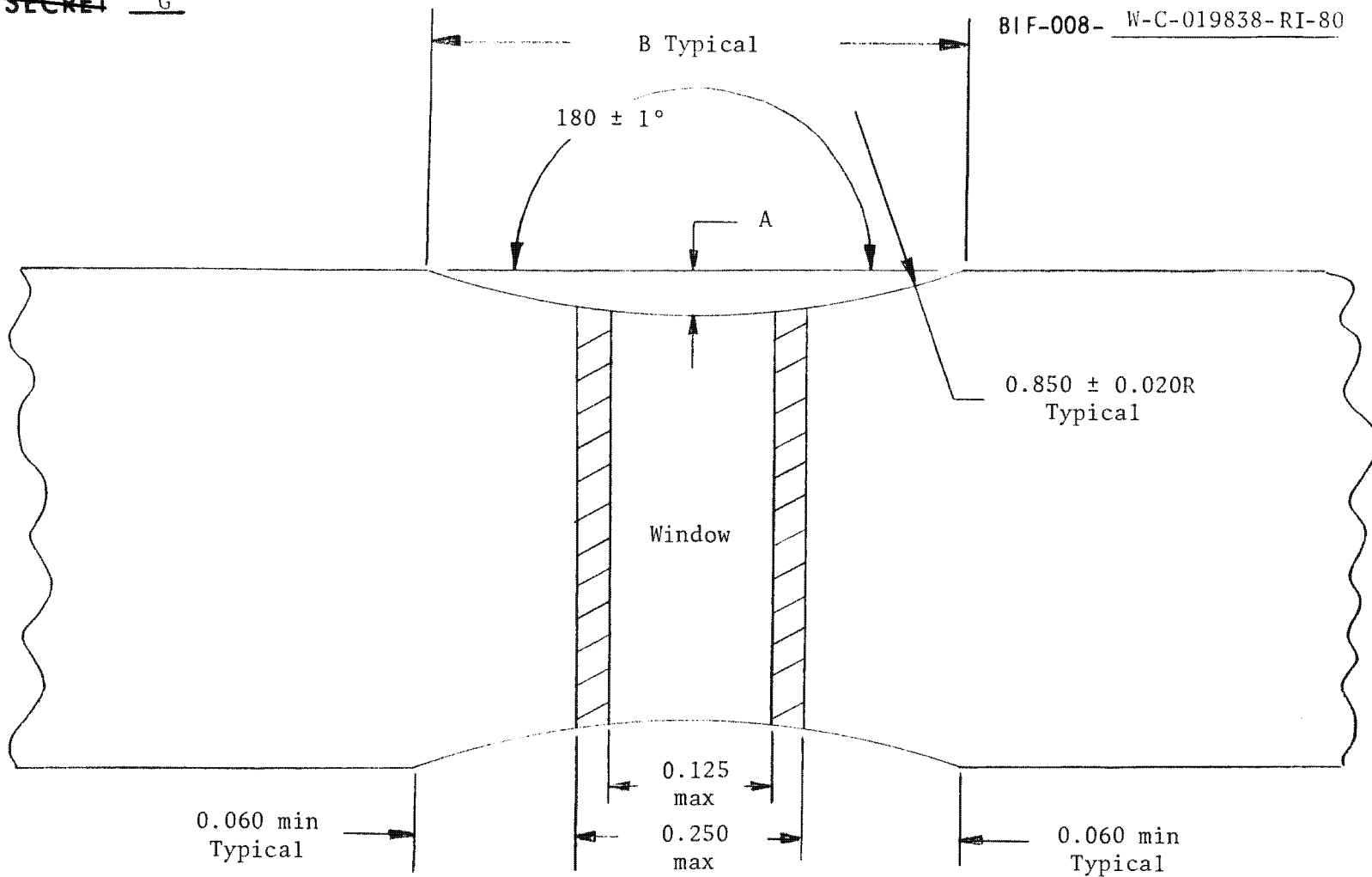
7.1.7.2 Curl. Curl is the effect of forces that cause film to assume an arc-like shape. These forces stem from two distinct phenomena: (1) The difference in behavior between support and emulsion in response to changes in relative humidity, (2) plastic flow induced when film is wound on a roll.

The standard testing procedure involves cutting 3-inch circular samples, allowing them to come into equilibrium with an environment of known relative humidity, and measuring the curvature against a template. While this method is useful in comparing characteristics of various films under standard test conditions, it provides little knowledge of how film behaves under tension and between rollers, that is, as used in a film handling system.

A typical case is illustrated schematically in Figure 2.7-5. When under tension between rollers, the parameter of interest is the separation of edge and center, shown as dimension s . Tests in the as-installed configuration, with representative values of d , have shown that the separation (s) is well below 1.0-inch for w (film width) of 9.5 inches (nominal) and the expected relative humidity range.

2.7-7

~~TOP SECRET~~ GHandle via BYEMAN
Control System Only



2.7-8

Depth A = 0.030 ± 0.010

Width B = 0.367 ± 0.020 for A = 0.020

B = 0.448 ± 0.020 for A = 0.030

B = 0.515 ± 0.020 for A = 0.040

NOTE: Dimensions in Inches

Figure 2.7-3. Window Splice

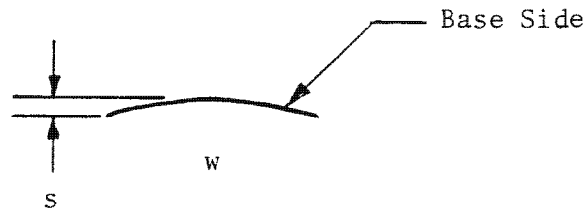
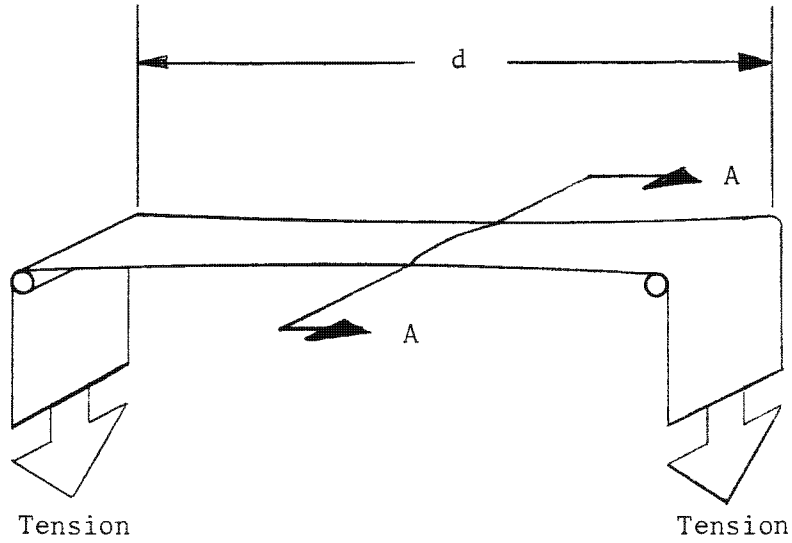
Handle via BYEMAN
Control System Only

Approved for Release: 2017/02/14 C05097211

Approved for Release: 2017/02/14 C05097211

~~TOP SECRET~~ G

BIF-008- W-C-019838-RI-80



Section A-A

Figure 2.7-5. Typical Curl

2.7-10

~~TOP SECRET~~ G

Handle via BYEMAN
Control System Only

~~TOP SECRET~~ GBIF-008- W-C-019838-RI-80

7.1.7.3 Electrical Properties. The electrical properties of photographic film are of importance because they, along with environmental factors, influence the rate at which electrical charges are accumulated and dissipated. Electrochemical potential is a function of material identity. When two dissimilar materials, having different electrochemical potentials, are placed in contact with one another, a non-equilibrium condition will arise. The difference in potential will cause an electrostatic charge of electrons to move from one material to the other. This flow of electrons will continue until the electrochemical potentials equalize, or until the materials are separated. Frequently, the two unlike surfaces are found to have a static charge after separation. In general, separation of similar surfaces such as gelatin-from-gelatin results in less static charge than separation of unlike surfaces, such as gelatin-from-base.

Statically charged materials seek to return to a neutral state by movement of electrons. If both materials are good conductors, they cannot be separated rapidly enough to prevent the electrons from "flowing" back through the points of contact and the potential between the two materials thus disappears. However, if either or both materials are poor conductors, the electrons will not flow back so rapidly through the contacting areas. It is then possible to retain some of the static charge on the materials after separation. Figure 2.7-6 illustrates the electrification of a film strand.

The surface resistivity of a material provides a measure of the ease with which static charges may dissipate. Surface resistivity is expressed in ohms per square (the size of the square is immaterial). Figure 2.7-7 shows typical surface resistivity for emulsion and gel backing.

~~TOP SECRET~~ Handle via BYEMAN
Control System Only

~~TOP SECRET~~ G

BIF-008- W-C-019838-RI-80

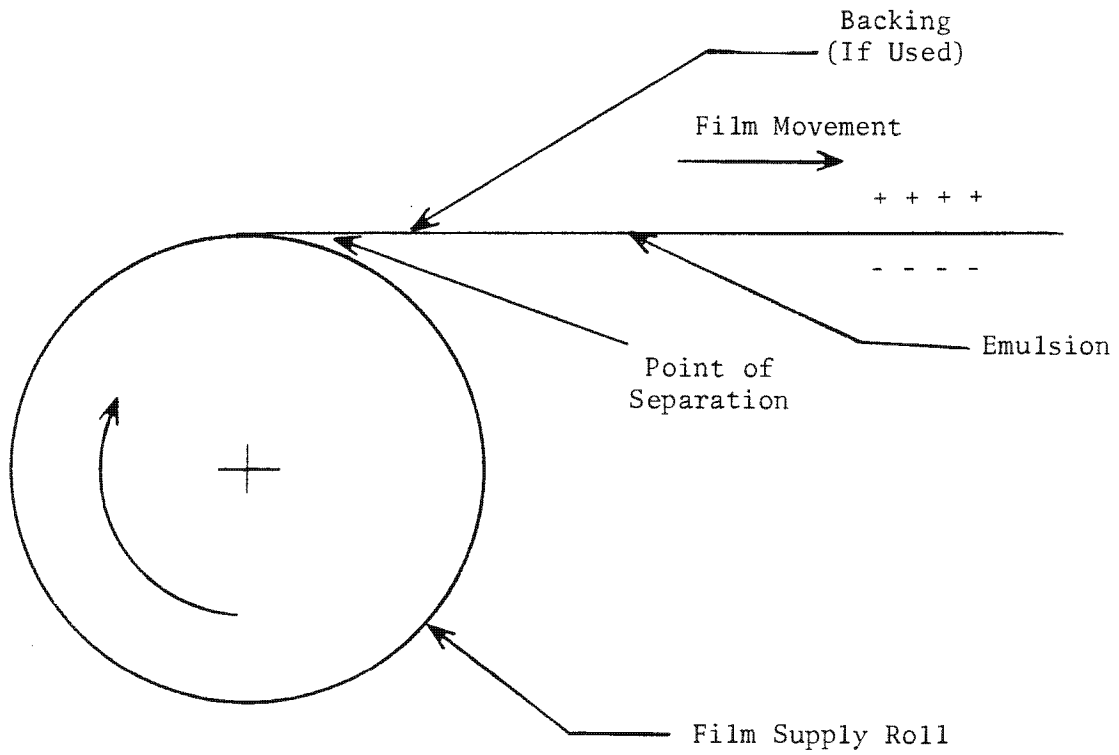


Figure 2.7-6. Electrification of a Film Strand

~~TOP SECRET~~ G

Handle via **BYEMAN**
Control System Only

~~TOP SECRET~~ G

BIF-008- W-C-019838-RI-80

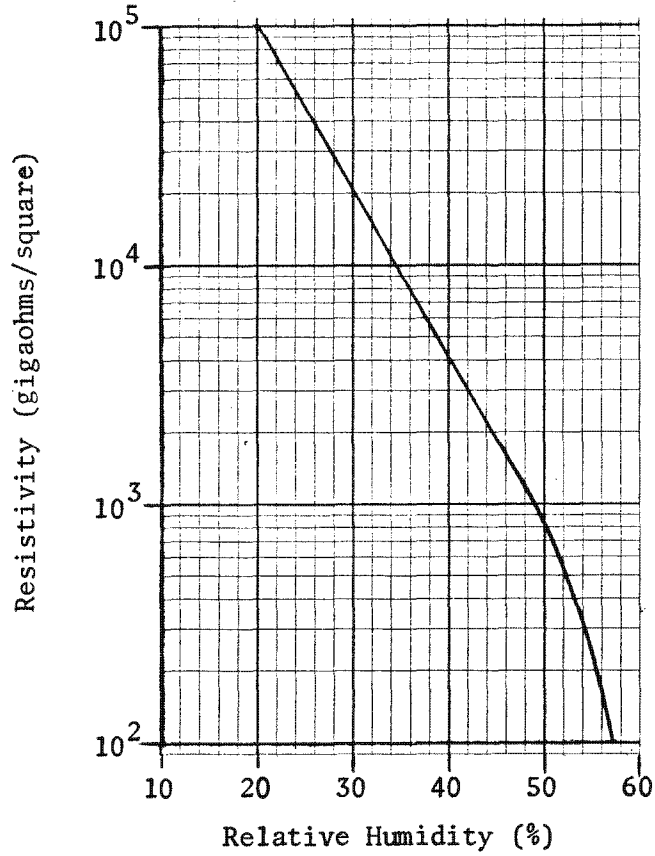


Figure 2.7-7. Typical Resistivity of Emulsion and Gel Backings

2.7-13

~~TOP SECRET~~ G

Handle via BYEMAN
Control System Only

~~TOP SECRET~~ GBIF-008- W-C-019838-RI-80

In the Gambit film handling system, the very low pressure (typically < 0.5 mm of mercury) results in an insufficient number of charge carriers to support an arc or corona. Increased relative humidity during operation when film is de-spooled and the presence of matte particles in the backing, which reduces the intimacy of contact between film and rollers, act to reduce the chance of arc by reducing electron charge accumulation.

7.1.7.4 Film Response to Environments. Physical and sensitometric characteristics of photographic film will vary widely under varying conditions of temperature and humidity.

7.1.7.4.1 Temperature Equilibration. The heat capacities and thermal conductivities of ESTAR base film and its components are shown in Table 2.7-1. Conditioning time in large rolls is long and film properties within the roll can vary as the temperature varies. Figure 2.7-8 shows estimated curves for temperature conditioning of the 9.5-inch and 5-inch film rolls used in the Gambit system.

7.1.7.4.2 Physical Temperature Effects. Film emulsion, backing and support melt at elevated temperatures. The melting point of ESTAR is about 500F and the gel coatings can be heated to 340F when dry without any physical damage. Serious photographic effects can occur however, so films should not normally be subjected to these temperatures. Wet melting points of gelatin coatings are much lower, in the range of 212F to 284F. Ignition temperature of ESTAR base films is about 900F.

7.1.7.4.3 Keeping Limits. Keeping limits as a function of temperature and relative humidity for film are given in Figure 2.7-9. The keeping limit represents the maximum storage time consistent with acceptable photographic quality for the stated conditions.

2.7-14

~~TOP SECRET~~ GHandle via BYEMAN
Control System Only

~~TOP SECRET~~ GBIF-008- W-C-019838-RI-80

TABLE 2.7-1
THERMAL PROPERTIES OF FILM

Heat Capacity	
<u>Material</u>	<u>Capacity</u> $\frac{(\text{BTU}/\text{lb})}{\text{F}}$
ESTAR base	0.35
Gelatin	0.37
Film (0.00025-inch emulsion and 0.00023-inch gel backing on 0.0015-inch ESTAR base)	0.36

Thermal Conductivity	
<u>Material</u>	<u>Conductivity</u> $\frac{(\text{BTU}) (\text{ft})}{(\text{hr}) (\text{ft}^2) (\text{F})}$
ESTAR base *	0.08 - 0.09

* For temperatures between 120F and 150F

2.7-15

~~TOP SECRET~~ G

Handle via **BYEMAN**
Control System Only

~~TOP SECRET~~ G

BIF-008- W-C-019838-RI-80

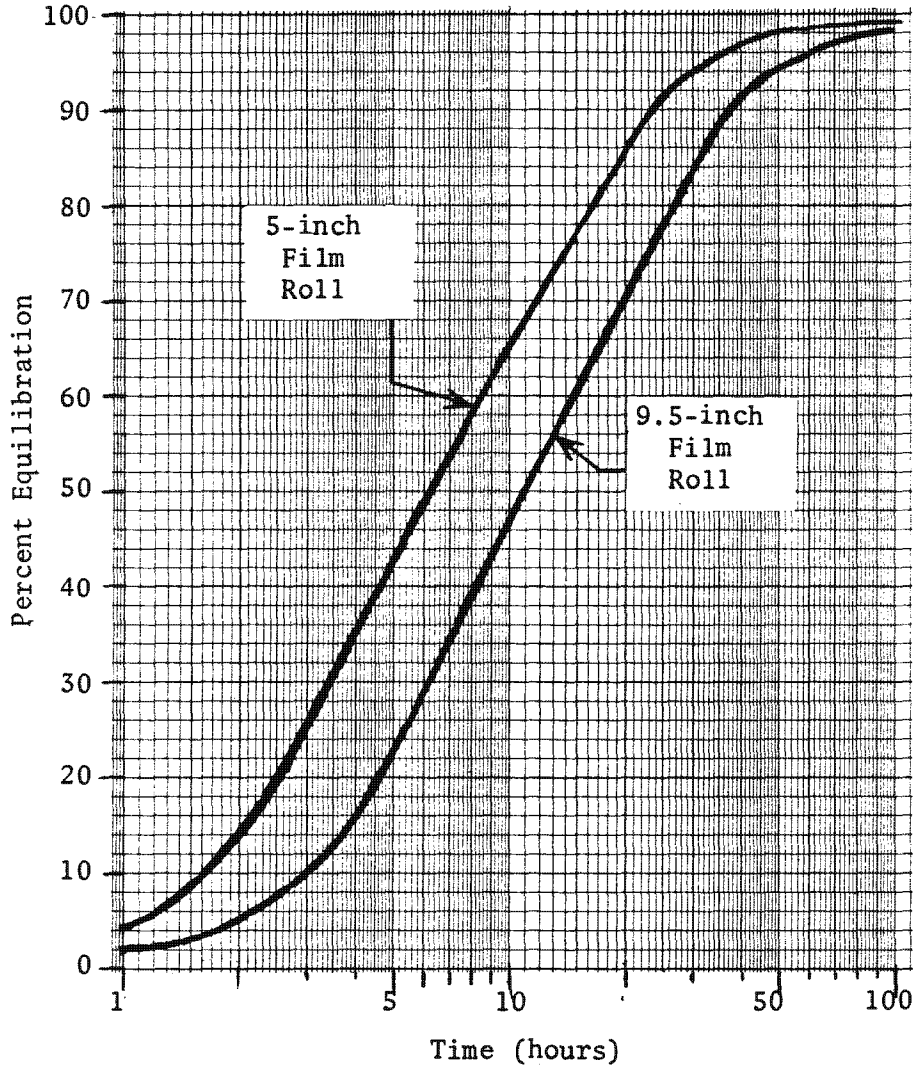


Figure 2.7-8. Temperature Conditioning Curves for 9.5- and 5-inch Wide Films

2.7-16

~~TOP SECRET~~ G

Handle via BYEMAN
Control System Only

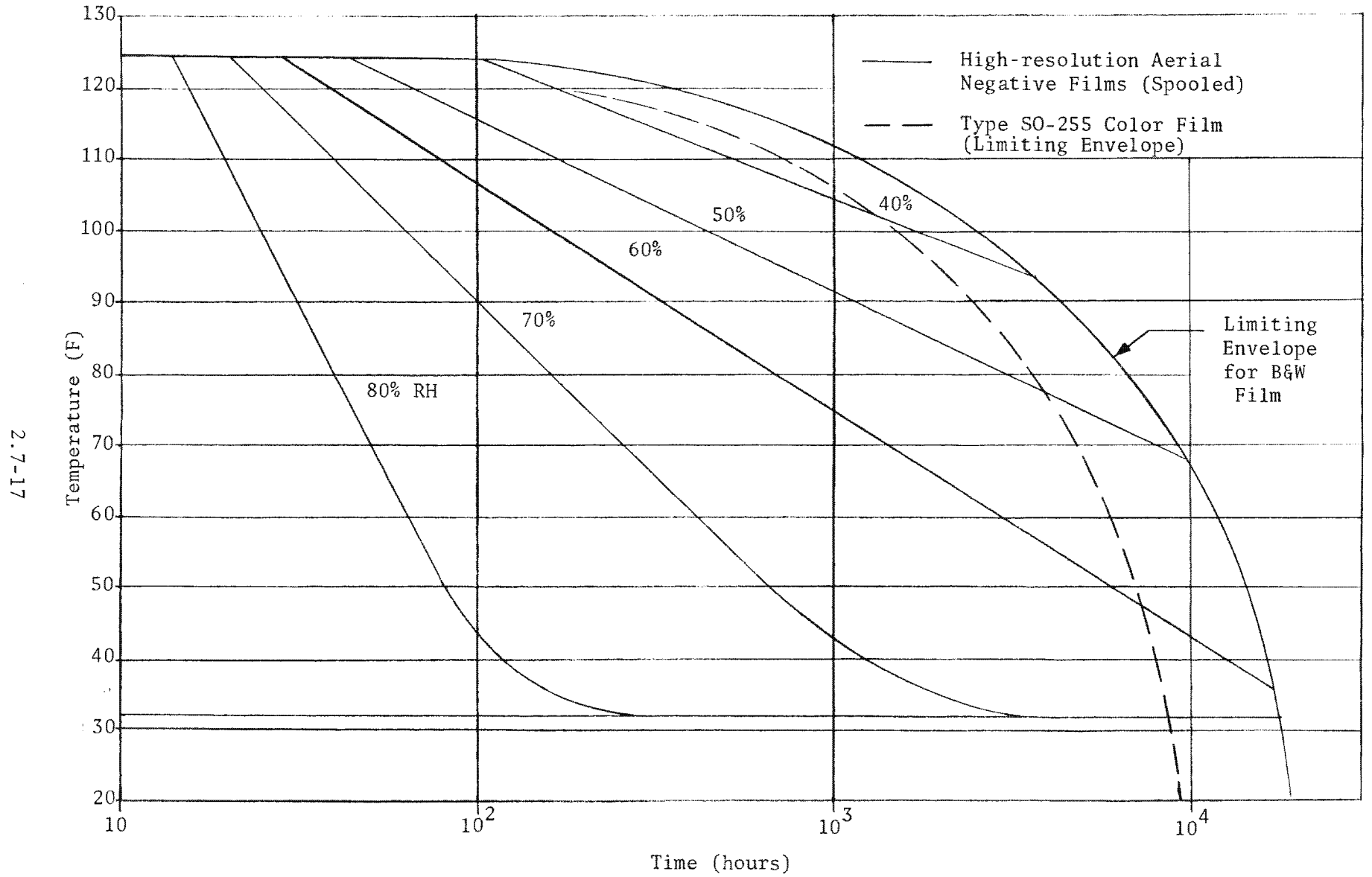


Figure 2.7-9. Film Keeping Limits

Handle via BYEMAN
Control System Only

Approved for Release: 2017/02/14 C05097211

2.7-17

Approved for Release: 2017/02/14 C05097211

~~TOP SECRET~~ GBIF-008- W-C-019838-RI-80

7.1.7.4.3 Moisture Capacity. ESTAR base has a very low moisture capacity in comparison with the gelatin layers. The gel/base ratio of a film determines moisture capacity. In black-and-white films on thin base, this ratio is 0.20 to 0.40 and the moisture capacity varies from 1.0 to 4.0 percent on a dry basis. (Moisture capacity data for Gambit films is provided in Table 2.7-2.)

7.1.7.4.4 Moisture Conditioning Rates. Film will gain or lose moisture depending on the relative humidity to which it is exposed. Conditioning rates depend on a number of factors but free-film strips will condition in minutes while film rolls will take several hours. Film width is a factor in roll conditioning and during conditioning a gradient will exist across the width. Of most practical importance is the fact that on exposure to even moderate vacuum, moisture loss in a strip takes place in seconds. The conditioning rate at 10^{-3} torr (0.001 mm of mercury) is 50 times that at one atmosphere. A strand of film will be equilibrated in less than 10 seconds.

7.1.7.5 Spectral Transmittance. The typical transmittance of clear ESTAR base and an unprocessed black-and-white film and a color film are shown in Figure 2.7-10. In any specific product, additional dyes may be added to prevent unwanted reflection from interlayer boundaries or from a camera platen behind the film. Absorbing dyes in the emulsion may be added to reduced light scattering. The transmittance curves for each product will therefore be different. In general, however, the ESTAR base films are open in the red/infrared region. Most dyes are removed during processing so that transmittance of the processed material in the visible region is determined by the silver or dye forming the processed image.

~~TOP SECRET~~ GHandle via BYEMAN
Control System Only

~~TOP SECRET~~ G

BIF-008-W-C-019838-RI-80

TABLE 2.7-2
 WEIGHT AND MOISTURE CONTENT, GAMBIT FILMS

<u>Film Type</u>	<u>Pounds/Linear ft</u> (70F and 35% RH)		<u>Moisture Content</u> <u>lb of water/lb of Film</u> (70F and 35% RH)
	<u>9.5-Inch</u>	<u>5-Inch</u>	
SO-130	0.01580	0.00827	0.033
SO-255	0.01580	0.00827	0.029
SO-312	0.00908	0.00476	0.017
SO-315	0.00927	0.00486	*
SO-409	0.00908	0.00476	0.017

*To Be Determined

2.7-19

~~TOP SECRET~~ G

Handle via **BYEMAN**
 Control System Only

~~TOP SECRET~~ G

BIF-008- W-C-019838-RI-80

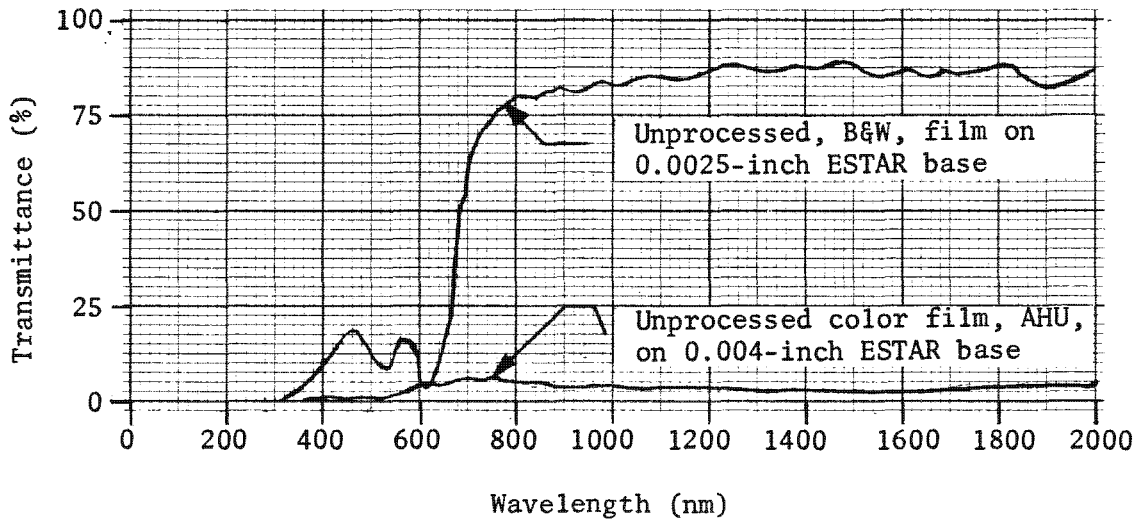


Figure 2.7-10. Spectral Transmission of Film

2.7-20

~~TOP SECRET~~ G

Handle via BYEMAN
Control System Only

~~TOP SECRET~~ GBIF-008- W-C-019838-RI-80

7.1.7.6 Weight and Moisture Summary. Table 2.7-2 provides a summary of the weight and moisture characteristics of the principal film types used in the Gambit system. The weight of a unit length of 9.5-inch wide and 5-inch wide film is provided at 70F and 35% relative humidity. Moisture content is given as the weight of water per weight of dry film.

7.2 Sensitometric Characteristics

Each film has specific and controlled sensitometric and image structure characteristics which define its information recording capabilities. The degree of utilization of this capability depends on the manner of exposing, processing and viewing or duplication of the material. Film manufacturing is controlled such that a given film will perform consistently in controlled laboratory testing. The actual performance in practical applications then depends on many other factors. Special tests and unique measurements of film performance should be made under conditions that match those expected in practice.

7.2.1 Characteristic Curve

Figure 2.7-11 is a typical characteristic curve relating exposure to the resulting photographic densities. Since this response varies according to the spectral distribution of the exposing light, the light used in testing should simulate that to which the film will be exposed in practice. Exposure time should be close to that anticipated in actual use. If these factors are standardized, the curve then depicts the photographic response of a specific film batch when processed in a prescribed manner. Processing can be modified to change the response curve. Other factors such as film age etc. can also modify the response curve.

2.7-21

~~TOP SECRET~~ GHandle via **BYEMAN**
Control System Only

~~TOP SECRET~~ G

BIF-008- W-C-019838-RI-80

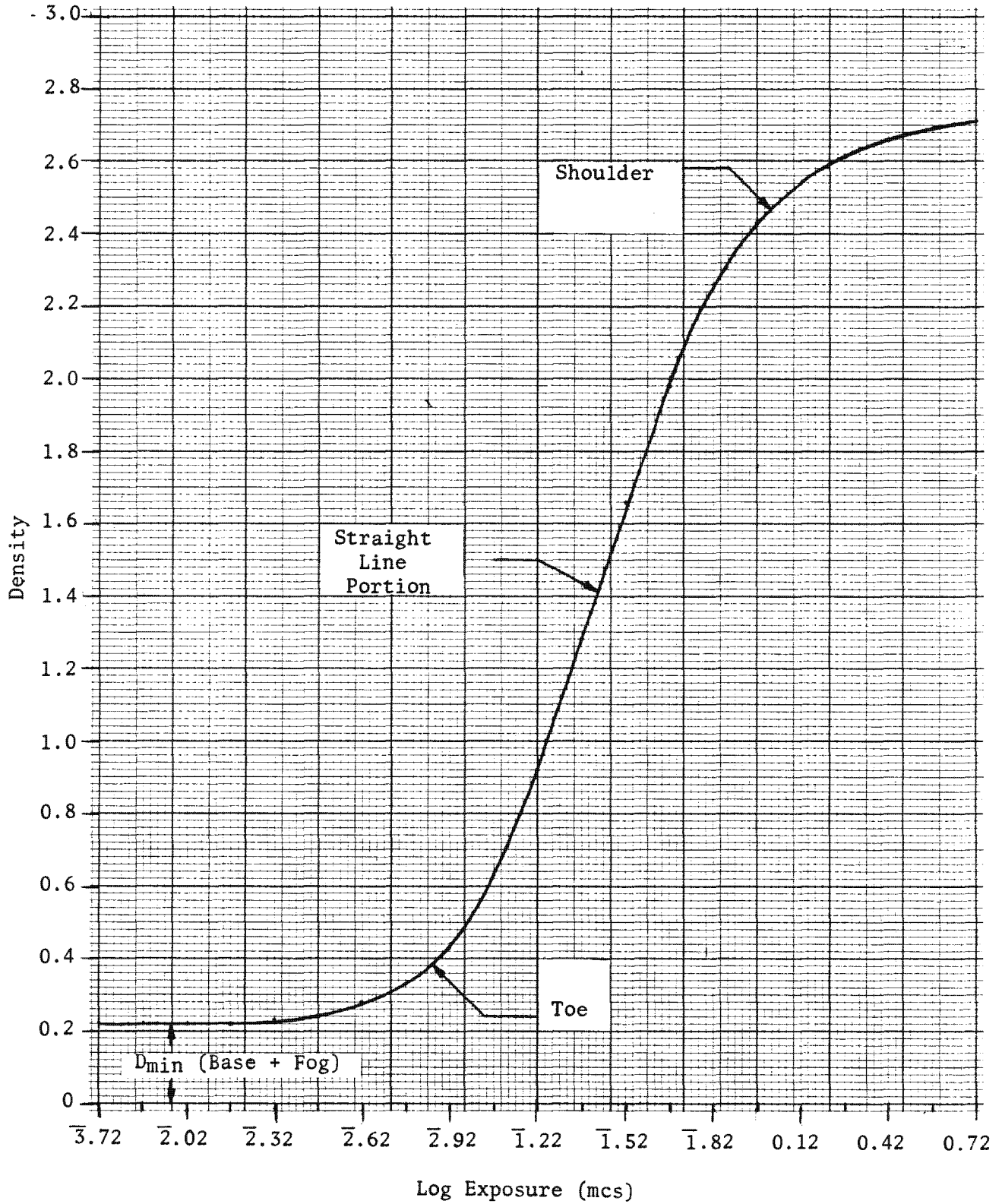


Figure 2.7-11. Typical Characteristic Curve

2.7-22

~~TOP SECRET~~ G

Handle via BYEMAN
Control System Only

~~TOP SECRET~~ GBIF-008- W-C-019838-RI-80

7.2.1.1 Density. Density is defined as the common logarithm of the opacity, or reciprocal transmittance of the film.

$$\text{Density} = \text{Log}_{10} \frac{1}{\text{Transmittance}}$$

The characteristic curve in Figure 2.7-11, (also called the sensitometric curve, the D-Log E curve, or the H&D curve) is plotted in this form because the eye judges brightness differences on a nearly logarithmic scale. Exposure is the product of the intensity of radiation and exposure time (Units: meter-candle-seconds). The curve is therefore in photometric terms. For aerial films, daylight response is measured by filtering the calibrated exposing source, or sensitometer, to simulate daylight. The range of exposures is obtained by placing a tablet with a series of 21 different, calibrated density or transmittance steps in contact with the film to vary the illumination reaching the film. The resultant image density is read on a densitometer and plotted in the form shown in Figure 2.7-11.

7.2.1.2 Fog. The minimum density, or the lower horizontal portion of the curve, represents gross fog or D_{\min} . It is the sum of the density of the support and the unexposed but processed emulsion.

7.2.1.3 Toe. The lower portion of the curve, above the fog level, with increasing slope is called the toe.

7.2.1.4 Straight Line. The midsection of the curve, with the steepest and nearly constant slope, is called the straight-line portion.

7.2.1.5 Shoulder. The upper portion of the curve, where the slope is decreasing, is called the shoulder.

2.7-23

~~TOP SECRET~~ GHandle via BYEMAN
Control System Only

~~TOP SECRET~~ GBIF-008- W-C-019838-RI-80

7.2.2 Sensitometric Parameters

Critical sensitometric parameters can be determined from the characteristic curve. These parameters define the characteristics of a given film-process combination. Figure 2.7-12 illustrates these parameters and they are discussed individually in the following paragraphs.

7.2.2.1 Speed. Photographic film speed is a measure of the sensitivity of the film to light. The higher the film speed, the "faster" the film or the lower the exposure required to produce an image. Many methods are used to determine speed values and there is a specific method for aerial film which is directly related to usage. The speed value is called aerial film speed (AFS) and, for black-and-white films, is defined as $3/2$ times the reciprocal of the exposure (in meter-candle-seconds) at the point on the characteristic curve where the density is 0.3 above gross fog, or D_{min} .

$$AFS = \frac{3}{2E}$$

7.2.2.2 Gamma. The slope of the straight-line portion of the characteristic curve (see Figure 2.7-12) is called gamma and is a measure of contrast. Gamma of aerial films is relatively high in order to enhance photography taken through atmospheric haze.

7.2.2.3 Processing Effects. The characteristic curve represents film response for a particular combination of film and process. A special process known as "Dual-Gamma" is used on black-and-white films in the Gambit system. Figure 2.7-13 shows a comparison of standard (Versamat) process and "Dual-Gamma" process for Type 1414 film.

~~TOP SECRET~~ G

~~TOP SECRET~~ G

BIF-008- W-C-019838-RI-80

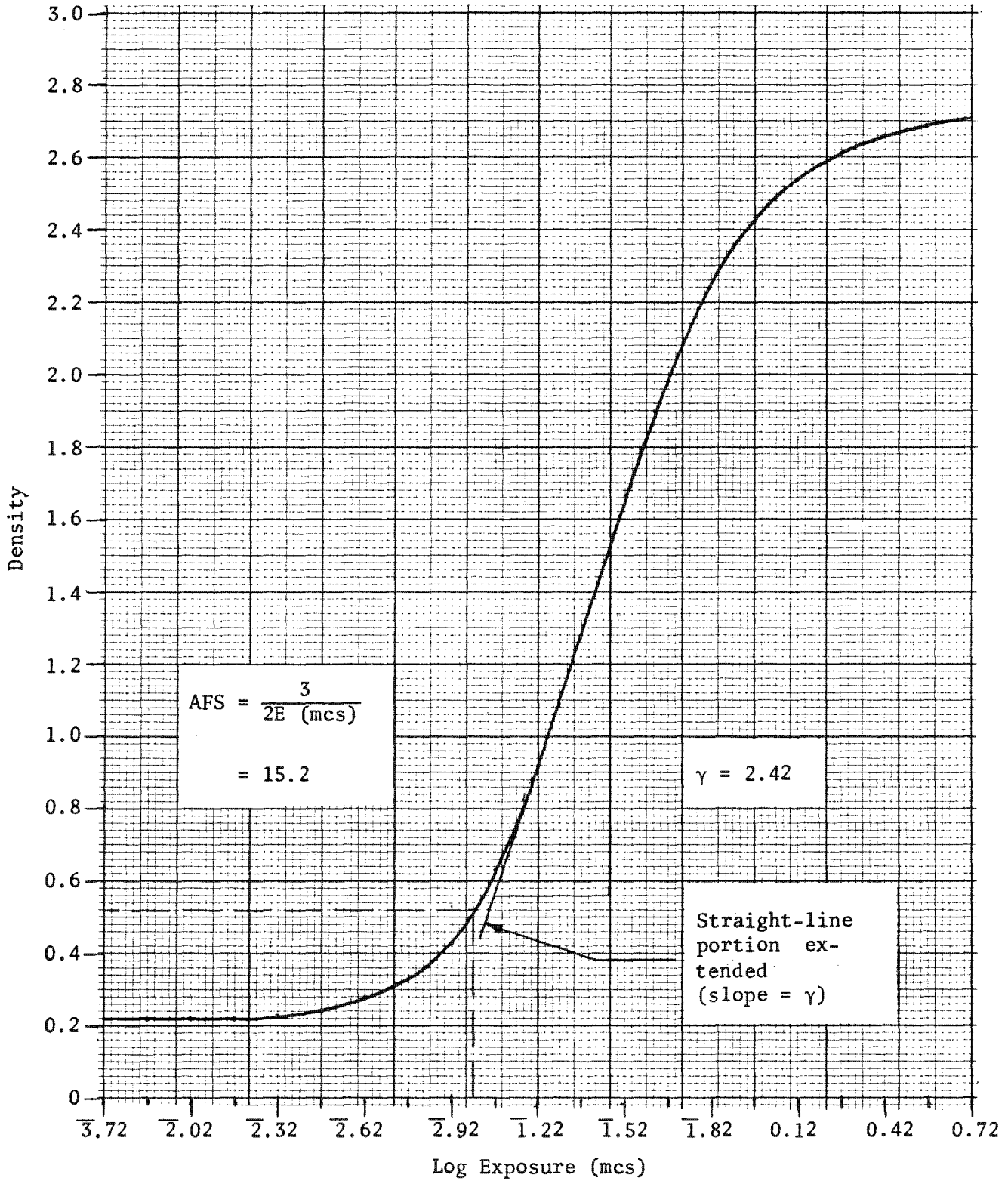


Figure 2.7-12. Sensitometric Properties

2.7-25

~~TOP SECRET~~ G

Handle via BYEMAN
Control System Only

~~TOP SECRET~~ G

BIF-008- W-C-019838-RI-80

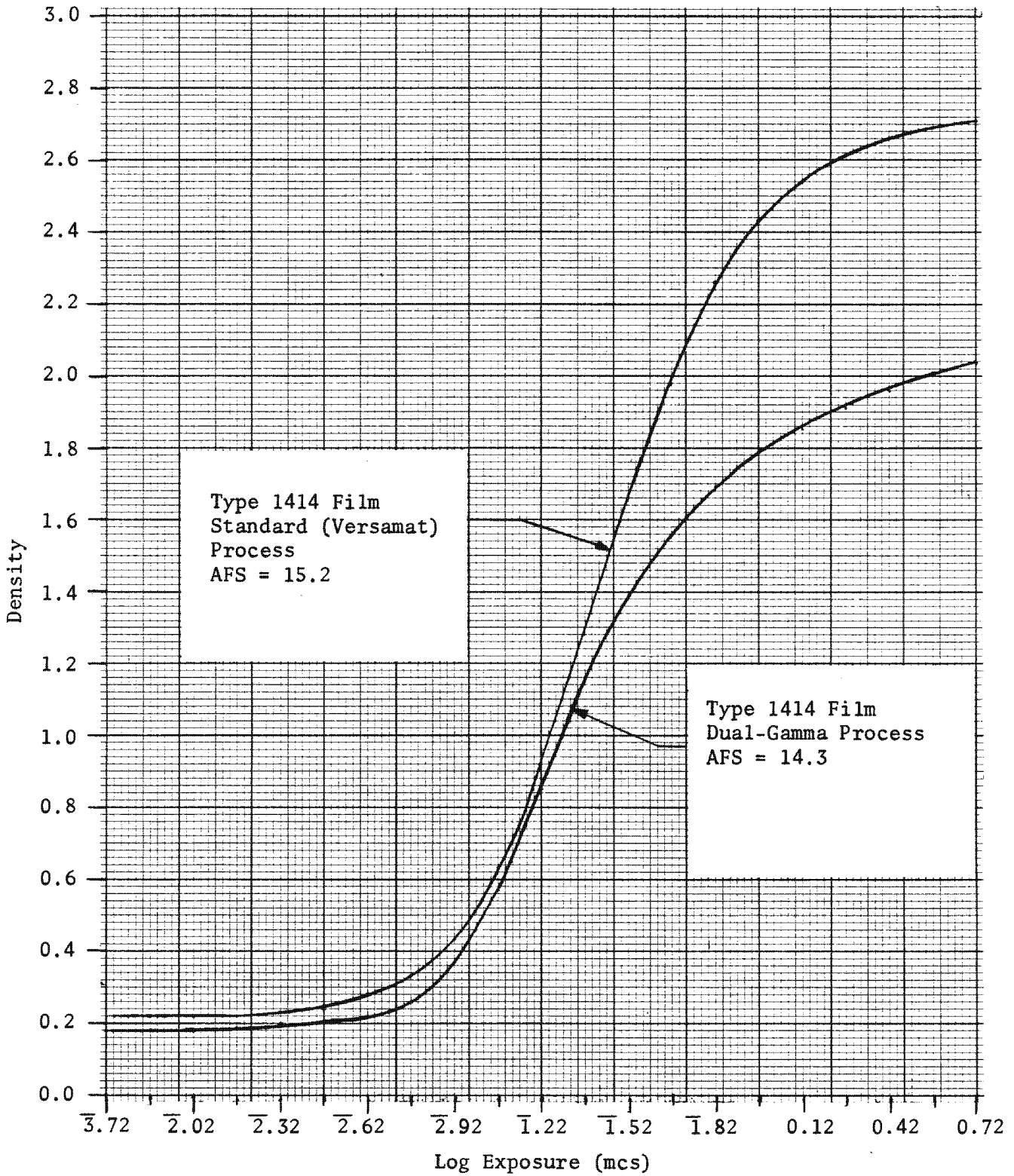


Figure 2.7-13. Process Comparison

2.7-26

~~TOP SECRET~~ G

Handle via BYEMAN
Control System Only

~~TOP SECRET~~ GBIF-008- W-C-019838-RI-80

7.2.3 Spectral Sensitivity

The spectral sensitivity of a film describes its response to radiation of various wavelengths. By special sensitizing techniques the response can be extended from the inherent blue response of silver halide to include green, red and near-infrared portions of the spectrum. Spectral sensitivity curves describe this response in the form shown in Figure 2.7-14. Spectral sensitivity information for a specific film-process combination may be found in the vendor's data sheets for that film. The black-and-white aerial films are panchromatic, that is, sensitive to red, green and blue light. Most films for high altitude use have extended red sensitivity to about 720 nanometers to better penetrate atmospheric haze. Light scattered from the atmosphere, or haze light, is strongly blue and ultraviolet. This unwanted, non-image forming light is further reduced by filtration in the optical system.

7.2.4 Fog

Fog increases the number of developable silver halide crystals over large areas of film. It is associated with non-image forming light or other influences having a similar effect. Fog increases D_{\min} (see Figure 2.7-11), thereby altering the effective speed (AFS) of the film.

Fog may arise from stray illumination, static discharge, and charged-particle or quantum radiation. Additionally, the age of film and the type of processing applied may influence fog levels attained in practice.

7.2.5 Special Films

Films are available with specialized sensitometric characteristics which may be appropriate in certain applications of Gambit photography.

~~TOP SECRET~~ GHandle via **BYEMAN**
Control System Only

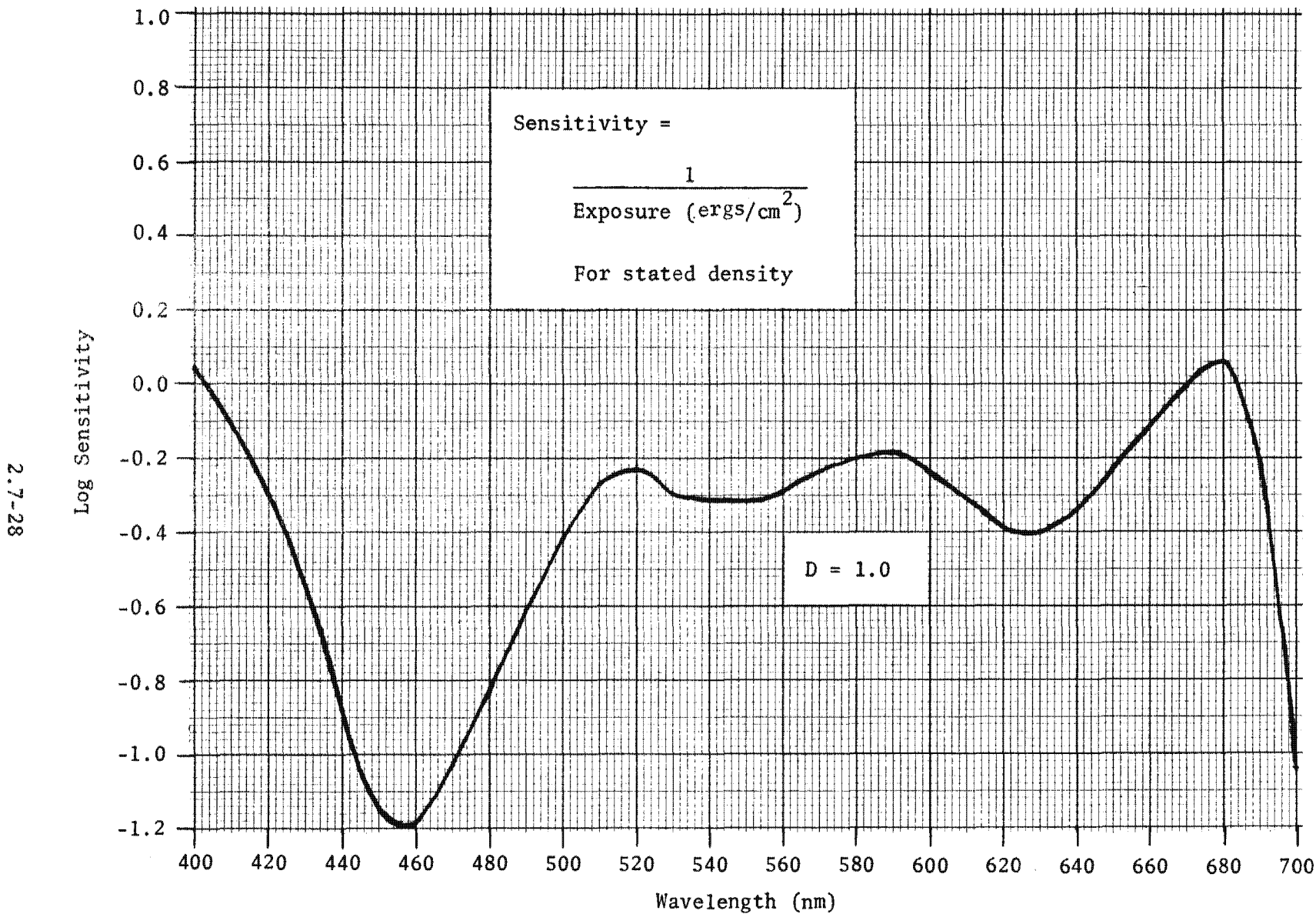


Figure 2.7-14. Typical Spectral Sensitivity, Black-and-White Film

Handle via BYEMAN
Control System Only

Approved for Release: 2017/02/14 C05097211

Approved for Release: 2017/02/14 C05097211

~~TOP SECRET~~ G

BIF-008-W-C-019838-RI-80

7.2.5.1 Color Film. Conventional reversal color films have three photo-sensitive layers which are separately sensitized to the three primary colors; red, green, and blue. A complementary dye image is formed in each layer in inverse proportion to exposure of the layer. The integrated image is a close visual reproduction of the original scene.

7.2.5.2 Infrared Color Film (False Color IR). Any portion of the spectrum can be recorded in a color film if the emulsion layers are so sensitized. The color, or dye, developed in the layers is not directly related to the color of the light to which it is sensitized. An infrared color film emphasizes differences in infrared reflection of materials by having layers sensitive to green, red and infrared light in which are formed yellow, magenta and cyan dyes. A yellow filter layer is coated over the emulsion layers to prevent blue light from reaching the emulsion. These products are of value in evaluating differences in the condition of vegetation, in detecting camouflaged sites and in interpreting soil and water composition.

7.2.3.3 Special Black-and-White Films. Very high-speed black-and-white films can be employed for photography of light sources or even illuminated areas at night. Faster films also are of value in photography at low solar altitudes. Black-and-white films sensitized and filtered to record in the infrared spectrum are available. These films have very limited use in the Gambit system.

7.3 Noise Characteristics (Signal/Noise)

Film "noise", in the sense of that which may interfere with the detection of image modulation, is principally associated with film granularity. Furthermore, if "signal" is interpreted as the image modulation, then detection is not possible when the signal-to-noise ratio becomes equal to or less than 1.

~~TOP SECRET~~ G

~~TOP SECRET~~ GBIF-008- W-C-019838-RI-80

7.3.1 Film Granularity

While to the unaided eye, the densities in a black-and-white photographic image may appear to be homogeneous, microscopic examination will reveal a collection of discrete particles of metallic silver. These particles, called grains, form a granular pattern which becomes visible under enlargement. It is this pattern which is the major contributor to film "noise". When the dimensions describing the grain size and spacing are of the same order as the spacing of the image modulation, the signal-to-noise ratio is near unity and the image modulation can no longer be recorded by the film.

The standard numeric describing this effect is RMS granularity which represents 1000 times the standard deviation in density produced by the granular structure of the material when a uniformly exposed and developed sample having a density of 1.0 is scanned by a microdensitometer having an optical system aperture of $f/2.0$ and a circular scanning aperture 48 μm in diameter. For the finer grain aerial films, more meaningful data has been obtained by reducing the aperture to 12.7 μm and 2.0 μm . The 2.0 μm aperture is expected to become the standard.

7.3.2 Threshold Modulation

Threshold modulation (TM) is defined as the modulation at spatial frequency ν which must be supplied to a given film in order that the density variations after processing will be detectable (see Part 2, Section 12.3). This threshold of detection may be thought of as occurring when signal (image modulation)/noise (related to granularity) is equal to one.

As described elsewhere (Part 2, Section 9.1 and Part 2, Section 12.5.2), the intersection of a system's MTF curve with a film TM curve (adjusted for contrast) provides a useful estimate of a limiting system resolution

~~TOP SECRET~~ GHandle via BYEMAN
Control System Only

~~TOP SECRET~~ GBIF-008- W-C-019838-RI-80

on that film. Table 2.7-3 contains the mathematical expression for the TM curves for a number of films currently used in the Gambit system.

7.3.3 Duplication

Because of the multiple users of Gambit photography and also because of the desire to preserve the original material for archival use, most examinations of Gambit photography are done on duplicate materials. This duplication process results in some decrease in image quality at high spatial frequencies of up to 8 percent between the original negative and the duplicate. The influence of the base material in the light path and the turbidity of the emulsion contribute to this effect. In general, improvements in duplicating materials and equipment have kept pace with improvements in acquisition quality to minimize these losses.

7.4 Film Characteristics Summary

Table 2.7-4 presents the descriptive parameters of many films which have been or are expected to be employed in the Gambit Reconnaissance System. It should not be assumed that the characteristics shown in the table will be identical with those of any given batch of film. It is expected that the nominal characteristics shown will change from time-to-time and that film types will be added and deleted from the table.

~~TOP SECRET~~ GHandle via BYEMAN
Control System Only

~~TOP SECRET~~ GBIF-008- W-C-019838-RI-80TABLE 2.7-3
THRESHOLD MODULATION CURVES*

<u>Film Type</u>	<u>Exposure**</u>	<u>a</u>	<u>b</u>	<u>c</u>
3401/3411	0	1.78×10^{-7}	0	5.43×10^{-5}
	+1***	2.00×10^{-2}	0	6.50×10^{-5}
	-1***	2.00×10^{-2}	0	6.50×10^{-5}
SO-112/SO-312	0	2.23×10^{-2}	0	3.50×10^{-7}
	+1	2.94×10^{-2}	0	4.16×10^{-7}
	-1	2.41×10^{-2}	0	6.97×10^{-7}
SO-315	0	1.94×10^{-2}	0	9.06×10^{-7}
	+1	2.67×10^{-2}	0	9.84×10^{-7}
	-1	2.14×10^{-2}	0	1.40×10^{-6}
SO-409	0	1.7×10^{-2}	0	2.07×10^{-7}
	+1	2.0×10^{-2}	0	3.81×10^{-7}
	-1	-1.8×10^{-2}	0	9.55×10^{-7}
SO-130	0	4.32×10^{-2}	0	5.19×10^{-5}
	+1	4.50×10^{-2}	0	5.60×10^{-5}
	-1	3.91×10^{-2}	0	5.68×10^{-5}
SO-255	0	2.42×10^{-2}	0	4.50×10^{-6}
	+1	1.84×10^{-2}	0	6.21×10^{-6}
	-1	2.11×10^{-2}	0	6.40×10^{-6}

$$*TM = a + bv + cv^2$$

** 0 = nominal

+1 = 1 stop over

-1 = 1 stop under

***Estimated

2.7-32

~~TOP SECRET~~ GHandle via **BYEMAN**
Control System Only

TABLE 2.7-4
FILM CHARACTERISTICS

FILM TYPE		Description	AFS *	Long Wave- Length Cutoff (nm)	RMS Granularity	Base Thickness (Inches)	Emulsion Thickness (Inches)	Dyed Pelloid Backing Thickness (Inches)	Emulsion Matte **	Backing Matte **	AHU (Anti- Halation Undercoat)
Black-and-White Negative Films											
(1)	3401/3411†	Plus-X Aerial Film	212	710	380	0.00250	0.00030	0.00025	None	None	No
(2)	SO-312	High Definition Aerial Film	4.7	690	75	0.00120	0.00020	0.00018	None	F-P	No
(3)	SO-315	High Definition Aerial Film	9.3	690	80	0.00120	0.00016	0.00015	None	R-P	No
(4)	SO-409	High Definition Aerial Film	1.2	690	68	0.00120	0.00019	0.00014	None	F-P	No
<u>Special Films</u>											
(1)	SO-255	Aerial Color Film (Reversal)	10.7 ⁽¹⁾	690	13.1	0.00150	0.00075	0.00043***	MF-RM	MF-RM	No
(2)	SO-130	False Color, IR (Reversal)	9.5 ⁽¹⁾	870	36.2	0.00150	0.00082	0.00042***	R-P	R-P	No

* AFS listed is effective AFS in applications. However, these values can change significantly with time as processes are modified and smear/exposure trade-offs are applied.

** Matte designations are as follows: R = Regular; F = Fine; MF = Medium Fine; VF = Very Fine; P = Permanent; RM = Process Removable; L-P = Large Permanent.

*** Backing is clear gel

(1) Equivalent AFS: $AFS_E = \frac{3}{E(msc)}$ where E(mcs) is exposure to produce a green density of 1.5 with a Wratten 2E filter.

† These materials are no longer being manufactured. However, the manufacturer has adequate supplies of these films in storage to meet customer requests.

2.7-33/2.7-34

Handle via BYEMAN
Control System Only

Approved for Release: 2017/02/14 C05097211

Approved for Release: 2017/02/14 C05097211

~~TOP SECRET~~ GBIF-008- W-C-019838-RI-80

8.0 MISSION SIMULATIONS

This section contains simulation results for both a low and a high mode mission.

The low-mode simulation was run with Mission Simulation and Analysis (MSA) software developed for use in the analysis of PPS/DP EAC equipment response under varying conditions. A description of the software is given in Appendix C. Because of the large number of mission aspects modeled by the software, no attempt has been made to define and systematically analyze the limiting cases. These results are shown in paragraphs 8.1 through 8.7.

The high-mode results were derived by from a simulation generated by the Intelligence Requirements Satisfaction Simulator (IRSS). These results are shown in paragraphs 8.8 through 8.11. This simulation is intended to illustrate the 9-inch camera coverage which could be expected on a 120-day high-mode mission. Any change in the various mission aspects including use of the 5-inch camera will result in different coverage results.

25X1

8.1 Orbit Generation

Two 60-day missions were simulated with identical orbits but with different launch dates and times. These orbits were devised to give full earth coverage above 20 degrees north latitude. The effects of orbit decay due to drag were included and orbit adjusts were simulated. The calculations were ended after an 8-day closure period.* The 8 days were spread uniformly throughout the 60-day period. The important orbital parameters used are given in Table 2.8-1.

*Closure - Ground track repeat.

2.8-1
~~TOP SECRET~~ GHandle via BYEMAN
Control System Only

~~TOP SECRET~~ GBIF-008- W-C-019838-RI-80

TABLE 2.8-1
 ORBITAL PARAMETERS

(1) Orbit inclination	110.5°	
(2) Height of perigee	68 nmi	
(3) Eccentricity range	0.0234 to 0.0218	
(4) Latitudes of perigee	40° to 48.5°	
(5) Days simulated	8	
(6) Launch dates, Pacific Standard times (AM)	4/1 8:00 AM	9/1 7:30 AM
(7) Dates simulated	April 9-10 April 23-24 May 7-8 May 21-22	September 9-10 September 23-24 October 7-8 October 21-22
(8) Orbit adjusts	1 per 16 revs	
(9) Drag coefficient	138 lb/ft ²	

2.8-2

~~TOP SECRET~~ G

Handle via BYEMAN
 Control System Only

~~TOP SECRET~~ GBIF-008- W-C-019838-RI-808.2 Target Acquisition

The determination of which targets were potentially available for photography on each rev of the two missions was done using a subset of the master list of 13871 targets used on Mission 40. Figure 2.8-1 gives an indication of the geographical location of these 13871 targets. The subset used for the simulation reduced the density of targets while maintaining their geographical distribution. Acceptable targets were limited to those acquirable within the prescribed PPS/DP EAC limits. These limits are given in Table 2.8-2.

8.3 Target Selection

Because of the simulation-model hardware constraints, only a fraction of the available targets may be selected for photography. The MSA selection process eliminates hardware conflicts while emphasizing the selection of stereo photographs of high-priority targets at low obliquity. Monoscopic photographs are then fit in where the average rate of film usage must be budgeted and regularly adjusted to sustain the entire mission. This film management function is introduced by providing a Monte Carlo weather model which assigns assumed cloud conditions to each target. Then, by assigning weather thresholds to targets by priority, deleting targets not passing the weather thresholds in effect when they are acquired, and periodically adjusting the thresholds, the film rate is brought into line with the required rate. The weather statistics, which consist of average cloud conditions over the area of interest during each month of the year, were provided by the Air Weather Service. Tables 2.8-3 through 2.8-6 summarize the basis of the selection process carried out for the two simulated missions. Table 2.8-3 outlines the basic constraints in effect. Table 2.8-4 gives the weather statistics for the months simulated. Tables 2.8-5 and 2.8-6 summarize the weather thresholds used to control the rate of film use.

2.8-3

~~TOP SECRET~~ GHandle via BYEMAN
Control System Only

~~TOP SECRET~~ G

B1 F-008-W-C-019838-RI-80

This Page Intentionally Blank

2.8-4

~~TOP SECRET~~ G

Handle via **BYEMAN**
Control System Only

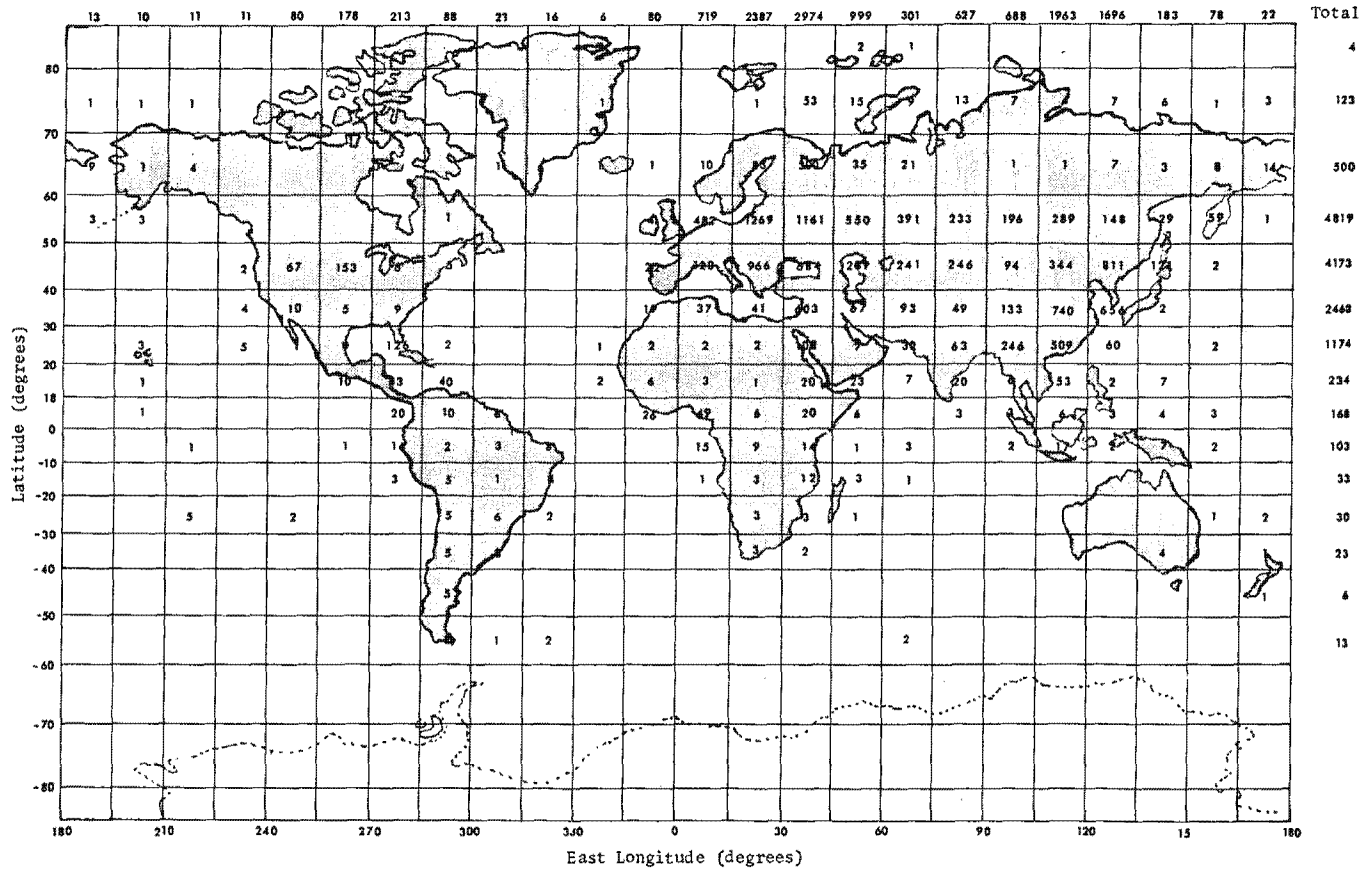


Figure 2.8-1. Target Distribution

2.8-5/2.8-6

Handle via BYEMAN
Control System Only

Approved for Release: 2017/02/14 C05097211

Approved for Release: 2017/02/14 C05097211

~~TOP SECRET~~ GBIF-008- W-C-019838-RI-80

TABLE 2.8-2

ACQUISITION LIMITS

- | | |
|---------------------------------------|--------------------------|
| (1) Obliquity limit | $\pm 45^\circ$ |
| (2) Lower sun angle limit | 5° |
| (3) Range of photographic acquisition | Ascending and Descending |
| (4) Slant range limit | 210 nmi |
| (5) Master list of targets: | |

A number of priority (4-9) targets, which were in clusters or in high-density areas, were removed from the original master list of 13871 targets derived from Mission 40. The remaining total of 9302 targets was the master list used for this simulation.

2.8-7
~~TOP SECRET~~ GHandle via **BYEMAN**
Control System Only

~~TOP SECRET~~ GBIF-008- W-C-019838-RI-80

TABLE 2.8-3

CONSTRAINTS ON TARGET SELECTION

(1) Stereo LOS angle	±8.65°	
(2) In-track ephemeris uncertainty (1σ)	2500 ft*	
(3) LOS pointing uncertainty (1σ)	0.113°	
(4) Target diameters	From Mission 40 target tape	
(5) Target location uncertainties (1σ)	From Mission 40 target tape	
(6) Clock granularity	0.2 sec	
(7) Burst time pad multipliers	<u>Priority</u>	<u>Pad Multiplier*</u>
	0	1.5
	1	1.3
	2	1.2
	3	1.1
	4	1.0
	5-9	0.7
(8) Roll rate equation	$\Delta t = \frac{\Delta\Omega}{5.5} + 0.82 - 0.82 e^{-\frac{\Delta\Omega}{0.9} \text{ sec}}^{**}$	
(9) Stereo slew time	3 sec	
(10) Mission length	60 days	
(11) Total film load	13,800 ft (See Table 2.8-7)	
(12) Weather conditions	See Table 2.8-4	
(13) Weather threshold	See Tables 2.8-5 and 2.8-6	

* Obtained from Customer TWX.

** Best engineering estimate, LMSC

2.8-8
~~TOP SECRET~~ G

Handle via BYEMAN
 Control System Only

TABLE 2.8-4
CLOUD CONDITIONS FOR THE MONTHS OF SIMULATIONS

Probability of Exceeding Indicated
Cloudfreeness

<u>Percent Cloudfree</u>	<u>April</u>	<u>May</u>	<u>September</u>	<u>October</u>
0	1.000	1.000	1.0000	1.0000
10	0.675	0.697	0.7042	0.6711
20	0.515	0.507	0.5260	0.5121
30	0.440	0.414	0.4467	0.4421
40	0.382	0.347	0.3880	0.3885
50	0.333	0.293	0.3396	0.3431
60	0.288	0.247	0.2957	0.3020
70	0.243	0.201	0.2499	0.2602
80	0.188	0.144	0.1889	0.2038
90	0.127	0.085	0.1141	0.1257
100	0.000	0.000	0.0000	0.0000
*	0.528	0.523	0.5440	0.5540

* Correlation Coefficient between cloud conditions in adjoining weather cells

2.8-9

TABLE 2.8-5

WEATHER THRESHOLDS FOR ACQUISITION

Range of Cloudfree Conditions for which Photography was Allowed*

Priority Category	Date of Launch	
	4/1	9/1
0	0	0
1	0-14	0-10
2	0-14	0-10
3	0-18	0-18
4	0-18	0-18
5	0-24	0-24
6	0-30	0-30
7	8-40	0-40
8	5-45	0-45
9	15-50	5-50

* Since the thresholds were changed periodically during the simulation to adjust film usage rates, a range of thresholds was used in each priority category except 0.

Handle via BYEMAN
Control System Only

Approved for Release: 2017/02/14 C05097211

2.8-10

Approved for Release: 2017/02/14 C05097211

TABLE 2.8-6

WEATHER THRESHOLD AVERAGES

Rev Average of Cloudfree Conditions for which Photography was Allowed

<u>Priority Category</u>	<u>Date of Launch</u>	
	<u>4/1</u>	<u>9/1</u>
0	0	0
1	3.5	3.6
2	3.5	3.6
3	5.9	5.8
4	6.9	7.3
5	10.4	10.8
6	13.9	11.5
7	23.8	17.3
8	24.7	16.8
9	32.6	23.7

2.8-11

~~TOP SECRET~~ GBIF-008- W-C-019838-RI-808.4 Photographic Performance Model

Photographic performance is determined by the mission parameters, the hardware design, and the planned mission use. Tables 2.8-7 and 2.8-8 summarize the remaining factors contributing to the performance results for the two missions. Table 2.8-7 outlines all the system parameters modeled, except smear. The servo granularity and the optical parameters are typical of the Block 48 design. The two-platen camera was modeled by assuming that different film types were used with each platen. The choice of which platen to use for a given photograph was based on the sun angle at the target. Contrast was modeled using a modification of the AMOS model from the KALEIDOSCOPE program. It assumes a constant target high and low reflectance value. The smear for each frame was the algebraic sum of the smear from each of the many contributors. The smear due to each contributor was determined by a Monte Carlo sample from the distribution for each contributor. Table 2.8-8 gives a description of the distributions for the individual contributors.

8.5 Equipment Usage Model

The estimate of the PPS EAC equipment usage for the two missions was based on a model of the nominal Block 48 hardware designs. The model computes both the servo steps selected and the cumulative servo motor ON times. Since simulations were based on 8-day segments, the mission totals for equipment usage were obtained simply by scaling up the simulation totals by a factor of 60/8. This simple scaling is valid because of the control of film use maintained by the software film management monitor.

2.8-12

~~TOP SECRET~~ GHandle via BYEMAN
Control System Only

~~TOP SECRET~~ GBIF-008- W-C-019838-RI-80

TABLE 2.8-7

PHOTOGRAPHIC PERFORMANCE MODEL

(1)	Focal length	175 inches	
(2)	1σ defocus	0.0005 inch	
(3)	Smear contributors	See Table 2.8-8	
(4)	Film-drive speeds	3.37 to 11.8 ips (1024 steps)	
(5)	Crab steps	0.35°	
(6)	Slits	Block 48 design (See Part 3, Section 2)	
(7)	Film load	1414 (AFS 14.7) on 5-inch platen S0124-101 (AFS 5.7) on 9-inch platen	
(8)	Camera use algorithm	1414 for targets with sun angles below indicated angles. S0124 for targets with sun angles above indicated angles.	
		$\frac{4/1}{32.0^\circ}$	$\frac{9/1}{21.4^\circ}$
(9)	MTF	current R-5 formula	
(10)	OQF	0.88	
(11)	Effective \underline{f} -number*	4.3	
(12)	Slit-to-emulsion spacing	0.0065 inch	
(13)	TMs	$TM_{1414} = 0.017 + 0.00037 f$ $TM_{124-101} = 0.028 + 1.9 \times 10^{-5} f + 8.7 \times 10^{-7} f^2$ (Where f is spatial frequency in cycles/mm)	

* \underline{f} -number - indicates aperture size~~TOP SECRET~~ GHandle via **BYEMAN**
Control System Only

~~TOP SECRET~~ G

BIF-008- W-C-019838-RI-80

TABLE 2.8-7 (CONTINUED)

- | | |
|---------------------------------------|---|
| (14) Contrast ratios | (1) Variable from a contrast model for a tribar target with a high/low reflectance of 33/7
(2) Constant at 2:1
(3) Variable from a contrast model for a 12% GM reflectance "average" target with a high/low reflectance of 16/9 |
| (15) Exposure versus sun angle tables | 1414 from Mission 43 data base, AFS 14.7
124-101 from Mission 43 data base, AFS 5.7 |

NOTE: Film types 1414 and SO-124 are no longer used. Because of other, more specific performance studies undertaken with respect to the newer monodispersed films (SO-312, SO-315, SO-409), a full simulation using MSA was not considered necessary.

2.8-14

~~TOP SECRET~~ G

Handle via BYEMAN
Control System Only

~~TOP SECRET~~ GBIF-008- W-C-019838-RI-80

TABLE 2.8-8

MISSION SIMULATION SMEAR CONTRIBUTOR MATRIX

	<u>Smear Contributor</u>	<u>Units</u>	<u>Error Magnitude</u>
(1)	Altitude distribution (1- σ)	nmi	0.10000
(2)	Roll attitude (1- σ)	Degrees	0.08707
(3)	Pitch attitude (1- σ)	Degrees	0.07459
(4)	Yaw attitude (1- σ)	Degrees	0.07880
(5)	Roll rate (1- σ)	Deg/Sec	0.00260
(6)	Pitch rate (1- σ)	Deg/Sec	0.00100
(7)	Yaw rate (1- σ)	Deg/Sec	0.00100
(8)	Crab granularity ($\pm b$)	Degrees	0.17500
(9)	Crab reproducibility (1- σ)	Degrees	0.00330
(10)	Stereo reproducibility (1- σ)	Degrees	0.00330
(11)	Film-drive speed granularity ($\pm b$)	Percent	0.04400
(12)	Film-drive speed drift (1- σ)	Percent	0.03300
(13)	Focal length error (1- σ)	Inches	0.10000
(14)	K distortion	Percent	0.21800
(15)	Roll step granularity ($\pm b$)	Degrees	0.00000*
(16)	Roll attitude offset (μ)	Degrees	0.00000
(17)	Pitch attitude offset (μ)	Degrees	0.00410
(18)	Yaw attitude offset (μ)	Degrees	-0.01360
(19)	Roll rate offset (μ)	Deg/Sec	0.00000
(20)	Pitch rate offset (μ)	Deg/Sec	0.00000
(21)	Yaw rate offset (μ)	Deg/Sec	0.00000
(22)	Target location (1- σ)	nmi	0.21400
(23)	Cross-track ephemeris (1- σ)	nmi	0.10000

* Roll step granularity error ($\pm b$) included in roll step granularity via PPS crab step granularity

μ = Mean bias

1- σ = 1 standard deviation

$\pm b$ = uniform distribution range

2.8-15

~~TOP SECRET~~ G

Handle via BYEMAN
Control System Only

~~TOP SECRET~~ GBIF-008- W-C-019838-RI-808.6 Photographic Performance Estimates

Figures 2.8-2 through 2.8-4 are cumulative Geometric Mean (GM) ground resolution curves for the two missions. They show the estimated number of frames exceeding a given resolution for each of three contrast conditions. They are based on a total of 26933 frames for the April-May mission and a total of 26430 frames for the September-October mission. Table 2.8-9 summarizes some of the data from these graphs. The results for all three contrast conditions show that the April launch resulted in generally better resolution than the September launch. Table 2.8-10 compares the factors which influenced the resolution for the two missions. The major factor was the difference in the sun angle distributions which resulted from the solar declination being higher in the April-May period than in the September-October period. However, the contrast distributions for the two periods tend to lessen the difference caused by sun angle. This occurs because the haze level is more favorable in the fall than in the spring. This is illustrated in Figure 2.8-5 which shows a distinct shift in the distribution of film plane contrasts for the tribar target to higher values for the September launch. In fact, as Table 2.8-9 shows, the highest resolution values were obtained in the September-October mission for just this reason. The slant range and smear distributions for the two missions were nearly identical and thus did not account for much of the difference in performance.

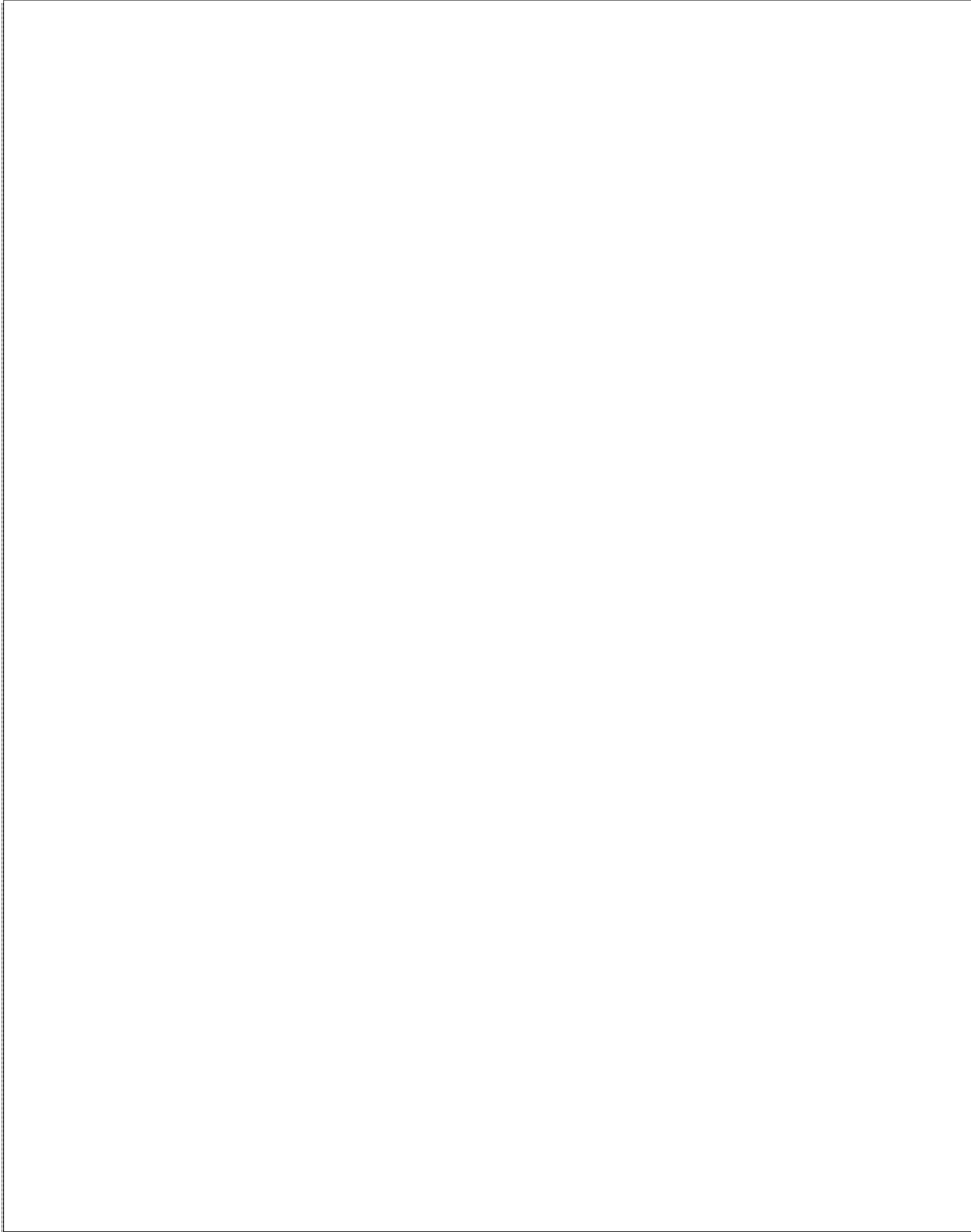
As expected, the contrast model for the tribar target gives a broader distribution of resolutions than does a constant contrast of 2 to 1. However, using 2 to 1 results in a reasonable representation of the tribar resolutions. Operational photography is done on generally lower contrast targets, in this case represented by a target with high and low reflectance values of 16 and 9 percent. This results

2.8-16

~~TOP SECRET~~ GHandle via BYEMAN
Control System Only

25X1

BI F-008-- W-C-019838-RI-80



Geometric Mean Resolution
(Inches)

Figure 2.8-2. Cumulative Simulated Resolution (Tribar)

Number Exceeding Stated Resolution (10^3)

2.8-17

~~TOP SECRET~~ G

Handle via **BYEMAN**
Control System Only

~~TOP SECRET~~ G



2.8-18

Figure 2.8-3. Cumulative Simulated Resolution (2:1 Contrast)

25X1

Handle via BYEMAN
Control System Only



2.8-19

Figure 2.8-4. Cumulative Simulated Resolution (Operational)

25X1

Approved for Release: 2017/02/14 C05097211

Approved for Release: 2017/02/14 C05097211

~~TOP SECRET~~ G

BIF-008- W-C-019838-RI-80

TABLE 2.8-9

9 PLUS 5 COMBINED GEOMETRIC MEAN GROUND RESOLUTION
(FROM MISSION SIMULATIONS)

<u>Launch Date</u>	<u>Contrast</u>	<u>GM Ground Resolution (inches)</u>			
		<u>Best</u>	<u>Median</u>	<u>95% Point</u>	
4/1	Tribar 33/7			14.52	25X1
	Constant 2:1			14.16	
	Operational 16/9			28.26	
9/1	Tribar 33/7			14.66	
	Constant 2:1			15.08	
	Operational 16/9			25.44	

2.8-20

~~TOP SECRET~~ G

Handle via BYEMAN
Control System Only

~~TOP SECRET~~ GBIF-008- W-C-019838-RI-80

TABLE 2.8-10

RESOLUTION CONTRIBUTORS

<u>Contributor</u>	<u>Launch Dates</u>	
	<u>4/1</u>	<u>9/1</u>
Average Sun Angle (Degrees)	40.90	33.90
Average Slant Range (nmi)	89.30	90.10
Average Image Plane Contrast		
R_{HI}/R_{LO} of 33/7 (Tribar)	2.51	2.63
R_{HI}/R_{LO} of 16/9 (Operational)	1.36	1.39
In-track Smear Rates (μ rad/sec)		
μ_F	74.30	75.10
σ_F	59.00	60.90
0.68σ	64.50	65.70
Cross-track Smear Rates (μ rad/sec)		
μ_F	102.70	101.80
σ_F	76.90	76.90
0.68σ	87.20	86.80

Note: μ_F - mean of folded normal distribution σ_F - standard deviation of folded normal distribution 0.68σ - median of normal distribution

2.8-21

~~TOP SECRET~~ GHandle via BYEMAN
Control System Only

TOP SECRET G

BIF-008 - W-C-019838-RI-80

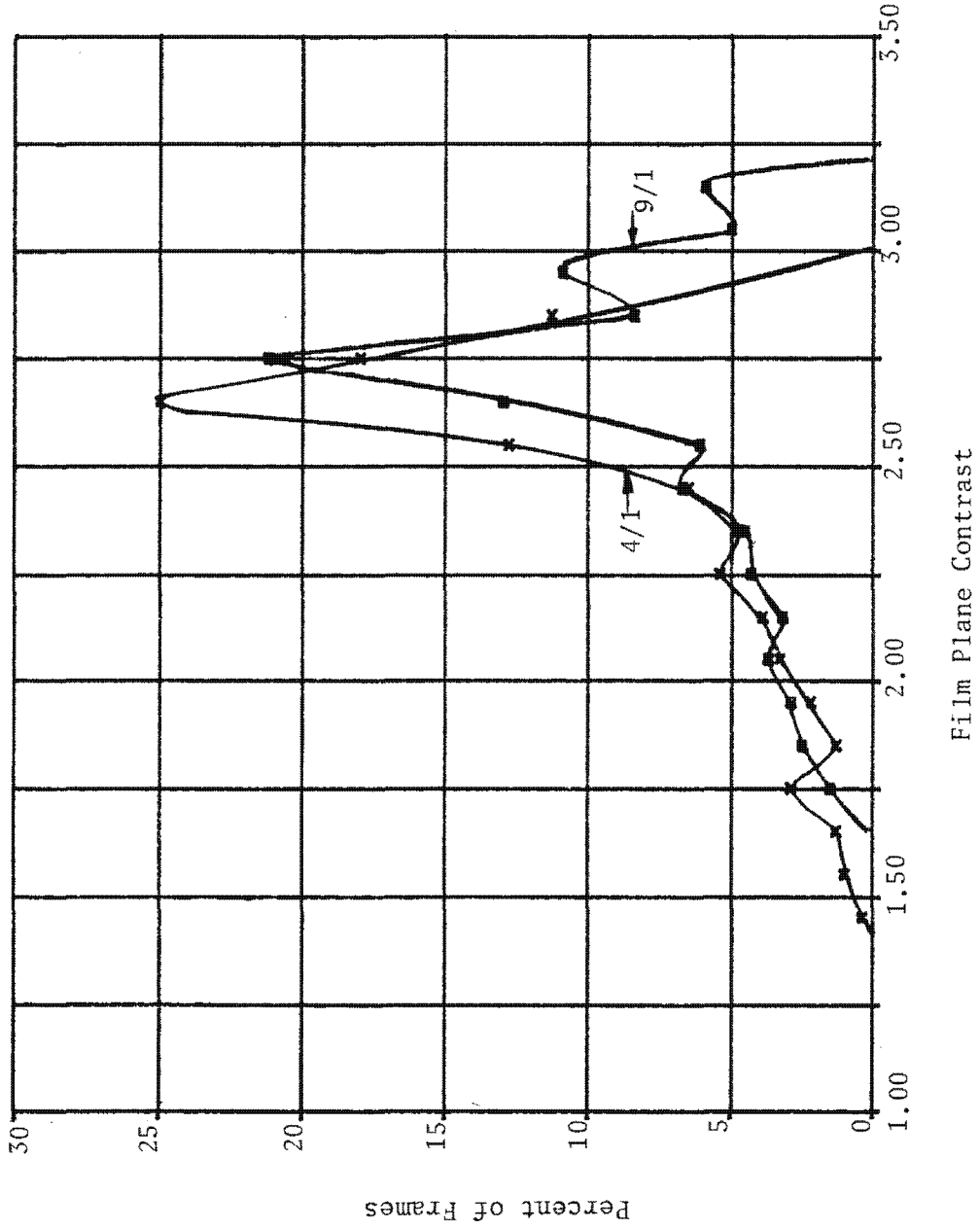


Figure 2.8-5. Contrast Distribution

2.8-22

Handle via **BYEMAN**
Control System Only

TOP SECRET G

~~TOP SECRET~~ GBIF-008- W-C-019838-RI-80

in considerably lower resolution values than are achieved with tribar targets. This also lessens the differences due to sun angle.

Target acquisition is another important factor in performance. Pointing errors are only a minor factor in the loss of useable photography. The major factor is cloud cover. Table 2.8-11 gives an indication of the number of photographs of targets in each priority category that would be acquired without cloud obscuration at least once on the two missions. It is based on the results of the interaction between the film management monitor and the weather model. It shows that, in order to use up the film, over half of the targets acquired must be in the low priority (4-9) groups. The distribution of priorities for targets acquired depends strongly on the mission length, the weather, and the weather threshold policy. Changes in the priority distribution of the targets acquired are one of the main performance related differences in missions of various lengths.

8.7 Equipment Usage Estimates

Table 2.8-12 gives an estimate of the PPS equipment usage for the two missions. The cycles of operation indicate the required orbit lifetimes for the various components. The ON times can be used to determine energy requirements for the equipment. The telemetry includes radar station contact. Because of the shorter average frame length expected for Block 48 operations, the 9-inch camera operations are expected to exceed 19000 cycles, which represents a significant increase over pre-Block 48 usage. The large value for stereo actuations arises from a built-in bias toward stereo pairs and the fact that simultaneous operation of both systems is not modeled.

~~TOP SECRET~~ G

TABLE 2.8-11

NUMBER OF TARGETS WITH A 95% PROBABILITY OF AT LEAST ONE CLEAR ACQUISITION

<u>Priority Category</u>	<u>Launch Date</u>	
	<u>4/1</u>	<u>9/1</u>
0	86	87
1	317	248
2	245	229
3	1549	1496
4	184	164
5	121	121
6	183	122
7	98	84
8	314	272
9	1750	1852
0-3 (Subtotal)	2197	2060
4-9 (Subtotal)	2650	2615
Total	4847	4675

2.8-24

TABLE 2.8-12

EQUIPMENT USAGE SUMMARY

Hardware Component	Launch Date	Cycles Operation		On Time (Hours)	
		<u>4/1</u>	<u>9/1</u>	<u>4/1</u>	<u>9/1</u>
Camera, 9-inch		19545	19635	4.01	4.09
Camera, 5-inch		7388	6795	1.41	1.34
SRC, 9-inch		8955	9128	0.25	0.26
SRC, 5-inch		3330	3053	0.09	0.08
Slit, 9-inch		4275	4260	1.08	1.24
Slit, 5-inch		2205	1965	0.80	0.62
Crab		8723	8565	11.21	10.32
Stereo		23198	22868	16.11	15.88
9/5-inch camera power		1560	1463	143.77	149.75
Telemetry		2700	2603	215.68	221.65

2.8-25

~~TOP SECRET~~ G

BIF-008-W-C-019838-RI-80

8.8 High-Mode Orbit Generation

Two 120-day missions were simulated. Each mission was run for the entire orbital period at a single altitude. Pertinent orbital parameters are shown in Table 2.8-13.

TABLE 2.8-13
ORBITAL PARAMETERS

Orbit Inclination	96.4°
Height of Perigee	350/450 nmi
Eccentricity	Circular
Days Simulated	120
Launch Date	1 May
Launch Time	1830 Z
Closure	4 Days

8.9 Target Acquisition/Selection

The targets available for photography were acquired from the 1214 Standing Search Target file. The following tables describes the Standing Search Target file.

<u>Interval</u>	<u># Cells</u>	<u>Type Photography</u>
2-month	868	Stereo
4-month	5,214	Stereo
6-month	4,571	Stereo
9-month	7,927	Stereo
12-month	17,285	Mono
	<hr/> 35,865	

2.8-26
~~TOP SECRET~~ G

Handle via BYEMAN
Control System Only

~~TOP SECRET~~ GBIF-008- W-C-019838-RI-80

Details of the target selection criteria may be found in the Block 1.0 software description.

Constraints on target selection are shown below. These constraints are essentially identical to the low-mode simulation except for the weather threshold model, total film load considered, and GRD requirement.

Stereo LOS* Angle	±8.65 degrees
In-Track Ephemeris Uncertainty 1σ	0.5 nmi
LOS Pointing Uncertainty	0.0
Clock Granularity	0.2 second
Roll Rate Equation	$\Delta t = \frac{\Delta\Omega}{5.5} + 0.82 - 0.82 e^{-\frac{\Delta\Omega}{0.9 \text{ second}}}$
Stereo Slew Time	3 seconds
Total Film Load	11,800 (SO-112)
Weather Conditions	ETAC Data
Weather Threshold	90%
GRD Maximum	48 inches/450 nmi, 32 inches/350 nmi
Lower Sun Angle Limit	-2 degrees

Figures 2.8-6 through 2.8-9 illustrate the Gambit vehicle's rate of satisfaction of specific area requirements when

- (1) All target requirements are initialized at the zero satisfaction level. This assumes no other search mission for 12 months prior to launch. (Not probable.)
- (2) The target requirements are initialized at satisfaction levels reflecting the aging of cells previously acquired by the primary search vehicle. This assumes no other search mission for 3 months prior to launch. (More probable.)

*Line-of-sight.

2.8-27

~~TOP SECRET~~ GHandle via **BYEMAN**
Control System Only

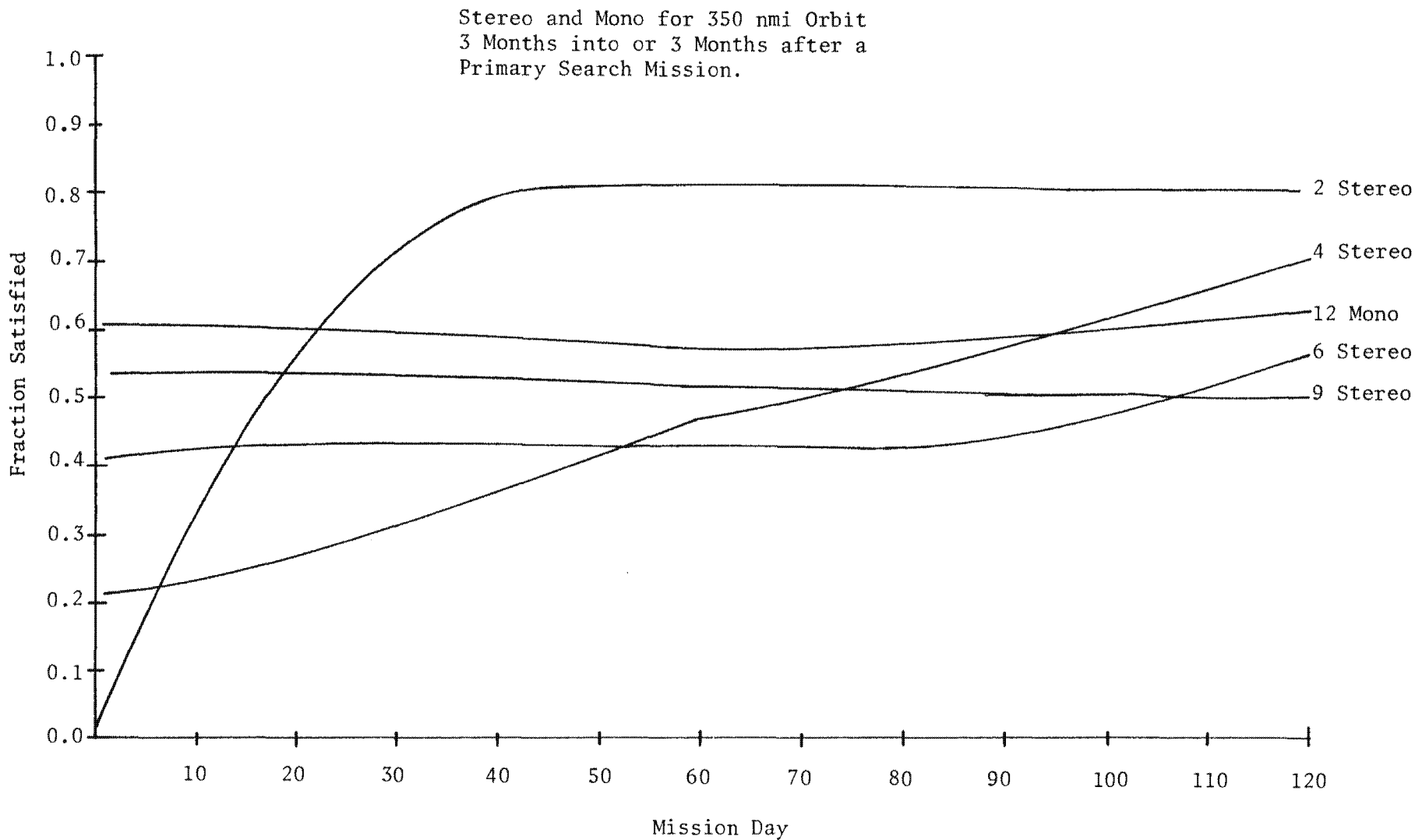


Figure 2.8-6. Gambit Dual Mode Search Satisfaction

Handle via BYEMAN
Control System Only

Approved for Release: 2017/02/14 C05097211

2.8-28

Approved for Release: 2017/02/14 C05097211

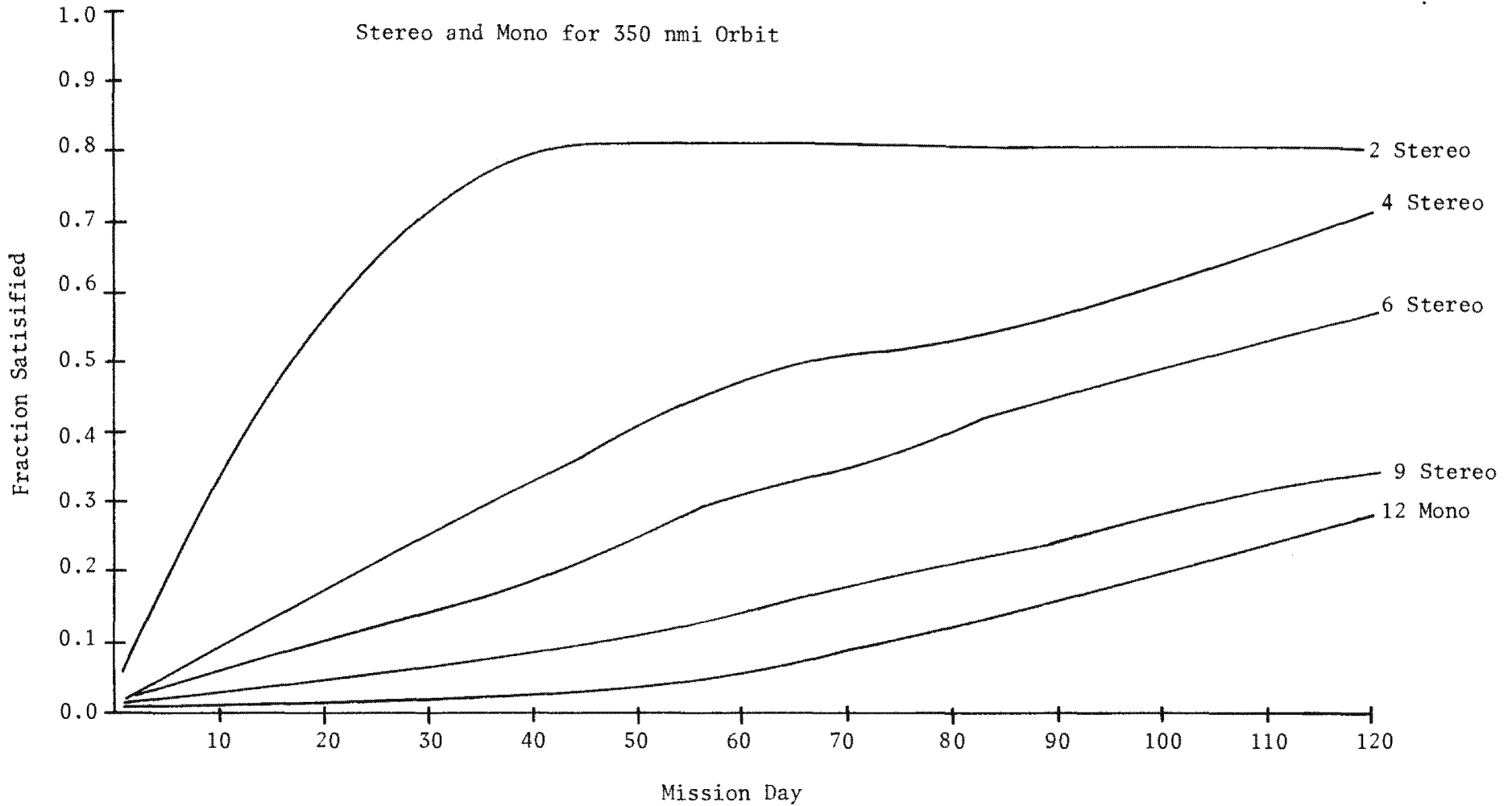


Figure 2.8-7. Gambit Dual Mode Search Accomplishment

Handle via BYEMAN
Control System Only

Approved for Release: 2017/02/14 C05097211

2.8-29

Approved for Release: 2017/02/14 C05097211

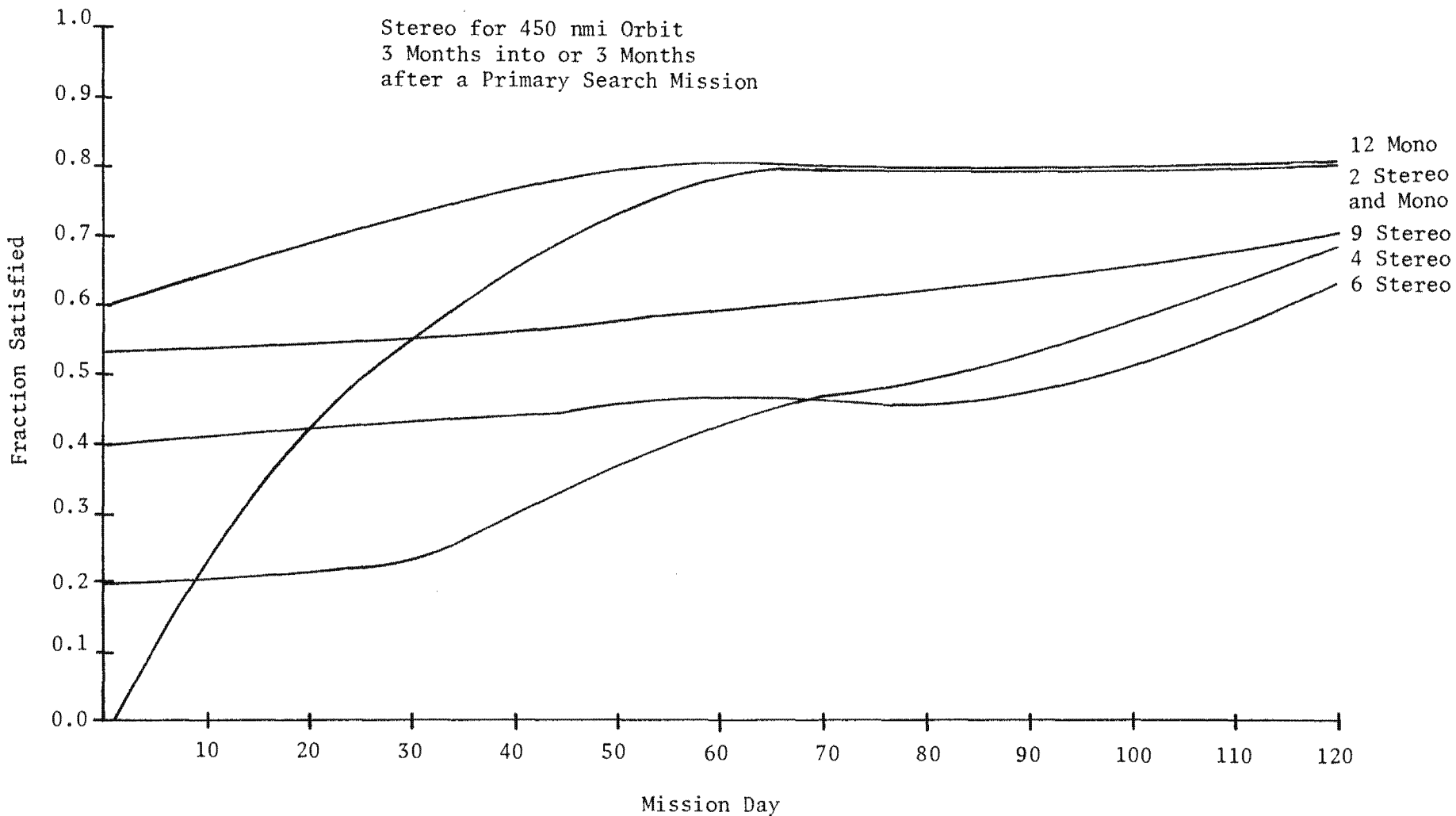


Figure 2.8-8. Gambit Dual Mode Search Satisfaction

Handle via BYEMAN
Core System Only

Approved for Release: 2017/02/14 C05097211

2.8-30

Approved for Release: 2017/02/14 C05097211

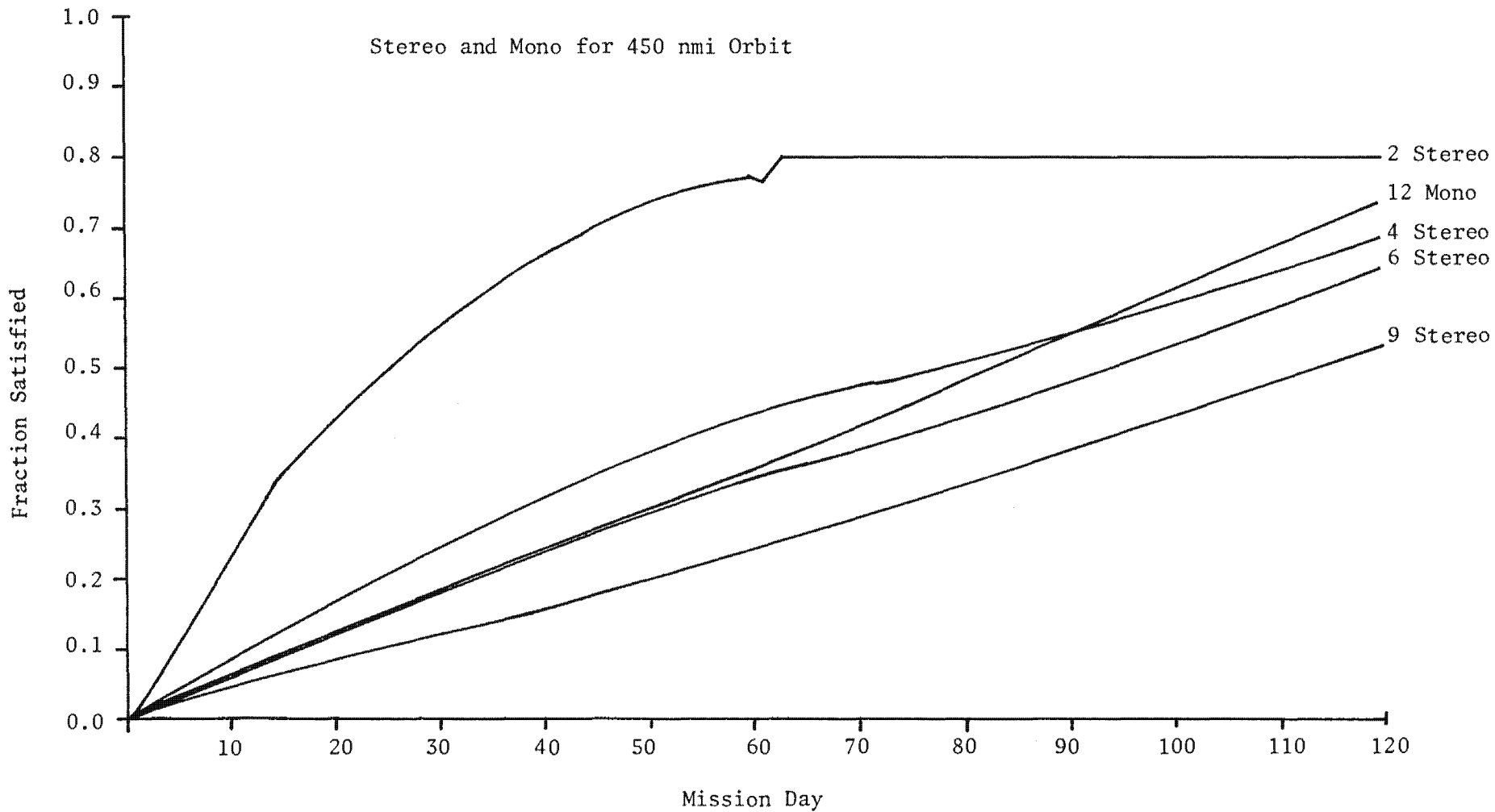


Figure 2.8-9. Gambit Dual Mode Search Accomplishment

Approved for Release: 2017/02/14 C05097211

2.8-31

Approved for Release: 2017/02/14 C05097211

~~TOP SECRET~~ G

BIF-008- W-C-019838-RI-80

In each case, the film usage rate was adjusted such that an equal amount of film was used each day of the mission. It can be seen from the graphs that the Gambit vehicle in most cases meets the targetting strategy of 50 percent satisfaction of each category after 50 percent of the aging requirement has elapsed. Note that 80 percent satisfaction ratio is counted as fully satisfied.

Figure 2.8-10 displays the approximate NIIRS distribution of the two orbit cases that were run.

2.8-32

~~TOP SECRET~~ G

Handle via BYEMAN
Control System Only

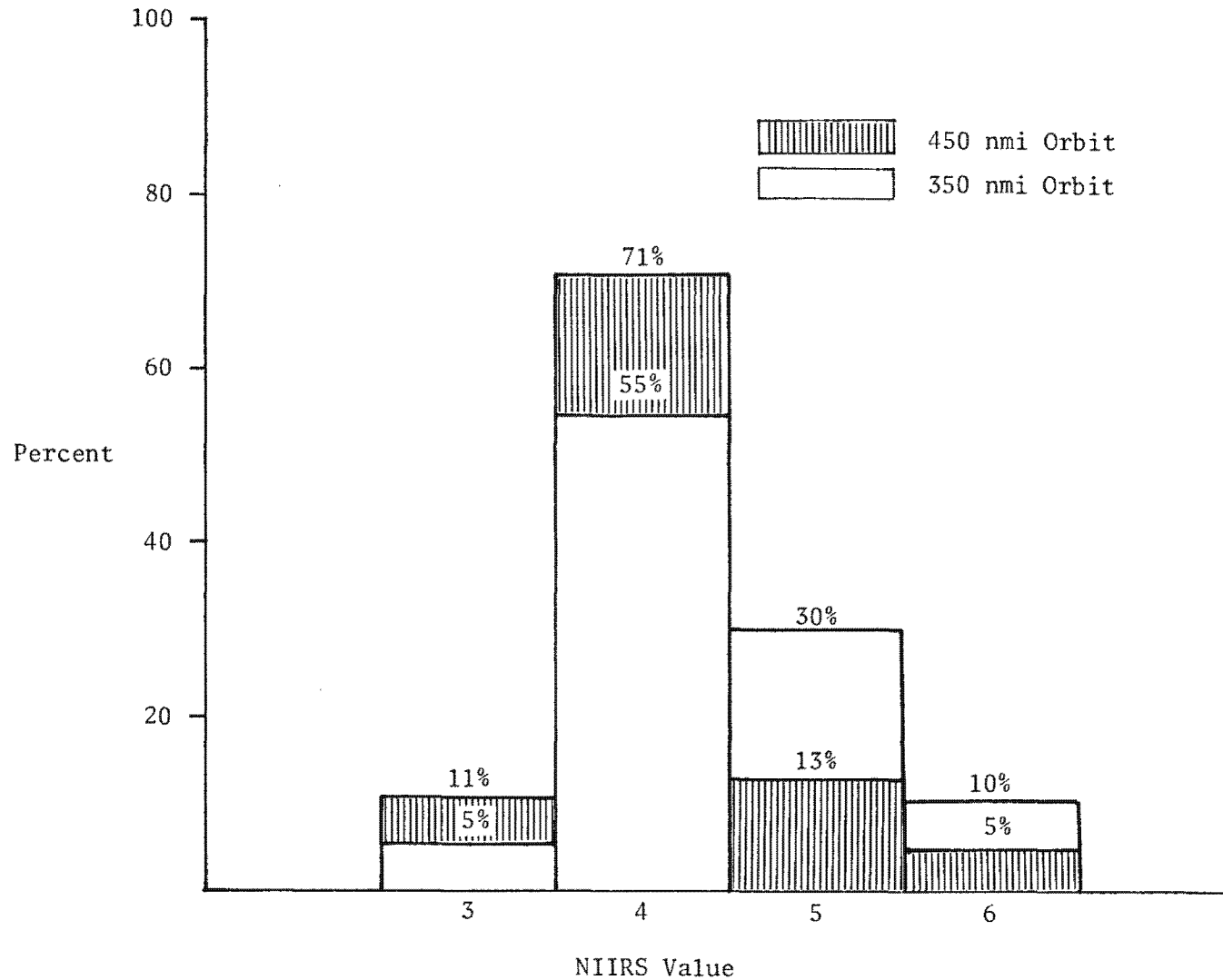


Figure 2.8-10. NIIRS Distribution

Approved for Release: 2017/02/14 C05097211

2.8-33

Approved for Release: 2017/02/14 C05097211

~~TOP SECRET~~ G

BIF-008-W-C-019838-RI-80

This Page Intentionally Blank

2.8-34

~~TOP SECRET~~ G

Handle via **BYEMAN**
Control System Only

~~TOP SECRET~~ GBIF-008- W-C-019838-RI-80

9.0 IMAGE QUALITY EVALUATION

Image quality may be considered to be the degree of excellence of a developed photographic image. The traditional numeric for assessing photographic image quality is limiting resolution, or the size of the smallest distinguishable detail. Because of the very small size of the image details obtained in aerial reconnaissance, and the consequent need to magnify the image to search for important fine detail, it seems intuitively correct that subjective assessment of image quality be highly correlated with limiting resolution. This is true, but it is also important to recognize that resolution is only one aspect (a threshold numeric) of image excellence and therefore does not uniquely define image quality.

Measures which are concerned with the mid-spatial frequencies and which are derivable from certain considerations of information theory correlate better with subjective quality estimates than does the threshold numeric. These newer techniques have the added advantage of not requiring deployment of ground targets for their estimation and are therefore available on any frame. Current understanding does not, however, allow an attachment of significance to the absolute level of these measures, but the relative comparison of frames (Is frame "A" better than frame "B"?) is easily accomplished. These objective measures (determined by power-spectrum analysis machines) are functions, to a greater or lesser extent, of defocus, contrast, smear, exposure level, scene type, etc., all of which will vary frame-to-frame.

2.9-1

~~TOP SECRET~~ GHandle via **BYEMAN**
Control System Only

~~TOP SECRET~~ GBIF-008- W-C-019838-RI-809.1 Limiting Resolution

A value for limiting resolution may be calculated from system parameters before a flight and also may be determined after a flight from examination of selected frames.

9.1.1 Prediction

The prediction of limiting resolution requires specification of a system modulation transfer function (MTF) and a film threshold modulation (TM) curve. The system MTF can be derived from the MTF of the various components by simple multiplication since it is a Fourier-space representation of processes which, in configuration space, must be convolved. For example, the system MTF corresponding to an in-focus optic in the presence of s micrometers of linear smear is:

$$\text{MTF}(\nu) = [\text{MTF}_O(\nu)] [\text{MTF}_S(\nu)]$$

where:

$$\text{MTF}_O(\nu) = \text{in-focus optical MTF}$$

$$\text{MTF}_S(\nu) = \frac{\sin \pi s \nu (10)^{-3}}{\pi s \nu (10)^{-3}} = \text{linear smear MTF}$$

$$\nu = \text{spatial frequency in cycles per mm}$$

$$10^{-3} = \text{conversion of mm to } \mu\text{m}$$

$$s = \text{amount of linear smear in micrometers}$$

The film TM is the minimum modulation required to record information at a given spatial frequency. TM curves are published for various films for an infinite contrast condition. To apply them in any practical situation they must be adjusted for the appropriate contrast (C) as follows:

$$\text{TM}_C(\nu) = \text{TM}_\infty(\nu) \frac{C+1}{C-1}$$

2.9-2

~~TOP SECRET~~ GHandle via **BYEMAN**
Control System Only

~~TOP SECRET~~ GBIF-008- W-C-019838-RI-80

For example, if the contrast is 2:1, $C=2$, and the infinite contrast TM is multiplied at every spatial frequency by 3 to obtain the 2:1 contrast TM curve.

For purposes of prediction, limiting resolution is defined as that spatial frequency corresponding to the intersection of the system MTF and film TM curves. The MTF is interpreted as representing the modulation passed by the system and available as image modulation at the film plane, while the TM curve represents the modulation required by the film in order that the image be just discernible (threshold) at that spatial frequency. The foregoing is represented graphically in Figure 2.9-1 below:

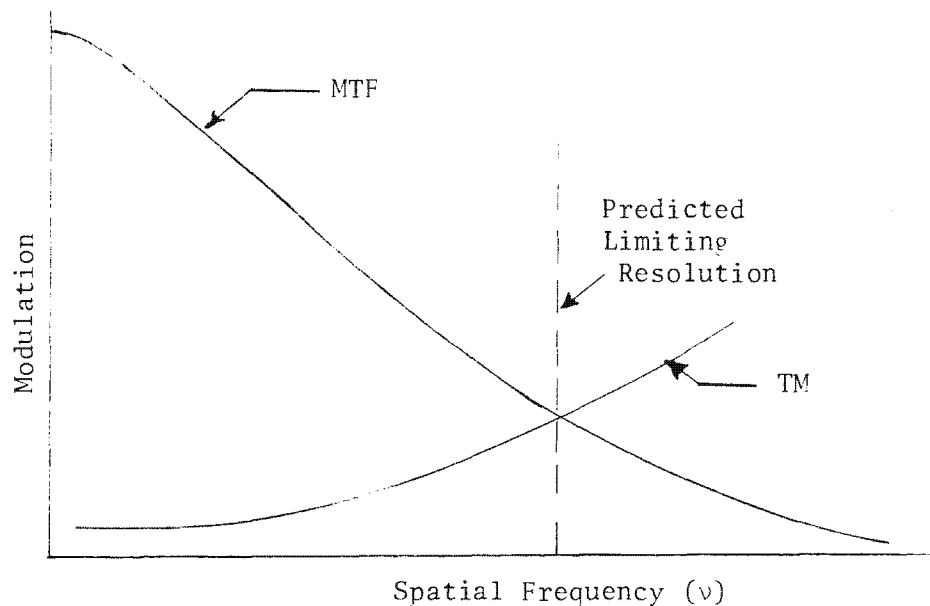


Figure 2.9-1. Limiting Resolution Illustration

2.9-3

~~TOP SECRET~~ G

Handle via BYEMAN
Control System Only

~~TOP SECRET~~ GBIF-008- W-C-019838-RI-80

9.1.2 Measurement

The measurement of limiting resolution is carried out by examination of an operational photograph. The photography to be evaluated must contain a ground-deployed resolution target known as a Controlled Range Network or CORN target. Because of their configuration, these targets are also known as tribar targets. A typical CORN target is illustrated in Figure 2.9-2.

The photographic image of the tribar target is examined under magnification and the smallest set in which the bars and spaces are distinguishable is noted. Knowing the physical size of the limiting tribar set, the limiting ground resolution may be established for the particular acquisition conditions.

9.2 Objective Quality Measures

All measures of objective quality utilize power-spectrum analysis (PSA) machines which provide measurements of power spectral density in the spatial frequency domain. Means have been devised to generate estimates of the image noise present so that specific objective quality measures may be found.

9.2.1 Power Spectral Analysis

Power spectral analysis utilizes elements of electromagnetic theory, Fourier analysis, and solid-state electronics.

9.2.1.1 Electromagnetic Theory. Electromagnetic radiation can be characterized by an electric field vector E and a magnetic field vector H oscillating perpendicular to each other and perpendicular to the direction of motion of the wave as illustrated in Figure 2.9-3.

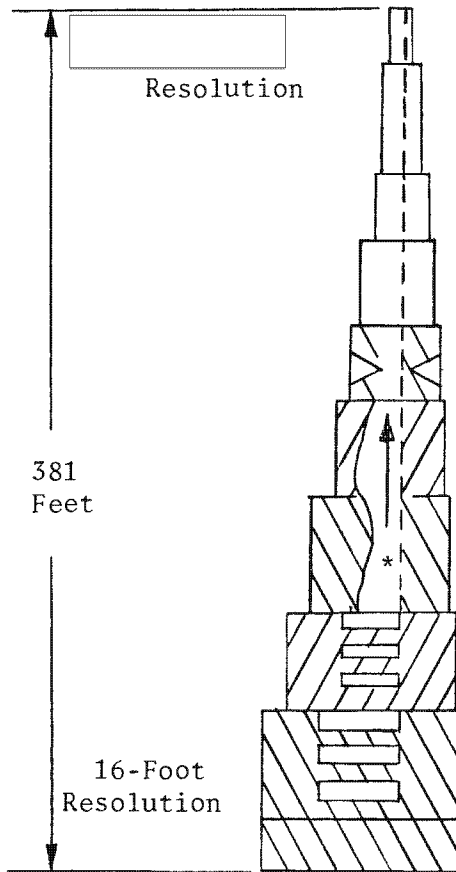
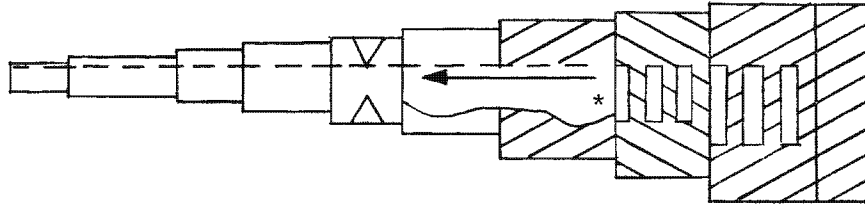
2.9-4

~~TOP SECRET~~ GHandle via BYEMAN
Control System Only

~~TOP SECRET~~ G

BIF-008- W-C-019838-RI-80

Same as other leg.



Panel 9

Legs are perpendicular to each other.

25X1

*Bar and space width decreases by for each group of 3.

Note: A panel may have more than one group.

Figure 2.9-2. Controlled Range Network (CORN) Target

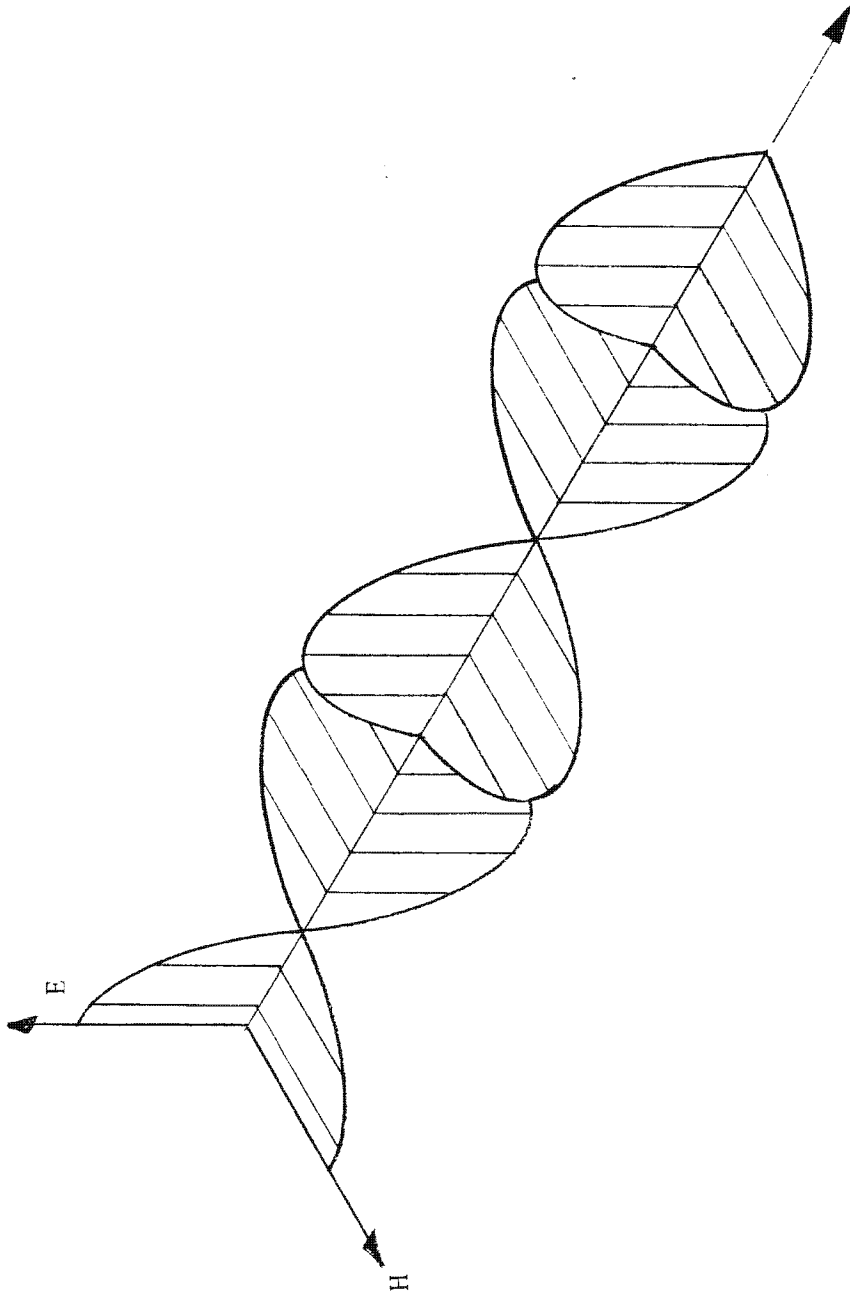
2.9-5

~~TOP SECRET~~ G

Handle via BYEMAN Control System Only

BI F-008 - W-C-019838-RI-80

~~TOP SECRET~~ G



2.9-6

Figure 2.9-3. Electromagnetic Field Vectors

Handle via BYEMAN
Control System Only

~~TOP SECRET~~ G

~~TOP SECRET~~ GBIF-008- W-C-019838-RI-80

A monochromatic (and therefore coherent) electromagnetic wave can be described by the amplitude $A(x,y)$ and phase $\theta(x,y)$ of one of the field vectors:

$$\hat{E} = A(x,y) e^{i\theta(x,y)}$$

where: \hat{E} represents the complex amplitude of the electric field.

9.2.1.2 Fourier Transform. If a photographic transparency of a scene is placed on a light table, the variations in density characteristic of the image present different degrees of opacity to the incoming light. It is this differential light-stopping property which renders the image visible to the eye. A highly simplified version of this situation is shown in Figure 2.9-4 where the "scene" consists of a transparent area in an otherwise opaque screen.

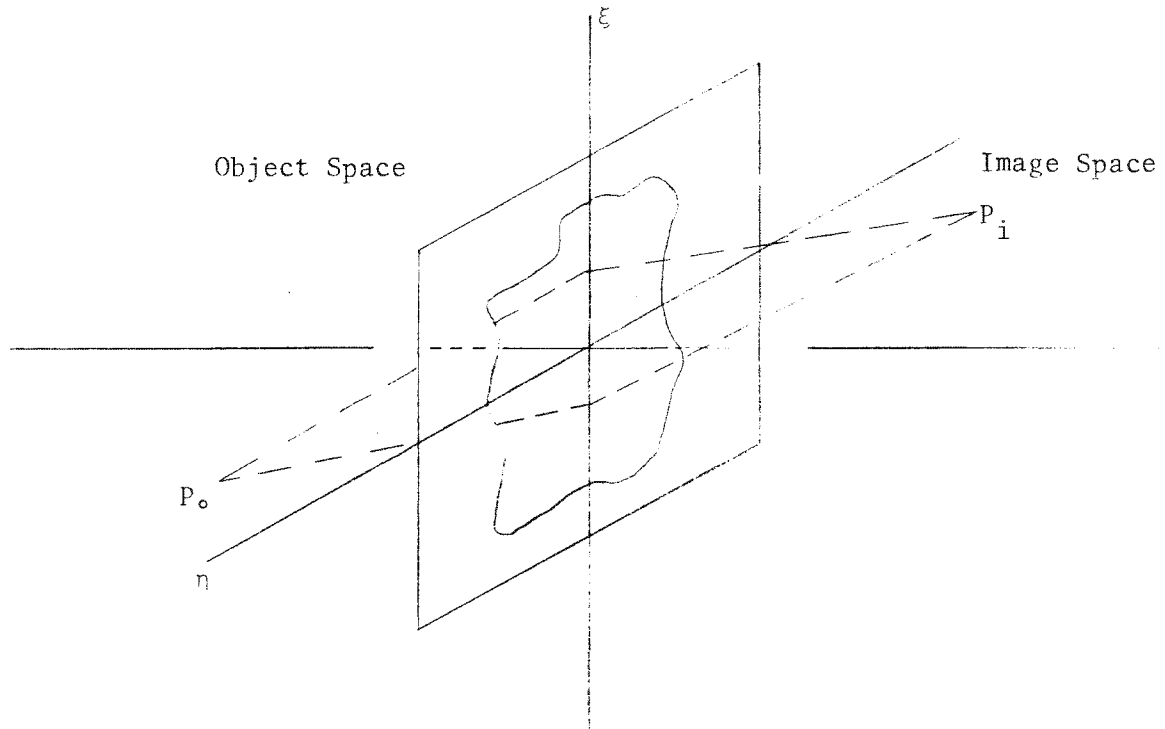


Figure 2.9-4: Simplified Scene Transparency

2.9-7

~~TOP SECRET~~ G

Handle via BYEMAN
Control System Only

~~TOP SECRET~~ GBIF-008- W-C-019838-RI-80

If the screen is now illuminated with coherent light emanating from the point P_0 , the complex amplitude \hat{E}_i associated with a point P_i in image space is found from Fresnel-Kirchoff diffraction theory to have the form (in Fraunhofer approximation):

$$\hat{E}_i(p, q) = C \iint_A e^{-ik(p\xi + q\eta)} d\xi d\eta$$

where p and q are angular coordinates corresponding to the relative positions of P_0 and P_i and k is the wave number $2\pi/\lambda$ of the light. Now a pupil function is defined:

$$\hat{g}(\xi, \eta) = \begin{cases} C & \text{for points within the aperture } A \\ 0 & \text{for points outside the aperture } A \end{cases}$$

Then

$$\hat{E}(p, q) = \iint_{-\infty}^{\infty} \hat{g}(\xi, \eta) e^{-ik(p\xi + q\eta)} d\xi d\eta$$

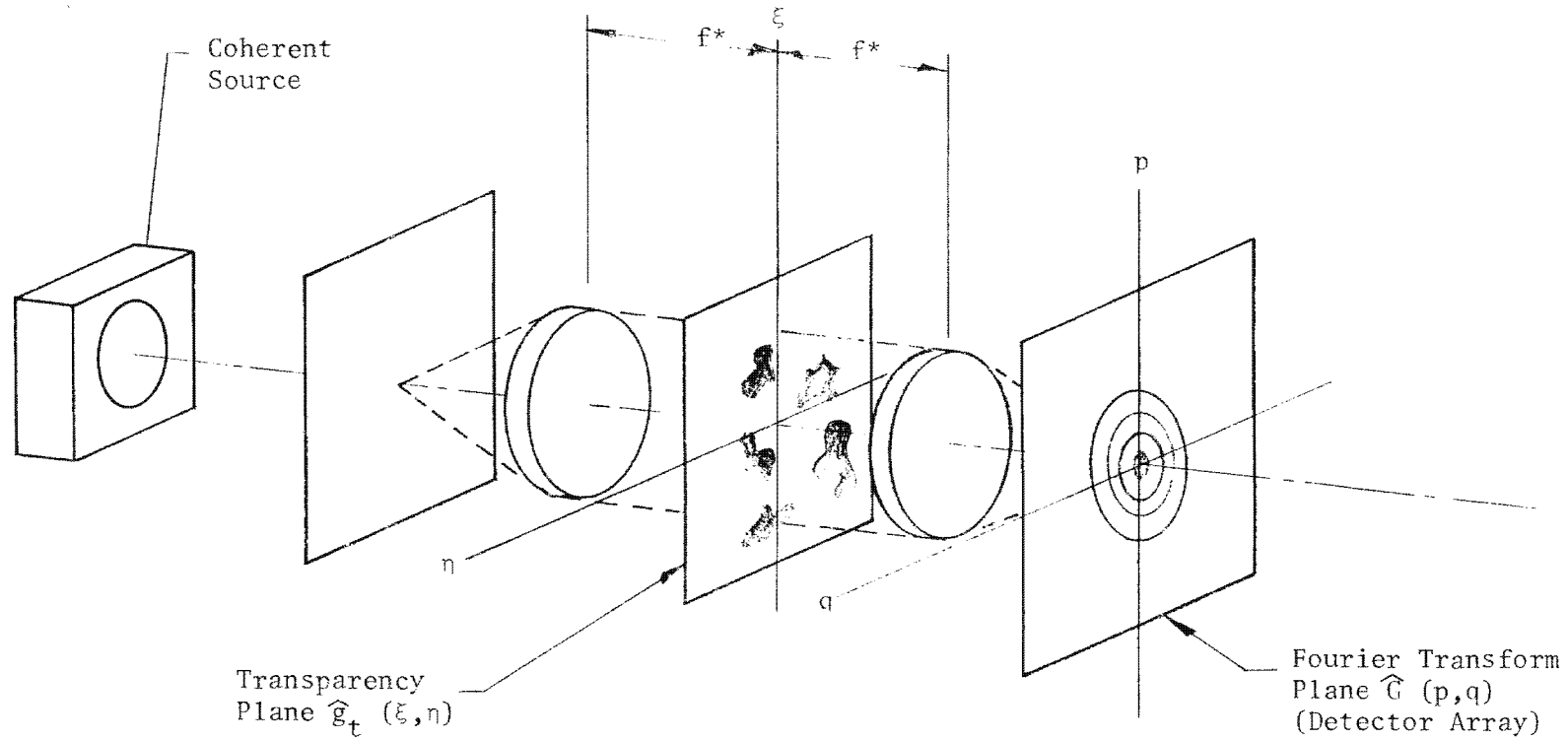
which has the form of a Fourier Transform (FT). If the spatial distribution of the transparency image is described by some function $\hat{g}_t(\xi, \eta)$, the FT of this spatial distribution is given by:

$$\hat{G}(p, q) = \iint_{-\infty}^{\infty} \hat{g}_t(\xi, \eta) e^{-ik(p\xi + q\eta)} d\xi d\eta$$

The basis, then, for all objective measures of image quality lies in the fact that a transparency illuminated with coherent light yields the Fourier Transform of the spatial distribution of the image. Fraunhofer approximation demands, however, that the source (P_0) and image plane (P_i) be infinitely distant from the screen. This is not practical to do directly but is very easy to do optically, as shown in Figure 2.9-5.

If quantities derivable from the transparency Fourier Transform $\hat{G}(p, q)$ are to provide a measure of photographic image quality, the detector in the FT

~~TOP SECRET~~ GHandle via BYEMAN
Control System Only



2.9-9

*An exact Fourier Transform is obtained only if the two lenses are spaced as shown ($f =$ focal length).

Figure 2.9-5. Optically Generated Fourier Transform

Handle via **BYEMAN**
Control System Only

Approved for Release: 2017/02/14 C05097211

Approved for Release: 2017/02/14 C05097211

~~TOP SECRET~~ GBIF-008- W-C-019838-RI-90

plane and its associated electronics must provide an output relatable to film response. Photographic film response (density) is proportional to $\int I dt$, and since intensity (I) is the squared modulus of the complex amplitude, an output is required which is proportional to $\hat{G}^* (p,q) \hat{G} (p,q)$. Power spectral density, given by

$$PSD = \lim_{T \rightarrow \infty} \frac{\hat{G}^* (p,q) \hat{G} (p,q)}{2T} ,$$

satisfies these requirements.

The limit implies that the detector integration time must be long compared to the period of the electromagnetic wave vector oscillations (a very good approximation.)

9.2.1.3 Detector/Electronics. A solid-state detector array is shown in Figure 2.9-6. Note that there are 20 equally spaced annular rings (counting the central spot as ring number 1). If the dimensions are such that the width of each ring spans 10 cpmm of spatial frequency, then

Ring or Band	1	=	0-10 cpmm
	2	=	10-20 cpmm
	3	=	20-30 cpmm
	.	.	
	.	.	
	.	.	
	20	=	190-200 cpmm

All rings are of equal width which results in an area weighting effect; the farther a ring is from the central band (which measures the undiffracted power or dc power), the larger its area and hence the more weight attached to power diffracted into it.

2.9-10

~~TOP SECRET~~ GHandle via BYEMAN
Control System Only

~~TOP SECRET~~ G

BIF-008- W-C-019838-RI-80

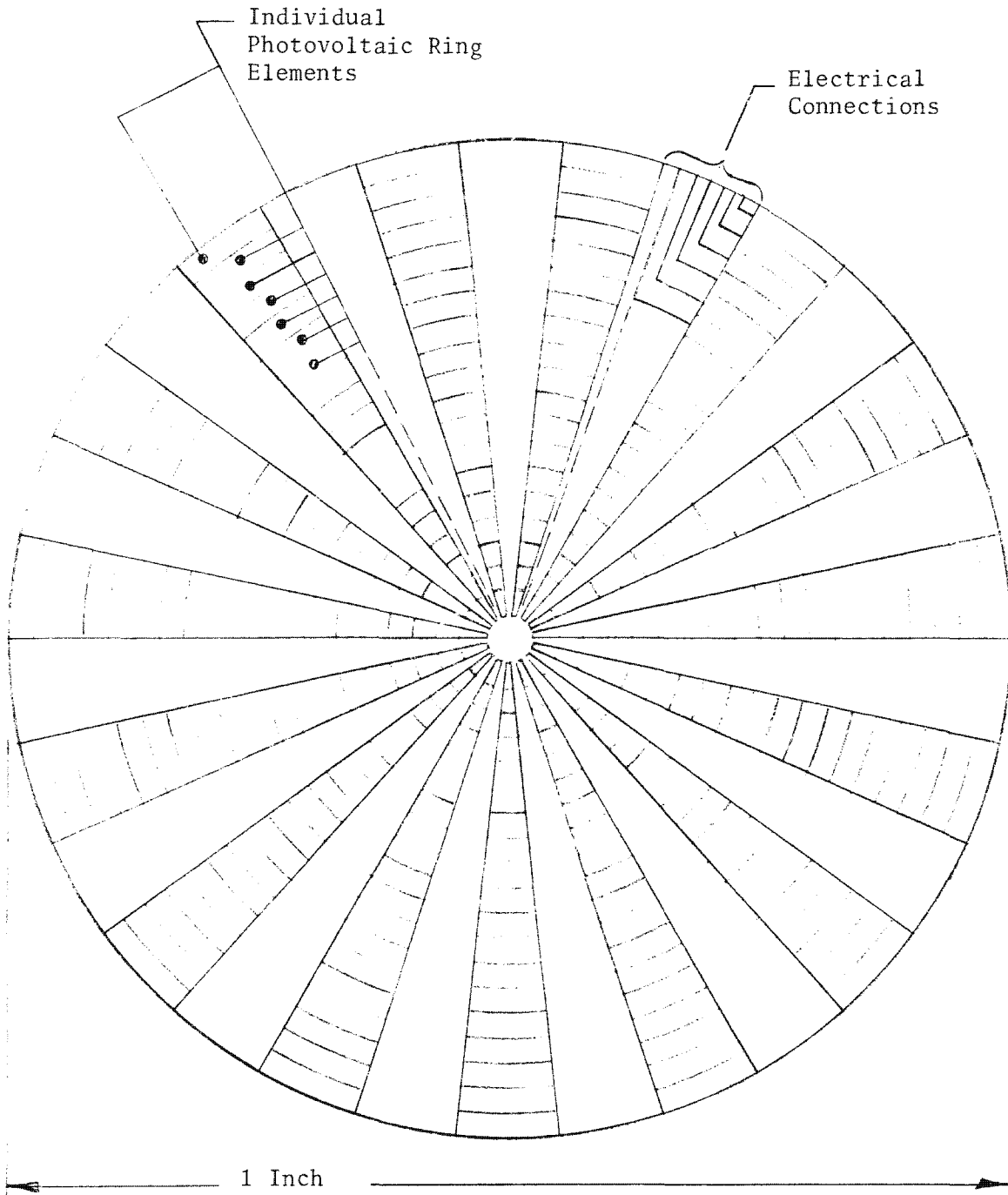


Figure 2.9-6. Solid-State Detector For PSD Analysis

2.9-11

~~TOP SECRET~~ G

Handle via **BYEMAN**
Control System Only

~~TOP SECRET~~ GBIF-008- W-C-019838-RI-80

9.2.2 Image Noise

Noise present in the image is of two types: grain noise and phase noise.

9.2.2.1 Grain Noise. The grain noise power spectral density, $PSD_{NG}(\nu)$, is measured as a function of spatial frequency, ν , by scanning a uniformly exposed ("flat patch") film sample with the optical power spectrum analysis (PSA) machine. Since granularity is not independent of density however, $PSD_{NG}(\nu)$ is a function of the mean density of the patch and therefore the grain noise dependence on spatial frequency is required over a range of densities.

9.2.2.2 Phase Noise. Phase noise arises because the phase relationship between different parts of a coherent beam are not random. Noise contributors associated with the coherence of the illuminating source are surface noise and relief image noise (associated with image depth within the emulsion). Because light experiences a phase change on reflection, irregularities in the emulsion surface (scratches, and the fact that the emulsion surface is actually somewhat rippled) cause phase differences to appear in the reflected beam which interfere, both constructively and destructively, with the incoming light. Similarly, as the beam proceeds into the emulsion itself, areas of varying density (peculiar to the image of the scene) act as "surfaces" from which reflections and the consequent phase interferences result.

These phase effects produce scene-correlated noise, the presence of which prevents a general theoretical description of the process. Furthermore, they significantly affect the noise in every practical application of PSA. One technique for estimating the phase noise contribution to the total noise utilizes the grain noise power spectrum, $PSD_{NG}(\nu)$, just described. Experience has shown that the total signal plus noise power spectrum, $PSD_{S+N}(\nu)$, is

2.9-12

~~TOP SECRET~~ GHandle via BYEMAN
Control System Only

~~TOP SECRET~~ GBIF-008- W-C-019838-RI-80

devoid of scene specific information by band number 11 (100-110 cpmm)* for virtually all Gambit photographs. This means that for the spatial frequency range beyond 105 cpmm (the middle of band number 11), $PSD_{S+N}(\nu)$ equals $PSD_N(\nu)$ where $PSD_N(\nu)$ is the total PSD noise (phase + grain). An estimate of the phase noise ($PSD_{NP}(\nu)$) contribution at frequencies below 105 cpmm is determined by extrapolating the difference between $PSD_{S+N}(\nu)$ and $PSD_{NG}(\nu)$ in the region from 105 cpmm to 195 cpmm (see Figure 2.9-7) back to zero (phase noise is known to increase as spatial frequency decreases). The total noise ($PSD_N(\nu)$) used at all frequencies is then $PSD_{NG}(\nu) + PSD_{NP}(\nu)$.

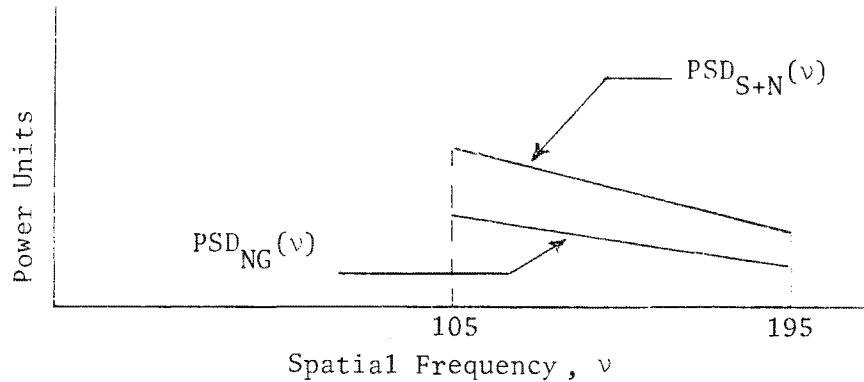


Figure 2.9-7. Estimation Of Phase Noise

*These spatial frequencies have no relationship to those associated with limiting tribar resolution.

~~TOP SECRET~~ G

~~TOP SECRET~~ GBIF-008- W-C-019838-RI-80

9.2.3 Specific Quality Measures

There are several image quality numerics which are derived from the PSD distribution.

9.2.3.1 LOCMO. LOCMO is the local first moment of the PSD distribution defined mathematically as:

$$\text{LOCMO} = \sum_{\nu = 30}^{70} \nu \text{PSD}_{\text{S+N}}(\nu)$$

where: $\text{PSD}_{\text{S+N}}$ is power spectral density of signal plus noise (both grain and phase)

Note that LOCMO is not corrected for noise; the total scene plus noise (PSD), as measured, is used in its definition. LOCMO is, therefore, a useful measure when examining different film types where relative noise characteristics are not certain. It is also appropriate when examining images on a single film type when only relative quality measure is desired. A typical LOCMO calculation is illustrated in Figure 2.9-8.

9.2.3.2 Information Theory. It can be shown that the information content of a photographic image in bits can be written as a function of PSD as:

$$I(\nu_{\text{max}}) = 2 Ak \int_0^{\nu_{\text{max}}} \log_2 \left[\frac{\text{PSD}_{\text{S+N}}(\nu_x, \nu_y)}{\text{PSD}_{\text{N}}(\nu_x, \nu_y)} \right] d\nu_x, d\nu_y$$

where: A = the area of the scanning aperture
 k = normalization constant
 (information is usually normalized so that the height of the dc peak is 100 bits.)

2.9-14

~~TOP SECRET~~ GHandle via **BYEMAN**
Control System Only

~~TOP SECRET~~ G

BIF-008- W-C-019838-RI-80

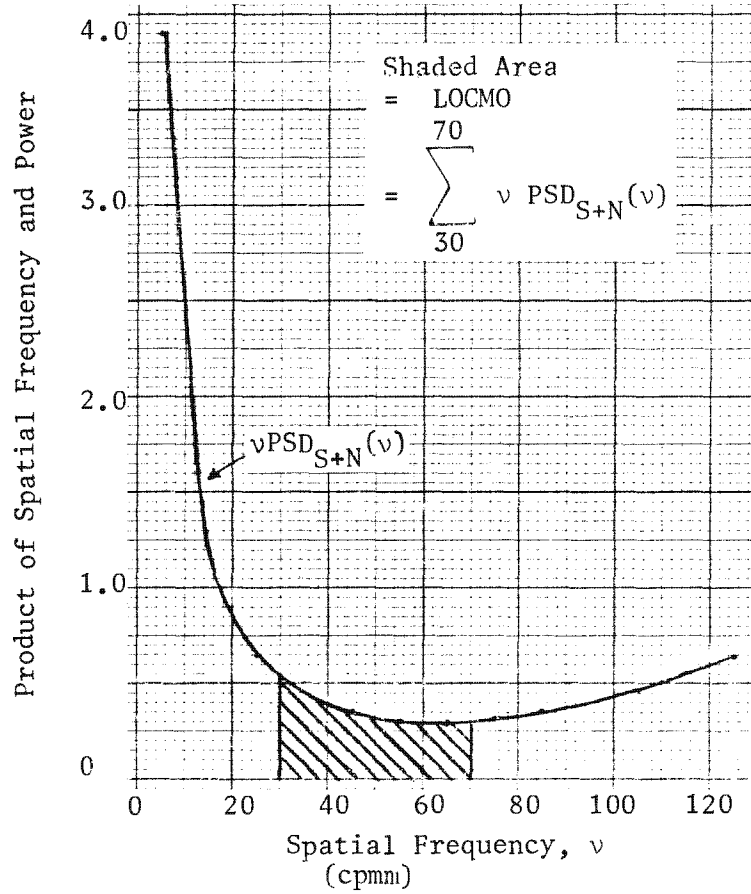


Figure 2.9-8. LOCMO

2.9-15

~~TOP SECRET~~ G

Handle via **BYEMAN**
Control System Only

~~TOP SECRET~~ GBIF-008- W-C-019838-RI-80

If the assumption is made that the aperture is filled with random scene edges so that the imagery is isotropic, then $dv_x dv_y = v dv d\theta$ and the integration can be performed over θ :

$$I(v_{\max}) = 4\pi Ak \int_0^{v_{\max}} \log_2 \left[\frac{\text{PSD}_{S+N}(v)}{\text{PSD}_N(v)} \right] v dv$$

If the further assumption is made that the noise is Gaussian uncorrelated so that

$$\text{PSD}_{S+N} = \text{PSD}_S + \text{PSD}_N,$$

the integral may be rewritten as

$$I(v_{\max}) = 4\pi Ak \int_0^{v_{\max}} \log_2 \left[1 + \frac{\text{PSD}_S(v)}{\text{PSD}_N(v)} \right] v dv.$$

This latter assumption is known to be not strictly true, but it is necessary in order to write $I(v_{\max})$ in terms of the PSD signal-to-noise ratio. Furthermore, in practical cases, the estimate of phase noise makes use of the same assumption (see Section 9.2.2.2).

Figure 2.9-9 shows a display of information content as a function of spatial frequency obtained by analyzing the 10-cpmm spatial frequency bands corresponding to the detector rings (see Figure 2.9-6). Note the peak in the normalized ($I(v_{\max})$) function occurring in band 4. A curve fitted to the normalized information peaks in bands adjacent to band 4 provides the location of the band of peak information (or BPI). BPI is thus dependent on the information contained in bands covering a wide spatial frequency range.

2.9-16

~~TOP SECRET~~ GHandle via BYEMAN
Control System Only

~~TOP SECRET~~ G

BIF-008- W-C-019838-RI-80

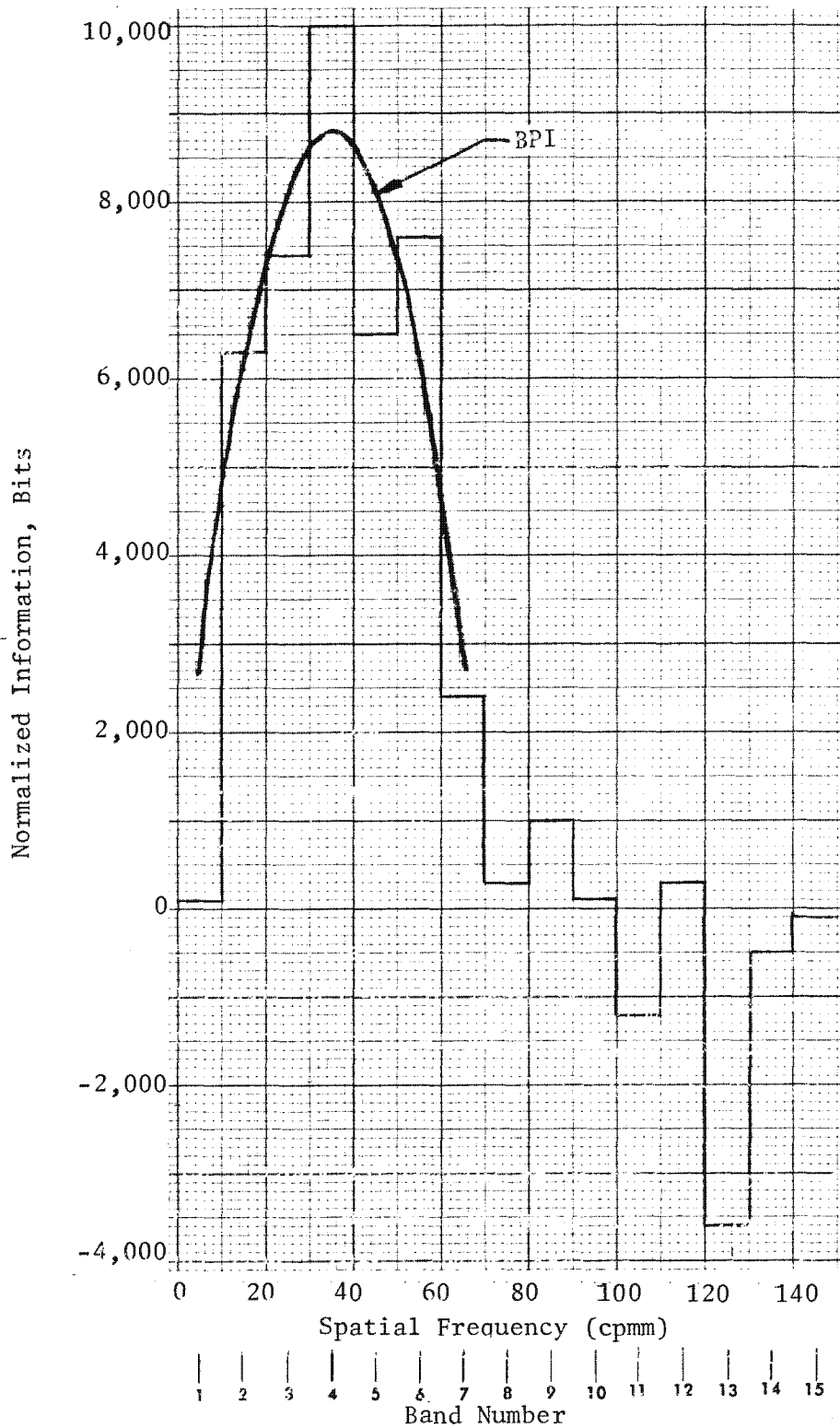


Figure 2.9-9. Information Content And BPI

2.9-17

~~TOP SECRET~~ G

Handle via BYEMAN
Control System Only

~~TOP SECRET~~ GBIF-008- W-C-019838-RI-80

Information density, another useful quality measure, is the area under the normalized information curve over the same frequency range as LOCMO.

The spatial frequency range chosen for LOCMO and information density calculations gives precedence to the higher frequency information (up to the cut-off where signal = noise) as being more indicative of image quality. Better image quality means sharper edges and better detail rendition, both of which serve to diffract the coherent laser light through larger angles (into the outer higher frequency rings of the detector). This is why the LOCMO and information density ranges were chosen as they were and why it is that given two frames, the one with the higher BPI will prove to be subjectively preferred.

9.2.4 Reliability of Quality Measures

For highest reliability when using PSD derived quality measures, certain ground rules must be observed. These include the following.

- (1) All measurements should be taken from original negative material.
- (2) Caution must be exercised when comparing results for different films as uncertainties in the noise estimates are aggravated when film type is changed.
- (3) The machine aperture must be filled with random scene edges so that the scene isotropy assumption is valid.
- (4) In a series of measurements which together lead to an estimate of a system parameter (such as defocus), all measurements should be as nearly alike as possible (i.e., same film type, field position, obliquity, etc.).

~~TOP SECRET~~ GHandle via BYEMAN
Control System Only

~~TOP SECRET~~ GBIF-008- W-C-019838-RI-80

9.3 National Imagery Interpretability Rating Scale (NIIRS)

The National Imagery Interpretability Rating Scale (NIIRS) developed from the need within the intelligence community for a uniform method of rating and specifying photographic quality. At present NIIRS is the only rating scheme which numerically ranks the exploitation suitability of reconnaissance imagery.

9.3.1 Construction of the Rating Scale

One obvious numeric to use as a rating scale would be ground resolved distance, or GRD. This is not practical since measurement of GRD requires that a tribar target be in the frame. Ground resolution (a subjective estimate made without tribars) is possible but the standard scale, based on the appearance of automobiles, is not appropriate to technical intelligence targets.

It was decided to construct a pseudo ground resolution scale like the auto scale but appropriate to technical intelligence objects. Such a scale is best constructed by requiring the photo-interpreter to answer a sequence of very precisely formulated questions about the target. (The sequence proceeds from questions of discernment to recognition and finally to identification.) Such a procedure necessarily demands a set of questions for each order of battle (ground forces, aircraft, missile, electronic, naval, etc). The questions (or criteria, as they are called) within each group or NIIRS category generally refer to ground objects of nearly the same size.

9.3.2 Design Objectives

The selection of questions which refer to ground objects of essentially the same size is designed to provide a good correlation between NIIRS and GRD. This has, in general, been achieved. A further design objective of the NIIRS, that of being system-independent, apparently has not been achieved as yet.

2.9-19

~~TOP SECRET~~ GHandle via **BYEMAN**
Control System Only

~~TOP SECRET~~ GBIF-008- W-C-019838-RI-809.4 Data Tracks As User Aids

The vehicle clock time is encoded on both 9-inch and 5-inch film as a permanent, unambiguous record of when a given frame was exposed. The precise time at which a target within a frame was exposed may also be determined.

9.4.1 Data Track Decoding

Two data tracks, A and B, provide timing information on the film as described in Part 3, Sections 2.2.2.2.3.1 and 2.5.4.2.4.

Each data track consists of a continuous 500 hertz pulse train interrupted at 200-millisecond intervals with a code word representing vehicle clock time. Each time word consists of 25 pulses, the first of which is a sync pulse. Location of the sync pulse corresponds to the time of the associated time word. As seen on the film, the absence of a pulse signifies a binary bit "1" and the presence of a pulse signifies a binary bit "0". Data tracks A and B are identical but are offset in-track on the film. When viewing the film from head to tail, the sync bit is represented by the first missing pulse. The next 24 pulses represent the vehicle clock time word. (Least Significant Bit toward the head and Most Significant Bit toward the tail.) Refer to Figure 2.9-10.

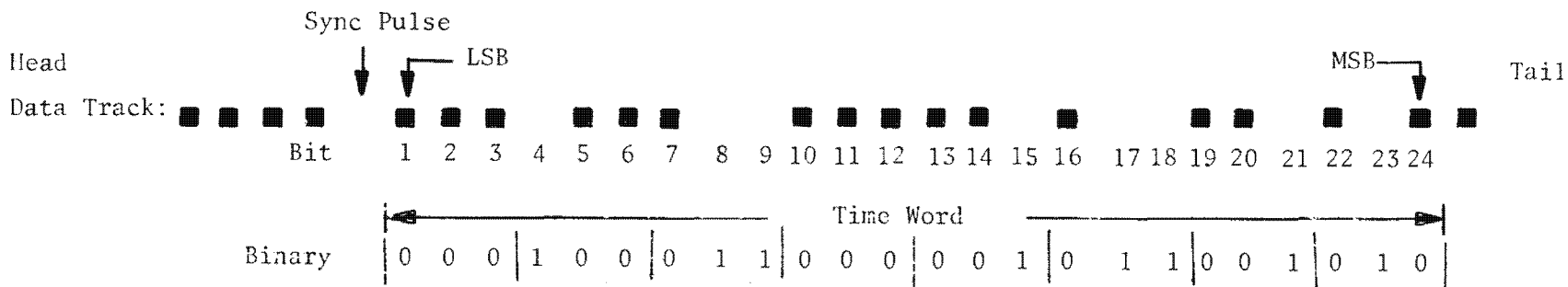
9.4.2 Decoding Procedure

There are four different time conventions which may be encountered:

- (a) Vehicle Clock - This is the 24-bit clock register which is recorded on the film data tracks. Each binary count is 0.2 second and the register recycles after 3355443.0_{10} seconds (38.8 days).
- (b) ECS or Vehicle Time (V/T) - The first 22 bits of the vehicle clock are used by the Extended Command System (ECS) for command control functions. Each binary count is 0.2

2.9-20

~~TOP SECRET~~ GHandle via **BYEMAN**
Control System Only



Example 1

Octal: | 0 | 1 | 6 | 0 | 4 | 6 | 4 | 2 |

MCD Octal Time: 24640610

Octal: | 0 | 1 | 6 | 0 | 4 | 6 | 4 | 0* |

*Always 0 or 1 because bits 23 and 24 are not used.

Conversion: 8^0 8^1 8^2 8^3 8^4 8^5 8^6 8^7

 1261960

Clock Granularity = 0.2

Vehicle Time: 1261960 x 0.2 = 252392.0

Figure 2.9-10. Time Word Decoding

Approved for Release: 2017/02/14 C05097211

2.9-21

Approved for Release: 2017/02/14 C05097211

~~TOP SECRET~~ GBIF-008- W-C-019838-RI-80

second and the register recycles after 838860.6₁₀ seconds (9.7 days). It is Vehicle Time expressed in decimal which is reported in the Chronological Command List (Chrono) and the Mission History Display (MHD).

- (c) System Time - The system time does not appear on the film. System time is Greenwich Mean Time (GMT) expressed in seconds. System time recycles daily after 86400.0 seconds. System time is listed in the Chrono, the MHD and the Mission Correlation Data (MCD)* listings. The Chrono and the MHD also list the Vehicle Time, enabling the relation between Vehicle Time and System Time to be established. Since the vehicle clock is accurate to within one part in 10⁶, the V/T to System Time relationship does not change rapidly.
- (d) Mission Correlation Display (MCD) Octal - The MCD listing contains the 24 bits of the vehicle clock expressed in octal to facilitate simple, rapid correlation with the 24 binary pulses printed on the film data tracks. Data tracks read in three-bit groups can be easily converted to the MCD octal form as shown in Figure 2.9-10.

9.4.2.1 MCD Octal Time

- (a) Record all 24 bits of the time word.
- (b) Divide these into 8 groups of 3 bits.
- (c) Convert each group of 3 bits to a single octal digit. (Bit significance is 1, 2 and 4 from left to right.)
- (d) Reverse the resultant octal number. This is the MCD Octal time.

*MCD = Mission Correlation Data - a computer output providing vehicle parameters for all frames.

2.9-22

~~TOP SECRET~~ GHandle via BYEMAN
Control System Only

~~TOP SECRET G~~

BIF-008-W-C-019838-RI-80

9.4.2.2 Vehicle Time. To convert a time word to vehicle time, proceed as follows:

- (a) Record all of the first 24 bits of the time word.
- (b) Divide these into 8 groups of 3 bits. (Set bits 23 and 24 to zero since they are not used for V/T.)
- (c) Convert each group of 3 bits to a single octal digit. (Bit significance is 1, 2 and 4 from left to right.)
- (d) Multiply each of the 8 octal digits times the corresponding decimal significance as defined thusly:

$$8^0 \mid 8^1 \mid 8^2 \mid 8^3 \mid 8^4 \mid 8^5 \mid 8^6 \mid 8^7, \text{ i.e.,}$$

$$1 \mid 8 \mid 64 \mid 512 \mid 4096 \mid 32768 \mid 262144 \mid 2097152$$

- (e) Add the products from step d) and multiply the sum times the clock granularity (0.2). The result is V/T. See Figure 2.9-10 for an example.

2.9-23

~~TOP SECRET G~~Handle via BYEMAN
Control System Only

~~TOP SECRET~~ G

BIF-008-W-C-019838-RI-80

This Page Intentionally Blank

2.9-24

~~TOP SECRET~~ G

Handle via BYEMAN
Control System Only

~~TOP SECRET~~ GBIF-008- W-C-019838-RI-80

10.0 OPERATIONAL ENVELOPE

The following paragraphs describe limiting values for various operational parameters for both Surveillance and Search missions. In some cases, requirements encompass a broader range than is generally encountered during a mission. For these parameters, values for typical Surveillance and Search missions are shown.

10.1 Launch, Orbit and Recovery Limits

Table 2.10-1 shows launch, orbit and recovery information, including system requirement and typical values for Surveillance and Search mission.

10.2 Photographic Limits

The photographic range is defined as the altitude at which in-focus photographs can be obtained with the correct drive speed. The PPS/DP EAC operating altitude is 68 to 470 nmi. The presence of the secondary recording system has no degrading effect on the primary recording system.

10.2.1 Timing Constraints

25X1

10.2.1.1 Stereo Mode. The design of the PPS/DP EAC is optimized for the execution of high-resolution stereo photography. A stereo pair consists of two frames covering the same target from different look angles. (See Figure 2.10-1) A frame includes not only the high resolution photography but also the film used during the starting and stopping transients (maximum of 0.15 second each). During the time it takes to rotate the stereo mirror from the forward to aft

2.10-1

~~TOP SECRET~~ GHandle via BYEMAN
Control System Only

TABLE 2.10-1
LAUNCH, ORBIT, AND RECOVERY INFORMATION

Parameter	Requirement	Typical Surveillance	Typical Search
Launch Site	Space Launch Complex - 4 - West (SCL-4-W)	--	--
Launch Azimuth	172 to 187 Degrees	--	--
Launch Window	Any Nominal Time \pm 1 Hour Given 3 Days Advance Notice(1)	--	--
Altitude Range On-Orbit	68 - 470 nmi	75 - 200 nmi	450 - 470 nmi
Altitude Range for Photography	68 - 470 nmi	75 - 200 nmi	450 - 470 nmi
Direction of Travel During Photography	Northbound or Southbound	Southbound	Southbound
Inclination	82 - 120 Degrees	96.4 Degrees (2)	98.75 Degrees (2)
Eccentricity	0.00128 to 0.0525	0.0185	0.00192
Beta Angle Range	\pm 40 Degrees	\pm 6 Degrees (3)	\pm 6 Degrees (3)
Perigee Altitude	68 - 460 nmi	75 nmi	455 nmi
Apogee Altitude	175 - 470 nmi	200 nmi	470 nmi
Orbital Flight Attitude			
Nose Forward	Continuous		
Nose Aft	3 Consecutive Revs		
Inertial	1 Revolution		
Tumbling (4)	3 Consecutive Revs	DOES NOT OCCUR	
Mission Duration	120 Days	40 Days (5)	80 Days (5)
Recovery Site	Between 18° and 24° N 147° and 170° W	--	-- (6)
Recovery Method	Northbound or Southbound Air Snatch by Day; Water Snatch by Night	Southbound Air Snatch by Day	Southbound Air Snatch by Day

(1) Assumes that the PPS/DP EAC is at SLC-4-W.
(2) Inclinations shown are for a full mission. For missions involving an altitude change, an intermediate inclination near 97.5 is probable.
(3) Assumes 40 days at 75 - 200 nmi followed by 80 days at 450 nmi circular; launch time chosen to optimize initial beta.
(4) Damage may result if photographic operations are commanded during a tumbling episode.
(5) For a combined mission, either portion may have a duration of up to 120 days.
(6) "Footprint" may be expanded for recovery from high altitude.

2.10-2
2-01.3

Approved for Release: 2017/02/14 C05097211

Approved for Release: 2017/02/14 C05097211

- T₀ = Camera ON
- T₁ = Film movement begins
- T₂ = High-resolution
- T₃ = Camera OFF
- T₄ = Film stopped
- T₅ = Camera ON
- T₆ = Film movement begins
- T₇ = High-resolution
- T₈ = Camera OFF
- T₉ = Film stopped
- T₆ - T₄ = Interframe time

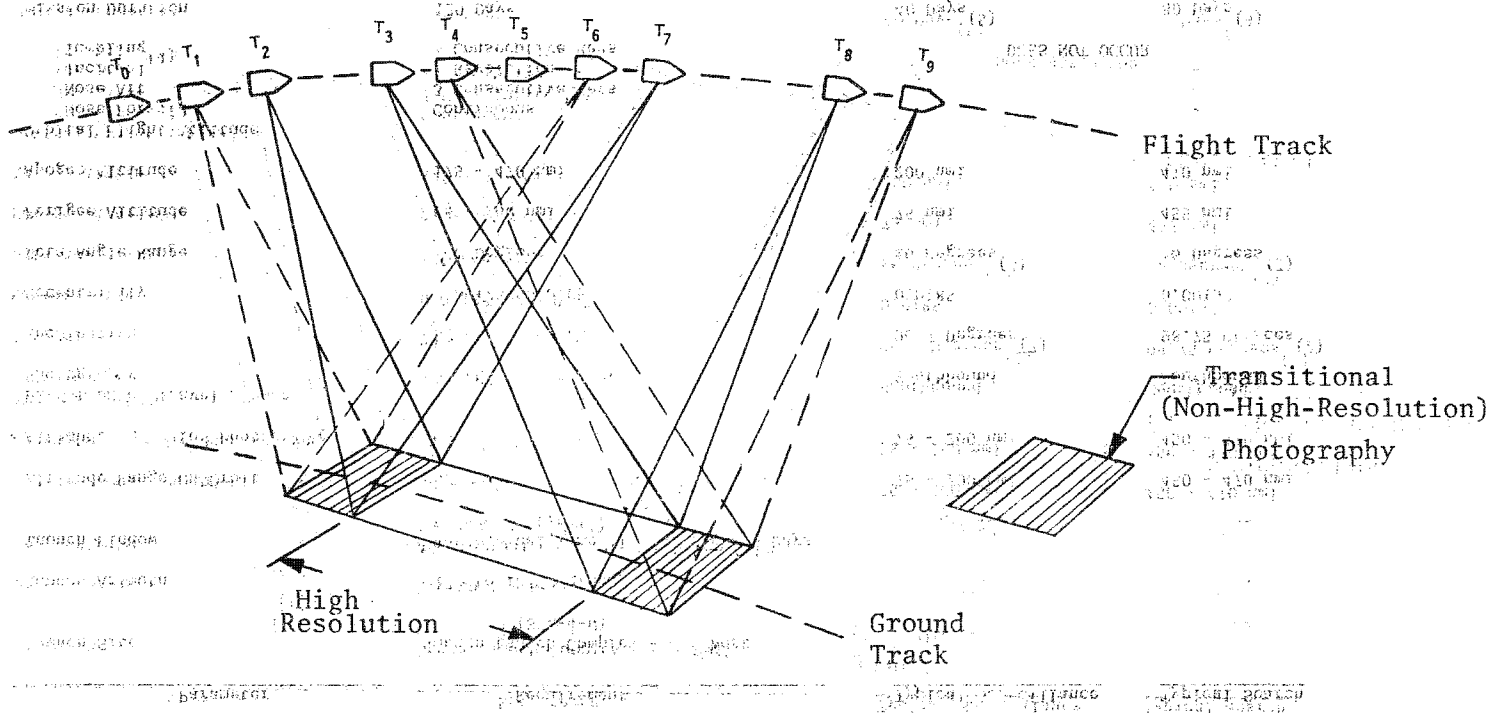


Figure 2.10-1 Stereo Timing

2.10-3
S-01.3

Approved for Release: 2017/02/14 C05097211

Approved for Release: 2017/02/14 C05097211

~~TOP SECRET G~~

08-12-22291/2-10-4

BIF-008- W-C-019838-RI-80

position (3 seconds maximum) the stereo mirror may also be crabbed to accommodate for relative target velocity changes and the vertical motion of the vehicle. Also, during this time, the vehicle can be rolled, if necessary. The film take-up mechanism does not normally operate during stereo photography. Because stereo photography is basically a sequence of two short strip photographs, a similar command sequence is used to obtain stereo pairs, or strip shots. Limits on high-resolution ground coverage available in full stereo are a function of stereo inter-frame time (3.0 seconds minimum) as well as start and stop times, and command granularity considerations.* Figure 2.2-8, found in Part 2, Section 2, may be used to estimate maximum stereo high-resolution coverage.

10.2.1.2 Strip Mode. A secondary manner for programming the dual platen camera results in a strip photograph. In this mode, photography occurs for any desired length of time. If the photograph requires more film than is available in the film storage looper, the supply and take-up reels are actuated during photography. During extended strip photography, occasional film-drive speed changes may be necessary to optimize image motion compensation.

Strip photography may be degraded by take-up/supply operation and/or film-drive speed changes. Because the PPS/DP EAC is optimized for stereo photography, no redesign is contemplated solely to improve strip photography.

10.2.1.3 Single Frame, High-Resolution Limits. When the camera is commanded ON, there is a delay before the film reaches the commanded speed. Similarly, the film does not stop instantaneously when the camera is commanded OFF. The total film length for a given frame is given by the following equation:

*Interframe time for half-stereo (forward-to-nadir or nadir-to-aft transitions) is 2.0 seconds.

BYEMAN
Control System Only

2-10-4
~~TOP SECRET G~~

Handle via BYEMAN
Control System Only

~~TOP SECRET~~

1A-327010-0-7-8000118

61F-008-W-C-019838-RI-80

$$FL = \left[\frac{1}{2}(T_{start}) + T_{set} \right] V_f + T_{HR} V_f + \frac{1}{2}(T_{stop}) V_f$$

where: T_{start} = start-up time (sec)
 T_{set} = settling time (sec)
 FL = frame length (inches)
 V_f = film-drive speed (inches/sec)
 T_{HR} = time of high-resolution (sec)
 T_{stop} = stop time (sec)

A typical film velocity for a single frame is shown in Figure 2.10-2.

The high-resolution frame length is limited by the length of film (36.8 inches maximum) which can be stored in the looper between electrical stops. (Performance specifications do not require high-resolution photography during take-up operation.)

The maximum in-track ground distance which could be photographed in high-resolution is shown in Figure 2.10-3 as a function of slant range for zero stereo and zero and 45-degree obliquity. Nominal values for T_{start} , T_{set} , and T_{stop} were utilized in the equation along with a limiting frame length (FL of 36.8 inches. The approximation for film-drive speed of $V_f = \frac{V_g R}{h}$ was used. Ground velocity, V_g , is

the velocity associated with a circular orbit at the altitude given. Values in the figure assume a completely empty (electrical stop) looper; any film in the looper from a previous frame will reduce the possibility of high-resolution ground coverage.

10.2.1.4 Time Dependent Events. Most of the hardware and pointing parameters which must be set for high-resolution photography of a given target vary from frame-to-frame. The time required to change one or another of these parameters may become a limiting value in certain cases. These parameters are summarized in Table 2.10-2.

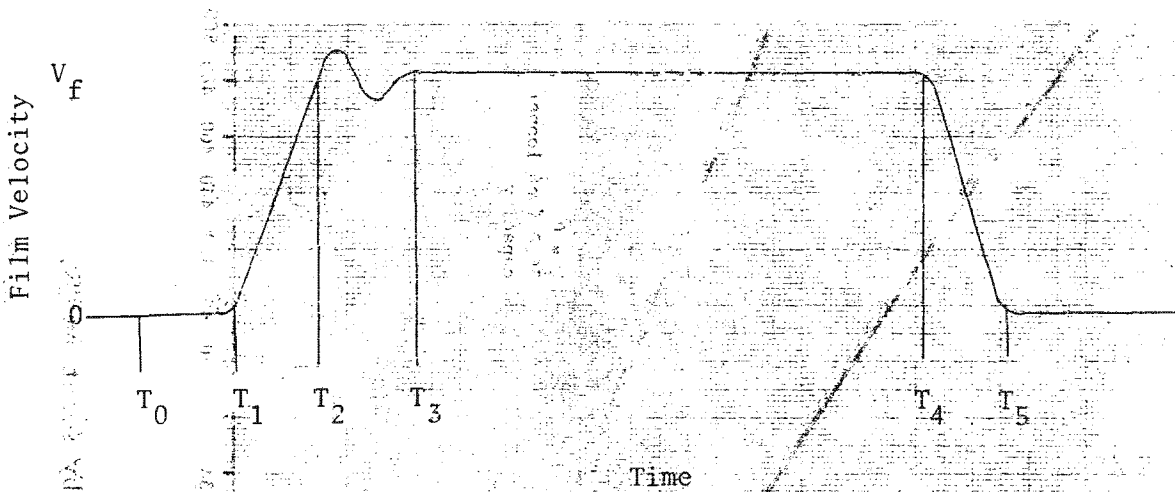
2-10-5
~~TOP SECRET~~

Handle via BYEMAN
 Control System Only

~~TOP SECRET~~ G

BIF-008- W-C-019838-RI-80

TOP SECRET G



- T_0 = ON command received at FPLLE
- T_1 = Begin film movement
- T_2 = Film velocity reaches commanded value
- T_3 = Film velocity settled; begin high-resolution photography
- T_4 = OFF command received at FPLLE
- T_5 = Film movement ceases
- $T_1 - T_0$ = FPLLE delay (0.150 sec)
- $T_2 - T_1$ = Start-up time, T_{start} (0.08 sec nominal)*
- $T_3 - T_1$ = Start-up and settle time (0.15 sec maximum)*
- $T_3 - T_2$ = Settling time, T_{set} (0.07 sec nominal)*
- $T_4 - T_3$ = Time of high-resolution photography, T_{HR} *
- $T_5 - T_4$ = Stopping time, T_{stop} (0.150 sec maximum, 0.07 sec nominal)*

*Figures apply to normal range only. These represent design goals for operation.

25X1

Figure 2.10-2. Typical Film Velocity Profile

2.10-6

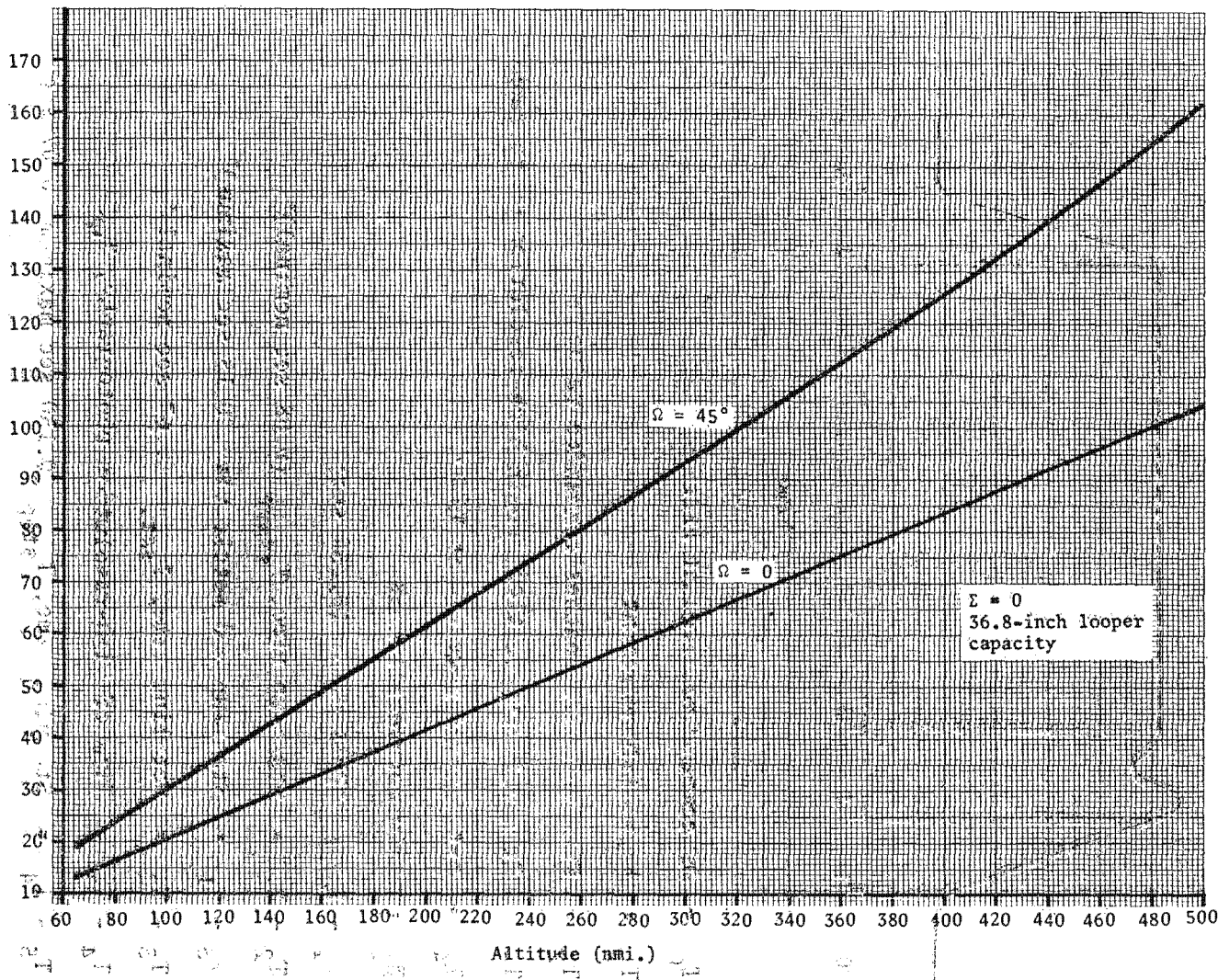
~~TOP SECRET~~ G

Handle via BYEMAN
Control System Only

0-01.5
2.10-7
~~TOP SECRET~~

Maximum High Resolution Ground Distance (nmi.)

Altitude (nmi.)



NOTE: High resolution distance may be scaled by slant range.

Figure 2.10-3. High Resolution Distance

Handle via BYEMAN
Control System Only

~~TOP SECRET~~ G

BIF-008--W-C-019838-RTL-80

10.2.2 Focus Limits

To maintain high-resolution throughout the mission, the position of the emulsion (generally spoken of as the platen position) and the position of the image plane must be matched very closely. The optical design of the primary and secondary cameras is such that no image-plane shifts, except those caused by changes in object distance, should occur on-orbit. (See Part 2, Section 5.) Axial position of the image plane is related to the object distance (slant range) by Newton's formula:

$$\Delta Z = F^2 (1.3714 \times 10^{-5}) \left(\frac{1}{a_2} - \frac{1}{a_1} \right)$$

- where: ΔZ is the image plane shift in inches
- F is the lens' focal length in inches
- a_1 is the initial slant range in nmi
- a_2 is the final slant range in nmi
- 1.3715×10^{-5} is the conversion factor, inches to nmi

Film drive speeds can be matched to image velocity for slant ranges from 65 nmi to 710 nmi. Only in the region from 3.37 in./sec (~212 nmi) to 11.8 in./sec (~65 nmi) is the slant range compensation automatic (i.e., tied to film drive speed). For all operation in an EAC range, the platen is driven to the step 1 position (+0.00275 inch) and automatic SRC is disabled. Needed platen shifts are identified in operational software and explicit commands are sent to accomplish the required platen movement. Required changes are expected to be small. (See Figure 2.10-4.)

08-14-88 010-2-1
BIF-008--W-C-019838-RTL-80

5-01.8 SHAF
1944 5-10-5

88-011 85

2.10-9

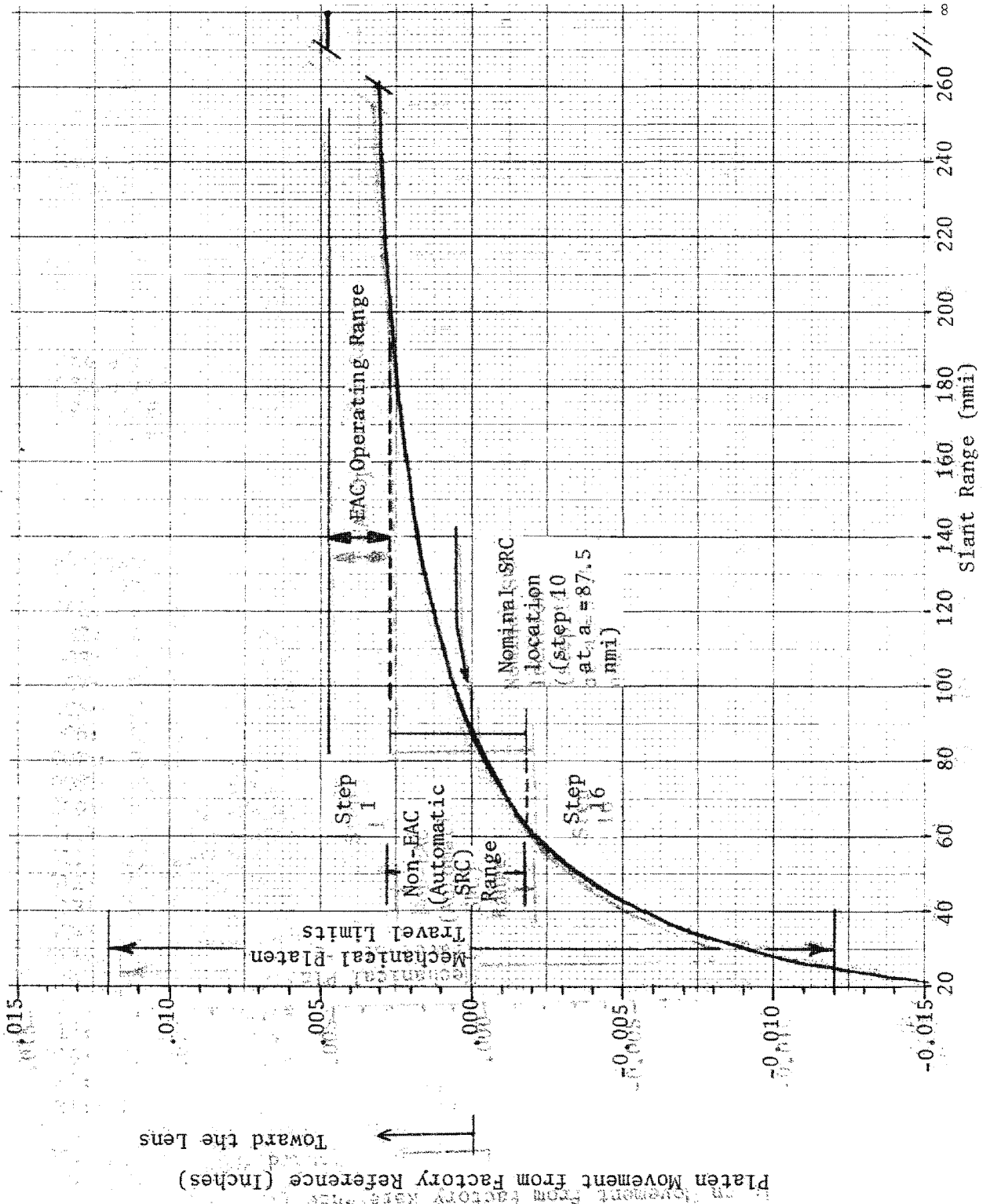
~~TOP SECRET~~ G

Handle via BYEMAN
Control System Only

~~TOP SECRET~~ G

REF ID: A66008 - W-C-019838-RI-80

TOP SECRET G



2.10-10

Figure 2.10-4. Focus Limits

Handle via BYEMAN Control System Only

TOP SECRET G